TECHNISCHE UNIVERSITÄT MÜNCHEN

Lehrstuhl für Biochemische Pflanzenpathologie

Mode of Action of *de novo* designed Antimicrobial Peptides against Human and Plant Pathogens

Alexandra Stefanie Dangel

Vollständiger Abdruck der von der Fakultät Wissenschaftszentrum Weihenstephan für Ernährung, Landnutzung und Umwelt der Technischen Universität München zur Erlangung des akademischen Grades eines

Doktors der Naturwissenschaften

genehmigten Dissertation.

Vorsitzender: Univ.-Prof. Dr. W. Liebl

Prüfer der Dissertation: 1. Univ.-Prof. Dr. J. Durner
2. Univ.-Prof. Dr. S. Scherer

Die Dissertation wurde am 11.04.2012 bei der Technischen Universität München eingereicht und durch die Fakultät Wissenschaftszentrum Weihenstephan für Ernährung, Landnutzung und Umwelt am 12.09.2012 angenommen.

Publications:

B. Zeitler, A. Dangel, M. Tellmann, H. Meyer, M. Sattler, J. Durner, C. Lindermayr "*De-novo* Design of Antimicrobial Peptides for Plant Protection", ***submitted to Molecular Plant-Microbe Interactions (MPMI), in resubmission process***

A. Dangel, N. Ackermann, O. Abdelhadi, K. Oender, P. Fracois, J. Schrenzel, J. Heesemann, C. Lindermayr „ A *de novo* Designed Antimicrobial Peptide with Activity Against Multi-Resistant *Staphylococcus aureus* Acting on Intracellular Bacterial Targets ", ***in preparation***

Table of Contents

I Abbreviations

6x His-tag	Polyhistidine tag of 6 histidine residues
A	Absorption
aa	Amino acid(s)
AB	Antibiotic(s)
Ab	Antibody
ADP	Adenosine diphosphate
AMP	Antimicrobial peptide
AMPPNP	5'-Adenylylimidodiphosphate
AP	Alkaline phosphatase
ATP	Adenosine triphosphate
bp	Base pairs
cfu	Colony forming units
CV	Column volume
core RNAP	RNA Polymerase core enzyme
DEPC	Diethyl pyrocarbonate
$DiSC_3(5)$	3,3’-dipropylthiadicarbocyanine iodide
DMPC	1,2’-dimyristoylphosphatidylcholine
DMPE	1,2’-dimyristoylphosphatidylethanolamine
DMPG	1,2’-dimyristoylphosphatidylglycerol
DNA	Deoxyribonucleic acid
DTT	Dithiothreitol
FPLC	Fast protein liquid chromatography
GOI	Gene of interest
GST	Glutathione S-transferase
h	Hour(s)
HCl	Hydrochloric acid
Kb	Kilobases
kDa	Kilodalton
LB	Luria-Bertani
mAb	Monoclonal antibody
mAU	Milli absorbance units
MBC	Minimal bactericidal concentration
MIC	Minimal inhibitory concentration
ml	Milliliter(s)
min	Minute(s)
mM	Millimolar
MOPS	3-morpholinopropane-1-sulfonic acid (IUPAC nomenclature)

MS	Mass spectrometry
NA	nucleic acid
NanoSIMS	Nanometer-scaled secondary ion mass spectrometry
ND	Not determined
nM	Nanomolar
nt(s)	Nucleotide(s)
OD	Optical density
oN	Overnight
ORF	Open reading frame
PAGE	Polyacrylamide gel electrophoresis
PCR	Polymerase chain reaction
PFA	Para-formaldehyde
PVDF	Polyvinylidene fluoride
RNA	Ribonucleic acid
ROI	Region of interest
RPC	Reversed phase chromatography
rpm	Revolutions per minute
RT	Room temperature
SD/-xxx	Selective deficiency for substance/nutrient: xxx
SDS	Sodium dodecyl sulphate
SEC	Size exclusion chromatography
SigB	Transcription factor sigma B
SP	Synthetic peptide
Vol	Volume(s)
v/v	Volume per volume
w/v	Weight per volume
wt	Wild type
Y2H	Yeast-Two-Hybrid
µl	Microliter(s)
µM	Micromolar
λ_{ex}	Extinction wavelength
λ_{em}	Emission wavelength

Amino acids and nucleotides are expressed according to the IUPAC code (International Union of Pure and Applied Chemistry). All base units and derived units are used following the convention of the SI-system (Système International d'unitès).

II Summary

Antimicrobial peptides (AMPs) are important defense molecules of the innate immunity of higher organisms. Made up of 10 – 50 amino acids they are relatively short in length and often exhibit a positive net charge due to high portions of cationic and hydrophobic amino acids. According to these features, four structural groups of AMPs have been designed at the Institute of Biochemical Plant Pathology prior to this study, differing in size and position of charged and hydrophobic amino acid clusters. Due to their previousely tested high and broad ranged activity against phytopathogens these AMPs provided the basis of this study.

Bacterial resistance to commercial antibiotics is a growing problem world-wide, with multi-resistant *Staphylococcus aureus* being one of the most threatening human pathogens in this context. Regarding the consequent need of new antibiotic agents, AMPs can serve as putative alternative antibiotics. Based on the knowledge about mode and site of action, the activity of newly designed AMP generations can be improved. The antibacterial activities of our newly designed AMPs against multi-resistant *S. aureus* and their mode and site of action, with regard to major putative targets such as membranes, nucleic acids or bacterial proteins, were analyzed within this study.

Regarding antibacterial activity against multi-resistant *S. aureus,* several AMPs with high antibacterial activities in the low micromolar range could be identified. Especially derivates of SP1 (SP1-13) and SP10 (SP10-2, SP10-4, SP10-8) were highly active at concentrations of 1 µg/ml.

A huge number of known AMPs act via pore formation or lysis of bacterial membranes. We could exclude these mechanisms for the *de novo* designed peptides. However, SP10-4, SP10-8 and SP13-2 from structural groups III and IV showed strong influence on the bacterial membrane potential and thereby dissipated membrane integrity. Hydrophobic amino acids turned out to be especially important for this mechanism.

For peptide SP1-1 the strong antimicrobial activity could not be explained by membrane effects. In contrast, localization of heavy isotope labeled SP1-1 using nanometer scaled secondary ion mass spectrometry (NanoSIMS) revealed the ability of SP1-1 to enter *S. aureus* cells and its intracellular accumulation.

For SP1-1 from structural group I and representatives of groups III (SP10-2) and IV (SP13) dose dependent nucleic acid binding by gel retardation experiments was detected. Subsequent microarray analysis revealed numerous genes involved in cell wall and amino acid metabolism, transport mechanisms, virulence and pigmentation differentially expressed by the influence of SP1-1.

Performing a yeast-two-hybrid screen, a strong peptide – protein interaction between SP1-1 and a serine kinase in *S. aureus* (RsbW) was discovered. RsbW acts as an anti-

sigma factor of stress dependent transcription factor Sigma B (SigB) in *S. aureus,* with the ability to perform a partner switching between SigB and its substrate for phosphorylation, RsbV. Due to the instability of RsbW studies of the binding event between SP1-1 and RsbW were not possible. An inhibiting influence of SP1-1 on the kinase function of RsbW as well as on its binding ability to SigB and RsbV, however, was demonstrated *in vitro* by *in-gel* assays. Furthermore, the inhibiting influence of SP1-1 on RsbW was proven to be part of the mode of action, by *in vivo* tests with *S. aureus* deletion mutants of regulon *sigB.* Those revealed that several of the SP1-1 triggered gene expression changes affected RsbW and SigB dependent genes.

In sum, candidates of the *de novo* designed peptides show high activities against *S. aureus* and have diverse targets and multiple modes of action. They act on very specific target molecules, like SP1-1 on kinase RsbW, but also on membranes by influencing membrane homeostasis, and on nucleic acids by dose dependent binding. SP1-1 has to be highlighted as a kinase inhibitor which can be an important agent also with regard to other medical fields. With further elucidation of the molecular mechanism of action and development, the *de novo* designed AMPs can serve as promising new tools, of particular interest in the fight against resistant pathogens.

III List of Figures and Tables

Figures

Tables

1 Introduction

1.1 Antimicrobial peptides

In natural environments every organism has to defend itself against the attack of pathogens. In this context, antimicrobial peptides (AMPs) belong to the most ancient molecules of pathogen defense. They are part of the innate immunity and play an important role in the first line defense of a widespread variety of higher organisms throughout the phylogenetic tree, e.g. invertebrates, plants and animals (Brogden, 2005). There they act as effective weapons against a broad variety of invading pathogens (Zasloff, 2002).

1.1.1 The role of antimicrobial peptides in the innate immunity of higher organisms

Innate immunity is evolutionary the eldest form of immunity, active in nearly all kinds of living organisms, including plants, fungi, insects, mammals and to a certain extent even in organisms such as algae (Ezekowitz and Hoffmann, 2003; Bouarab et al., 2004). To activate this first step of host protection there is no need of an earlier event of pathogen exposition (Ezekowitz and Hoffmann, 2003). The effects that are carried out by antimicrobial peptides are therefore understood as the first host protective barrier. This can even be taken literally, as these types of molecules often occur in the skin or the epithelia of respiratory and gastrointestinal tract of the host organism. They protect these primary shields against invading pathogens mainly by directly killing of the pathogenic organism (Dommett et al., 2005; Glaser, 2011; King et al., 2011). The defense mechanisms, mediated by antimicrobial peptides, take place much faster than the mobilization of compounds of the adaptive immune response and the time span needed for activation of AMP effects is in most cases much faster than a standard microbe generation time (Mangoni, 2011).

The research on antimicrobial peptides started in the 1980s, when the first peptides with antimicrobial activity were discovered in insects (Steiner et al., 1981). These antimicrobial peptides were cecropins, found in pupae of the moth *Hyalophora cecropia* by Boman, Steiner and coworkers (Steiner et al., 1981). Some years later magainins were detected in the skin of African claw frogs (Zasloff, 1987) and defensins in rabbit neutrophils (Ganz et al., 1990).

Until now there are several structural groups known. Even though mode and site of action for some of these first identified peptides have been identified not long after their discovery (Boman et al., 1991; Boman et al., 1993), mechanisms or target sites of most of the peptides are still not well elucidated (Epand and Vogel, 1999; Landon et al., 2008; Wimley and Hristova, 2011).

Although antimicrobial peptides are often active against a broad range of pathogens, the addressed organisms are differing from peptide to peptide. Effective concentrations are also highly variable among these peptides. For one of the first detected AMPs, magainin 2, the antibacterial activity ranged from 5 to 100 µg/ml, depending on the pathogenic bacterial strain (Zasloff, 1987). For most peptides that are under investigation today, activities in the lower µM range have been shown and peptides that exhibit activities in this or sometimes even the middle µM concentration range attract further interest of researchers (Hernandez-Aponte et al.; Haigh et al., 2008; Lu et al., 2008). However, many research groups work on further enhancement of activity and lower possible cytotoxic effects on eukaryotic cells by small structural changes of the peptides (Friedrich et al., 2000; Haines et al., 2009). Derivates of the frog-skin peptide Temporin 1Ta for example, differing only in single or few amino acid residues from the parental peptide, exhibited two- to four-fold lower minimal inhibitory concentrations (MICs) than the original peptide (Grieco et al., 2011).

1.1.2 Chemical and structural characteristics

For the different antimicrobial peptides, produced in diverse host organisms, several structural and motif conformities are known. Most of the molecules share cationic and amphipathic properties (Peschel and Sahl, 2006). Although there are also anionic antimicrobial peptides known (Harris et al., 2009), the majority exhibits high portions of basic amino acids, such as lysine and arginine. Those lead to the cationic character, with a positive net charge of around +2 to +7. Therefore, these AMPs can also be subsumed under the conceptual cationic antimicrobial peptides (CAMPs). Generally, these amphipathic molecules are composed of 10 – 50 amino acids, with about 50% or more of the amino acid residues being hydrophobic (Hancock and Diamond, 2000).

Within this umbrella term there are a wide variety of sequences and sequence features and the AMPs/CAMPs can be sub-grouped by their secondary and tertiary structures (Figure 1). In this way often three to five main groups are differentiated (Hancock and Lehrer, 1998; Epand and Vogel, 1999; Powers and Hancock, 2003; Giuliani et al., 2007).

The first group (A) is composed of peptides that share the feature of an α-helical structure (Huang et al., 2010). The frog derived magainin 2 (Maloy and Kari, 1995) and the human cathelicidin LL-37 (Bucki et al., 2010) are well known examples of this group (Nguyen et al., 2011). However, the helical structure is often not observed until the

peptide approaches a lipid environment, for example a bacterial membrane. In aqueous solutions an unstructured or randomly coiled structure can often be observed (Hancock and Diamond, 2000). ß-structured peptides form a second group (B), which in some cases can be further differentiated into ß-sheet peptides, e.g. human ß-defensins (Taylor et al., 2008) and peptides with a ß-hairpin structure, like the arginine rich protegrin-1 (Tang and Hong, 2009) or lactoferricin B (Giuliani et al., 2007).

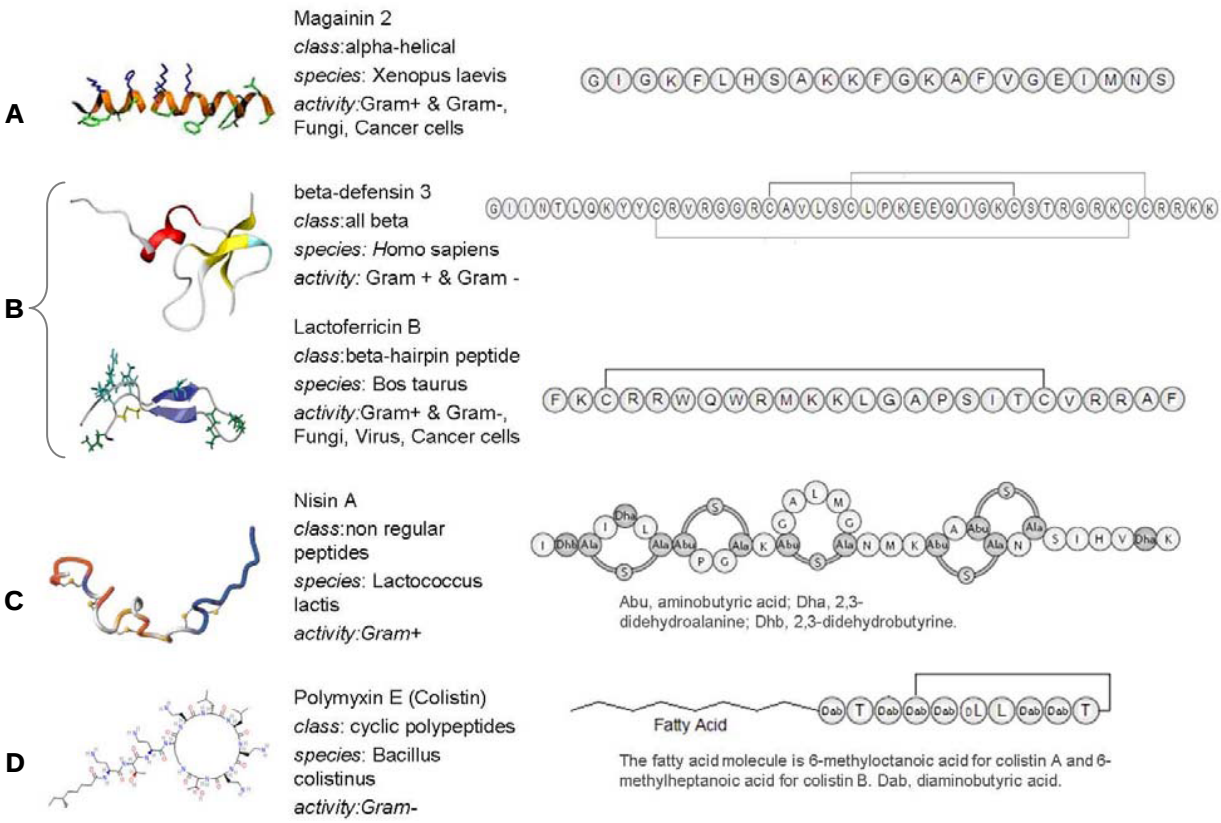

Figure 1 - Structural diversity of antimicrobial peptides
Antimicrobial peptides can be classified into different structural groups: (A) the alpha-helical, (B) the general beta and beta-hairpin, (C) the non-regular and (D) the cyclic peptides. The groups are described by well-studied representatives, including their origin and activity spectrum (middle column), their primary (right column) and their characteristic tertiary structure (left column). (Giuliani et al., 2007)

The most common classes of AMPs are those with ß-sheet and α-helical structures. But there is also a bulk of AMPs that do not fit into these characteristics. One of these other structural groups (C) is formed by AMPs that are characterized by an irregular amino acid composition. Those are called non-regular peptides. The sequence of these AMPs is often extremely rich in a particular amino acid, as it is the case for the histidine rich peptide group of histatins from human saliva (Dale and Fredericks, 2005) or the anti-fungal cysteine rich peptides RS-AFP1 and 2 from radish (Terras et al., 1995). Also the proline rich AMPs, that selectively kill gram-negative bacteria, fit into this class. They often show repeated motifs of proline interspersed with arginine residues (Scocchi et al., 2011). In other cases, non-abundant amino acids are important for structure and action of the

peptide, like tryptophan in indolicidin (Podorieszach and Huttunen-Hennelly, 2010). Also bacterially derived peptides fall into these groups. An example is nisin from lactic acid bacteria with its irregular aminobutyric acid (Dalmau et al., 2002). This peptide belongs to the lantibiotics, which are characterized by their intramolecular thio-ether rings (Herzner et al., 2011). The last group of peptides (D) are general loop- or ring-building peptides. Plant derived cyclotides belonging to this group show a macrocyclic cysteine knot motif. Their ring closing affects about twice as many of the amino acid residues than in other cyclic peptides, where the ring covers normally less than 15 amino acid residues (Craik et al., 2007). This group gained interest within the last years because the knotted ring structure seemed to provide a very stable scaffold for defense molecules (Jagadish and Camarero, 2010).
Transition between groups is smooth for many peptides, as for example ß-structured peptides can also be cyclic, leading to a lesser extent of entropy loss (Zanetti-Polzi et al., 2009). The ring structure is often formed by disulfide bonds (tachyplesins) or by cyclization of the peptidic backbone, like in gramicidin S or polymyxin B (Epand and Vogel, 1999). Although most classifications are done in an equal manner, especially regarding the most abundant α-helical and ß-peptides, this arrangment of AMPs is not 100% consistent among different authors (Hancock and Lehrer, 1998; Epand and Vogel, 1999; Hancock and Diamond, 2000; Giuliani et al., 2007).

1.1.3 Proposed mechanism of action

Since antimicrobial peptides have been identified as extremely potent molecules of defense against pathogens, their mode of action has been subject of intense research. Over the last decades it has been assumed that antimicrobial peptides mainly attack the cell membrane of pathogens. It has been suggested that peptides incorporate into the membrane, form pores and thereby or by other lytic mechanisms destroy the membrane. This mode of action has indeed been shown for a number of antimicrobial peptides (Zasloff, 2002; Boland and Separovic, 2006; Semrau et al., 2010; Amiche and Galanth, 2011).

1.1.3.1 Bacterial membranes as targets of antimicrobial peptides

The membranes of microbes differ significantly from those of eukaryotic organisms. Lipids occurring in big portions in eukaryotic membranes are mostly uncharged, like the phospholipids phosphatidylcholine (PC) and phosphatidylethanolamine (PE). Further lipids from eukaryotic membranes are also generally neutral in charge, like sphingomyelin (SM) and sterols like cholesterol or ergosterol. In contrast, prokaryotic membranes are predominantly composed of hydroxylated phospholipids, such as phosphatidylglycerol (PG), its dimer cardiolipin (CL), and phosphatidylserine (PS). These confer a negative net

charge to the membranes. Thereby, attraction of antimicrobial peptides to microbe membranes can be explained by electrostatic bonding between the cationic AMPs and the negatively charged outer surface of the membranes (Yeaman and Yount, 2003). Subsequently, pore forming or membrane disruption can occur. This is for example the mode of antimicrobial action of nisin (Wiedemann et al., 2004), salmon and human calcitonin (Stipani et al., 2001), lactacin F (Dalmau et al., 2002) and some protegrins (Sokolov et al., 1999). For a more detailed view on the disruptive mechanism, several models of incorporation into the bacterial membrane and following destruction of the membrane integrity were devised (Brogden, 2005; Park and Hahm, 2005; Palffy et al., 2009).

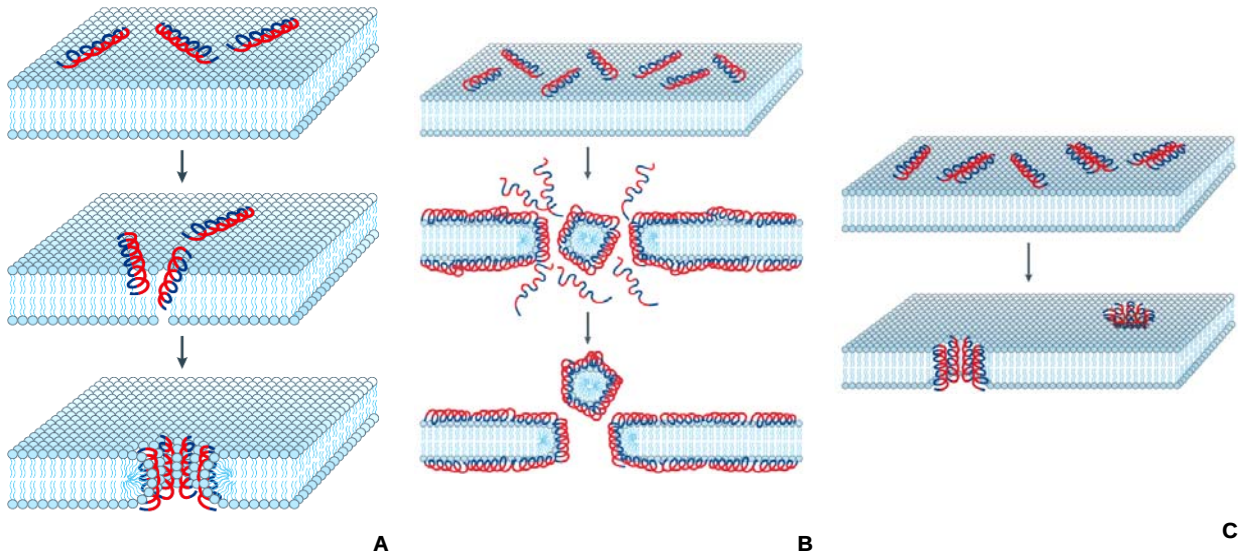

Figure 2 - Proposed models of antimicrobial peptide action at bacterial membranes
Shown are the three most prominent basic models to explain AMP action at bacterial membranes. (A) In the "toroidal-pore" model peptides aggregate and force the membrane to build a pore by bending around. (B) In the "carpet" model the peptides disrupt the membrane in an irregular way by a parallel orientation towards the lipids. (C) In the "barrel-stave" model the peptides form an aqueous pore by facing hydrophobic parts towards the lipids and hydrophilic parts to the interior part of the pore. Hydrophilic regions of the peptide are shown in red, hydrophobic regions are shown in blue. (Brogden, 2005)

One of the three most prominent models is the "toroidal-pore" model (Figure 2A). Here the peptides aggregate in such a way that the lipid bilayer is forced to bend around. In that way, the lipid head groups form an interior pore region together with the hydrophilic parts of the peptides. For magainins, for example, such toroidal pore forming is well known (Rzepiela et al., 2010). In the second model, the "carpet" model (Figure 2B), the peptides are oriented parallel with regard to the surface of the lipid bilayer. There they build an extensive layer on the membrane which leads to a disordered disruption of the membrane. This mechanism applies for example to the cathelicidin derivate LL7-27 (Thennarasu et al., 2010). The third model is called the "barrel stave" model (Figure 2C). Here the peptides aggregate in such a way that the hydrophobic parts are directed towards the lipids of the membrane and the hydrophilic parts form an aqueous interior

part of the pore (Oren and Shai, 1998; Shai, 1999). The barrel stave model could even be observed for peptides that actually are too short to span the lipid bilayer. But by thinning of the membrane at the peptides insertion site a membrane spanning pore can be achieved (Bocchinfuso et al., 2009).

However, some AMPs are able to influence membrane integrity, but not via one of these models. Influence on the membrane in a non-lytic way but with some kind of effect on the membrane stability appears to be important for the peptide CP10A. This indolicidin derivate does not show any membrane disruption or pore formation. Nonetheless it interacts with the membrane. This leads to the appearance of intracellular lamellar membrane structures in peptide-treated cells (Friedrich et al., 2001). Other membrane interactions, differing from the above models, can also cause damage to the membrane homeostasis and transport systems by membrane depolarization. In recent studies additional mechanisms of AMP - membrane interactions have been reported, for example membrane thickening or thinning, which happens due to charge and hydrophobic interactions after parallel orientation of peptides towards the lipid bilayer. In this way the dynamics of the lipid bilayer are affected. Such membrane interactions can be important for peptides even if they do not unfold their killing potential on the membranes themselves, but just translocate through membranes to reach intracellular targets (Friedrich et al., 2000; Nguyen et al., 2011). For cell-penetrating peptides (CPPs), different uptake mechanisms into at least eukaryotic cells are under discussion (Nakase et al., 2008). These include endocytic mechanisms, as macro pinocytosis (Jones, 2007), as well as non-endocytic mechanisms, like direct penetration (Madani et al., 2011). Derossi and colleagues (1996) for example already proposed a model for internalisation of a 16-amino acid long polypeptide by the formation of peptide uptaking phospholipid micelles that internalize into the cells and release the peptides into the intracellular compartments.

1.1.3.2 Bacterial intracellular targets of antimicrobial peptides

Many known AMPs act by membrane disturbing or lytic activity. However, there is also the possibility, that AMPs do not interact with the membrane directly, but with membrane associated or intracellular targets such as proteins or nucleic acids. This can result in inhibition or activation of transcription, translation or enzyme functions (Figure 3, Brogden, 2005).

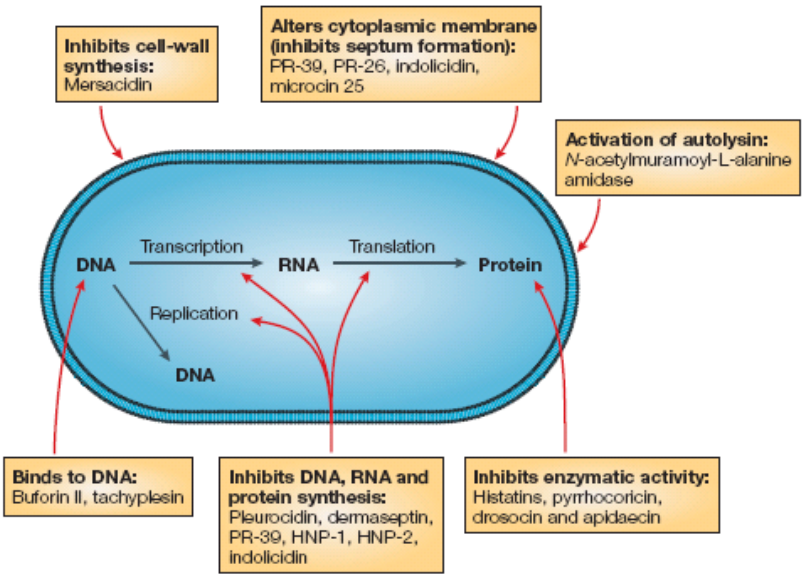

Figure 3 - Modes of action of antimicrobial peptides beyond membrane disruption
Antimicrobial peptides can have effects on a number of targets in bacterial cells. In addition to membrane disruption they can also inhibit cell wall synthesis or alter the cytoplasmic membrane. They can also affect transcription, translation or enzymatic activity by binding to intracellular targets like DNA, RNA or enzymes. Examples of non-membrane lytic antimicrobial effects in *E. coli* are shown with representative peptides. (Brogden, 2005)

Buforin II for example, is a very potent derivate of an antimicrobial peptide, isolated from the stomach tissue of the Asian toad *Bufo bufo gargarizans* (Park et al., 1996). It was demonstrated to penetrate the cell membrane of *E. coli* without lytic effects. It accumulates in the intracellular space of the bacteria and binds to DNA and RNA, indicating the inhibition or alteration of intracellular functions like DNA replication, transcription, or translation as killing mechanism (Park et al., 1998). For pleuricidin, an AMP derived from winter flounder, an inhibition of macromolecular synthesis was reported in *E. coli* in the context of initial membrane depolarization (Patrzykat et al., 2002). Additionally, effects on intracellular enzymes have already been described. For example antimicrobial peptides derived from insects such as drosicin, apidaecin and pyrrhocidin affect bacterial heat shock proteins (Otvos, 2000b; Otvos et al., 2000a). They interact in a specific manner with the 70 kDa DnaK chaperone, and in a nonspecific manner with the 60 kDa chaperonin GroEL. Thereby they inhibit their ATPase action and prevent chaperone-assisted protein folding (Kragol et al., 2001; Markossian et al., 2004). Furthermore, up-regulating effects on the immune system of the infected host have been shown. Agerbert et al. (2000) reported that peptide LL-37 induced chemotactic effects *in*

vitro, triggering selective migration of human peripheral blood monocytes, neutrophils, and CD4 T-cells. Furthermore, cumulative effects are described for some AMPs, demonstrating that AMPs may have multiple modes of action and diverse targets within a microorganism (Otvos, 2005).

1.1.4 *De novo* designed antimicrobial peptides of the Institute of Biochemical Plant Pathology

At the Institute of Biochemical Plant Pathology a number of peptides have been sequentially designed after the structural model of potent AMPs that are naturally occurring in the environment (Zeitler et al., 2012). The primary amino acid sequences have been chosen to achieve a positive net charge, by usage of the positively charged amino acids lysine or arginine. Furthermore, hydrophobic regions have been generated by leucine, valine, isoleucine, phenylalanine, proline, methionine and alanine. The α-helical structure has been generated by alanine, leucine and methionine residues. Such an α-helical structure of AMPs is often associated with membrane activity (Nguyen et al., 2011). The hydrophobic and positively charged amino acids have been arranged in clusters, since this amphipathic composition seems to be one fundamental criterion of naturally occurring peptides (Zasloff, 2002). Altogether four different groups of peptides have been designed, differing in size and localization of the hydrophobic and charged clusters (Figure 4).

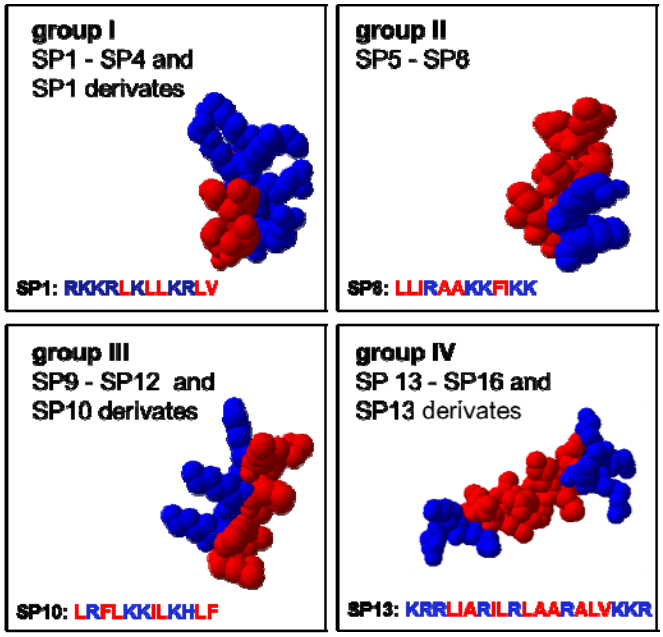

Figure 4 - Structure of the *de novo* designed antimicrobial peptides
According to the natural model four peptide groups with different hydrophobic and charged clusters and a predicted α-helical structure were developed. Cluster arrangement of the different groups and examples for amino acid sequences of representatives of each group are shown. Hydrophobic amino acids are shown in red, charged amino acids in blue.

The first group was composed of a larger cationic and a smaller hydrophobic part, whereas group II showed hydrophobic and cationic clusters in reversed proportions. Group III was designed by unilateral arrangement of similar sized hydrophobic and cationic clusters. Group I, II and III thereby were built of a length of 10 – 12 amino acid residues. Group IV was generated as a "bone"-like structure, by a hydrophobic part in the middle of the molecule, bounded by smaller cationic clusters at both ends. With the sequence enlarged to 18 – 20 amino acid residues this group should serve as a model for putative membrane spanning ability (Figure 4).
The first generation of the thus obtained *de novo* designed antimicrobial peptides (SP1 – SP16) was tested against plant pathogens. Furthermore, toxicity assays were carried out with human red blood cells. Several peptides showed promising activities in the single digit micromolar range against a broad range of phytopathogenic bacteria, including several *Pseudomonas* strains, *Pectobacterium sp.*, *Clavibacter sp.* and *Xanthomonas sp..* The most active peptides (SP1, SP10 and SP13) were used as lead structures to develop a second generation (SP1-1 – SP1-22, SP10-1 – SP10-11, SP13-1 – SP13-14) by single or few changes of the amino acid sequence (Supplementary Table 1). The peptides of the second generation were again tested for activity and toxicity. Representatives with activities ranging from the low micromolar level even down to the nanomolar concentration could be identified ((Zeitler et al., 2012), Supplementary Table 1). Candidates with high activity against phytopathogenic bacteria were used as the basis of this study.

1.2 Increasing resistance of bacteria necessitates for new antibiotic agents

There is a big demand for antimicrobial agents in all medical fields, including plant protection, veterinary and human medicine. In plant protection, bacterial infections are a big problem, as 14% of the total crop loss worldwide is due to infectious diseases and additional losses of 6 – 12% that occur after harvest (Agrios G. N., 2005). Those infections are mainly controlled by chemical pesticides, which, however, are subjected to strong restrictions and regulatory requirements (Montesinos, 2007). Their infiltration in soil and groundwater can additionally cause severe problems to the environment and contamination risks for the food supply chain (Flury, 1996; Dabrowski et al., 2002; Gonzalez-Rodriguez et al., 2011). However, decreasing possibilities regarding alternative antibiotics for the fight against pathogens affect not only plant protection but the entire medical field. One of the major problems is the growing number of bacterial resistances. In general, resistance to antibiotics in bacteria is defined as the ability to withstand the inhibitory concentration of an antibiotic. Throughout evolution, resistance mechanisms

are continuously evolving as long as microbes are exposed to any kind of antibiotic substance. Naturally occurring resistances are characteristic for particular bacterial species or even whole genera. They result in the inability of an antibiotic to reach and affect a target, because of either low affinity, the existence of efflux pumps or other genetically encoded mechanisms (Woodford and Ellington, 2007). The bigger problem occurs from the growing number of acquired resistances (Zhang et al., 2006; Werner et al., 2008). They are often mediated by horizontal gene transfer and the resistance carrying gene elements can be collected in a number of ways by bacteria. This makes the spreading of resistance features throughout whole microbial populations possible (Chroma and Kolar, 2010). Due to the haploidity and the typical short generation times of many pathogenic bacteria the resistance underlying mutations, especially under selection pressure situations by antibiotic occurrence in the environment, can accumulate very fast (Woodford and Ellington, 2007).

A special issue regarding resistant bacteria is given by the multi-resistant strains of *Staphylococcus aureus*. This bacterium is a facultative anaerobic, gram-positive coccus, belonging to the class of *Bacilli*, that forms grape like clusters in culture (Baron, 1996). Its carotenoid pigment staphyloxanthin is responsible for the golden color and thus for the species name "aureus" (Liu and Nizet, 2009). In around one third of the healthy population it can be found on the mucous membranes and the skin without causing any symptoms (Kluytmans et al., 1997; Gorwitz et al., 2008). However, it carries a number of virulence factors and can also cause a range of illnesses from minor skin infections, to life-threatening diseases such as pneumonia, meningitis, and sepsis (Defres et al., 2009; Larkin et al., 2009; Sinha and Fraunholz, 2010). This pathogen is naturally susceptible to every kind of antibiotic but it has a special ability to acquire resistances, often via horizontal gene transfer. Since the 1940s more and more resistances against commercial antibiotics were reported and the number of nosocomial infections caused especially by methicillin-resistant *S. aureus* (MRSA) strains constantly increased. Many MRSA strains now are resistant to multiple antibiotic classes and outbreaks and epidemics occur worldwide (Chambers and Deleo, 2009). The severe infections caused by multi-resistant bacteria are a medical challenge and also a financial burden for hospitals and health care systems (Wilke, 2010) and the spreading resistances are further advancing (Mainous et al., 2011). Therefore, the need for new strategies and agents in the fight against MRSA is an important topic of current medicine (Burda et al., 2011).

In this context AMPs are often regarded as putative alternatives to common antibiotics (Sperstad et al., 2011). At least the first interaction between peptide and the microbe happens by a rather unspecific attraction of charges and hydrophobic interactions with lipids (Huang et al., 2010). Since many AMPs act on bacterial membranes or generalized targets they have considerable advantages compared to standard antibiotics with very distinct targets, as the possibility for the microbe to acquire resistance in those general

and essential pathways is much lower (Perron et al., 2006; Peschel and Sahl, 2006). Moreover, some peptides even use multiple or a combination of mechanisms, making it even more difficult for bacteria to acquire resistance (Nguyen et al., 2011). Due to these differences AMPs are attracting interest of researchers as they can putatively serve as alternative therapeutic agents in the fight against bacterial pathogens (Mangoni, 2011).

1.3 Aim of this study and strategy

A lot of research has been done on antimicrobial peptides in terms of their antimicrobial potential and regarding their mode and site of action. But although activity ranges of many naturally occurring peptides seem to be promising, they need to be further improved for their possible future application in the fight against pathogens. The AMPs used in this study have been designed previously to achieve high activities against pathogens with a preferably negligible or low toxicity. For decades site and mode of action of antimicrobial peptides have mainly been assigned to bacterial membranes. However, it is well established now that different kinds of peptides can have very different targets and also a multiple mode of action.

In this study the previously designed AMPs were to be analyzed for antibacterial activity against the important human pathogen *S. aureus,* and their mode of action regarding major possible targets.

The analyses covered the following items:

- Antibacterial activity against multi-resistant strains of *S. aureus* should be elucidated. With its capacity to acquire multiple resistances against common antibiotics this pathogen requires urgent attention and new effective antibiotic agents.
- Effects on membrane integrity, disruption and interaction ability of the peptides should be tested with artificial membranes and membranes of living bacteria cells.
- Furthermore, localization of the peptides at the pathogens should be conducted by microscopic and nanometer scaled secondary ion mass spectrometry (NanoSIMS) approaches to elucidate main target sites.
- Additionally, the interaction with possible intracellular targets should be investigated. The binding to nucleic acids should be studied by gel shift assays and, in addition, protein – protein interactions should be elucidated by a yeast-two hybrid screen.

The gained knowledge about target sites and mechanisms could be useful for future development of the AMPs by targeted changes in peptide structure to improve activity by enhanced target peptide fitting.

2 Material and Methods

2.1 Material

2.1.1 Chemicals

The chemicals used in this study were obtained in high purity grade and purchased either from Sigma Aldrich GmbH (Taufkirchen, Germany), Carl Roth GmbH (Karlsruhe, Germany), or other sources as indicated.

2.1.2 Peptides

Unlabeled synthetic peptides

Peptides were obtained from Hanhong Chemicals Co. Ltd (Shang Hai, China) in a purity grade of >80% and with C-terminal amidation. Mino acid sequences and physico-chemical characteristics are in Table 1:

Table 1 - Amino acid sequences and physico-chemical characteristics of the used AMPs

peptide	Sequence	Theoretical PI / MW	Charge at neutral pH
SP1	RKKRLKLLKRLV	12.31 / 1551.04	+7
SP1-1	RKKRLKLLKRLL	12.31 / 1565.07	+7
SP1-2	RKKRVKLLKRLV	12.31 / 1537.02	+7
SP1-3	RKKKVKLLKRLV	12.04 / 1509.00	+7
SP1-4	RKKRLKVVKRLV	12.31 / 1522.99	+7
SP1-5	RKKRLRVVRRLV	12.60 / 1579.02	+7
SP1-6	RKKKLKVVKRLV	12.04 / 1494.98	+7
SP1-7	RKKKLKIIKRLI	12.04 / 1537.06	+7
SP1-8	RKKKIKIIKRLI	12.04 / 1537.06	+7
SP1-9	RKKKIKIIKKII	11.43 / 1509.04	+7
SP1-10	RKKKAKIIKKII	11.43 / 1466.96	+7
SP1-11	RKKKLKFFKRLF	12.04 / 1639.11	+7
SP1-12	RKKKFKFFKRLF	12.04 / 1673.13	+7
SP1-13	RKKKFKFFKRFF	12.04 / 1707.14	+7
SP1-14	RKKKFKIFKRLF	12.04 / 1639.11	+7
SP1-15	KRKKLLKRLL	12.03 / 1295.72	+6
SP1-16	KRKKLLKRLI	12.03 / 1295.72	+6
SP1-17	KKKKIIKRLI	11.39 / 1267.71	+6
SP7	LLIKFLKRFIK	11.26 / 1418.88	+4
SP8	LLIRAAKKFIKK	11.33 / 1428.87	+5
SP9	LLKALKKLLKKLL	10.60 / 1522.08	+5
SP10	LRFLKKILKHLF	11.26 / 1556.02	+5
SP10-1	LRFLKKILKKLF	11.33 / 1547.05	+5
SP10-2	LRFLKKALKKLF	11.33 / 1504.97	+5

Table 1 - continued

SP10-4	LRFIKKILKKLI	11.33 / 1513.03	+5
SP10-5	LRIIKKILKKLI	11.33 / 1479.01	+5
SP10-6	LRIIRRILRRLI	12.60 / 1591.07	+5
SP10-7	LRILRRLLRRLF	12.60 / 1625.09	+5
SP10-8	LRFLRRILRRLL	12.60 / 1625.09	+5
SP10-10	LRKLKKILKKLF	11.39 / 1528.05	+6
SP10-11	LRKAKKIAKKLF	11.39 / 1443.89	+6
SP11	LRALAKALKHKL	11.26 / 1361.74	+4
SP12	LKALRKALKHLA	11.26 / 1361.74	+4
SP13	KRRLIARILRLAARALVKKR	12.70 / 2402.07	+8
SP13-2	KRRLILRILRLAIRALVKK	12.61 / 2330.04	+9
SP13-6	KRRKLIKILKLIIKLIRKKR	12.49 / 2558.42	+11
SP13-7	KRRKLIKILKLIAKLIRKKR	12.49 / 2516.34	+11
SP13-12	KRRLFLFRLFRLFLRLFLKK	12.61 / 2711.47	+8
SP13-14	KRRKLAFRLFRLFLKLVLKK	12.49 / 2574.33	+9

Indolicidin was purchased from Bachem (Weil am Rhein, Germany) and protegrin1 (purity >95%) was synthesized by Metabion (Munich, Germany).

Peptides were dissolved in HPLC grade water or peptide buffer (0.2% BSA, 0.01% acetic acid in HPLC grade water), filter sterilized and stored as aliquots at -20°C for short time and at -80°C for long time storage.

Labeled synthetic peptides

Peptides were obtained in a purity grade of >80% and with C-terminal amidation. Sequences and physico-chemical characteristics as follows:

SP10-9-TAMRA SP10-11-TAMRA SP13-14-FAM	N-terminal TAMRA (5(6)tetramethyl-rodamine) and FAM (5(6)-carboxy-fluorescein), labeled peptides were purchased from Metabion International AG (Martinsried, Germany)
^{15}N-SP1-1	L (5,8,12) ^{15}N labeled SP1-1 was purchased from Genscript Inc. (Piscataway, NJ, United States)

2.1.3 Buffers and Solutions

Peptide buffer	0.2% BSA, 0.01% acetic acid (sterile filtrated)
PBS	137 mM NaCl
	2.7 mM KCl
	4.3 mM Na_2HPO_4
	1.47 mM KH_2PO_4
	pH 7.4

TE	10 mM Tris-HCl pH 8.0
	1 mM EDTA pH 8.0
50x TAE running buffer	2.0 M Tris
	5.71% (v/v) glacial acetic acid
	50 mM EDTA
10x DNA loading buffer	50% (w/v) glycerol
	10 mM EDTA, pH 8.0
	0.25% (w/v) bromphenol blue
	0.25% (w/v) xylene cyanol FF
Kinase activity buffer	50 mM Tris pH 7.5
	50 mM KCl
	10 mM $MgCl_2$

SDS-PAGE (according to Laemmli, 1970)

2x reducing sample buffer	100 mM Tris/HCl, pH 6.8
	4% (w/v) SDS
	0.2% (w/v) bromphenol blue
	20% (w/v) glycerol
	200 mM DTT
Resolving gel buffer	1.5 M Tris/HCl, pH 8.8
	0.4% (w/v) SDS
Stacking gel buffer	0.5 M Tris/HCl, pH 6.8
	0.4% (w/v) SDS
10x SDS running buffer	250 mM Tris base
	2 M glycine
	1% (w/v) SDS

Tricine-SDS-PAGE (accordig to Schagger, 2006)

Fixing solution	50% (v/v) methanol
	10% (v/v) glacial acetic acid
	100 mM ammonium acetate (*added just before use*)
10x anode buffer	1.0 M Tris base
	225 mM HCl
10x cathode buffer	1.0 M Tris base
	1.0 M tricine
	1.0% (w/v) SDS
3x gel buffer	3.0 M Tris base
	1.0 M HCl
	0.3% (v/v) SDS

4x reducing sample buffer	150 mM Tris/HCl, pH 7.0
	12% (w/v) SDS
	0.05% (w/v) Coomassie blue G-250
	30% (w/v) glycerol
	6% (v/v) ß-mercaptoethanol

Native PAGE (modified from Laemmli, 1970)

Resolving gel buffer	1.5 M Tris/HCl, pH 8.8
Stacking gel buffer	0.5 M Tris/HCl, pH 6.8
10x native PAGE running buffer	250 mM Tris
	2 M glycine

4x non-reducing sample buffer	200 mM Tris/HCl, pH 6.8
	0.4% (w/v) bromophenol blue
	40% (w/v) glycerol
	400 mM DTT

Staining of proteins on polyacrylamid gels

Coomassie R-250 staining solution	0.25% (w/v) Coomassie Brilliant Blue R-250 in 50% (v/v) methanol, 10% (v/v) glacial acetic acid
Coomassie R-250 destaining solution	30% (v/v) methanol 10% (v/v) glacial acetic acid
Coomassie G-250 staining solution	0.25% (w/v) Coomassie Brilliant Blue G-250 in 50% (v/v) methanol, 10% (v/v) glacial acetic acid
Coomassie G-250 destaining solution	10% (v/v) glacial acetic acid

Protein transfer and immunoblotting

Transfer buffer	40 mM Tris
(Duchesne and Fernig, 2007)	40 mM Tricine
	0.04% (w/v) SDS
	20% (v/v) methanol
Ponceau-S solution	0.2% (w/v) ponceau-S in 3% acetic acid
TBS	10 mM Tris/HCl, pH 7.4
	150 mM NaCl
	1 mM MgCl2
TBS-T	0.5% (w/v) Tween 20 in TBS

Blocking buffer	1% (w/v) dry milk powder
	1% (w/v) BSA
	in TBS-T
Alkaline phosphatase (AP) buffer	0.1 M Tris/HCl, pH 9.5
	0.1 M NaCl
BCIP solution	5% (w/v) 5-bromo-4-chloro-3'-indolyphosphate in 100% DMF
NBT solution	10% (w/v) nitro blue tetrazolium chloride in 70% DMF

Cell lysis

For recombinant SP1-1	50 mM NaH_2PO_4
	150 mM NaCl
	10 mM Imidazole
	Adjust pH to 8.0 using NaOH
For recombinant RsbW, RsbV	50 mM KCl
	50 mM Tris
	2 mM $MgCl_2$
	1 mM DTT
	pH 8.0
For recombinant SigB	150 mM NaCl
	100 mM Tris
	1 mM EDTA
	1 mM DTT
	pH 8.0

Affinity chromatography

Binding buffer

For binding of GST-tag	PBS, pH 7.4
For binding of 6x His-tag	50 mM NaH_2PO_4
	150 mM NaCl
	10 mM imidazole
	pH 8.0
For binding of Strep-tag	50 mM Tris
	300 mM NaCl
	pH 8.0

Elution buffer

For elution of GST-tag	50 mM
	100 mM NaCl
	20 mM L-Glutathione reduced
	pH 8.5

For elution of 6x His-tag	50 mM NaH_2PO_4 or 50 mM Tris
	150 mM NaCl
	400 mM imidazole
	pH 8.0
For elution of Strep-tag	50 mM Tris-HCl, pH 8.0
	300 mM NaCl
	2.5 mM d-desthiobiotin
Washing buffer (Ni-NTA Matrix)	50 mM NaH_2PO_4
	150 mM NaCl
	20 mM imidazole
	pH 8.0

2.1.4 Media

All media were prepared in dd H_2O and autoclaved at 121°C for 10 min or sterile filtrated through 0.22 µm sterile filters (Millipore, Billerica, MA, United States).

LB medium	1% (w/v) tryptone
	0.5% (w/v) yeast extract
	0.5% (w/v) NaCl
	pH 7.0
	1.5% (w/v) agar for solid media
King´s B medium	2% (w/v) peptone
	0.15% (w/v) K_2HPO_4
	0.15% (w/v) Mg_2SO_4-$7H_2O$
	1.5% (w/v) agar for solid media
	pH 7.2
BHI medium	Bacto Brain Heart Infusion, Porcine, Difco (BD Diagnostics Franklin Lakes, USA) prepared according to the supplier´s instructions
TFB1	30 mM CH_3CO_2K
	100 mM RbCl
	10 mM $CaCl_2$
	50 mM $MnCl_2$
	15% glycerol
	pH 5.8 (adjusted with acetic acid), filter sterilized

TFB2	10 mM MOPS
	75 mM $CaCl_2$
	10 mM RbCl
	15% glycerol
	pH 6.5 (adjusted with KOH), filter sterilized
$^{(13C)15}$N-M9 minimal medium	33.7 mM Na_2HPO_4
	22 mM KH_2PO_4
	8.55 mM NaCl
	9.35 mM $^{15}NH_4Cl$
	0.4% (w/v) glucose (or ^{13}C glucose)
	1 mM $MgSO_4$
	0.3 mM $CuCl_2$
	1 µg biotin
	1 µg thiamine
	1x trace elements solution
100 x trace elements (for M9):	13.4 mM EDTA
	3.1 mM $FeCl_3$-$6H_2O$
	0.62 mM $ZnCl_2$
	76 µM $CuCl_2$-$2H_2O$
	42 µM $CoCl_2$-$2H_2O$
	162 µM H_3BO_3
	8.1 µM $MnCl_2$-$4H_2O$

2.1.5 Antibiotic stock solutions

Working concentrations were 1:1000 of stock solutions. Stock solutions were sterile filtered through 0.22 µm sterile filters (Millipore, Billerica, MA, United States) and stored as aliquots at -20°C.

Ampicillin (Amp)	100 mg/ml in water
Carbenicillin (Carb)	100 mg/ml in 20% (v/v) EtOH
Chloramphenicol (Cam)	35 mg/ml in EtOH
Kanamycin (Kan)	50 mg/ml in water
Erythromycin (Ery)	10 mg/ml in EtOH
Spectinomycin (Spec)	50 mg/ml in water

2.1.6 Plasmids

Name	Origin	AB resistance	description
pDONR221	Invitrogen, Karlsruhe, Germany	Kan	Gateway® cloning vector
pAGRO:T2SB:SP1.1cc	(Zeitler, 2011)	Amp/Carb	
pAGRO:T2SB-SP10-2	(Zeitler, 2011)	Amp/Carb	
pDest15	Invitrogen, Karlsruhe, Germany	Amp	Gateway® expression vector
pDest15:T2SB:SP1.1cc	this work	Amp/Carb	
pDest17	Invitrogen, Karlsruhe, Germany	Amp/Carb	Gateway® expression vector
pDest17:RsbW	this work	Amp/Carb	
pET-Dest42	Invitrogen, Karlsruhe, Germany	Amp/Carb	Gateway® expression vector
pET-Dest42:RsbW	this work	Amp/Carb	
pPR-IBA1	IBA GmbH, Göttingen, Germany	Amp	Strep-tagged bacterial expression vector
pPR-IBA:RsbW	[1]	Amp	
pPR-IBA:RsbV	[1]	Amp	
pPR-IBA:sigB	[1]	Amp	
pET-GB1a	[3]	Kan	6x His-tagged bacterial expression vector, GB1a fusion protein containing
pET-GB1a: SP1-1	this work	Kan	
pCDF11	[3]	Spec	N-terminal 6x His-tagged bacterial expression vector
pCDF13	[3]	Spec	bacterial expression vector
pCDF11:sigB	this work	Spec	
pCDF13:sigB	this work	Spec	
pGBKT7	(Clontech, Mountain View,CA, USA)	Kana	Y2H bait plasmid
pGADT7	(Clontech, Mountain View,CA, USA)	Amp	Y2H prey plasmid
pDONR/Zeo	Invitrogen	Kan	Gateway® cloning vector
pENTRY Zeo/ScaI	[2]	Kan	Entry vector designed for Gateway® cloning
pAD-Gate2	(Maier et al., 2008)	Amp	Gateway compatible Y2H prey vector
pBD-Gate2	(Maier et al., 2008)	Kan	Gateway compatible Y2H bait vector

[1] Institute of Microbiology, Ernst-Moritz-Arndt University of Greifswald (Greifswald, Germany)
[2] Department of Dermatology, Paracelsus Medical University Salzburg (Salzburg, Austria)
[3] Protein Expression and Purification Facility, Helmholtz Zentrum München (Munich, Germany)

2.1.7 Microorganisms

2.1.7.1 Bacterial Strains

Plant pathogens

Clavibacter michiganensis ssp. michiganensis (DSM 46294)
Pectobacterium carotovorum ssp. carotovorum (DSM 30168)
Pseudomonas corrugata (DSM 7228)
Pseudomonas syringae pv. syringae (DSM 10604)
Pseudomonas syringae pv. tomato (DSM 50315)
Xanthomonas vesicatoria (DSM 50861)

Human pathogens (*Staphylococcus aureus* strains and isolates)

Strain	**Methicillin resistance**	**Further AB resistances**	**Reference, Source**
S. aureus clinical isolate 90857	yes	penicillin, oxacillin, erythromycin, clindamycin, gentamycin, amikacin, ciprofloxacin, moxifloxacin	Max-von-Pettenkofer Institute, Munich, Germany
S. aureus COL	yes	n.d.	[1)], (Shafer and Iandolo, 1979)
S. aureus RN1HG (= *S. aureus* HG001)	no	-	[1)], (Herbert et al., 2010)
S. aureus RN1HG Δ*sigB* (deletion mutant)	no	Ery	[1)]
S. aureus RN1HG Δ*sigB* complemented (complemented deletion mutant)	no	Ery/Cam	[1)]
S. aureus Newman	no	n.d.	[2)], (Duthie, 1952)

[1)] Institute of Microbiology, Ernst-Moritz-Arndt University of Greifswald (Greifswald, Germany)
[2)] Department of Dermatology, Paracelsus Medical University Salzburg (Salzburg, Austria)
n.d.: not determined in the context of this study

E. coli strains for cloning and protein expression

Strain	**Resistance**	**Description / Usage**
E.coli TOP10		Electrocompetent cloning strain
E.coli DH5α		Chemically competent cloning strain
E.coli DB 3.1		Chemically competent cloning strain
E.coli BL21 (DE3) plysS	Cam	Chemically competent expression strain
E.coli BL21 Star (DE3) pRARE 2	Cam	Electrocompetent expression strain

Culture and growth conditions

E. coli cell cultures were grown in LB medium with appropriate antibiotics at 30 - 37°C. Phytopathogens were grown in LB medium or King´s B medium (*Pseudomonas sp.*) at 28 - 30°C. *S. aureus* strains were grown in BHI medium (Bacto Brain Heart Infusion, Porcine, Difco, BD Diagnostics Franklin Lakes, USA), or LB with appropriate antibiotics at 37°C. Liquid cultures were incubated with shaking (200 – 300 rpm).

2.1.7.2 Yeast strain

AH109 (MATα)	haploid yeast strain, Matchmaker™ Two-Hybrid System (Clontech, Mountain View, CA, USA)

Transformation, used media and buffers according to the manufacturer´s instructions.

2.1.7.3 Fungus

Botrytis cinerea

Grown on 2% malt extract agar at room temperature in the dark and transferred to light to induce sporulation.

2.1.8 Oligonucleotides

Name	Sequence
M13F_mediGX	5´- TGTAAAACGACGGCCAGT-3´
M13R2_mediGX	5´- GGAAACAGCTATGACCATG-3´
T7	5´- TAATACGACTCACTATAGGG-3´
SP1-1 sense	5´- ATGAGAAAGAAGAGACTTAAGCTTCTTAAGAGATTGCTTTGA -3´
SP1-1 antisense	5´- TCAAAGCAATCTCTTAAGAAGCTTAAGTCTCTTCTTTCTCAT -3´
SP10-2 sense	5´- ATGTTGAGGTTCCTTAAGAAGGCTCTTAAGAAGCTTTTCTGA -3´
SP10-2 antisense	5´- TCAGAAAAGCTTCTTAAGACCTTCTTAAGGAACCTCAACAT -3´
sigB_nco_F2	5´- AAGAAGGAGATATACCCATGGCGAAAGAGTCGAAATCAGCTAATGAA-3´
sigB_st_hind_R3	5´- CGGATCAAGCTTATTATTTTTCGAACTGCGGGTGGCTACAAGCGCTTTGAT-3
attb1_coatprot	5´- GGGGACAAGTTTGTACAAAAAAGCAGGCTTTTCTTACAGTATCACTACT-3´
attb2_coat_SP1-1	5´- GGGGACCACTTTGTACAAGAAAGCTGGGTTCAAAGCAATCTCTTAAG-3´
attB1_f	5´- GGGGACAAGTTTGTACAAAAAAGCAGGCT-3´
attB2_r	5´- GGGGACCACTTTGTACAAGAAAGCTGGGT-3´
SP1-1_pET_F	5´- CATGGGAATGCGCAAAAAACGCCTGAAACTGCTGAAACGCCTGCTGTAAGAGCT-3´
SP1-1_pET_R	5´- CTTACAGCAGGCGTTTCAGCAGTTTCAGGCGTTTTTTGCGCATTCC-3´

DNA-sequencing was performed by the value read service of Eurofins MWG Operon (Ebersberg, Germany).

2.1.9 Antibodies

antibody	Working concentration / dilution	origin
Primary antibodies		
Anti-SP mAb containing supernatants of hybridoma cells (description: see supplementary data, chapter 6.3)	1 : 20 – 1 : 100	Core Facility for Generation of Monoclonal Antibodies and Cell Sorting, Institute of Molecular Immunology, Helmholtz Zentrum München (München, Germany)
StrepMAB-Classic (2-1507-001)	0.1 µg/ml	IBA GmbH (Göttingen, Germany)
Anti-Histidine-tagged protein mouse mAb (OB05)	1 µg/ml	Calbiochem (Darmstadt, Germany)
Anti-Biotin-Alkaline Phosphatase mouse mAB	1 : 10 000	Sigma-Aldrich GmbH (Taufkirchen, Germany)
Secondary antibodies		
Anti-Rat IgG-AP (A8438)	1 : 30 000	Sigma-Aldrich GmbH (Taufkirchen, Germany)
Anti-Mouse-IgG AP (A5153)	1 : 10 000	Sigma-Aldrich GmbH (Taufkirchen, Germany)
Alexa-Fluor 546 goat anti-rat IgG	1 : 30 000	Invitogen (Karlsruhe, Germany)

2.1.10 Kits

Name	Company
Gateway® BP Clonase™ Enzyme Mix, No.11789-013	Invitrogen, Karlsruhe, Germany
Gateway® LR Clonase™ Enzyme Mix, No.11791-019	Invitrogen, Karlsruhe, Germany
MinElute® PCR Purification Kit, No. 28004	Qiagen GmbH, Hilden, Germany
QIAprep® Spin Miniprep Kit, No. 27104	Qiagen GmbH, Hilden, Germany
QIAquick® Gel Extraction Kit, No. 28704	Qiagen GmbH, Hilden, Germany
QIAquick® PCR Purification Kit, No. 28104	Qiagen GmbH, Hilden, Germany
GenElute™ HP Plasmid Maxiprep Kit	Sigma, St. Louis, MO, USA
Wizard® SV gel and PCR clean-up system	Promega, Madison, WI,USA

2.2 Methods

2.2.1 General molecular cloning techniques

2.2.1.1 Purification of PCR products and DNA reaction mixtures

If necessary for downstream experiments DNA products from PCR or after enzymatic cleavage were cleaned with the QIAquick PCR purification Kit, according to the manufacturer´s instructions (Qiagen, Hilden, Germany). The concentration of the DNA was analyzed by measuring the absorption at 260 nm and the purity by measuring the absorption at 280 nm and 230 nm, calculating the ratios of A_{260nm}/A_{230nm} and A_{260nm}/A_{280nm} with the Nanodrop ND-1000 spectrophotometer (NanoDrop Technologies, Wilmington, USA).

2.2.1.2 RNA extraction from bacteria cells

Total bacterial RNA extraction was carried out with the Qiagen RNeasy Mini Kit according to the manufacturer´s instructions (Qiagen, Hilden, Germany) after growing bacteria in liquid cultures and harvesting cells (5×10^8 cells per reaction) by centrifugation (3000 g, 4°C, 10 min).

2.2.1.3 Nucleic acid agarose gel electrophoresis

The separation of nucleic acids according to fragment size was done in 1% agarose gels in TAE buffer. After dissolving agarose in TAE buffer by cooking and cooling down to about 50°C, 0.05 µg/ml ethidium bromide was added and the gel was casted. Samples were mixed with 6x loading dye (MBI Fermentas, St Leon-Rot, Germany) to a final dye concentration of 1x and the gels were run at a voltage of 100 V. After separation, nucleic acids were visualized with UV light (302 nm) on a Benchtop 2UV™ Transilluminator and photographed with a UV PhotoDocIt™ Imaging System (UVP, LLC, Upland, CA, United States) equipped with a Canon PC1251 digital camera.

2.2.1.4 Extraction and purification of DNA from agarose gels

After agarose gel electrophoresis DNA bands were cut under UV light with a scalpel and transferred to a 2 ml reaction tube. The purification was done with the QIAquick Gel Extraction Kit according to the manufacturer´s instructions (Qiagen, Hilden, Germany). The concentration and purity of the DNA was analyzed with the Nanodrop ND-1000 spectrophotometer as described in 2.2.1.1.

2.2.1.5 Restriction enzyme cleavage

Cleavage of DNA molecules by restriction enzymes was performed with enzymes and corresponding buffers of MBI Fermentas (St Leon-Rot, Germany) or New England Biolabs

(Frankfurt am Main, Germany). The procedures for single and double reactions were performed according to the manufacturer´s recommendations.

2.2.1.6 Preparation of competent cells

For preparation of competent cells all solutions were used sterilized. Additionally, beginning with the harvesting of the cells, all solutions and containers were used ice-cold. Therefore the materials were prechilled before use.

Preparation of electrocompetent *E. coli*

Electrocompetent *E. coli* were prepared by a method modified from Sambrook and Russel (2001). A single colony from an LB agar plate was used to inoculate 30 ml LB and incubated oN at 37°C. With 10 ml of the oN culture 300 ml of LB were inoculated and grown at 37°C until the OD_{600nm} reached 0.4 - 0.5. The flask was then cooled for 20 min on ice with slight swirling. The cells were harvested by centrifugation at 3000 g for 20 min at 4°C. The cells were washed twice in dd H_2O and then twice in 10% (w/v) glycerol. Afterwards the cells were resuspended in 250 µl 10% (w/v) glycerol and the OD_{600nm} of a 1:100 dilution of the suspension was measured. The concentration of cells was adjusted to 2x 10^{10} cells/ml (1.0 OD_{600nm} = 2.5x 10^8 cells/ml) with 10% (v/v) glycerol and 40 µl aliquots were immediately frozen in liquid nitrogen and stored at -80°C.

Preparation of chemically competent *E. coli*

For preparation of chemically competent *E. coli* a single colony from a LB agar plate was used to inoculate 2.5 ml LB and incubated oN at 37°C. With the oN culture 250 ml of LB, (including 20 mM $MgSO_4$) were inoculated and grown at 37°C until the OD_{600nm} reached 0.4 - 0.6. The flask was then cooled on ice with slight swirling. The cells were harvested by centrifugation at 3000x g for 5 min at 4°C. The cells were then resuspended in 40% culture volume of TFB1 and incubated on ice for 5 min. The cells were again harvested by centrifugation, resuspended in 4% of original culture volume of TFB2 and incubated on ice for 15 - 60 min. 40 µl aliquots of the cell suspension were immediately frozen in liquid nitrogen and stored at -80°C.

2.2.1.7 Transformation of competent **E. coli**

Chemical Transformation

For transformation of competent bacteria by heat shock an aliquot of 40 µl competent *E. coli* cells was thawed on ice for 10 min and then mixed with 1 – 20 ng plasmid DNA or 0.5 – 2 µl of an enzymatic reaction mixture. The reaction mixture was incubated on ice for 30 min. Afterwards the cells were transformed by incubation at 42°C for 30 s with subsequent immediate cooling on ice. The cells were suspended in 1 ml LB media and

shaken (250 rpm) for one hour at 37°C. Then 20 – 200 µl were plated on LB plates with appropriate antibiotics. Single colonies were used for further experiments after incubation of the plates at 37°C oN.
For double transformation of *E. coli* BL 21(DE3) plys S with either pPRIBA1:RsbW and pCDF11:SigB or pPRIBA1:RsbW and pCDF13:SigB, the two used plasmids were mixed in equimolar ratio and 50, 70 or 100 ng of the plasmid mixture was mixed with the thawed cells and processed further as described above.

Transformation by Electroporation
For electroporation, an aliquot of electrocompetent *E. coli* cells was thawed on ice for 10 min, mixed with either 1 - 10 ng plasmid DNA or with 0.5 - 1 µl of an enzymatic reaction and transferred to a prechilled 1mm Gene Pulser cuvette (Bio-Rad, Munich, Germany). An electric pulse of 25 µF capacitance, 1.7 kV and 200 Ω resistance was applied. Afterwards, cells were immediately suspended in 1 ml LB medium and shaken (250 rpm) for one hour at 37°C. Then 20 – 200 µl were plated on LB plates with appropriate antibiotics. Single colonies were used for further experiments after incubation of the plates at 37°C oN.

2.2.1.8 Gateway® cloning

Unless otherwise indicated the Gateway® cloning reactions were performed according to the manufacturer´s instructions (Gateway® Technology with Clonase™ II, Invitrogen, Karlsruhe, Germany).

Polymerase Chain Reaction
Amplification of the gene of interest (GOI) was performed by standard PCR protocol with the following conditions:

20 ng template plasmid DNA
4 µl 5x phusion HF buffer
200 µM 10 mM dNTPs
0.5 µM forward primer
0.5 µM reverse primer
3% DMSO (p.a.)
0.2 µl phusion™ high fidelity DNA polymerase (Finnzymes, Keilaranta, Finland)
In a total reaction volume of 20 µl by addition of dd H_2O

The PCR was executed in a Hybaid PCR-Express thermocycler with the following programme:

Step	temperature	duration	cycles
1 Initial denaturation	98°C	30 s	1x
2 DNA amplification			
Denaturation	98°C	10 s	
Annealing	58 – 65°C	15 - 30 s	30x
Extension	72°C	20 s	
3 Final Extension	72°C	10 min	1 x
4 Holding temperature	4°C		

For the initial Gateway® PCR reaction the GOI was amplified with attb-recombination-sites introducing primers from the template plasmid.

Gateway® reactions

For ligation into the Gateway® donor vector pDONR221, the PCR product was subjected to a Gateway® BP reaction according to the instructions in the manufacturer´s handbook with the following variables. Plasmid and insert were used in an equimolar ratio.

100 ng (32 fmol) pDONR221 plasmid DNA
Equimolar amount of PCR product
2 µl 5x Clonase reaction buffer
Adjusted to a total reaction volume of 10 µl with TE buffer
2µl Clonase

The reaction mixture was incubated oN at 25°C, then 1 µl Proteinase K (2 µg/µl) was added and incubated 10 min at 37°. *E. coli* TOP10 or DH5α were transformed with 0.5 µl of the B/P reaction mixture, plated on LB agar plates (Kan). A single colony was used to inoculate 5 ml LB (Kan) and grown oN. The plasmid DNA from the oN culture was purified. The assembly of the insert was checked with restriction enzyme cleavage of 100 ng DNA, following separation of the DNA fragments on 1% agarose gel and sequencing the GOI and flanking regions with M13F_mediGX and M13R2_mediGX sequencing primers.
After ensuring the correct sequence, the plasmid pDONR221:x was subjected to the Gateway® L/R reaction for transferring the inserted region into the destination vector. The reaction was performed according to the manufacturer´s handbook (Gateway® Technology with Clonase ™ II, Invitrogen, Karlsruhe, Germany) and 0.5 µl was transformed into *E. coli* TOP10 or DH5α. A single colony was used to inoculate 5 ml LB (Carb) and after oN growth the plasmid DNA was purified. The sequence was checked

with T7 sequencing primer, and the plasmid was transformed into *E. coli* BL 21 for recombinant expression.

2.2.1.9 Recombinant protein and peptide production in E. coli *BL 21*

Recombinant protein production was carried out by inoculation of 10 ml LB medium with appropriate antibiotics with a single colony of *E. coli* BL 21. The culture was incubated oN at 37°C with shaking (200 rpm). The oN culture was used to inoculate LB medium to an OD_{600nm} of 0.05 - 0.1 which was further incubated at 37°C with shaking. After reaching an OD_{600nm} of 0.5, protein expression was induced by the addition of 1 mM IPTG and incubation at 30°C oN or 37°C for 2.5 – 18 h with 200 rpm shaking. The cells were harvested by centrifugation (3000x g, 30 min, 4°C) and the pellets were immediately frozen to -80°C.

2.2.2 Protein purification and analyses

2.2.2.1 Protein extraction from bacterial cultures

Cell lysis under native conditions was started by thawing bacterial cell pellets for 10 min on ice and subsequent resuspending in lysis buffer, following addition of 1 mg/ml of lysozyme. After incubation on ice for 30 min, 10 µg/ml RNAse A and 5 µg/ml DNAse I were added and cell disruption was further propagated by 6x 10 s bursts of ultra-sonication (step 5, 50% power) with 10 s cooling between each burst. After another 15 min of incubation on ice cell debris was removed by centrifugation (12 000x g, 30 min, 4°C) and the clear supernatant (crude extract of soluble proteins), was further used.
For protein extraction under denaturing conditions 4 M urea was added to the lysis buffer.

2.2.2.2 Determination of protein concentration

Determination of protein concentration was done with the Bradford Bio-Rad Protein Assay (Bio-Rad Laboratories GmbH, München, Germany) and carried out as suggested by the manufacturer.

2.2.2.3 Acetone precipitation of proteins

Proteins were precipitated by addition of 4 sample Vol of ice cold acetone p.a. and incubation for at least 3 h at -20°C. The precipitates were collected by centrifugation at 18000x g for 30 min at 4°C and the supernatant was discarded. The pellet was washed by addition of the same Vol of ice cold acetone and a second centrifugation step. After removing the supernatant the protein pellet was air dried at RT and resuspended in an appropriate amount of water or buffer.

2.2.2.4 Affinity chromatography by FPLC

The protein of interest was affinity purified from a crude bacterial protein extract using prepacked columns with either immobilized strep-tactin (strep-tactin superflow plus 1ml catrige, IBA, Göttingen, Germany), Ni-NTA matrix (Ni-NTA Superflow FF 1ml, GE Healthcare, Freiburg, Germany) or Glutathione matrix (GSTrap FF 1 ml GE Healthcare, Freiburg, Germany) with an ÄKTA Explorer 10 liquid chromatography system, including a Frac-901 fraction collector, operated by the UNICORN control software version 5.11, used according to the manufacturer´s instructions. Affinity chromatography was carried out at 16°C with a 0 – 100% gradient elution and the following method details:

Column equilibration volume: 10 CV
Monitoring wavelength: 215 nm, 280 nm
Emptying loop volume: 10 ml, followed by 5 CV column wash
Wash out flow rate: 0.5 ml/min
Gradient length (binding buffer to elution buffer): 20 CV

The strep-tactin column was regenerated after each purification cycle by washing with 5 CV of 0.5 M NaOH, 5 CV of H_2O and re-equilibrated by 5 CV binding buffer with a flow of 1 ml/min.

2.2.2.5 Affinity purification of 6x His-tagged proteins by Ni-NTA matrix

6x His-tagged peptide-fusion proteins were affinity purified using Ni-NTA agarose (Qiagen, Hillden, Germany). The matrix was equilibrated by addition of 2.5 Vol lysis buffer, gentle mixing, 1 min centrifugation at 100x g and discarding the supernatant. 600 µl of 50% Ni-NTA agarose slurry were used for 5 ml cleared cell lysate. Further purification steps were carried out according to the batch purification protocol of the manufacturer (the QIA*expressionist*^{TM} - A handbook for high-level expression and purification of 6x His-tagged proteins, 2003/06 pages 82 f.).

2.2.2.6 Size exclusion chromatography (SEC) by FPLC

Affinity purified protein solutions were applied to size exclusion chromatography (SEC) using a superdex 75 or superdex 200 column (GE Healthcare, Freiburg, Germany) by FPLC (see affinity chromatography). The concentrated protein sample was manually applied by a 200 µl sample loop and separated at 16°C in separation buffer (RsbW: 25 mM Tris, 150 mM NaCl, pH 8.0, recombinant, SP1-1: 5% acetonitrile, 150 mM NaCl, 10 mM HCl) with the following method details:

Column equilibration volume: 1 CV
Monitoring wavelength: 215 nm, 280 nm
Emtying loop volume: 400 µl
Flow rate: 1 ml/min

The column was washed with 50 ml of H_2O and 20% EtOH with a flow of 0.5 ml/min after each run, and equilibrated with 50 ml H_2O and separation buffer before each use.

2.2.2.7 Reversed Phase Chromatography (RPC) by FPLC

RPC was performed according to the protocol of Zeitler (2011). SEC fractions were dried under vacuum and resuspended in 5% acetonitrile, 10 mM HCl. The separation was performed with a 1 ml in-house packed RPC column with C8-substituted silica based matrix with 10 µm particle size (*LiChrosorb RP-8,* Merck, Darmstadt, Germany) by FPLC (see affinity chromatography). The samples were injected in a 1 ml sample loop and separated using a gradient elution (5% acetonitrile, 0.01 M HCl – 80% acetonitrile, 0.01 M HCl) at RT with the following details:

Flow rate: 1 ml/min
Monitoring wavelength: 215 nm, 280 nm
Emptying loop volume: 8 ml, followed by 4 CV column wash
Gradient length: 20 CV
1 ml fractions were collected, dried again and checked for correct size and purity on Tricine-SDS-PAGE.

2.2.2.8 Polyacrylamid gel electrophoresis of proteins

Separation of proteins on polyacrylamid gels was carried out with a Hoefer SE 250 Mini-Vertical Gel Electrophoresis unit (GE Healthcare, Freiburg, Germany). The gels were casted in an 8 x 7 x 1 cm Hoefer Mighty Small dual gel caster (GE Healthcare, Freiburg, Germany) according to the manufacturer´s handbook. Gels for native and glycine SDS-PAGE were run at a constant current of 25 mA per gel with an Electrophoresis Power Supply EPS 601 (GE Healthcare, Freiburg, Germany). All gels were run until the bromophenol dye front reached the bottom of the gel.

A – SDS-PAGE

Proteins were separated according to their molecular weight with 12% or 15% resolving gels and 4% glycine-SDS-polyacrylamide-stacking-gels. Gels were prepared as described by Sambrook and Russell (2001) according to Laemmli (1970). Protein extracts were mixed 1:1 with 2x reducing sample buffer, heated 5 min (95°C) and loaded into the gel pockets. Bacterial cell pellets were dissolved in 1/10 – 1/20 Vol (of culture volume) in 2x

reducing sample buffer, heated 10 min at 95°C, centrifuged 15 min at 13200 rpm at RT and 1/5 - 1/10 Vol of the supernatant was loaded into the gel pockets.

B - Tricine-SDS-PAGE

Proteins and peptides with a mass of < 10 kDa, were separated by Tricine-SDS-PAGE with buffers and preparation of gels according to Schägger (2006). Samples were mixed with 4x sample buffer to a final concentration of 1x, incubated 30 min at 37°C and shortly centrifuged. Then a maximum of 5 - 10 µl of sample was loaded per well. Gels were run at an initial voltage of 30 V till the samples entered the resolving gel. The voltage was increased to 120 V and the gel was further run until the samples reached the middle of the resolving gel. For the remaining gel run 130 V were applied. The run was performed at 4 - 6°C in a cold room. Proteins were fixed by 30 min of incubation in fixing solution.

C - Native PAGE

Proteins were separated under non-denaturing conditions with 15% resolving and 4% stacking gels. Gels were prepared as described by Sambrock and Russel (2001), (according to Laemmli, 1970) without the addition of SDS or ß-mercaptoethanol to any buffer. Samples were mixed with 4x non-denaturing sample buffer to a final concentration of 1x, incubated on ice until the run and then applied to the gel pockets.

D - Staining of proteins after PAGE separation

Native and SDS-PAGE gels were stained by incubation and shaking in Coomassie R-250 staining solution for 1 h followed by destaining in Coomassie R-250 destaining solution until the background became completely clear. For Tricine-SDS-PAGE Coomassie G-250 staining solution and Coomassie G-250 destaining solution were used in the same way.

2.2.2.9 Protein transfer on membranes by Western- or Dot-Blotting and immunodetection

Proteins were transferred from polyacrylamide gels to Hybond-LFP PVDF membranes with 0.2 µm pore size (GE Healthcare, Freiburg, Germany) by semi dry western blotting with a Hoefer SemiPhor semi-dry transfer unit (GE Healthcare, Freiburg, Germany). The membrane was activated by short incubation in methanol, following water and finally transfer buffer. A blotting sandwich consisting of 3 sheets of blotting paper, wetted with transfer buffer, the activated membrane, the polyacrylamide gel and again 3 sheets of wetted blotting paper was assembled. Protein transfer was performed by application of 1.5 mA current per cm^2 of gel/membrane area for 1 h. The membrane was removed from the blot and shortly rinsed in TBS buffer. If necessary, proteins were stained for 15 min with Ponceau-S and destained by three washing steps of 10 min in water. The membrane

was blocked for 1 h by shaking in blocking buffer and subsequently 2 x 10 min washed in TBS-T. The appropriate first Ab, reactive against specific epitopes or tags was applied for 1 h, followed by three times 10 min of washing in TBS-T. If unlabeled first Ab was used, a secondary labeled IgG, species specific for the first Ab was then applied for 1 h and again unbound Ab was removed by three washing steps in TBS-T and one in TBS buffer. When fluorescent labeled Ab was used the membrane was dried in the dark and the fluorescent stain of protein was visualized with a Typhoon Trio+, Variable Mode Imager (GE Healthcare, Freiburg, Germany) at the appropriate wavelength. When alkaline phosphatase (AP) coupled Ab was used, the precipitate of the forming AP product was detected after application of 33 µl BCIP and 33 µl NBT solution in 10 ml AP buffer.

For dot blotting, peptide or protein samples in a volume of 2 - 5 µl were dropped on Hybond-LFP PVDF membranes with 0.2 µm pore size (GE Healthcare, Freiburg, Germany), activated and wetted in transfer buffer. The membrane was air dried. Small molecules were fixed to prevent their elution during washing steps by 1 x 5 min and 1x 10 min rinsing in TBS (1% glutaraldehyde), 5 min rinsing in TBS (50 mM glycine) and washing with TBS. After the fixation the membrane was blocked and further processed as described for western-blotted samples.

2.2.3 Molecular cloning and recombinant protein expression of RsbW, RsbV, and SigB

2.2.3.1 Gateway® cloning of RsbW and expression from plasmids pDest17 and pET-Dest42

The gateway® cloning of RsbW from the template plasmid pAD-Gate2, that included the RsbW ORF was carried out as described in chapter 2.2.1.8, with the following details.
For the initial PCR 5 ng of template DNA were used to amplify RsbW with primers attb1_f and attb2_r and the annealing step was carried out at 56°C for 15 s.
For B/P reaction 10 ng (32 fmol) of the 420 bp PCR product were used.
After the B/P reaction the assembly of the insert was checked by restriction enzyme cleavage with AvrII, following separation of the DNA fragments on 1% agarose gels and sequencing the region of interest. The obtained sequences were compared with *rsbW* Gene-ID: 2861460 from *S. aureus* MRSA 252 (http://www.ncbi.nlm.nih.gov/gene?term=rsbw%20mrsa252), as the Y2H screen was established with the genomic sequences of *S. aureus* Mu50 but the translated protein from the ORF of the prey plasmid was changed in one amino acid due to a mutation and the DNA sequence thus corresponded exactly to RsbW sequence of MRSA252.
By L/R reaction the ROI was ligated into expression vectors pDest17 and pET-Dest42 and generated plasmids pDest17:RsbW and pET-Dest42:RsbW were transformed into *E. coli* BL 21 (De3) plys S.

RsbW was recombinantly expressed as described in 2.2.1.9, by growing the bacterial culture at 37°C for 5 h or at 30°C oN. Protein was extracted and 6x His-tagged protein was purified by affinity chromatography. To achieve this protease inhibitor cocktail in a final concentration of 1x (complete, EDTA free Protease Inhibitor Cocktail tablets/ Roche Diagnostics GmbH, Mannheim Germany) was added to the samples. Aliquots were analyzed by SDS-PAGE as described in chapter 2.2.2., and samples were used for further experiments.

2.2.3.2 Transformation and recombinant protein expression of RsbW, RsbV, SigB from plasmid pPR-IBA1

RsbW, RsbV and SigB, cloned into the BSAI restriction site in plasmid pPR-IBA1 (kindly provided by Dr. J. Pané-Farré, Institute of Microbiology, Ernst-Moritz-Arndt-University of Greifswald, Greifswald, Germany) were transformed, expressed and purified by a modified method of Pané-Farré et al. (2009). The plasmid was transformed into expression strain *E. coli* BL 21 (DE3) plys S and a single colony was used to inoculate LB medium (Cam, Amp) and grown oN. With the oN culture fresh medium was inoculated to an OD_{600nm} of 0.05 and grown at 37°C. After reaching an OD_{600nm} of 0.5, protein expression was induced by addition of 1 mM IPTG. After further 2.5 h of growth at 37°C and 200 rpm shaking the cells were harvested by centrifugation (3000x g, 30 min, 4°C) and the pellets were immediately frozen to -80°C for later purification steps described in chapters 2.2.2.3 to 2.2.2.6.

2.2.4 Cloning and recombinant protein expression of peptide SP1-1

2.2.4.1 Gateway® cloning of SP1-1 and expression from plasmids pDest15 and pET-Dest42

Gateway reactions were carried out, as described in chapter 2.2.1.8, with the following details.

For the initial PCR 20 ng plasmid pAGRO:T2SP:SP1.1cc (Zeitler, 2011) was used as template to amplify SP1-1 with CNBr cleavage site, charge compensation and attb-recombination-sites with primers attb1_coatprot and attb2_coat_SP1-1. The annealing step was carried out at 60°C for 30 s.

For B/P reaction 12 ng (32 fmol) of the 580 bp PCR product were used.

After the B/P reaction the assembly of the insert in pDONR221:T2SP:SP1.1cc was checked by restriction enzyme cleavage with ApaLI, following separation of the DNA fragments on 1% agarose gels and sequencing with M13F_mediGX and M13R2_mediGX oligonucleotides. By L/R reaction the ROI was ligated into the expression vector pDest15 and the derived pDest15:T2SP:SP1.1cc was transformed into *E. coli* BL 21 Star (DE3) RARE 2. SP1-1 was recombinantly expressed as described in 2.2.1.9, by growing the

bacterial culture at 30°C oN. Protein was extracted, the GST-tagged proteins purified by affinity chromatography and analyzed by SDS-PAGE as described in chapter 2.2.2.

2.2.4.2 Cloning of SP1-1 and expression from plasmids pET-GB1a, pET-Trx1a, pET-Z2a

To increase the amount of produced SP1-1 the plasmids pET-GB1a, pET-Trx1a and pET-Z21a (kindly provided by Dr. A. Geerlof, Protein Expression and Purification Facility, Helmholtz Zentrum München, Munich, Germany) were used as expression vectors. Primers encoding the sequence of SP1-1, stop codon, restriction sites for enzymes NcoI and SacI and CNBr cleavage site, with codons optimized for *E. coli* were used.
The plasmids were restriction digested with NcoI and SacI oN, separated by 1% agarose gel electrophoresis and the linear vector band at 5.5 kb was cut off and purified from the gel as described in chapter 2.2.1.4. Forward and reverse primers for SP1-1 were annealed to a double stranded construct by heating to 95°C and slow cooling in a Hybaid PCR-Express thermocycler with the following programme details:

Step	temperature
1	25°C 2 min
2	ramp step: 25°C to 95°C ramp rate: 0.1°C/s
3	95°C 10 min
4	ramp step: 95°C to 4°C ramp rate: 0.1°C/s (with 30 s incubation steps at: 85, 75, 65, 55, 45, 35, 25, 15°C)
5	4°C hold

Ligation of the double stranded oligonucleotide-fragments and the plasmid-fragment was performed with 90 ng of linearized plasmid DNA (25 fmol) with a molar ratio of plasmid to insert of 1:3 or 1:5, with T4 ligase (MBI Fermentas, St Leon-Rot, Germany) according to the manufacturer´s instructions at 16°C oN.
The DNA was transformed into *E. coli* DH5α which was then plated on LB agar plates (Amp). The positively transformed clones were used to inoculate 5 ml of the same medium and after oN growth at 37°C plasmid DNA was extracted.
The sequence was checked by sequencing with T7 sequencing primers. 6x His-tagged plasmids with correct sequences were chemically transformed into *E. coli* BL 21 (DE3) plys S and submitted to recombinant protein expression as described in chapter 2.2.1.9. Protein was extracted (chapter 2.2.2.1), affinity purified using a Ni-NTA matrix (chapter 2.2.2.5) and samples were acetone precipitated (chapter 2.2.2.3).

Reduction of oxidized methionine residues (according to Zeitler, 2011)
Acetone precipitated samples were resuspended in 1 ml 200 mM NH_4HCO_3, 5% ß-mercaptoethanol, blanked with argon and incubated oN at RT with inverting. The reduced protein was dried under vacuum in a speedvac evaporator with heating.

Chemical cleavage of SP1-1 from the fusion partner (according to Zeitler, 2011)
The dried samples were dissolved in 800 µl 88% (v/v) formic acid and 200 µl 5 M CNBr in acetonitrile (final concentration of formic acid: 70%). The samples were immediately mixed by vortexing. The samples were overlaid with argon, covered by aluminium foil and incubated 24 h in the dark. Samples were dried under vacuum in a speedvac evaporator, resuspended in 500 µl H_2O and stored at -20°C until further purification steps.
After cleavage peptide samples were further purified by SEC and RPC (chapters 2.2.2.6 and 2.2.2.7) separation and analyzed by Tricine-SDS-PAGE (chapter 2.2.2.8B)

2.2.5 Sub-cloning and recombinant protein expression of SigB

For co-expression with RsbW in plasmid pPR-IBA1:RsbW, *sigB* was sub-cloned from pPRIBA1:SigB into a plasmid with a different origin of recombination. Plasmids pCDF11 (N-terminal His tag) and pCDF13 (kindly provided by Dr. A. Geerlof, Protein Expression and Purification Facility, Helmholtz Zentrum München, Munich, Germany) were used. The plasmids were restriction digested with NcoI and HindIII at 37°C oN, separated by 1% agarose gel electrophoresis. The linear vector band at 3.5 kb was cut off and purified from the gel as described in 2.2.1.4.
SigB was amplified by PCR with primers sigB_nco_F2 and sigB_st_hind_R3 (including stop codon, 5´-restriction site for NcoI and 3´-restriction site for HindIII) from plasmid pPR-IBA1:SigB, sequenced with T7 sequencing primers and checked for sequence homology with *sigB* from http://www.ncbi.nlm.nih.gov/nuccore/Y09929.1.
The PCR was carried out as described in chapter 2.2.1.8, with the following modifications:

PCR reaction mixture modifications:
Template: pPRIBA1:SigB
Forward primer: sigB_nco_F2
Reverse primer: sigB_st_hind_R3

PCR programme modifications:
Annealing cycles: 65 °C, 15 s
Extension cycles: 25 s

The PCR product was purified, restriction enzyme cleavage was performed with NcoI and HindIII at 37°C oN and again purified. The digested DNA fragment was de-phosphorylated with calf intestine phosphatase CIP (MBI Fermentas, St Leon-Rot, Germany) according to the manufacturer´s instructions at 37°C for 4 h and again purified. Ligation of the *sigB* insert into pCDF11 or pCDF13 plasmid-fragments (828 bp) was performed with 90 ng of linearized plasmid DNA (38 fmol) with a molar ratio of plasmid: insert of 1:3 (61 ng *sigB* insert) or 1:5 (100 ng *sigB* insert), with T4 ligase (MBI Fermentas, St Leon-Rot, Germany) according to the manufacturer´s instructions at 16°C oN. The DNA was transformed into *E. coli* DH5α by heat shock and plated on LB agar plates (Spec). The positively transformed clones were used to inoculate a 5 ml oN culture in the same medium and after oN growth at 37°C plasmid DNA was extracted.
The sequence was checked by sequencing with T7 sequencing primers. Plasmids with correct sequences were transformed into *E. coli* BL 21 (DE3) plys S and submitted to recombinant protein expression.

2.2.6 Antibacterial activity test

The *in vitro* test for antibacterial activity of the synthetic peptides was performed by a modified microbroth dilution assay of the Clinical and Laboratory Standards Institute (CLSI/NCCLS). The assays were performed in sterile flat bottom 96-well plates (Greiner-bio-one, Frickenhausen). Dilutions of peptides (10 fold concentration of final assay concentration) were prepared in peptide buffer (0.2% BSA, 0.01% acetic acid) and 10 µl of each dilution step were loaded per well.
Bacteria from fresh agar plates were collected with an inoculation loop and suspended in BHI (*S. aureus* 90857) or LB liquid medium in an OD_{600nm} of 0.08 – 0.1. When *S. aureus* mutant strains were used, they were grown in appropriate antibiotics (*S. aureus* RN1HG *ΔsigB*: Ery, *S. aureus* RN1HG *ΔsigB* complemented: Ery/Cam). The suspension was diluted to 1.1 x 10^6 cfu/ml in the same medium. 90 µl of this bacterial suspension were loaded into each well to achieve 10^5 cfu/well (final peptide concentration was: 0.1, 0.5, 1, 2.5, 5, 10, 20, 40, 100 µg/ml). 10 µl peptide buffer without peptide addition served as control. After incubation at 28°C for 1 - 2 days (plant pathogenic bacteria) or 37 °C 18 – 24 h (*S. aureus*), OD_{600nm} was determined with a Tecan Genios microplate reader (Tecan, Crailsheim, Germany). Minimal inhibitory concentrations (MIC), defined as the lowest concentration (µg/ml) of the AMP that prevents visible growth (Wiegand et al., 2008) after 18h and minimal bactericidal concentrations (MBC), defined as the concentration of AMP where at least 99.9% of the initial inoculum were killed (Barry et al., 1999), were determined after 24 h. For every peptide the test was performed in duplicates.

2.2.7 Hemolytic activity of synthetic peptides

The ability of the peptides to lyse red blood cells was determined by release of hemoglobin from human erythrocytes after incubation with peptides. Dilutions of peptides (10 fold concentration of final assay concentration) were prepared in peptide buffer (0.2% BSA, 0.01% acetic acid) and 10 µl of each dilution step was loaded per well. Fresh human erythrocytes (Deutscher Blutspendedienst, München, Germany) were washed three times with 10 mM Tris, 150 mM NaCl, pH 7.4, with centrifugation (1500x g, 5 min, 20°C) before each washing step. 1.5 x 10^9 cells in 90 µl volume were added to peptide dilutions in 96-well plates. Final peptide concentrations were 0, 0.1, 0.5, 1, 2.5, 5, 10, 20, 40, 100 and 200 µg/ml. The reactions were then incubated for 45 min at 37°C. Afterwards, the suspensions were centrifuged, 30 µl of the supernatants were added to 100 µl of water and hemoglobin release was determined by measurement of the OD_{405nm}. 2% SDS served as a control for 100% cell lysis.

2.2.8 Analyses of peptide – membrane interactions

To investigate the peptides' ability to interfere with bacterial membranes, different model systems for bacterial membranes were tested for their behavior in the presence of the synthetic AMPs.

2.2.8.1 Pore forming ability at artificial membranes

For building artificial membranes, Teflon chambers were used with two aqueous compartments connected by small circular holes (diameter 0.5mm). Black lipid bilayers were formed by painting a 1% (w/v) solution of di-phytanoyl–phosphatidylcholine (DiPhPC) or a mixture of di-phytanoyl-phosphatidylcholine/di-phytanoyl-phosphatidylserine (DiPhPC/PS) in a molar ratio of 4:1 in n-decane, across the holes. The aqueous solutions, containing 0.15 M or 1 M KCl, were buffered with 10 mM HEPES to pH 7. After blackening of membranes, 0.1 – 10 µg/ml peptides were added to the *cis*-side and increasing positive and negative voltages (+/-20 to +/-300mV) were applied. Membrane conductance was measured as resulting current with a pair of Ag/AgCl electrodes with salt bridges switched in series with a voltage source and a highly sensitive current amplifier. Current was boosted 10^9 - 10^{10} fold, monitored on an oscilloscope and recorded on a strip chart recorder. The single-channel instrumentation had a time resolution of 1 – 10 msec, depending on the magnitude of the single-channel conductance. The voltage polarity was defined in respect to the side where AMP was added (*cis*-side).

2.2.8.2 Phospholipid micelle disruption

The peptides´ ability to disrupt phospholipid micelles was tested by a method developed by Kolusheva et al. (2000a; 2000b). Phospholipid-polydiacetylene (PDA) vesicles were built of 1,2,-dimyristoylphosphatidylcholine (DMPC), or 1,2,-dimyristoylphosphatidylglycerol (DMPG) that were suspended in chloroform : isopropanol : water (10 : 2 : 0.2) and mixed in a molar ratio of 2 : 3 with trycosadiynoic-acid to a final lipid concentration of 100 mM. Lipids were dried together under vacuum, resuspended in water to a concentration of 10 mM and ultrasonicated for 10 min at 70°C. After slow cooling the lipid suspension was kept at 4°C overnight and the PDA backbone was polymerized with UV-light (254 nm, 500 µJ/cm^2, 5 min). The solution was diluted to a concentration of 1 mM in 2 mM Tris (pH 8.5) in 96 well plates. Different peptide concentrations (0.1 – 100 µg/ml) were added in a total volume of 100 µl/assay and incubated with the lipids for 5 min. The shift of the absorption maximum from 620 nm to 490 nm was measured with a Tecan Safire2 plate reader (Tecan, Crailsheim, Germany). The percentage of colorimetric reaction (%CR) for every sample was calculated as follows:

$$\%CR = [(PB_0 - PB_I)/PB_0] \times 100$$

with

$$PB = A_{620nm}/(A_{620nm}+A_{490nm}) \times 100$$

PB_0 is the absorbance of the control sample (micelles only treated with buffer) and PB_I is absorbance of a distinct treated sample after addition of peptide. The %CR after peptide addition was compared to that of 1% SDS or that after protegrin 1 treatment.

2.2.8.3 Bacterial membrane potential measurements

The peptide´s potential to depolarize bacterial membranes was determined by a method of Friedrich et al. (2001). Bacteria (*P. syringae pv. syringae* or *Clavibacter michiganensis ssp. michiganensis*) were grown oN, diluted to a OD_{600nm} of 0.01 and grown at 30°C to the mid-logarithmic phase (OD_{600nm}: 0.4 – 0.5). Cells were harvested by centrifugation (3000x g, 4°C, 10 min). They were washed twice with 5 mM HEPES, pH 7.2, diluted to an OD_{600nm} of 0.05 in the same buffer with additional 0.1 M KCl, and incubated for 10 min at 30°C to equilibrate the outer and inner side of the membrane. The membrane potential sensitive dye 3,3'-dipropylthiadicarbocyanine iodide ($DiSC_3(5)$) was added to a final concentration of 0.4 µM and the cells were incubated for further 30 min until the reduction in fluorescence was stable (about 90%). 0, 0.5, 1, 10, 50 or 100 µg/ml of peptides, in peptide buffer (0.2% BSA, 0.01% acetic acid), were added in a total volume of 100 µl. Changes in the membrane potential were measured by the detection of the dye at an excitation wavelength of 622 nm and an emission wavelength of 670 nm for 2 h after peptide addition with a Tecan Safire 2 microplate reader (Tecan, Crailsheim, Germany). As controls, 1% SDS, for cell lysis, and the pore forming antimicrobial peptide

indolicidin were used. To test at which concentration the peptides under consideration show antimicrobial activity for the used amount of cells 10 µl aliquots were plated on LB plates after 0, 10, 30 and 60 minutes after peptide addition, incubated oN and checked for growth.

2.2.9 Localization experiments

2.2.9.1 Fluorescence microscopy

Bacterial cells from mid-logarithmic phase in LB medium, were harvested by centrifugation, resuspended in LB and used in a concentration of 10^8 cfu/ml. Fungi were grown on 2% malt-agar plates at RT in the dark. Sporulation was induced by incubation of the plates for 3 - 4 days in the light and spores were collected by wiping a sterile plate loop over the fungus, rinsing the plate with water to remove the spores and collecting the spore containing water. They were used in a concentration of 10^6 spores/ml.

Antimicrobial peptides, labeled with the two different fluorescent dyes 5(6)-carboxyfluoresceine (FAM, λ_{ex}: 494nm, λ_{em}: 519nm) and 5(6)-carboxy-tetramethyl-rodamine (TAMRA, λ_{ex}: 541nm, λ_{em}: 565nm) were incubated at a concentration of 25 or 100 µg/ml with the bacterial cells or the fungal spores in a volume of 200 µl for 1 to 3 hours in the dark. The cells were harvested by centrifugation, washed three times with PBS (bacteria) or water (spores) and resuspended in 1/10 Vol of media or water. Laser scanning confocal microscopy was carried out with a Zeiss laser scanning microscope (LSM) 510 Meta (Carl Zeiss AG, Jena, Germany). Images were processed with the Zeiss LSM Image Browser software, Version 4,2,0,121 (Carl Zeiss AG, Jena, Germany).

2.2.9.2 NanoSIMS experiments

S. aureus 90857 was grown in BHI medium oN and diluted to an amount of 4 x 10^6 cfu. The cells were incubated with 100 µg/ml ^{15}N-SP1-1 in peptide buffer or the same volume of only peptide buffer (mock) in a total volume of 4 ml. Usage of sub-lethal SP1-1 concentrations was made sure for the used amount of cells by plating of 10 µl aliquots, 1:10 and 1:100 dilutions of the reaction mixtures after incubation times of 10 or 30 min peptide treatment and checking for growth after 18 h at 37°C. Fixing and filter preparation was carried out following a protocol of Musat et al. (2008) with slight modifications. After 10 and 30 min cells were harvested by centrifugation at 3000x g, 10 min, 4°C, and the pellet was resuspended in 6 ml PBS (1% paraformaldehyde) for fixation. The mixture was fixed by incubation oN at 4°C and cells were pelleted again at 3000x g, 10 min, 4°C and washed three times with PBS. Finally, the sample was resuspended in 100 µl a mixture of PBS and glycerol (1:1; v/v) and filtered on polycarbonate filters (GTTP type, pore-size 0.22 µm, diameter, 13 mm, Millipore), sputtered for 5 min (~ 40 nm layer) with gold (80%) and palladium (20%). Filtering was

done by using a dot blotter with dot diameter of 3 mm (Carl Roth GmbH & Co. KG, Karlsruhe, Germany) by application of vacuum. The samples were air dried and fixed with copper adhesive foil on aluminium stacks for electron-microscopy and kept at -20 °C until further processing. Samples were analyzed by NanoSIMS 50L (Cameca, Gennevilliers cedex, France) by the NanoSIMS facility at the Chair of Soil Science, Department Ecology and Ecosystem Management of the Center of Life and Food Sciences Weihenstephan (TU München, Munich, Germany). Around 60-Z directed cycles of ion beam sections with secondary ion mass spectra of secondary ^{12}C, ^{13}C, ^{16}O and ^{32}S ions $^{12}C^{14}N$ $^{12}C^{15}N$ and the images of all measured secondary electrons, generated by primary Cs^+ ion, were recorded. Image analysis was done with WinImage (Cameca, Gennevilliers Cedex, France) by accumulation and drift correction of signal count images of relevant cycles.

2.2.10 Analyses of intracellular peptide targets

2.2.10.1 Nucleic acid binding of AMPs

For extraction of total bacterial RNA mid-logarithmic growing cells of *Clavibacter michiganensis ssp. michiganensis* were used. Extraction of the RNA was performed with the Qiagen RNeasy Mini Kit (Qiagen, Hilden, Germany) as described under 2.2.1.2. The used DNA fragment, with a size of 2.5 kb was prepared from a bacterial plasmid pDONR221, cultivated in *E. coli* DB 3.1 and extracted with the QIAprep® Spin Miniprep Kit (Qiagen, Hilden Germany). The fragment was amplified by PCR and reaction was carried out as described in chapter 2.2.1.8, with the following modifications:

PCR reaction mixture modifications:
Template: pDONR221
Forward primer: M13F_mediGX
Reverse primer: M13R2_mediGX

PCR programme modifications:
Annealing cycles: 58°C, 30 s
Extension cycles: 2 min

Gel retardation experiments were performed by a method of Park et al. (1998) with minor modifications. 100 ng of bacterial plasmid DNA (2.5 kB fragment of pDONR221 vector) or 1 µg of total bacterial RNA were mixed with peptides, resulting in peptide:nucleic acid ratios (w/w) of 0.1 – 4.0, in 10 µl of binding buffer (5% glycerol, 10 mM Tris-HCl (pH 8.0), 1 mM EDTA, 1 mM DTT, 20 mM KCl and 50 µg/ml BSA). The reaction mixtures were incubated at room temperature for 1 h. Subsequently, 2 µl of 6 fold-DNA-loading buffer (MBI Fermentas, St. Leon-Rot, Germany) were added and the samples were applied to 1% non-denaturing agarose-gel electrophoresis.

2.2.10.2 Microarray analysis

Gene expression studies of *S. aureus* COL (kindly provided by Dr. J. Pané-Farré, Ernst-Moritz-Arndt University of Greifswald, Greifswald, Germany) after treatment of SP1-1 were performed. RNA extraction and microarray design and analysis (2.2.10.2B - D) were carried out at the University of Geneva Hospitals, Genomic Research Laboratory, Service of Infectious Diseases, in the research group of Prof. Jaques Schrenzel.

A - Growth conditions and peptide treatment

The experiment was performed based on a protocol of Pietiäinen et al. (2009) with modifications. *S. aureus* COL from an oN culture in BHI medium was diluted to an OD_{600nm} of 0.05. The bacteria were grown at 37°C to the exponential phase (OD_{600nm}: 0.6) and 1.8 ml cultures were either treated with 200 µl of SP1-1 in a sub-lethal concentration of 4 µg/ 10^6 cfu (400 µg/ml) in peptide buffer or the same amount of buffer (mock). Cells were grown for further 10 min and harvested by centrifugation (10 min, 4000x g, 4°C). Cell pellets were resuspended in 500 µl acetone:ethanol (1:1; v/v) and stored at -80°C until RNA purification.

Sub-lethal concentrations were determined by growth curve experiments with measurement of OD_{600nm} values 5, 10, 30, 60 and 120 min after SP1-1 or buffer treatment at an OD_{600nm} of 0.6. 200 µl culture volume and peptide concentrations of 0, 1, 2, 4 µg/ 10^6 cfu were used.

B - Microarray design and manufacturing

The microarray was manufactured by in situ synthesis of 10807 60-mer long oligonucleotide probes (Agilent, Palo Alto, CA, USA), selected as previously described (Charbonnier et al., 2005). These covered >95% of all ORFs annotated in strains N315 and Mu50 (Kuroda et al., 2001), MW2 (Baba et al., 2002) and COL (Gill et al., 2005), NCTC8325 (Gillaspy et al., 2007), USA300 (Diep et al., 2006), MRSA252 an MSSA476 (Holden et al., 2004), and Newman (Baba et al., 2008) including their respective plasmids. Experimental validation of the array was done, using CGH, mapping of deletion, specific PCR and quantitative RT-PCR (Charbonnier et al., 2005; Koessler et al., 2006).

C - RNA extraction and expression microarray analysis

Total RNA was extracted as previously described (Renzoni et al., 2006; Scherl et al., 2006). DNA-free total RNA was obtained after DNase treatment using RNeasy columns (Qiagen, Hilden, Germany). The absence of DNA traces was checked by quantitative PCR (Mx 3005, Agilent) with assays specific for 16S rRNA (Renzoni et al., 2006; Scherl et al., 2006). Batches of 5 µg total *S. aureus* RNA were labeled by Cy-3 using SuperScript II (Invitrogen, Basel, Switzerland) following the manufacturer's instructions. Purified

genomic DNA from the reference sequenced strains used for the design of the microarray was labeled with Cy-5 dCTP (Charbonnier et al., 2005) and used in microarray normalization (Talaat et al., 2002). Mixtures of Cy-5-labeled DNA and Cy3-labeled cDNA were further processed as described by Scherl et al. (2006). Labeled products were purified by QiaQuick columns (Qiagen, Hilden, Germany). A mixture of them was diluted in 50 µl Agilent hybridization buffer, and hybridized at a temperature of 60°C for 17 h in a hybridization oven (Robbins Scientific, Sunnyvale, CA, USA). Slides were washed with Agilent proprietary buffers, dried under nitrogen flow, and scanned (Agilent, Palo Alto, CA, USA) using 100% PMT power for both wavelengths.

D - Microarray data analysis

Fluorescence intensities were extracted using the Feature extraction™ software (Agilent, version 8). Local background-subtracted signals were corrected for unequal dye incorporation or unequal load of labeled product. Using a rank consistency filter and a curve fitting algorithm per the default LOWESS (locally weighted linear regression) method. Data from three independent biological experiments were analyzed using GeneSpring 8.0 (Silicon Genetics, Redwood City, CA, USA) as previously described (Scherl et al., 2006) with a 5% *P* value (cutoff, 0.05) and an arbitrary threshold of 3-fold for defining significant differences in expression ratios of peptide-treated cells compared non-treated. The complete microarray dataset is posted on the Gene Expression Omnibus database http://www.ncbi.nlm.nih.gov/geo/, accession number GPL7137 for the platform design and GSE1207 for the original dataset.

2.2.10.3 Analysis of intracellular protein interactions by Yeast-two-Hybrid screening

The yeast-two hybrid screen and the downstream quantification of protein-protein interactions of SP1-1 and SP10-2 against an open reading frame library of *Staphylococcus aureus* Mu50 (Brandner et al., 2008) was carried out by the group of Dr. Kamil Önder at the Department of Dermatology, Paracelsus Medical University Salzburg (Salzburg, Austria) following a method of Maier et al. (2008).

A - Yeast Two-Hybrid library and peptide coding plasmid construction

A Yeast Two-Hybrid (Y2H) library representing almost every *S. aureus* gene was produced using a pool of PCR products generated by Brandner et al. (2008). First the pool of 2697 PCR products, each flanked with attB1 and attB2 sites for recombinational cloning or Gateway® cloning (Hartley et al., 2000; Walhout et al., 2000), was recombined into the Gateway® compatible pDONR™/Zeo vector by attB x attP recombination using 450 ng PCR product, 300 ng pDONR™/Zeo plasmid, 2 µl BP Clonase™II Enzym Mix (Invitrogen) and TE buffer, pH 8.0 up to 10 µl. The reaction was

incubated overnight at 25°C. After adding 1 µg proteinase K solution (Invitrogen, Karlsruhe, Germany) at 37°C for 30 min, 3 µl of the reaction were used directly for bacterial transformation. The resulting 0.5 x 10^6 individual colonies were cultured and plasmids isolated using the GenElute™ HP Plasmid Maxiprep Kit (Sigma, St.Louis, MO, USA). As second step in the Y2H prey library construction 800 ng of the created library in pDONR™/Zeo were recombined by attL x attR reaction (Hartley et al., 2000) into 300 ng of the Gateway compatible pAD-Gate2 vector (Maier et al., 2008) by adding 2 µl LR Clonase™ II Enzyme Mix (Invitrogen, Karlsruhe, Germany) and TE buffer pH 8.0 up to 10 µl. The reaction was stopped with proteinase K solution and directly used for bacterial transformation. Overall, 1.1 x 10^6 primary colonies were cultured and subsequently used for plasmid isolation using the GenElute™ HP Plasmid Maxiprep Kit.

As bait plasmids coding sequences of SP1-1 or SP10-2 were cloned by recombination into the Y2H Destination vector pBD-Gate2 (Maier et al., 2008). For that, the SP1-1 or SP10-2 sense oligonucleotide was annealed with the respective anti-sense oligonucleotide and cloned into an entry vector designed for Gateway® cloning (pENTRY Zeo/ScaI). This vector harbors the blunt-end restriction site ScaI between the attL1 and the attL2 site. After transformation and plasmid preparation positive clones were sequenced. Positive clones in pENTRY/Zeo/ScaI were used for attL x attR recombination (Hartley et al., 2000) into pBD-Gate2 using the LR Clonase™ II Enzyme Mix Kit (Invitrogen, Karlsruhe, Germany) according to the kit manual. After transformation, selected positive clones were subjected again to sequencing and plasmid preparation using the GenElute™ HP Plasmid Maxiprep Kit.

B - Standard Y2H analysis, Y2H screen and quantification of protein-protein interactions

For single Y2H protein-protein interaction (PPI) analysis bait and prey vectors were transformed together into the haploid yeast strain AH109 (MATα) from the Matchmaker™ Two-Hybrid System (Clontech, Mountain View,CA, USA) according to the kit manual. One half of each transformation was plated onto a nutritionally selective plate deficient in tryptophan and leucine (SD/-leu-trp) to test for positive transformation and one half on a nutritionally selective plates deficient in tryptophan, leucine, adenine and histidine (SD/-leu-trp-ade-his) to test for putative interactions. The plates were incubated at least 5 days at 28°C. To exclude autoactivation of the examined bait and prey combinations each prey plasmid was co-transformed with empty pGBKT7 vector and each bait plasmid with empty pGADT7 vector (both Clontech) and examined in the same way.

To detect possible weak interactions and to exclude spurious autoactivation, all transformants were additionally analyzed under less stringent conditions, since direct plating of transformants onto PPI selective SD/-leu-trp-ade-his medium represents a very stringent condition. After growing the yeast colonies on SD/-leu-trp plates, several

random colonies were picked, resuspended in water, dropped out and grown on SD/-leu-trp and SD/-leu-trp-ade-his media.
A large-scale Y2H screen was performed by the co-transformation of 180 µg SP1-1 or SP10-2 in pBD-Gate2 together with 180 µg *S. aureus* ORF library in pAD-Gate2 in an upscaled yeast transformation protocol. Finally a part of the transformation was plated onto one SD/-leu-trp plate to test for positive plasmid uptake and general transformation efficiency and on SD/-trp-leu-ade-his plates to screen for novel PPIs. The plates were incubated for at least 5 days at 28°C. The grown primary positive yeast clones were recovered by plasmid isolation via digestion with 10 U Lyticase (Sigma Aldrich GmbH, Taufkichen, Germany), addition of 10% SDS, one freeze-thaw cycle, and purification by using a Wizard® SV gel and PCR clean-up system (Promega, Madison, WI,USA). The plasmids were then amplified in *E. coli* DH5α, sequenced and reintroduced back into the yeast strain AH109 to verify the putative interaction.

For quantification of the PPI, Y2H clones from transformation selective plates were cultivated in liquid SD/-leu-trp oN at 28°C with gentle shaking and analyzed for ß-galactosidase activity. The cultures were diluted to OD_{600}: 0.1, an equal volume of Beta-Glo® Reagent (Promega, Madison, WI, USA) was added and the mixture was incubated for one hour at room temperature (3 replicates each). Luminescence counts were detected with a luminescence reader, the PARADIGM™ detection platform (Molecular Devices, Sunnyvale, CA, USA).

2.2.10.4 Structural analysis of the kinase - peptide interaction

A - NMR analysis

For NMR analysis of kinase – peptide interaction, RsbW was recombinantly produced and purified as described in chapter 2.2.3.2. To this end the *E. coli* expression host was grown in ^{15}N-M9 medium, ensuring ^{15}N as the single nitrogen source during expression. The protein was concentrated to 200 µM in 25 mM Tris, 150 mM NaCl pH 8, by 2 x 10 min centrifugation at 4000x g in a Amicon® Ultra Centrifugal filter, Ultracel 10K (Millipore Corporation, Billerica, MA, USA) and NMR analysis was performed at the Institute of Structural Biology of the Helmholtz Zentrum München (Munich, Germany). RsbW spectra were recorded at 298 K on a Bruker Avance III 750-MHz spectrometer equipped with a TXI probe head, while titration drops of a 10 mM SP1-1 solution (in H_2O) to the sample during the measurement. The spectra were analyzed with Software NMRPipe and Sparky.

B – Thermo fluorescence (Melting curve measurement)

Recombinantly produced RsbW was used freshly purified either 1) without the addition of additives or 2) with addition of 2 mM ADP 3) with addition of 2 mM 5'-Adenylylimidodiphosphate (AMPPNP), or 4) after freezing to -80°C and thawing. For samples 2) and 3) 0.5 mM ADP were included in all chromatography running buffers. Reaction mixtures were prepared in optical 96 well plates (Applied Biosystems, Darmstadt, Germany) with subsequent sealing with optical adhesive covers (Applied Biosystems, Darmstadt, Germany) including the following components:

- 5 µl RsbW (5, 10, 20 µM or 10, 20, 40 or 50 µg/ml final concentration)
- 5 µl SYPRO® Orange (0.5, 1, 2 or 5x final concentration (Invitrogen, Karlsruhe, Germany))
- 40 µl 25 mM Tris, 150 mM NaCl, pH 8

The melting experiments were done in a Mx3000P® qPCR System (Stratagene, La Jolla, CA, USA) with the following programme settings:

Measurement mode: Dissociation curve

Step	Temperature	Duration	Cycles
1	25°C	5 min	1
2	+15°C/per cycle	30 s	141

Fluorescence data were collected and exported to Microsoft Office Excel (Microsoft Corporation, 2003) and melting-/dissociation curves were generated by plotting the measured fluorescence intensity against the temperature.

C - Aggregate separation and mass detection

Recombinantly produced RsbW was separated by mass and protein masses were detected by a light scattering detector (LSD). RsbW, freshly purified as described in chapters 2.2.4.1 - 2.2.4.3, in a concentration of 2 mg/ml in 25 mM Tris, 150 mM NaCl pH 8.0 was treated with following additives or buffers and incubated at 4°C oN in a total volume of 100 – 200 µl :

2 mg/ml RsbW (0.1 µM) +

1) / (in 25 mM Tris, 150 mM NaCl pH 8.0)
2) 2 mM ADP (in 25mM Tris, 150 mM NaCl pH 8.0)
3) 2 mM AMP-PNP (in 25mM Tris, 150 mM NaCl pH 8.0)
4) 0.5 mM SP1-1 (in 25mM Tris, 150 mM NaCl pH 8.0)
5) 0.5 mM SP1-13 (in 25mM Tris, 150 mM NaCl pH 8.0)
6) Co-purification with 1.3 mg/ml (0.1 µM) RsbV
7) / buffer exchanged to 50 mM Na_2HPO_4, 150 mM NaCl, pH 5.0

Only clear samples without any visible precipitates were applied to the SEC. They were separated on a superdex 200 column (as described in chapter 2.2.2.4) with a downstream LSD (GE Healthcare, Freiburg, Germany).

2.2.10.5 In vitro *RsbW binding and inhibition of phosphorylation reaction*

The inhibition of the phosphorylation of RsbV by RsbW, or the complex formation with the transcription factor Sigma B (SigB) by the AMPs was performed by a method established by Dr. J. Pané-Farré and colleagues of the Ernst-Moritz-Arndt University of Greifswald (Greifswald, Germany). 0.5 – 8 µg of AMPs in peptide buffer or the same amount of buffer were preincubated with 0.1 µM RsbW in kinase activity buffer in a final volume of 10 µl for 15 min at RT. Then RsbV or SigB (in a molar ratio RsbV:RsbW of 1:1 or SigB:RsbW of 1:2) were added and phosphorylation of RsbV (with subsequent addition of 1 mM ATP) or complex formation with SigB (without ATP addition) was carried out by incubation at RT for further 5 min. The reactions were stopped by addition of 50 mM EDTA (pH 8.0) and incubation of the samples immediately on ice. Then 4x native PAGE loading dye was added to a final concentration of 1x and the samples were applied to 15% native PAGE and stained with Coomassie protein stain.

2.2.10.6 In vivo *RsbW inhibition in S. aureus sigB deletion mutants*

To test the possibility of RsbW as a real *in vivo* target for SP1-1, antimicrobial activity tests with *S. aureus* RN1HG and its mutant strains were performed. *S. aureus* RN1HG (Herbert et al., 2010), a deletion mutant of this strain of *rsbU* and the *rsbW, rsbV, sigB* containing operon *sigB* (Δ*sigB*), and an episomal generated complemented mutant strain (Δ*sigB* complemented) were used. The strains were tested with regard to antibacterial activity of SP1-1 as described in chapter 2.2.5. Peptides SP8 and SP10-2 served as controls. Bacterial growth, measured as OD_{600nm} and calculated MIC values were measured after 18 h and compared between the three strains. The *S. aureus* strains were kindly provided by Dr. S. Engelmann and Dr. J. Pané-Farré, Ernst-Moritz-Arndt-University of Greifswald, Institute of Microbiology (Greifswald, Germany).

3 Results

At the Institute of Biochemical Plant Pathology more than 60 AMPs, differing in size and localization of hydrophobic and charged amino acid clusters had been designed previous to this study. Several of these peptides were highly active against a range of phytopathogenic bacteria. However, nothing was known about their site and mode of action at the bacteria.
So, the main aim of this study was to elucidate target sites and killing mechanisms of selected highly active AMPs.
Therefore, various target sites were analyzed and data are presented on:

- Antibacterial activity tests against multi-resistant strains of *S. aureus*
- Effects on bacterial membranes, including membrane perturbation and interaction ability with artificial membranes and membranes of living bacteria
- Localization of the peptides at the pathogens by microscopic approaches and nanometer scaled secondary ion mass spectrometry (NanoSIMS) approaches
- The interaction with possible intracellular targets:
    - Binding ability to nucleic acids by gel-shift assays
    - Identification of intracellular protein interaction partners within an Yeast-two-Hybrid screen.

  Furthermore, the elucidated interactions were characterized in detail by gene expression studies and enzyme tests.

3.1 Antibacterial activity of synthetic peptides against *S. aureus*

Since the *de novo* designed AMPs showed previously to this study high activities against phytopathogens, antibacterial tests were extended to a multi-resistant strain of the human pathogenic bacterium *Staphylococcus aureus.* The clinical isolate 90857 of *S. aureus* was chosen for the tests as it served as a representative for high level multi-resistance, including resistances against penicillin, methicillin, oxacillin, erythromycin, clindamycin, gentamycin, amikacin, ciprofloxacin and moxifloxacin. Various peptides from all structural design groups were used for a screen of antibacterial activity. In particular, derivates of SP1 as well as derivates of SP10 were selected, since some of their members have been identified before as highly active against phytopathogenic bacteria in the low micromolar or even nanomolar concentration ranges, starting at 0.1 µg/ml (Supplementary Table 1). To cover all structural groups SP7, SP8, SP9, SP13 and several SP13 derivates were also included in the test. Peptide dilutions were incubated with

bacterial cells for 18 to 24 h and the minimal inhibitory concentrations (MIC), defined as the lowest AMP concentration (µg/ml) that prevented visible growth (Wiegand et al., 2008) after 18h and the minimal bactericidal concentrations (MBC), defined as the concentration of AMP where at least 99.9 % of the initial inoculum were killed (Barry et al., 1999) after 24h were determined (Table 2). Against the investigated highly resistant strain, several peptides showed antibacterial activities in the low micromolar range, including SP1-13, SP10-2, SP10-4, SP10-8 with MIC values of 1 µg/ml, SP1-11, SP1-14, SP9, SP10-1 of 2.5 µg/ml and SP1-12, SP10-5 of 5 µg/ml. Additionally, peptides SP1-1, SP1-15, SP7, SP10-2, SP10-7, SP10-10, SP13, SP13-2, SP13-6, SP13-7 were active at concentrations of 10 – 20 µg/ml (Table 2). Interestingly, a clear discrimination of the MIC and MBC was often not possible. The lowest peptide concentration for which activity could be shown with regard to growth reduction, was in most cases already the concentration which killed all bacteria. For SP1-1, SP1-16, SP13-6 and SP13-7 one concentration step between the MIC and the MBC occurred (Table 2).

Table 2 - Antibacterial activity of selected peptides against MRSA clinical isolate 90857

peptide	**SP1**	**SP1-1**	**SP1-2**	**SP1-3**	**SP1-4**	**SP1-5**	**SP1-6**	**SP1-7**
MIC/MBC (µg/ml)	>40/>40	10/20	100/100	100/>100	>100/>100	>100/>100	>100/>100	>100/>100
peptide	**SP1-8**	**SP1-9**	**SP1-10**	**SP1-11**	**SP1-12**	**SP1-13**	**SP1-14**	**SP1-15**
MIC/MBC (µg/ml)	100/>100	100/100	>100/>100	2.5/2.5	5/5	1/1	2.5/5	10/10
peptide	**SP1-16**	**SP1-17**	**SP7**	**SP8**	**SP9**	**SP10**	**SP10-1**	**SP10-2**
MIC/MBC (µg/ml)	40/100	>100/>100	10/10	>100/>100	5/5	5/5	2.5/2.5	1/1
peptide	**SP10-4**	**SP10-5**	**SP10-6**	**SP10-7**	**SP10-8**	**SP10-10**	**SP10-11**	**SP13**
MIC/MBC (µg/ml)	1/1	5/5	40/>40	10/10	1/1	10/10	40/>40	20/20
peptide	**SP13-2**	**SP13-6**	**SP13-7**	**SP13-12**	**SP13-14**			
MIC/MBC (µg/ml)	10/10	5/10	5/10	10/40	40/40			

Synthetic antimicrobial peptides in concentrations of 0.1 – 100 µg/ml were incubated with 10^5 cfu of *S. aureus* clinical isolate 90857 in a total volume of 100 µl at 37°C for 18 – 24 h. OD_{600nm} was measured and minimal inhibitory concentration (MIC), defined as the lowest concentration (µg/ml) of the AMP that prevents visible growth after 18 h and minimal bactericidal concentration (MBC), defined as the concentration of AMP where ≥ 99.9% of the inoculum were killed after 24 h, were determined relatively to the not peptide treated cells as control for 100% growth.

Toxicity, determined previous to this study as the peptide concentration leading to 25% hemolysis of human erythrocytes, was at 20 µg/ml for SP13-6, at 50 µg/ml for SP9, SP10-8, SP13-2 and SP13-12 at 100 µg/ml for SP10 and SP13, and at or over 200 µg/ml for the SP10 and SP13 derivates. No hemolysis was detectable for SP1 and all tested derivates in the tested range up to 200 µg/ml (Supplementary Table 1). From these data SP1-1, as well as the phenylalanine-containing SP1-11 – SP1-15 and SP10-1 – SP10-5, SP10-7 and SP13-7 were identified as anti-*Staphylococcus* candidates with high activity against this pathogen but at the same time low toxicity against human cells. In sum, a number of candidates with high and broad ranged activity against several phytopathogenic bacteria as well as against MRSA were identified. For the following

analyses of mode of action, carried out in *S. aureus* and different phytopathogenic bacteria strains, mainly SP1-1, SP8, SP10-2, SP10-4, SP10-8, SP13 and SP13-2 from the different structural groups were selected. This selection covered peptides with high activity and low or no detectable toxicity from groups I, II and IV (SP1-1, SP10-2, SP10-4, SP13-2) but also peptides with high toxicity (SP10-8, SP13, SP13-2) for comparison. As within structural group II (SP5 – SP8) generally no high activities were observed only SP8 from this group was further used as control for no detectable antibacterial activity.

3.2 Bacterial membrane integrity

From the sequence of the designed peptides an α-helical tertiary structure was expected and could already be shown for representatives of the different structural groups in a previous study (Zeitler et al., 2012). Presence of α-helicity is often associated with membrane disturbing activity (Bocchinfuso et al., 2009; Rzepiela et al., 2010; Thennarasu et al., 2010). So, membrane disturbing ability was analyzed as a possible mode of action for the newly developed antimicrobial peptides.

3.2.1 The AMPs interact with artificial membranes but do not form pores

Many naturally occurring antimicrobial peptides act by the formation of pores in bacterial membranes. This leads to leaking of ions and other compounds from the cells and thus to the death of the bacteria (Kordel et al., 1989; Sokolov et al., 1999; Wu et al., 1999; Wiedemann et al., 2004). To analyze the pore forming ability of the synthetic AMPs, conductance measurements with artificial membranes were performed after AMP addition. Pore formation at artificial black lipid bilayers results in ascending conductance curves with discrete steps and plateaus (Stipani et al., 2001; Dalmau et al., 2002; Wiedemann et al., 2004; Polzien et al., 2009; 2010). Examples for conductance curves of pore forming substances, obtained during comparable experiments as described here, are given in Figure 5.

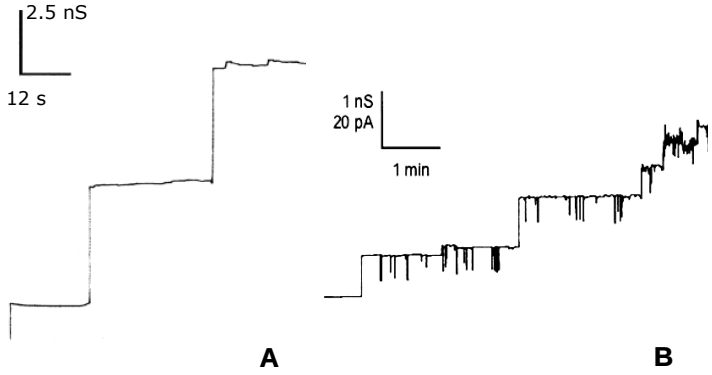

Figure 5 - Examples for conductance curves of pore formers
Pore formation at artificial lipid bilayers is shown by examples of conductance curves with discrete steps and plateaus of (A) human BAD (30 ng/ml) at pH 7 (1 M KCl) at +20 mV (Polzien et al., 2009) and (B) 2.5 nM *Clostridium perfringens* beta toxin at pH 7 (1M KCl, 10 mM Tris HCl) and 20 mV (Manich et al., 2008). The conductance curves were measured at lipid bilayers in a comparable setup as used in this study. Scale bars represent time in seconds (s) in x- and conduction current in pico ampere (pA) and nano Siemens (nS) in y-direction.

Peptides from all structural groups were used for the experiment. SP1-1, SP10-2, and 13, from groups I, III and IV with high antibacterial activity values were tested. Peptide SP8 from group II, with no antibacterial activity was used as a control. The resulting conductance curves were compared with data obtained from known pore forming substances (Figure 5). In general, the tested antimicrobial peptides did not cause the described curves, but intensive spontaneous spiking (Figure 6). This behavior displays interaction of the peptides with the membranes but without pore formation. The observed interaction depended on concentration, although within the tested range of 0.1 – 10 µg/ml peptide, the observed amplitude changes were only marginal. Furthermore, symmetric behavior was observed between negatively (4:1 mixture of di-phytanoyl-phosphatidylcholine/di-phytanoyl-phosphatidylserine) and neutrally charged membranes (di-phytanoyl–phosphatidylcholine) and between positive and negative applied voltages (Figure 6C compared to A, B, D). SP8 showed the same kind of curves in similar intensities as the highly active peptides (Figure 6C). For induction of conductance spiking by the peptides, application of voltages of around 100 mV were necessary. Conductance spiking was induced not only by negative applied voltages, similar to the bacterial membrane potential, but positive applied voltages also resulted in similar amplitudes. Once spiking was induced it could also be observed at lower voltages.

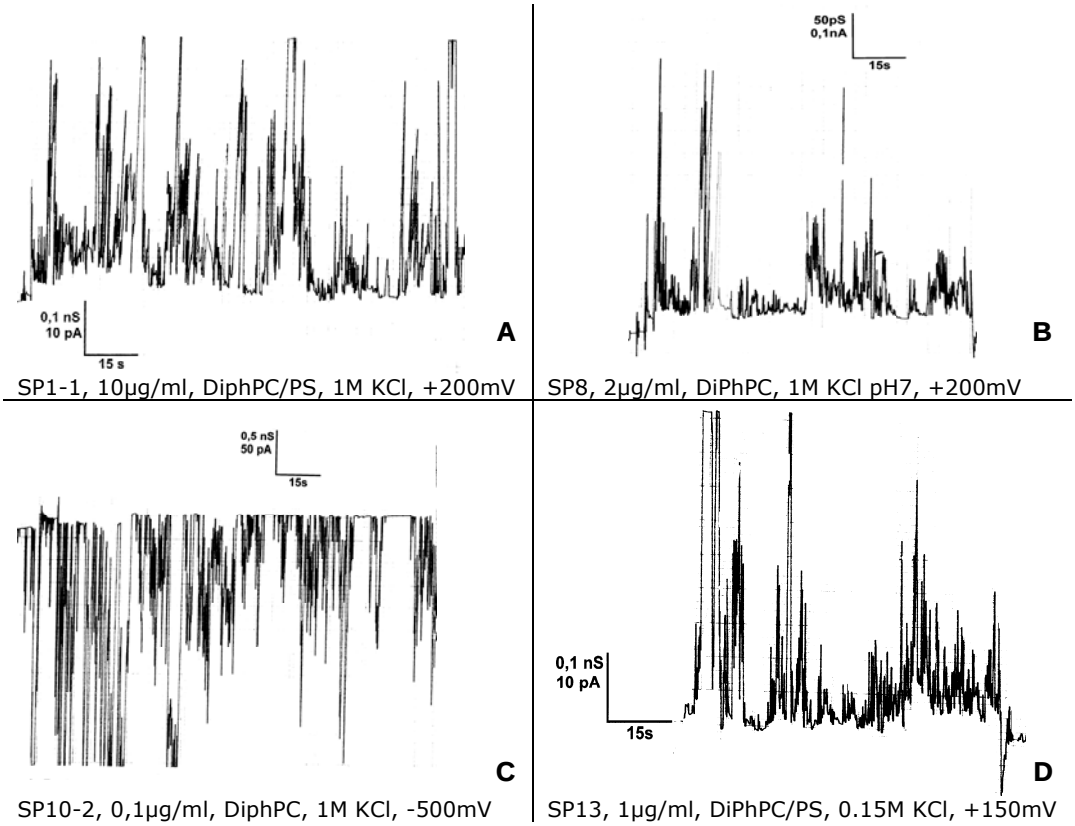

Figure 6 - Sections of conductance measurements of lipid bilayers treated with selected AMPs
Lipid bilayers were formed of 1% (w/v) di-phytanoyl–phosphatidylcholine (DiPhPC) or a 4:1 mixture of di-phytanoyl-phosphatidylcholine/di-phytanoyl-phosphatidylserine (DiPhPC/PS) in n-decane. Solutions of 0.15 or 1 M KCl at both membrane sides were buffered to pH 7. Conductance curves were recorded after addition of 0.1 – 10 µg/ml SP1-1, SP8, SP10-2 or SP13 to the *cis*-side of the membrane. Shown are representative sections of obtained conductance curves. Scale bars represent time in seconds (s) in x- and conduction current in pico ampere (pA) and nano Siemens (nS) in y-direction.

Thus, pore formation could be excluded as mode of action for all tested AMPs (SP1-1, SP8, SP10-2, SP13) from the four structural groups. However, the AMPs interacted with the membranes in slight concentration dependent manner. The type of interaction could not be defined in more detail with this experiment and had to be elucidated further.

3.2.2 The AMPs do not lyse phospholipid micelles

Since pore formation could be excluded, a generally lytic effect on phospholipid-micelles by the peptides was investigated. Using the method developed by Kolusheva et al. (2000a; 2000b), crosslinking of phospholipids within micelles results in a blue stained micelle solution due to the absorption maximum of the crosslinked polydiacetylene (PDA) backbone at 620 nm. After micelle lysis the breakdown of the PDA backbone leads to a switch of the absorption maximum to 490 nm (red) by the PDA fragments. The blue-to-red color shifts are directly related to adoption of helical conformations of the peptides, their association with lipids and the degree of penetration into the lipid bilayers (Kolusheva et al., 2000a; Kolusheva et al., 2000b). As the peptides were shown to interact with artificial membranes without pore formation (chapter 3.2.1), within the colorimetric experiment minor effects were expected due to this interaction. Strong effects would be a sign for micelle lysis by the AMPs.
Bacterial membranes mainly contain hydroxylated phospholipids like phosphatidylglycerol and are negatively charged. In eukaryotic membranes phospholipids like phosphatidylcholines occur, which lead to a neutral net charge (Zasloff, 2002; Yeaman and Yount, 2003). For the measurements negatively charged 1,2,-dimyristoylphosphatidylglycerol (DMPG) or neutral 1,2,-dimyristoylphosphatidylcholine (DMPC) phospholipid micelles were used. Again, SP1-1, SP10-2 and SP13 and SP8 as representatives of all structural groups were tested. SP1-1, SP10-2 and SP13 again served as representatives with high antibacterial activity (0.1 – 10 µg/ml), SP13 additionally for high hemolytic activity (100 µg/ml) and SP8 for no detectable activity. 2% SDS served as control for strong lytic effects (Figure 7). The naturally occurring AMP protegrin 1, derived from porc, served as a control for minor lytic effects (Figure 7), as it causes channel formation in lipid bilayers but not complete lysis (Sokolov et al., 1999). In the tested concentrations the synthetic AMPs showed much lower levels of colorimetric reactions than lysis by SDS, which led to a colorimetric reaction of 44% at DMPG (Figure 7A) and 43% at DMPC (Figure 7B) micelles. Slight effects by the AMPs were only observed at high concentrations. But these effects were at the same level for peptides SP1-1, SP10-2 and SP13 with high antimicrobial activity as well as for SP8. At those high peptide concentrations (40 – 100 µg/ml) blue-to-red switch ratios slightly below 20% occurred for the negatively charged micelles (Figure 7A) and at around 25% or less for the neutral lipids (Figure 7B). In negatively charged micelles the effects of synthetic

AMPs were clearly lower than of protegrin 1, which showed effects at concentrations of 20 to 100 µg/ml (Figure 7A). In non-charged micelles, the effects of the synthetic AMPs and protegrin 1 were with 20 – 25% at the same level (Figure 7B).

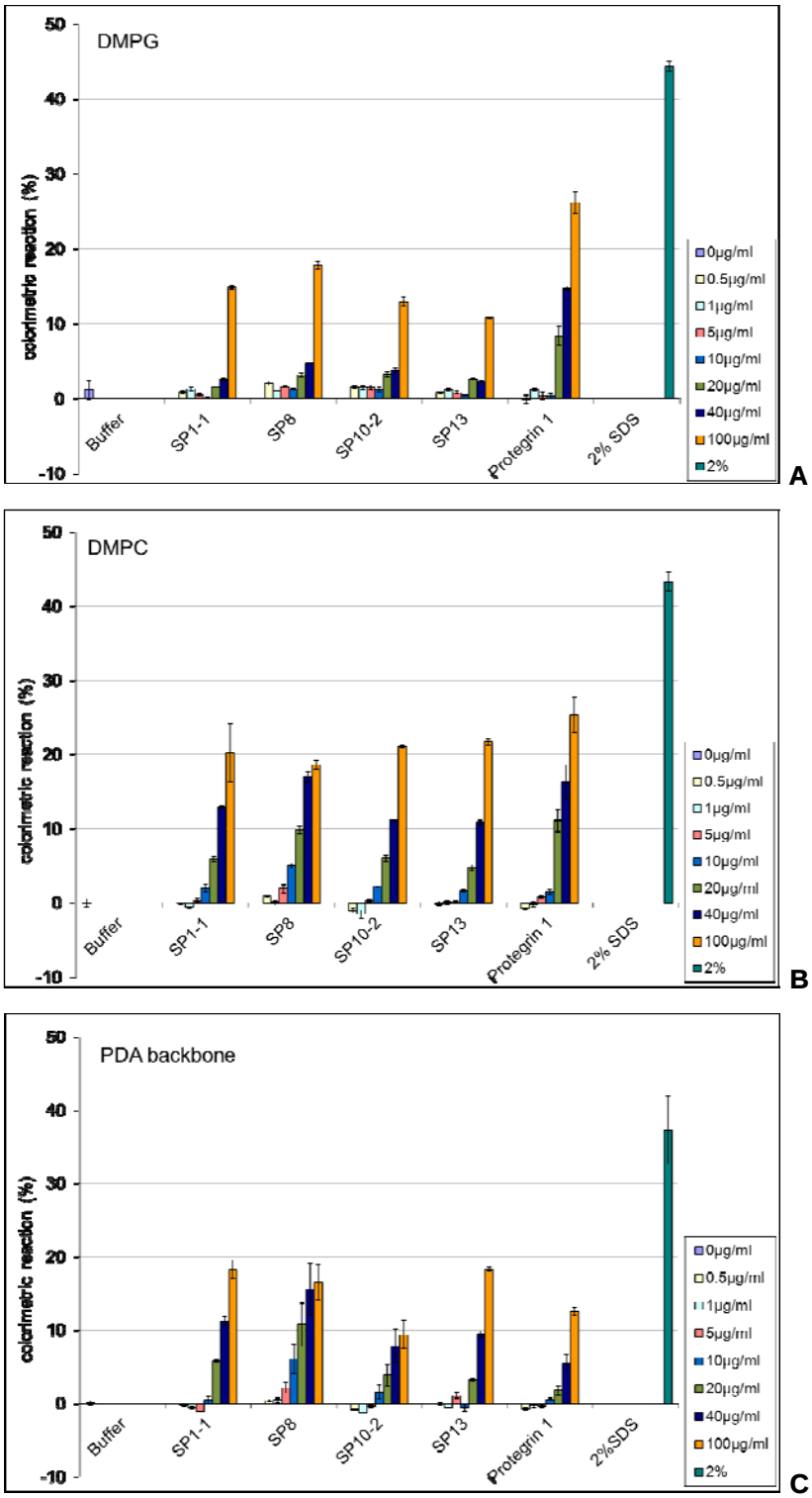

Figure 7 - Test for lytic effects of synthetic AMPs on phospholipid micelles
Phospholipid micelles were built of negatively charged 1,2,-dimyristoylphosphatidylglycerol (DMPG, A) or neutral 1,2,-dimyristoylphosphatidylcholine (DMPC, B) crosslinked with polydicosanoic acid (PDA). Micelles of only crosslinked PDA backbone were used as control (C). After addition of 0.5 – 100 µg/ml SP1-1, SP8, SP10-2, SP13 or buffer, micelle lysis was measured by the switch of the absorption maximum of the solution from 620 nm to 490 nm. 2% SDS was used as positive control. Protegrin 1 served as control for a pore forming peptide. Error bars represent standard deviation of 3 independent experiments.

As an additional control, the PDA backbone without phospholipid addition was used (Figure 7C). Here the effects were in a similar range for SP1-1, SP8 and SP13 but slightly lower for SP10-2 and protegrin 1, when compared to negatively charged phospholipids (Figure 7A and C). This implements that slight lytic effects at high peptide concentrations were mainly not caused by interaction of the peptides with phospholipids. The effects indicate interaction of the peptides with micelle membranes, as expected. However, generally much lower effects of the AMPs as compared to SDS and additionally, in negatively charged micelles lower effects as compared to protegrin 1 were detected. Together with the generally absence of preference of the AMPs for negatively charged lipids, also lytic effects can be excluded as a relevant mode of action.

3.2.3 SP10 and SP13 derivates depolarize bacterial membranes

The bacterial membrane potential is essential for transport mechanisms and ion homeostasis. The breakdown of this potential by depolarization of the cytoplasmic membrane can also be a possible mode of action of AMPs. To investigate the ability of selected synthetic peptides to affect the bacterial membrane potential, a membrane potential sensitive dye ($DiSC_3(5)$) was used. The dye is taken up by the cells and quenches on the inner side of the cell membrane in response to an intact membrane potential (Friedrich et al., 2000). Under depolarization, the quenching is attenuated and the increase of fluorescence can be measured photometrically. To test the influence on different membrane assemblies, two different strains of phytopathogenic bacteria, one gram-positive (*C. michiganensis ssp. michiganensis*) and one gram-negative strain (*P. syringae pv. syringae*) were loaded with the fluorescent dye and treated with 0.5 – 100 µg/ml peptides. Again representatives of all structural groups and of SP1-, SP10- and SP13-derivate groups were tested. SP1-1, SP10-4 and SP13-2 served as highly active and SP8 as non-active examples and SP10-8 for high hemolytic activity at a concentration of 50 µg/ml (Supplementary Table 1). SDS was used as positive control, as cell lysis by SDS leads to a complete breakdown of membrane potential. Indolicidin, a natural pore forming AMP from cattle (Falla et al., 1996), was used as control for influence on membrane potential by channel formation. Buffer treated samples served as control of background effects.

Figure 8 shows the results of treatment with 10 µg/ml peptide. A summary of treatments with the different peptide concentrations is given in Supplementary Figure 1. Especially at *C. michiganensis,* SP10-4 and SP13-2 showed strong depolarization of the membrane, comparable to indolicidin (Figure 8A). Treatment with SP10-8 resulted in similar levels of depolarization as treatment with 1% tensidic SDS (Figure 8A). For *P. syringae* the depolarization levels of SP10-4, SP10-8, SP13-2 and indolicidin were in the same range, but in general lower than for *C. michiganensis* (Figure 8B). SP8, that showed no

antibacterial activity in the tested concentration range, did not influence the membrane potential, as expected. Interestingly, SP1-1, exhibiting good antibacterial activity (0.1 – 2.5 µg/ml, Supplementary Table 1), revealed only moderate or low membrane depolarization with both bacterial strains – in gram-negative bacteria even comparable to non active SP8 (Figure 8A and B).

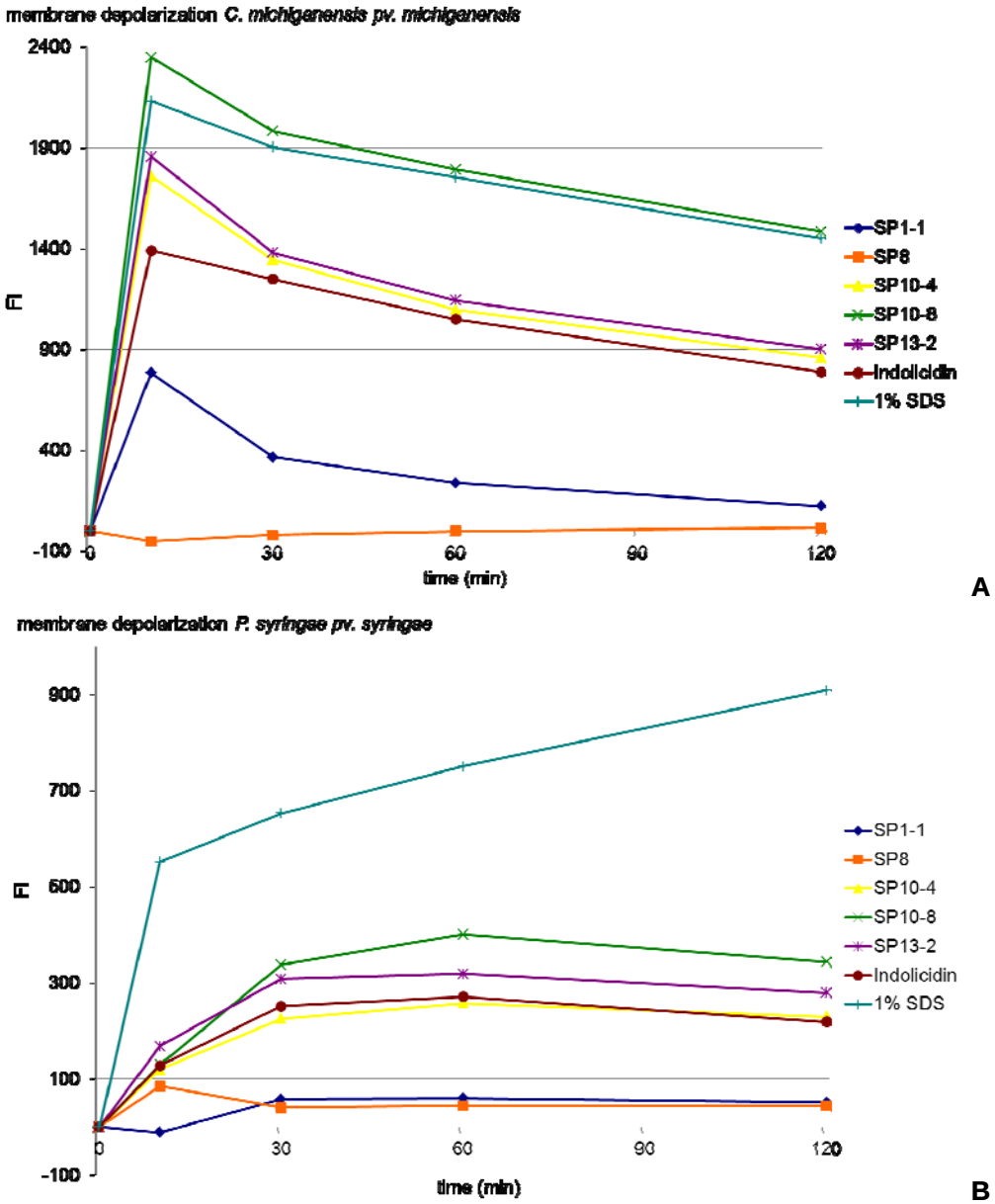

Figure 8 - Bacterial membrane depolarization activity of selected AMPs
Depolarization of bacterial membranes was determined by loading 5 x 10^7 cfu/ml gram-positive *C. michiganensis ssp. michiganensis* (A) or gram-negative *P. syringae pv. syringae* (B) with the dye $DiSC_3(5)$ and measuring fluorescence intensity (FI, at λ_{ex}: 622nm, λ_{em}: 670nm) 10, 30, 60 and 120 min after addition of 10 µg/ml SP1-1, SP8, SP10-4, SP10-8 or SP13-2. Indolicidin and 1% SDS were used as controls for membrane depolarization. Shown are the FI values of 3 independent measurements, normalized against buffer treatment.

The different levels of depolarization between the used peptides could also be observed when different peptide concentrations, ranging from 0.5 to 100 µg/ml were applied to the cells (Supplementary Figure 1). Summarizing these data, strong effects on the membrane potential by peptides of structural groups III and IV, especially SP10-4 and SP10-8, both derivates of SP10, but also of SP13 derivate SP13-2 could be shown. SP1-1

influenced the membrane potential only marginally. Additionally, at every measurement timepoint aliquots of the reaction mixtures were plated on LB agar plates. They were incubated for 24 hours and checked for growth. This displayed the killing ability of the AMPs within the reaction mixtures against the used amount of 5 x 10^7 cells. It became obvious, that antibacterial action of SP10-4, SP10-8 and SP13-2, and of the naturally occurring, pore forming AMP indolicidin proceeded faster than for peptide SP1-1 (Supplementary Figure 2).

3.2.4 Hydrophobic amino acids are important for the activity of SP10-4

To test the effect of specific amino acids at defined positions for antibacterial activity, an alanine scan was performed. SP10 derivates generally had high antibacterial activities. SP10-4 is a representative with high activity against *S. aureus* (1 µg/ml) and phytopathogens (0.1 – 2.5 µg/ml), and negligible hemolytic activity (> 200 µg/ml). It is therefore one of the most active AMPs. Furthermore, it exhibits clear influence on bacterial membrane potential (chapter 3.2.3). Due to these reasons SP10-4 was selected for the alanine scan. Derivates of SP10-4 with sequential alteration of one amino acid to alanine were used. Minimal inhibitory concentrations (MIC) against *S. aureus* 90857 as well as hemolytic activity were determined for each of the derivates (Table 3). Especially the hydrophobic amino acids leucine (L), isoleucine (I) and phenylalanine (F) were most important for antibacterial activity of this SP10-derivate. When these hydrophobic amino acids were substituted by alanine, the measured MIC values increased. This effect was most evident for leucine at specific positions 8 and 11. The antibacterial activity of SP10-4 (5 µg/ml) was even abolished within the tested concentration range of 0.1 – 100 µg/ml when one of these leucines was replaced by alanine (SP10-4-L(8)A, SP10-4-L-(11)A). With the replacement of cationic amino acids, the MIC concentrations of the SP10-4 derivates slightly decreased but the effects were very low. The MIC only changed one concentration step from 5 to 2.5 µg/ml when lysine at position 10 was substituted by alanine (SP10-4-K(10)A). The toxicity of SP10-4 was already very low with less than 25% hemolysis at the highest tested peptide concentration of 200 µg/ml. Additionally, the observed effects from the amino acid exchanges were generally much lower for hemolytic activity than for activity. However, as a general tendency higher antibacterial activity also resulted in higher hemolytic activity. So, for the peptides with leucine replaced by alanine, for which active concentrations were much lower or abolished within the tested concentration range, also hemolytic activity was abolished within the tested peptide concentrations. Only for the peptide with an exchange of lysine (K) at position 10 with alanine (SP10-4-K(10)A), activity and hemolytic concentrations decreased. But these effects on toxicity were only detectable to a very marginal extent and only one concentration step changed (>200 to 100 µg/ml).

Table 3 - Antibacterial and hemolytic activity of SP10-4 alanine scan peptide derivates

peptide	sequence	MIC (µg/ml)	hemolyt. conc. (µg/ml)
SP10-4	LRFIKKILKKLI-NH2	5	>200
SP10-4-L(1)A	ARFIKKILKKLI-NH2	100	-
SP10-4-R(2)A	LAFIKKILKKLI-NH2	5	>200
SP10-4-F(3)A	LRAIKKILKKLI-NH2	100	-
SP10-4-I(4)A	LRFAKKILKKLI-NH2	100	-
SP10-4-K(5)A	LRFIAKILKKLI-NH2	2,5	100
SP10-4-K(6)A	LRFIKAILKKLI-NH2	2,5	200
SP10-4-I(7)A	LRFIKKALKKLI-NH2	100	-
SP10-4-L(8)A	LRFIKKIAKKLI-NH2	>100	-
SP10-4-K(9)A	LRFIKKILAKLI-NH2	5	>200
SP10-4-K(10)A	LRFIKKILKALI-NH2	2,5	100
SP10-4-L(11)A	LRFIKKILKKAI-NH2	>100	-
SP10-4-I(12)A	LRFIKKILKKLA-NH2	40	-

SP10-4 derivates with sequential exchanges of one amino acid against alanine were used to identify sequence features that are important for antibacterial activity. Antibacterial activity was determined as minimal inhibitory concentration (MIC), by 18 h incubation of 10^5 cfu of *S. aureus* 90857 with dilution series of peptides (0, 0.1, 0.5, 1, 2.5, 5, 10, 20, 40, 100 µg/ml) and measurement of the OD_{600nm}. Hemolytic activity was determined with human red blood cells after incubation with 0, 0.1, 0.5, 1, 2.5, 5, 10, 20, 40, 100 or 200 µg/ml peptide for 45 min. Shown are the peptide concentrations leading to 25% hemoglobin release. > 200 describes a slight hemolytic activity at 200 µg/ml but below the above mentioned threshold. No value (-) indicates no detectable hemolytic activity up to the highest concentration tested.

3.3 Localization of the AMPs at the bacterial host

Experiments with membranes did not explain the mode of action of all peptide groups. To figure out if peptides are able to enter bacterial cells to reach intracellular targets localization experiments were carried out.

3.3.1 Localization by microscopy

To elucidate the localization of the AMPs and their ability to translocate into bacteria, microscopic localization of fluorescent labeled peptides, incubated with phytopathogenic bacteria was performed. After establishing the system, the experiment should also be adapted to *S. aureus*. Bacteria were incubated with the labeled AMPs and afterwards free AMPs were removed from the culture medium by washing steps. Finally, the samples were concentrated by centrifugation to allow visualization of the bacteria and analyzed by confocal microscopy. SP10-9 and SP10-11 exhibit high MIC values for the used bacteria strains of 2.5 µg/ml (SP10-9) against 10^6 cfu/ml of *Pectobacterium carotovorum* ssp. *carotovorum* and of 0.1 µg/ml (SP10-11) against the same amount of *Pseudomonas syringae pv. syringae* (Supplementary Table 1). As a 100-fold higher amount of bacteria (10^8 cfu/ml) compared to the amount used for activity tests was used, the peptide concentration was also enhanced to 25 µg/ml to obtain visible intensities but still sub-lethal concentrations. After 1 h incubation with the bacteria, the fluorescent labeled peptides SP10-9-TAMRA and SP10-11-TAMRA colocalized with the cells (Figure 9, red signals). After incubation with SP13-14-FAM, a fluorescent labeled peptide with lower

MIC values against the used bacteria strains (5 µg/ml for 10^6 cfu/ml of *P. syringae*, >10 µg/ml for *Pectobacterium carotovorum)* no interaction with the bacterial cells was observed. Contrariwise, SP13-14-FAM was either found freely as fluorescent debris in the medium (Figure 9A, green signals) or was not visible (Figure 9B), due to removal by the washing steps. No ring-like structures of fluorescent signal were detected and the distribution of the peptides could not be defined as a major occurrence at the cell surface. It could not be clearly distinguished, whether the signals of SP10-9-TAMRA and SP10-11-TAMRA, that colocalized with the bacteria, derived from the intracellular space or from the cell surface by scattering of fluorescent signals.

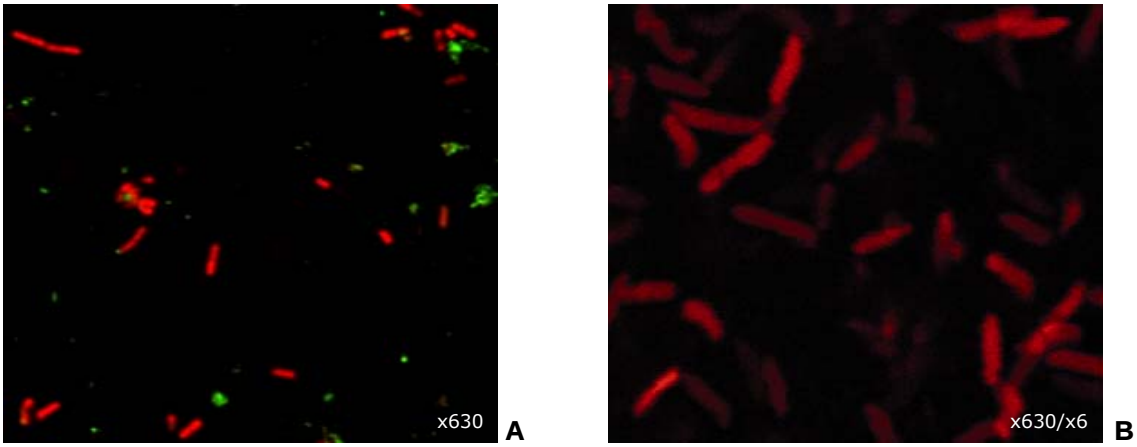

Figure 9 - Microscopic images of bacterial cells incubated with fluorescence-labeled AMPs
After 1h incubation of bacteria suspension cultures (10^8 cfu/ml) with fluorescent labeled AMPs and removal of excess peptides by 3 washing steps with PBS, the peptides were visualized by confocal fluorescence microscopy with a Zeiss laser scanning microscope (LSM) 510 Meta (Carl Zeiss AG, Jena, Germany). Image processing was done with the Zeiss LSM Image Browser software, Version 4,2,0,121 (Carl Zeiss AG, Jena, Germany). (A) *Pectobacterium carotovorum ssp. carotovorum,* incubated with 25 µg/ml of SP10-9-TAMRA (red, MIC: 2.5 µg/ml for 10^6 cfu/ml) and SP13-14-FAM (green, MIC: >10 µg/ml for 10^6 cfu/ml), 630x magnification. (B) *Pseudomonas syringae pv. syringae*, incubated with 25 µg/ml of SP10-11-TAMRA (red, MIC: 0.1µg/ml for 10^6 cfu/ml) and SP13-14-FAM (not visible, MIC: 5µg/ml for 10^6 cfu/ml), 630x magnification, 6x digital zoom.

To prove the principle of the approach, additional experiments were performed with spores of the fungus *Botrytis cinerea*. The bigger size of fungal spores as compared to bacterial cells and the therefore improved visibility at magnification levels achievable by fluorescence microscopy, provides easier applicability for localization studies. However, MIC values against fungal spores were not determined for the used peptides and the related peptides SP10 and SP13 showed low or no activity at the tested maximum concentrations of 100 µg/ml. Due to this fact high peptide concentrations (100 µg/ml) and long incubation times (2 h) were used. SP13-14-FAM that was incubated with *B. cinerea* spores was found attached to the cells and the image indicated localization at the cell membranes by ring-like fluorescent signals (Figure 10).

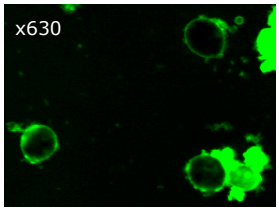

Figure 10 - Localization of synthetic AMP SP13-14-FAM at the cell surface of *B. cinerea* spores
Spores of the fungus *Botrytis cinerea* (10^6 spores /ml) were incubated with 100 µg/ml SP13-14-FAM for 2 h. After removal of excess dye in the medium, the fluorescence signal of the peptide was visualized at a 630x magnification with a confocal laser scanning microscope (LSM) 510 Meta (Carl Zeiss AG, Jena, Germany).

Due to these observations, the principle of the experiment was proven, but an explicit subcellular localization of the peptides on or in the bacteria was not possible with the magnification and the resolution of light microscopy.
Therefore, we decided to analyze the destination of the peptides by electron microscopy using an immunogold stain. Monoclonal antibodies (mAbs) were generated against SP1-1, SP10-2 and SP13 by the Core Facility for Generation of Monoclonal Antibodies and Cell Sorting of the Institute of Molecular Immunology (Helmholtz Zentrum München, Munich, Germany). However, dot-blot and western blot analyses of SP1-1, SP10-2, SP13 and mixtures of AMPs with BSA or crude bacterial protein extracts revealed that all of the antibodies were neither specific nor sensitive enough. (Supplementary Figure 3). Thus, the immunogold-labeling technique could not be applied.

3.3.2 Localization by Nanometer Scaled Secondary Ion Mass Spectrometry

As an alternative to electron microscopy and an independent approach of antibody usage, nanometer-scaled dynamic Secondary Ion Mass Spectrometry (NanoSIMS) was used for the localization of heavy isotope containing peptide. SP1-1, labeled with ^{15}N was used as this AMP did not show any membrane disturbing effects (chapter 3.2). The focus was directed towards *S. aureus*, since also intracellular protein interactions were to be tested in this bacterium (chapter 3.4.3), and the ability of SP1-1 to enter cells had to be elucidated first. The NanoSIMS technique is based on the mass spectrometry of secondary ions, extracted from surface layers (each of several nm) of the sample under the impact of an energetic ion beam. NanoSIMS 50L (Cameca, France) was used, exhibiting a spatial resolution of less than 50 nm with a primary Cs^+ ion and high transmissions at high mass resolutions of 60% at $M/\Delta M = 5000$ (Guerquin-Kern et al., 2005; CAMECA, 2009). Seven different secondary ion species can be detected simultaneously and the detection limit is in the parts per million (p.p.m.) and for some elements even in the parts per billion (p.p.b.) range (Musat et al., 2011). Using this method the secondary MS signals of the natural ^{14}N background of the bacteria cells and the ^{15}N enriched peptide signal can be measured at the same time, quantified and differentiated from each other, and the distribution can be read out by imaging of the MS signal. The MS data were therefore collected as $^{12}C^{14}N$ or $^{12}C^{15}N$, as the co-detection with ^{12}C enhances the signal and improves signal to noise ratios. Images of all collected secondary electrons and MS images of secondary ^{12}C, ^{13}C, ^{16}O and ^{32}S ions were recorded with every measurement of the $^{12}C^{14}N$ and $^{12}C^{15}N$ signals. By measuring the sum of all secondary electrons single cells became visible on the filter (Figure 11D, Figure 12D). The ^{12}C signal characterized the polycarbonate filter on which the cells were fixed. The ^{32}S signal served as marker for proteins and organic material and colocalized with the analyzed cells. ^{16}O and ^{13}C contaminations were very low or not detectable

(Supplementary Figure 8). Thus, it was ensured that bacteria cells and no other particles were analyzed. After incubation of *S. aureus* cells with ^{15}N-SP1-1 for 10 or 30 minutes, the signal of ^{15}N in comparison to ^{14}N was analyzed on a subcellular level for single cells (Figure 11, Figure 12). NanoSIMS images were collected for around 60 Z-directed layers of the selected sample region.

After 30 min of ^{15}N-SP1-1 incubation, ^{15}N and hence also SP1-1 was distributed all over the bacterial cell and intracellular space (Figure 11A - C). Additionally, ^{15}N signal intensities from the inner parts of the cells were stronger than from regions of the cell surface (Figure 11B). This data indicated, that ^{15}N-SP1-1 did not stick to the bacterial membrane but entered the bacteria and accumulated there.

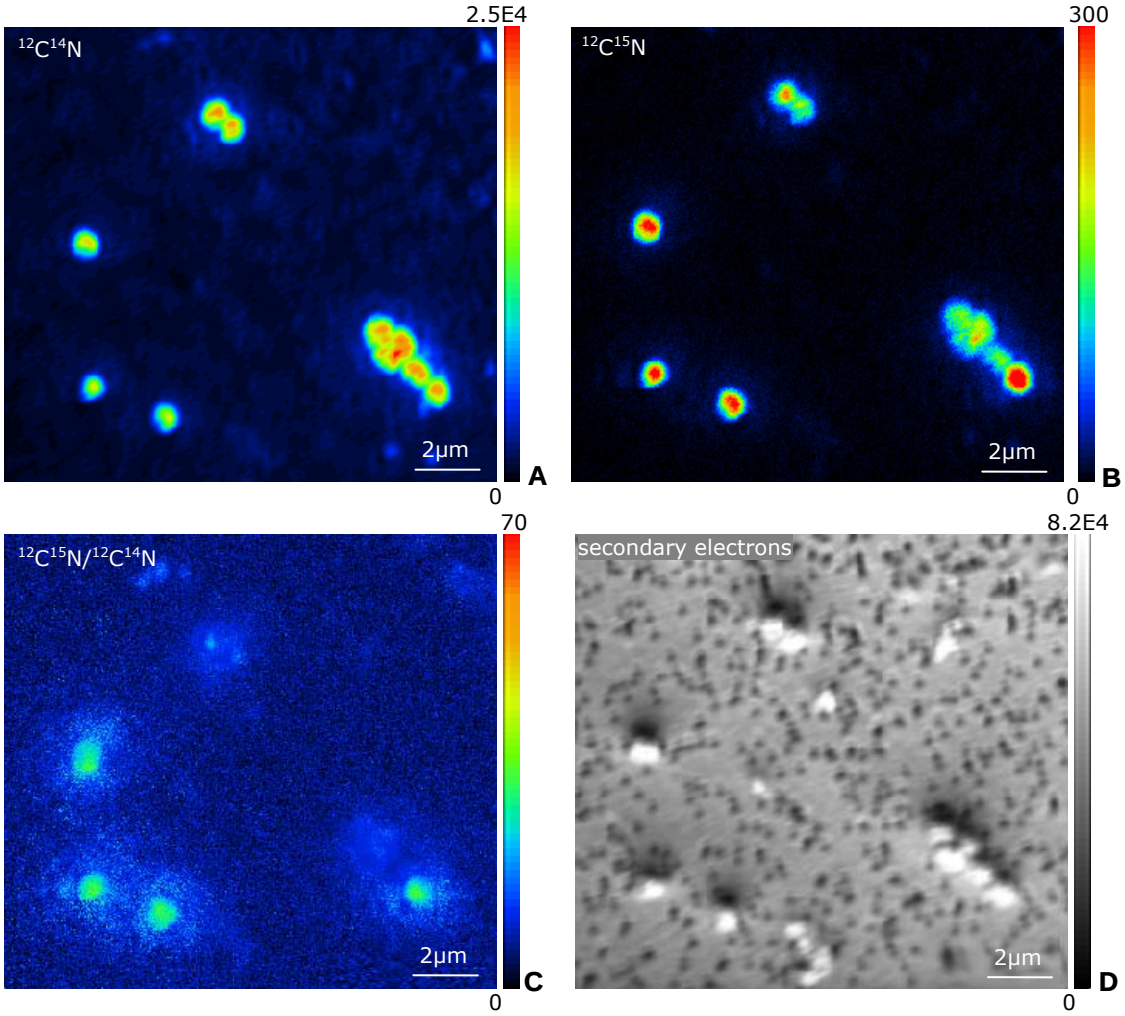

Figure 11 - NanoSIMS images of ^{15}N-SP1-1 deposition in *S. aureus* cells after 30 min incubation
S. aureus 90857 (4 x 10^6 cfu) was incubated with 100 µg/ml ^{15}N-SP1-1 for 30 min at 37°C, harvested by centrifugation and fixed with 1% PFA oN at 4°C. Samples were washed with PBS and filtered on gold/palladium sputtered filters. The filters were analyzed by NanoSIMS 50L with 60 cycles of ion beam sections and generation of secondary ion mass spectra. Image analysis was done with WinImage (Cameca, Gennevilliers Cedex, France). Shown are drift corrected and accumulated signals from cycles 10 to 50 and the recorded SIMS images of $^{12}C^{14}N$ (A), of $^{12}C^{15}N$ (B), the corresponding ratio (C) and the image of all measured secondary electrons (D).

Usage of sub-lethal ^{15}N-SP1-1 concentrations was ensured for the used amount of cells by plating 10 µl aliquots and dilutions of the reaction mixtures after the incubation times

and checking for growth after 18 h at 37°C (Supplementary Figure 4). By comparison of the $^{12}C^{15}N/^{12}C^{14}N$ signal count ratio of the measurement after 10 or 30 minutes of peptide treatment to non peptide treated cells or the background filter area, it was made sure that ^{15}N levels in or at analyzed cells were elevated from the natural background by a factor of 2.75 to 10 (Supplementary Figure 5 - 7).

To gain information about the time span of the ^{15}N-SP1-1 distribution over the cell, bacteria incubated 10 min with ^{15}N-SP1-1 were analyzed. Similar observations were made after 10 minutes compared to 30 minutes peptide treatment (Figure 12). Indeed, fewer bacteria cells gave ^{15}N signals after 10 min. But for cells with elevated ^{15}N levels, the SP1-1 derived ^{15}N signal was distributed over the whole cells and mostly accumulated within the cells (Figure 12A-C).

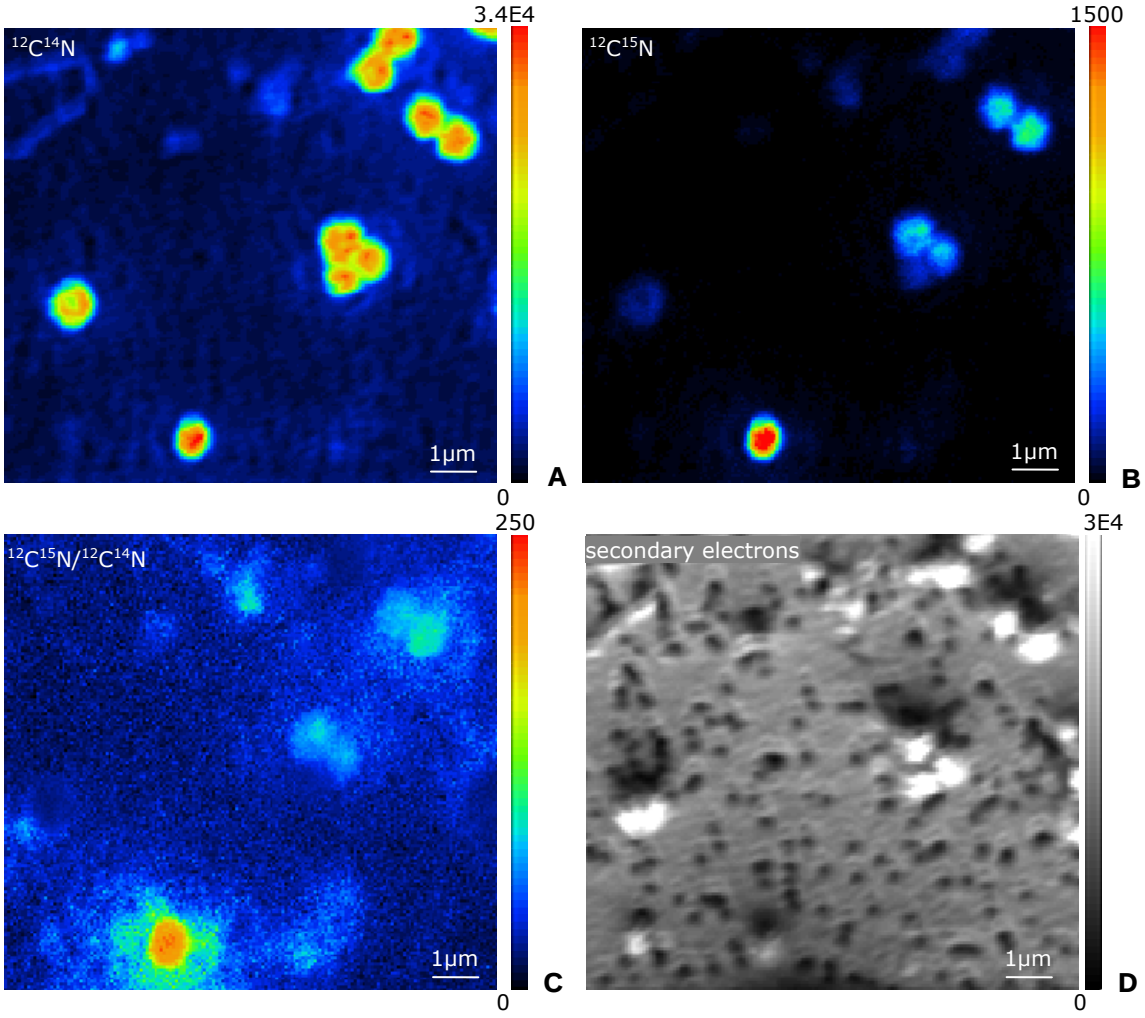

Figure 12 - NanoSIMS images of ^{15}N-SP1-1 deposition in *S. aureus* cells after 10 min incubation
S. aureus 90857 (4 x 10^6 cfu) was incubated with 100 µg/ml ^{15}N-SP1-1 for 10 min at 37°C, harvested by centrifugation and fixed with 1% PFA oN at 4°C. The cells were washed with PBS and filtered on gold/palladium sputtered filters. They were analyzed by NanoSIMS 50L with 63 cycles of ion beam sections and generation of secondary ion mass spectra. Image analysis was performed with WinImage (Cameca, Gennevilliers Cedex, France). Shown are drift corrected and accumulated signals from cycles 5 to 50 and the recorded SIMS images of $^{12}C^{14}N$ (A), of $^{12}C^{15}N$ (B), the corresponding ratio (C) and the image of all measured secondary electrons (D).

It was shown that SP1-1 translocated into and spread intracellularly in the *S. aureus* cells within 10 minutes and the major amount was still found intracellularly after 30 minutes.

3.4 Interaction with bacterial intracellular targets of the AMPs

Only for a small number of peptides including SP10-4, SP10-8 and SP13-2 membrane influencing ability was demonstrated that might be responsible for antibacterial activity. For other peptides, especially for SP1-1, such influence on membrane integrity does not seem to be the dominant mode of action. In addition, this peptide accumulated in the intracellular space. Besides biological membranes, intracellular molecules might be important putative targets for the AMPs. In this context the interaction ability of the peptides to different intracellular occurring biomolecules was tested.

3.4.1 Nucleic acid binding activity of the antimicrobial peptides

Due to their negative charge, nucleic acids are potential targets for the positively charged AMPs. The binding potential of the peptides can be shown by impeding of nucleic acid migration during agarose gel electrophoresis (Park et al., 1998). Again, to cover all structural groups, peptides SP1-1, SP8, SP10-2 and SP13 were used for the experiment. The AMPs were incubated with bacterial plasmid DNA in ratios (w/w) of 0.1 to 4.0 and DNA migration behavior was analyzed on agarose gels. SP1-1, SP10-2 and SP13 showed binding to the nucleic acids in a concentration dependent manner (Figure 13).

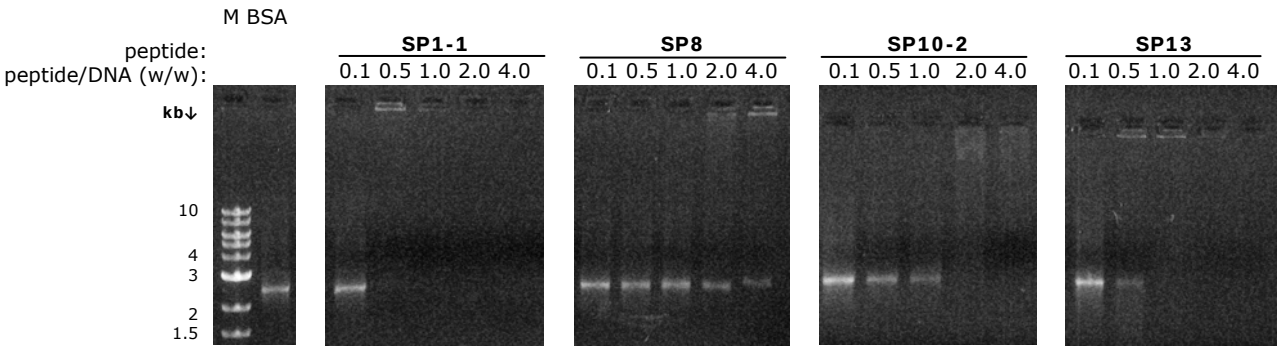

Figure 13 - Gel retardation experiments with bacterial DNA
10 – 400 ng of peptides SP1-1, SP8, SP10-2 or SP13 were incubated with 100 ng of a 2.5 kb bacterial plasmid DNA fragment at room temperature for 1 h and the reaction mixtures were applied to 1% agarose gel electrophoresis. The weight ratio (peptide / DNA) is indicated. 400 ng BSA served as a control. M: molecular weight marker in kilo bases (kb)

SP1-1 influenced DNA migration starting at a peptide / DNA weight ratio of 0.5 strongly, as no DNA band was detectable anymore at this ratio. Thereby, SP1-1 had the strongest influence on DNA migration compared to the other peptides used. SP10-2 started to inhibit DNA migration at ratios of 1.0 – 2.0 and SP13 at a ratio of 0.5. At higher peptide amounts, binding to the DNA did not only led to a shift in mobility, but the peptide-DNA complex did not migrate into the gel anymore. SP8 did not affect DNA migration clearly. Only very slight effects were visible at a very high SP8 / DNA ratio of 4.0, which can be attributed to unspecific charge compensating effects.

For binding of the peptides to bacterial RNA, the mobility behavior of the 16S and 23S rRNA from *Clavibacter michiganensis ssp. michiganensis* was analyzed by agarose gel electrophoresis. For testing dose dependent binding effects, the same peptides that were tested for dose dependent DNA interactions were used (SP1-1, SP8, SP10-2, and SP13). At high peptide / RNA ratios of 2.0, all peptides showed binding to RNA by a mobility shift or an abolished RNA migration (Figure 14). As non-reducing agarose gels were used for the separation of RNA, the gels show a band of high molecular weight nucleid acid aggregates (hmNA). After application of high peptide concentrations, disappearance of this band was detected. This can be regarded as an additional sign for peptide – nucleic acid interaction. For SP1-1, SP10-2 and SP13 dose dependent effects could be detected for RNA as well. Again, SP1-1 had the strongest effect. It influenced RNA migration, starting at peptide / RNA ratios of 0.25 – 0.5, SP10-2 at 1.0 and SP13 at a ratio of 2.0. However, the binding to bacterial RNA was not so clearly associated with activity, as in the case of DNA, as SP8 with no determinable antibacterial activity also seemed to interfere with RNA at ratios from 0.25 – 0.5 (Figure 14).

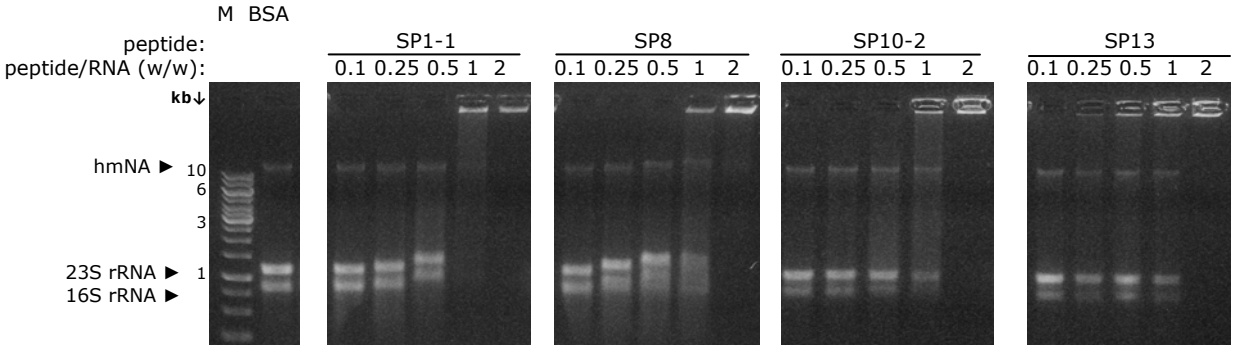

Figure 14 - Gel retardation experiments with bacterial RNA
0.1 – 2 µg of SP1-1, SP8, SP10-2 or SP13 were incubated with 1 µg bacterial RNA at room temperature for 1 h and the reaction mixtures were applied to agarose gel electrophoresis. The weight ratio (peptide / RNA) is indicated. 2 µg BSA served as a control. hmNA: high molecular weight nucleic acid aggregates. M: molecular weight marker in kilo bases (kb)

3.4.2 Microarray analysis of SP1-1 treated *S. aureus*

The tested AMP representatives SP1-1, SP10-2 and SP13, from structural groups I, III and IV showed dose dependent nucleic acid binding. Moreover, SP1-1 which had already been shown to localize intracellular in *S. aureus* (chapter 3.3.2), had the strongest DNA binding ability (chapter 3.4.1). The influence on gene expression by the binding to bacterial DNA was tested by a microarray analysis. The used *S. aureus* oligoarray covered 81% of the whole *S. aureus* COL genome with its 10807 oligoprobes (Charbonnier et al., 2005). RNA extraction, hybridization and microarray analysis (chapters 2.2.10.2 B - D) were carried out at the University Hospital of Geneva, by the group of Prof. Dr. Jaques Schrenzel (Geneva, Switzerland).

For the microarray analysis sub-lethal SP1-1 concentrations were determined for the amount of around 10^8 cells and the used strain (COL), since previously determined MIC values (10 µg/ml) were valid for 10^6 cfu/ml of strain 90857. *S. aureus* cells were grown to mid-logarithmic phase (OD_{600nm}: 0.58 - 0.6) and different SP1-1 concentrations (0, 1, 2, 4 µg/10^6 cfu) were added. OD_{600nm} values were monitored within the next 120 minutes. The peptide concentration of 4 µg/10^6 cfu, which slightly inhibited growth but did not kill the cells completely, was used for the subsequent experiments (Supplementary Figure 9). Gene expression changes were analyzed for samples treated 10 minutes with either 4 µg/10^6 cfu SP1-1 in peptide buffer or only buffer as mock treatment. This incubation time was chosen as it has been determined as suitable for the observation of AMP related gene expression changes in *S. aureus* in a previous study (Pietiainen et al., 2009).

The microarray analysis revealed a total of 115 genes with significantly changed expression. 18 genes were up-regulated more than three fold (Table 4) and 97 genes were down-regulated more than three fold (Table 5). Many cell metabolic pathways were affected and most of the differentially regulated genes could be grouped within the following functional categories, according to http://www.ncbi.nlm.nih.gov/COG/grace/fiew.cgi?g=158879: Amino acid transport and metabolism (E), nucleotide transport and metabolism (F), carbohydrate transport and metabolism (G), lipid transport and metabolism (I), cell wall/membrane/envelope biogenesis (M), secondary metabolite synthesis, transport and catabolism (Q), and only general predicted function (R). Within the up-regulated genes were several with functions in cell wall metabolism, like autolysin *atl,* (N-acetylmuramyl-L-alanine amidase and endo-b-N-acetylglucosaminidase) with a fold change of 3.19, peptidoglycan hydrolase gen *lytM* (fold change of 3.00), bifunctional autolysin SACOL1062 (fold change of 3.18) and the cell wall hydrolysing putative transglycolase gene *sceD* (3.25-fold change). The up-regulated gene for LysM domain-containing protein SACOL0507 has also a putative function in cell wall hydrolysis, comparable to glycosyl-hydrolase (Visweswaran et al., 2011). The two genes with the highest up-regulation were subunits I and II from cytochrome d ubiquinol oxidase with functions in oxidative phosphorylation and energy metabolism (Poole and Cook, 2000). Also the genes encoding for intracellular adhesion proteins (*icaA, B, D*), important for biofilm formation (O'Gara, 2007), were up-regulated. With functions in pigmentation and virulence, three genes involved in staphyloxanthin biosynthesis (SACOL2291, SACOL2295, SACOL2581) were induced 4.43-, 3.60- and 4.25-fold. Additionally, gene *ssaA* for secretory antigen precursor SsaA-like protein, a virulence determinant, was up-regulated 4.02-fold. Furthermore, genes for manganese transport protein MntH (SACOL1114), adenylsuccinate synthetase (SACOL0018) and hypothetical proteins SACOL0219 and SACOL1481 were up-regulated 3.07-, 3.68-, 3.11 and 3.81-fold by SP1-1.

Table 4 - Up-regulated genes after treatment of *S. aureus* with SP1-1

loci/gene	fold change	Function	COG
cell wall/membrane/envelope			
atl	3.19	autolysin, N-acetylmuramyl-L-alanine amidase and endo-b-N-acetylglucosaminidase	
lytM	3.00	peptidoglycan hydrolase	C
SACOL0507	3.44	LysM domain-containing protein	E
SACOL1062	3.18	bifunctional autolysin	
SACOL2088	3.25	sceD protein, putative transglycosylases (peptidoglycan hydrolases)	E
oxidative phosphorylation			
cydA	4.64	cytochrome d ubiquinol oxidase, subunit I	
cydB	5.34	cytochrome d ubiquinol oxidase, subunit II	
Transport			
SACOL1114	3.07	manganese transport protein MntH	E
biofilm formation			
icaA/SACOL2689	3.35	N-glucosaminyltransferase IcaA	E
icaB/SACOL2691	3.14	intercellular adhesion protein B	E
icaD/SACOL2690	3.33	intercellular adhesion protein D	IQ
virulence and pigmentation			
SACOL2291	4.43	staphyloxanthin biosynthesis protein	E
SACOL2295	3.60	staphyloxanthin biosynthesis protein, putative	C
SACOL2581	4.25	staphyloxanthin biosynthesis protein	C
ssaA	4.02	secretory antigen precursor SsaA-like protein	G
Others			
SACOL0018	3.68	adenylosuccinate synthetase	
SACOL0219	3.11	hypothetical protein	M
SACOL1481	3.81	hypothetical protein	E

Exponential growing *S. aureus* COL was treated 10 min with 4 µg/10^6 cfu SP1-1. Cells were harvested, RNA was extracted and transcriptional changes were analyzed with a *S. aureus* whole genome oligoarray (Charbonnier et al., 2005). Variance analysis was done for triplicates and fold changes of more than 3 were considered as significant. Shown are up-regulated genes with fold changes between 3 – 3.99 in light red and with fold changes of ≥ 4 in dark red. Functional categories (COGs after http://www.ncbi.nlm.nih.gov/COG/grace/fiew.cgi?g=158879): C, energy production and conservation; E, amino acid transport and metabolism; G, carbohydrate transport and metabolism; I, lipid transport and metabolism; M, cell wall/membrane/envelope biogenesis; Q, secondary metabolite synthesis, transport and catabolism.

A larger number of 97 genes were down-regulated by SP1-1. The biggest proportion of genes was thereby involved in amino acid and peptide metabolism. The genes of the histidine biosynthesis (*his*) operon displayed one of the most down-regulated groups with fold changes to 0.08 – 0.05. Further genes with functions in amino acid synthesis that were repressed were for example *dapA, B and D,* active in lysine biosynthesis, (Girish et al., 2011) with fold changes to 0.25, 0.23 and 0.25, and *gltA, B and D* (fold changes 0.20, 0.14, 0.16), from citrate and glutamate synthesis. Also genes with functions in carbohydrate, energy and amino acid transport were down-regulated. Especially many ABC transporters for maltose (SACOL0192 – 0195), peptides and amino acids (SACOL1915, 1916 and SACOL2441, 2471 – 2476) were affected with fold changes of 0.27 – 0.15. Furthermore, several genes involved in lipid metabolism were repressed by SP1-1 (*lysA, D; vraD, E, F*). Additionally, a number of genes with functions or at least putative functions in cell wall/membrane or envelope biogenesis (SACOL0196 – 0197, SACOL0198, SACOL0124, 0215, SACOL1847 – 1850) were down-regulated. The expression of genes *drp35* (SACOL2712) and *sgtB* was furthermore altered. Both gene products, the calcium dependent lactonase Drp35 and the glycosyltransferase SgtB

belong to the cell wall stress response regulon (Morikawa et al., 2005; Sass et al., 2008; Steidl et al., 2008).

Table 5 - Down-regulated genes after treatment of *S. aureus* with SP1-1

loci/gene	fold change	Function	COG
cell wall/membrane/envelope			
acsA	0.25	acetyl-CoA synthetase	
SACOL0196	0.18	Gfo/Idh/MocA family oxidoreductase	M
SACOL0197	0.13	Gfo/Idh/MocA family oxidoreductase	M
SACOL2712/drp35	0.15	DrP35 protein (drug responsive protein 35)	
sgtB	0.31	Glycosyltransferase	R
cell wall/membrane/envelope – putative			
SACOL0198	0.18	hypothetical protein	M
SACOL0214	0.16	long-chain-fatty-acid--CoA ligase, putative	M
SACOL0215	0.15	propionate CoA-transferase, putative	M
SACOL1847	0.15	hypothetical protein	M
SACOL1848	0.20	hypothetical protein	M
SACOL1849	0.26	hypothetical protein	M
SACOL1850	0.23	hypothetical protein	M
amino acid and protein metabolism			
ald	0.30	alanine dehydrogenase	
aldA	0.24	hypothetical protein	
alr	0.23	alanine racemase	
arcA	0.30	arginine deiminase	
arcB	0.26	ornithine carbamoyltransferase	
arcD	0.33	arginine/oirnithine antiporter	
Arg	0.27	Arginase	
asd	0.22	aspartate semialdehyde dehydrogenase	
citC	0.24	isocitrate dehydrogenase	
citZ	0.21	citrate synthase	
dal	0.23	putative alanine racemase	E
dapA	0.25	dihydrodipicolinate synthase	E
dapB	0.23	dihydrodipicolinate reductase	E
dapD	0.25	tetrahydrodipicolinate acetyltransferase	E
fadE	0.16	putative acyl-CoA synthetase	E
fadX	0.17	putative acetyl-CoA transferase	E
fbp	0.08	fructose-bisphosphatase	E
gcvT	0.30	glycine cleavage system aminomethyltransferase T	E
glcB	0.28	PTS system, glucose-specific IIABC component	E
glnQ	0.18	glutamine transport ATP-binding protein	E
glpF	0.17	glycerol uptake facilitator	E
glpT	0.20	glycerol-3-phosphate transporter	E
gltA	0.20	citrate synthase	F
gltB	0.14	glutamate synthase large subunit	F
gltD	0.16	glutamate synthase subunit beta	E
gntK	0.21	Gluconokinase	E
hisA	0.06	1-(5-phosphoribosyl)-5-[(5-phosphoribosylamino)methylideneamino] imidazole-4-carboxamide isomerase	E
hisB	0.05	imidazoleglycerol-phosphate dehydratase	E
hisC	0.06	histidinol-phosphate aminotransferase hisC	E
hisD	0.06	histidinol dehydrogenase	E
hisF	0.06	imidazole glycerol phosphate synthase subunit HisF	E
hisG	0.08	ATP phosphoribosyltransferase catalytic subunit	E
hisH	0.06	imidazole glycerol phosphate synthase subunit HisH	E
hisI	0.06	bifunctional phosphoribosyl-AMP cyclohydrolase/phosphoribosyl-ATP pyrophosphatase protein	E
hisZ	0.06	ATP phosphoribosyltransferase regulatory subunit	E
icd	0.24	isocitrate dehydrogenase	EM
SACOL0707	0.29	dihydroxyacetone kinase family protein	E
SACOL0708	0.26	DAK2 domain-containing protein	E

Table 5 – continued

SACOL1433	0.24	M20/M25/M40 family peptidase	E
SACOL1434	0.23	alanine racemase family protein	E
SACOL1593	0.32	glycine dehydrogenase subunit 2	E
SACOL1594	0.30	glycine dehydrogenase subunit 1	E
amino acid and protein metabolism – putative			
SACOL0625	0.12	hypothetical protein	E
SACOL0709	0.29	hypothetical protein	E
SACOL1705	0.26	hypothetical protein	E
energy and carbohydrate transport and metabolism			
msmX	0.27	multiple sugar-binding transport ATP-binding protein	C
SACOL2441	0.20	amino acid permease	C
SACOL2552	0.28	PTS system, IIABC components	C
SACOL2569	0.18	1-pyrroline-5-carboxylate dehydrogenase	C
SACOL2663	0.22	PTS system, fructose-specific IIABC components	R
SACOL2727	0.29	integrase/recombinase core subunit	G
sucA/SACOL1449	0.31	2-oxoglutarate dehydrogenase E1 component	G
sucB/SACOL1448	0.30	dihydrolipoamide succinyltransferase	G
energy and carbohydrate transport and metabolism – putative			
SACOL2478	0.22	hypothetical protein	C
SACOL2479	0.17	hypothetical protein	C
SACOL2521	0.18	transporter, putative	C
SACOL2527	0.08	fructose-1,6-bisphosphatase, putative	C
SACOL0174	0.26	hypothetical protein	G
transport – ABC transporters: energy, carbohydrate, amino acids, peptides			
SACOL0192	0.27	maltose ABC transporter, ATP-binding protein, putative	G
SACOL0193	0.25	maltose ABC transporter, maltose-binding protein, putative	G
SACOL0194	0.24	maltose ABC transporter, permease protein	G
SACOL0195	0.15	maltose ABC transporter, permease protein	M
SACOL1915	0.17	amino acid ABC transporter, ATP-binding protein	M
SACOL1916	0.17	amino acid ABC transporter, permease/substrate-binding protein	E
SACOL2471	0.30	transporter, putative	C
SACOL2472	0.23	peptide ABC transporter, ATP-binding protein	C
SACOL2473	0.19	peptide ABC transporter, ATP-binding protein	C
SACOL2474	0.18	peptide ABC transporter, permease protein	C
SACOL2475	0.16	peptide ABC transporter, permease protein, putative	C
SACOL2476	0.15	peptide ABC transporter, peptide-binding protein	C
SACOL2655	0.33	arginine/ornithine antiporter	
sirA/SACOL0099	0.28	Iron compound ABC transporter, lipoprotein	R
lipid transport and metabolism			
lysA	0.26	diaminopimelate decarboxylase	I
lysC	0.19	aspartate kinase	I
vraD	0.03	ABC transporter ATP-binding protein VraD	I
vraE	0.05	vraE protein	I
vraF	0.28	ABC transporter ATP-binding protein	I
Others			
SACOL0154	0.24	aldehyde dehydrogenase	
SACOL1428	0.19	aspartokinase, alpha and beta subunits	
SACOL1430	0.25	dihydrodipicolinate synthase	
SACOL1432	0.25	2,3,4,5-tetrahydropyridine-2,6-dicarboxylate N-succinyltransferase	
SACOL1742	0.20	methylcitrate synthase	
SACOL1783	0.25	acetyl-CoA synthetase	
SACOL1838	0.24	phosphoenolpyruvate carboxykinase	
SACOL2154	0.27	Arginase	

Exponentially growing *S. aureus* COL was treated 10 min with 4 µg/10^6 cfu SP1-1. Cells were harvested, RNA was extracted and transcriptional changes were analyzed with a *S. aureus* whole genome oligoarray (Charbonnier et al., 2005). Variance analysis was done for triplicates and fold changes of more than 3 were considered as significant. Genes with fold changes of 0.32 – 0.21 are indicated in light blue and ≤ 0.2 in dark blue. Functional categories (COG after http://www.ncbi.nlm.nih.gov/COG/grace/fiew.cgi?g=158879): C, energy production and conservation; E, amino acid transport and metabolism; G, carbohydrate transport and metabolism; I, lipid transport and metabolism;; M, cell wall/membrane/envelope biogenesis; R, general function only predicted.

3.4.3 Interaction with intracellular proteins

Intracellular proteins can also serve as potential targets for antimicrobial peptides. Hence, a Yeast-Two-Hybrid (Y2H) screen was used to identify possible protein binding partners in *S. aureus.* This pathogen represents a big medical threat due to its ability to acquire multiple resistances and the occurrence of an increasing number of highly resistant strains (Chambers and Deleo, 2009; Mainous et al., 2011). However, a number of AMPs with high antibacterial activities against highly resistant *S. aureus* were identified (Table 2). So, the focus of the analysis was directed towards this pathogen. Two peptides from different structural groups were used for the Y2H screen. SP10-2 from structural group III with high antibacterial activity (1 µg/ml) was used. SP1-1 from group I was also included in the test, although its MIC (10 µg/ml) was not in the range of the most active peptides. However, it seemed to act by a different mechanism. It showed lower influences on membrane potential (chapter 3.2.3) but stronger influence on nucleic acid binding (chapter 3.4.1) than SP10 derivates and an intracellular localization in *S. aureus* (chapter 3.3). The Y2H screen with peptides SP1-1 and SP10-2 and the following verification of the results by ß-galactosidase quantification were carried out by Dr. K. Önder and colleagues at the Department of Dermatology, Paracelsus Medical University Salzburg (Salzburg, Austria). The Y2H screen was performed with an ORFeome library, covering 2562 ORFs and thereby 95% of the identified 2697 open reading frames (ORFs) of strain Mu50 (Brandner et al., 2008; Maier et al., 2008). For single Y2H protein-protein interaction (PPI) coding sequences of SP1-1 and SP10-2 were cloned in Y2H bait vectors. SP1-1- und SP10-2-bait plasmids, containing the binding domain of transcription factor GAL4 (pBD-Gate2) were transformed together with the ORF-library-prey plasmid, containing the activation domain of GAL4 (pAD-Gate2), into the haploid yeast strain AH109. The strain has a defective GAL4 gene and is unable to synthesize adenine, tryptophan, histidine and leucine and thereby cannot grow on agar plates deficient in these nutrients. Positive transformation and delivery of both plasmids restores the ability to synthesize leucine (delivered by the prey plasmid) and tryptophan (delivered by the bait plasmid) and enables the yeast cells to grow on agar plates deficient in these nutrients (SD/-leu-trp). Positive interaction between SP1-1- or SP10-2-bait plasmids and interaction partners from the ORF library on the prey plasmid additionally leads to the approximation of both GAL4 domains. This results in activation of transcription and the ability of the yeast cells to synthesize adenine and histidine and to grow on agar plates selective for all four nutrients (SD/-leu-trp-ade-his).

Both peptide harboring plasmids exhibited high transformation efficiency with 10^6 primary transformants, indicating a full coverage of the library. After 7 days on selective agar plates, 7 positive colonies were identified. The prey plasmids were purified and amplified in *E. coli*. They were, together with original SP1-1- or SP10-2-bait plasmids,

transformed back to the yeast strain and monitored again for interaction on selective agar plates.

For SP1-1 two clones could be isolated, and sequence analysis revealed in both cases the identified interaction partner as the same serine-protein-kinase, namely RsbW. For SP10-2 two clones could be isolated as well. However, one candidate (hypothetical protein SAV0341) could not be verified by sequence analysis and another (hypothetical protein SAV1441) turned out as an autoactivator.

The interaction between SP1-1 and RsbW could be verified on selective agar plates, as the growth of the transformed yeast cultures indicated a very strong interaction. Regarding the interaction between SP10-2 and the kinase, the growth of the yeast cultures was visible but very weak, indicating either a low affinity interaction or a false positive. As positive control the strong interaction between mouse p53 und SV40 T-large antigen was used. As negative control the interactions of empty bait and prey plasmids were used (Figure 15).

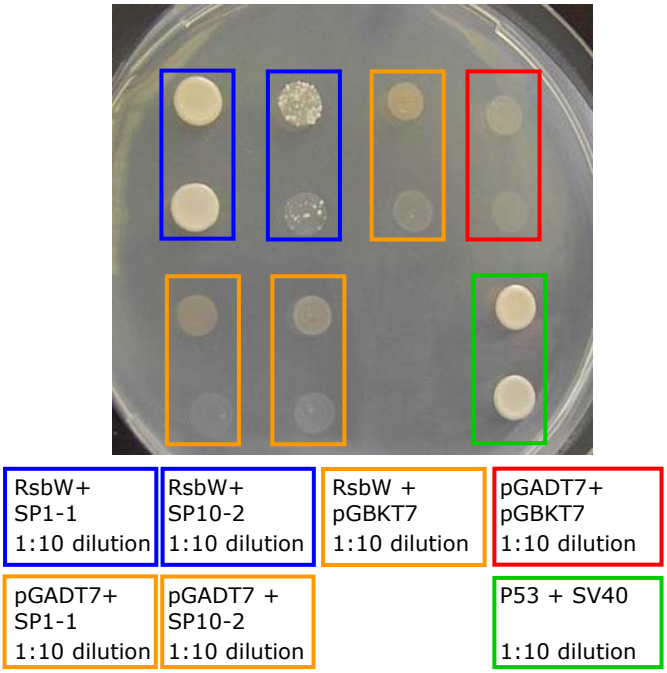

Figure 15 - Identification of the interaction of SP1-1 and RsbW of *S. aureus*
SP1-1 and SP10-2 coding sequences were transferred in Y2H compatible bait plasmids and screened in a Yeast-Two-Hybrid screen against 2562 *S. aureus* ORFs in prey plasmids. Positive yeast transformants were dropped on interaction-selective plates (-tryptophan, -leucine, -histidine, -adenine) and checked for growth. Shown are the plated colonies after 2 d of incubation on selective plates at 28°C. As controls served combinations of empty bait (pGBKT77) and prey (pGADT7) vectors and the strong interaction between mouse p53 und SV40 T-large antigen. The positive control is indicated in green, the negative control in red. Tests for autoactivation are indicated in orange and clear interactions in blue.

Quantification of ß-galactosidase activity is more suitable for the assessment of relative interaction intensities. The interactions between SP1-1 and SP10-2 and the identified serine-kinase RsbW were quantified by the restored activity of the lagZ gene by interaction of bait and prey plasmids, and the following substrate turnover by the gene product ß-galactosidase. As controls again interactions of empty bait and prey plasmids (negative) and between mouse p53 und SV40 T-large antigen (positive) were used. ß-galactosidase quantification demonstrated that interaction of SP1-1 and RsbW was specific and seemed to be strong (45%) compared to positive control. For SP10-2 the level of ß-galactosidase activity remained below that of the negative control and the interaction could not be verified (Figure 16).

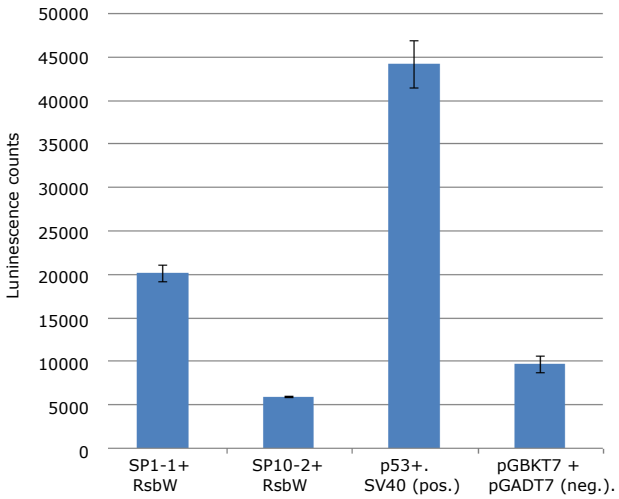

Figure 16 - ß-galactosidase quantification of the peptide - RsbW interaction
The interactions of peptides SP1-1 and SP10-2 with RsbW were relatively quantified by ß-galactosidase quantification. Clones from transformation selective plates were cultivated in liquid SD/-leu-trp oN at 28°C, and diluted to OD_{600}: 0.1. An equal volume of Beta-Glo® Reagent (Promega) was added, the mixture was incubated for one hour at RT and luminescence counts were measured. For SP1-1 a strong interaction of 45% of the positive control was observed. For SP10-2 the interaction could not be proven. As positive control the interaction of mouse p53 und SV40 T-large antigen was used. As negative control the interaction of the combination of the empty bait (pGBKT7) and prey (pGADT7) vector. Error bars represent standard error of 3 replicates.

Additionally, the prey plasmids were co-transformed with empty pGBKT7 vector and the bait plasmids with empty pGADT7. By subsequent dropping on selective plates and ß-galactosidase quantification, autoactivation could be excluded for the specific interaction (Figure 17).

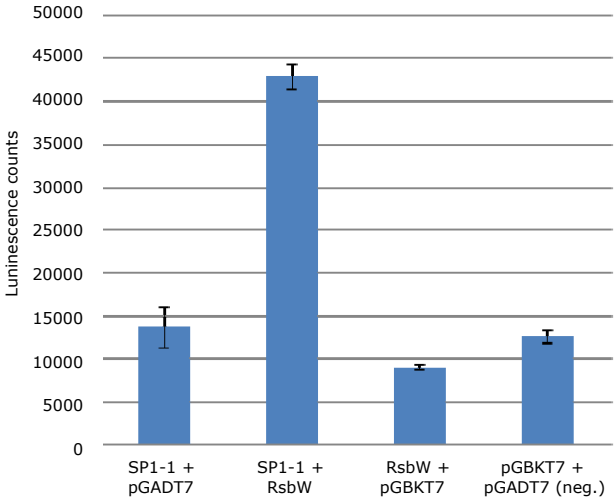

Figure 17 - Test for autoactivation of the interaction between SP1-1 and RsbW
To exclude autoactivation of bait and prey combinations from the Y2H screen, each prey plasmid was co-transformed with empty pGBKT7 vector and each bait plasmid with empty pGADT7 vector. The transformants were grown on selective plates deficient in tryptophan and leucine (SD/-leu-trp) for positive transformants, and deficient in tryptophan, leucine, adenine and histidine (SD/-leu-trp-ade-his) for putative interactions. They were then examined by ß-galactosidase quantification. Clones were cultivated in liquid SD/-leu-trp oN at 28 °C, and diluted to OD_{600nm}: 0.1. An equal volume of Beta-Glo® Reagent (Promega) was added, the mixture was incubated for one hour at RT and luminescence counts were measured. As negative control the interaction of the combination of the empty bait (pGBKT7) and prey (pGADT7) vector was used. Error bars represent standard error of 3 replicates.

Direct plating of transformants onto nutritionally deficient medium (SD/-leu-trp-ade-his) represents a very stringent condition, which only permits yeast cells with strong interactors to grow. Additionally, all transformants were analyzed under less stringent conditions to detect possible weak interactions and to exclude spurious autoactivity. After growing the yeast colonies on SD/-leu-trp plates and picking several random colonies, resuspending them in water and dropping them out, they were grown again on SD/-leu-trp and SD/-leu-trp-ade-his. With this approach the same results could be obtained and no further weak interactions were detected.

3.4.4 The role of kinase RsbW in *S. aureus*

RsbW, identified as a target protein of SP1-1 in *S. aureus*, is a serine-kinase with an important role in transcription regulation via an alternative transcription factor. In eubacteria promoter recognition is accomplished by a sigma factor, which can bind the DNA dependent RNA polymerase core enzyme, thus forming the holoenzyme and initiating transcription (Campbell et al., 2002; Pane-Farre et al., 2009). Additionally to the essential sigma factor A, responsible for house-keeping transcription, the cells usually possess a number of alternative sigma factors with different promoter specificities. With these, the bacteria can adapt to different environmental conditions with changes of their transcription patterns (Gruber and Gross, 2003). One of these is the stress dependent alternative transcription factor Sigma B (SigB). Its regulatory system is best characterized in *B. subtilis*. However, within this system the key domains and the core mechanisms of regulation and response are strongly conserved in related gram-positive bacteria, including *S. aureus* (Gruber and Gross, 2003; Senn et al., 2005; van Schaik et al., 2005; Hecker et al., 2007). For *S. aureus* not only the *sigB* operon, with its gene elements *sigB*, *rsbW* and *rsbV,* is extremely similar to that of *B. subtilis* but also the upstream corresponding phosphatase *rsbU*.

For the regulation of SigB, RsbW, which is active as a homodimer, plays an important role as an anti-sigma factor element (Miyazaki et al., 1999; Delumeau et al., 2002). Under normal conditions this anti-sigma factor is bound to SigB, by what the sigma factor is not able to interact with the RNA polymerase core enzyme and the transcription of the downstream, stress related genes is prevented (Figure 18).

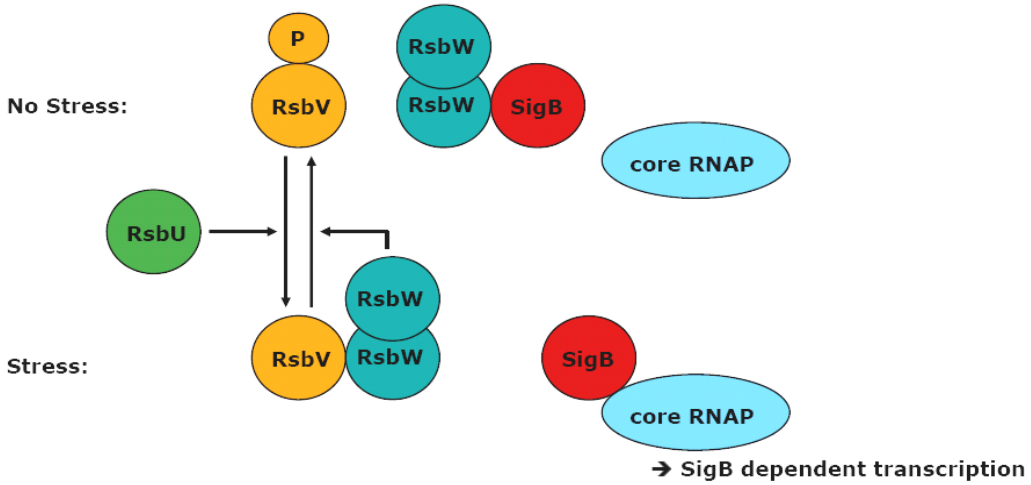

Figure 18 - The role of RsbW in regulation of transcription factor Sigma B
The RsbW homodimer regulates Sigma B (SigB) dependent transcription by a partner switching model. Under normal conditions it is bound to the transcription factor SigB and prevents its binding to the RNA polymerase core enzyme (core RNAP) and thereby inhibits transcription. Under stress conditions, RsbW binds to its second partner, RsbV that is phosphorylated by the RsbW serine-kinase. SigB is released, can bind to the RNA polymerase core enzyme and starts SigB dependent transcription. Under these stress conditions phosphatase RsbU dephosphorylates RsbV what leads again to binding of RsbW to RsbV and release of the transcription factor from the kinase. Figure created in accordance to van Schaik et al. (2005) and Pane-Farré et al. (2009).

Additionally, RsbW can perform a partner switching (Senn et al., 2005). Its binding to SigB is in competition to the binding to RsbV, the substrate which can be phosphorylated by RsbW at the serine residue at position 57 (Pane-Farre et al., 2009). As soon as RsbV is phosphorylated, the binding to RsbW is inhibited and the kinase can bind and inactivate the transcription factor. Under stress conditions or under the influence of certain environmental stimuli such as heat shock, addition of $MnCl_2$, NaCl or alkaline shock, RsbW binds to the non-phosphorylated RsbV and releases the transcription factor (Figure 18). SigB thereupon interacts with the core RNA polymerase, which leads to the transcription of the downstream stress related genes. Under these stress or stimulated conditions, RsbU acts as a further part of this dynamic system, namely by dephosphorylation of RsbV (Figure 18). This again leads to binding of RsbW to RsbV and release of the transcription factor from the kinase (Pane-Farre et al., 2009). There is also evidence that in *S. aureus*, unlike in *B. subtilis*, SigB does not only trigger stress dependent transcription but also general regulatory functions in cell wall metabolism, membrane transport processes and virulence. The affected genes differ between different environmental stimuli (Pane-Farre et al., 2009).
Perturbation of this regulatory network can have strong effects on gene and protein expression patterns. This has already been shown for a number of stress factors, such as heat or salt stress or the addition of chemicals like H_2O_2 or paraquat (Hecker et al., 2009). Antimicrobial agents or long chain fatty acids can also increase SigB dependent stress related transcription of staphyloxanthin and further factors that influence membrane stabilization (Kenny et al., 2009). Such altered gene expression by enhancement or reduction of SigB dependent gene expression can severely affect the fitness of the bacteria. For example, extracellular proteases - by influencing SigB – can inhibit protein-dependent biofilm formation in *S. aureus* and thereby decrease the survival rate (Marti et al., 2009). On the other hand, the antibiotic vancomycin, for example, can even enhance cytotoxicity by SigB dependent transcription in resistant strains (Chen et al., 2011a). It becomes obvious that influencing SigB activation or inactivation by an intervention into the regulatory mechanism of the regulon, can have multiple and possibly also severe effects on the growth or infectivity of the bacteria. Due to this, the interaction between RsbW and SP1-1 and the influence on its function were analyzed.

3.4.5 Recombinant expression of RsbW, RsbV and SigB

For analysis of the impact of SP1-1 on the function of RsbW, the serine-kinase, its natural substrate RsbV and the transcription factor SigB had to be expressed recombinantly. The production of RsbW was done in *E. coli* as 6x His-tagged fusion protein. For expression of the kinase, the coding sequence was amplified from the Y2H shuttle vector pAD-Gate2. It was cloned into expression vectors with either N- (pDest17) or C-terminal (pET-Dest42)

6x His-tag. Analysis of cell pellets by SDS-PAGE revealed high expression levels of pDest17:RsbW (Figure 19B) 18 hours after induction whereas for pET-Dest42:RsbW expression levels were negligible (Figure 19A).

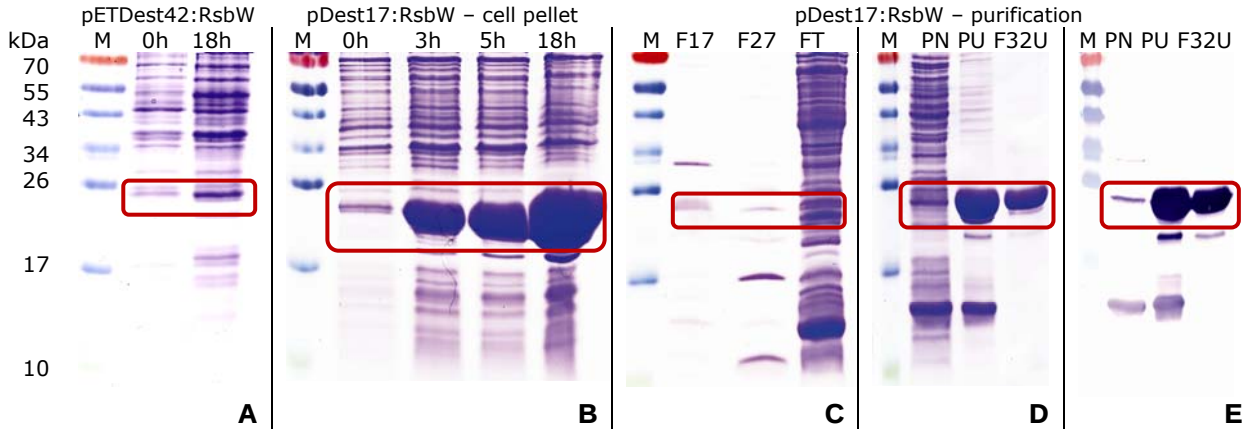

Figure 19 - Recombinant expression and purification of RsbW as 6x His-tagged protein
RsbW was inserted into pDest17 or pET-Dest42, recombinantly expressed in *E. coli* BL 21 (DE3) plys S and affinity purified under different conditions. Shown are Coomassie stained 15% SDS-PAGE (A – D) or western blot (E) analyses. RsbW containing bands are indicated by red boxes. M: molecular weight marker in kDa.
(A - B) Expression levels of recombinant RsbW after induction by 1 mM IPTG and 18 h growth at 30°C. Shown are analyses of cell pellets from 1 ml culture (0, 3, 5 or 18 h after induction). Cell pellets were resuspended in 50 µl SDS loading dye, shortly boiled and 1/5 Vol (10 µl) was loaded per lane. Expression from plasmids (A) pET-Dest42:RsbW or (B) pDest17:RsbW. (C-E) Analysis of RsbW during purification after protein extraction from 1l culture volume, expressed from pDest17:RsbW 18 h at 30°C. 10 µl of 1 ml eluted fractions from affinity chromatography or of 10 ml crude protein extracts were loaded per lane. (C) Fractions 17, 27 and the column flow through (FT) of affinity purification after protein extraction under native conditions. (D) Comparison of solubility of the eluted protein after extraction under native or denaturing conditions, using 4 M urea. Native protein extract (PN), protein extract from urea extraction (PU) and of fraction 32 of affinity purification after urea protein extraction (F32U). (D) Detection of recombinant RsbW, according to C, by western blotting and immunodetection of the 6x His-tag by Anti-Histidine-tagged protein mouse mAb OB05 (Calbiochem, Darmstadt, Germany).

The recombinant proteins expressed from pDest17:RsbW were extracted and purified under native conditions (Figure 19C). However, SDS PAGE analysis of the protein extract (Figure 19D, lane PN), eluted fractions (Figure 19, F17, F27) and column flow-through (Figure 19, FT) from affinity chromatography revealed a very low yield. It was assumed that most of the protein was stored in inclusion bodies. Neither expression at lower temperatures (30°C or 20°C) nor induction with lower amounts of IPTG (0.1 – 0.5 mM) could prevent the occurrence of a high portion of insoluble proteins. By treatment with 4 M urea, inclusion bodies could be broken down, denatured proteins were released (Figure 19D, lane PU) and could be purified (Figure 19D, lane F32U). The RsbW band was additionally detected by western blotting and immunodetection of the 6x His-tag (Figure 19E). Comparing the RsbW signals of natively (Figure 19E lane PN) with denaturing (Figure 19E lane PU) extracted proteins and eluted fractions from affinity purification after urea extraction (Figure 19E lane F32U) proved the result. Thus, after urea extraction and purification, the denatured protein would have to be refolded again by dialysis. Since the produced proteins should also be used for structural analyses of the SP1-1 – RsbW interaction, proper folding has to be considered as a critical point and a denaturing step is a risk regarding this.

Hence, although the production of kinase RsbW was successful, a second purification strategy was tested. RsbW, RsbV and SigB were produced from Strep-tagged plasmids, known for a higher amount of soluble protein expression. The plasmids pPRIBA1:RsbW, pPRIBA1:RsbV and pPRIBA1:SigB with the sequences of *rsbW, rsbV or sigB* from *S. aureus* COL ligated into pPRIBA1 at BsaI restriction sites, were kindly provided by Dr. J. Pané-Farré of the Institute of Microbiology at the Ernst Moritz Arndt-University of Greifswald (Greifswald, Germany). The plasmid pPRIBA1:RsbW was transformed into *E. coli* BL 21 (DE3) plys S and recombinant RsbW was expressed after induction with 1 mM IPTG for 2.5 h at 37°C. Protein was extracted and affinity purified by the Strep-tag. SDS-PAGE analysis of eluted fractions revealed a suitable amount of soluble protein of around 1 mg/ 100 ml culture volume (Figure 20A). By gelfiltration protein aggregates (Figure 20B, F8, F9) were separated from the active homodimeric form of RsbW (Figure 20B, F10, F11). Yield and purity of collected protein fractions after gelfiltration were analyzed by native PAGE analysis (Figure 20C) and only pure protein fractions without aggregates were used for further experiments (Figure 20C, F10).

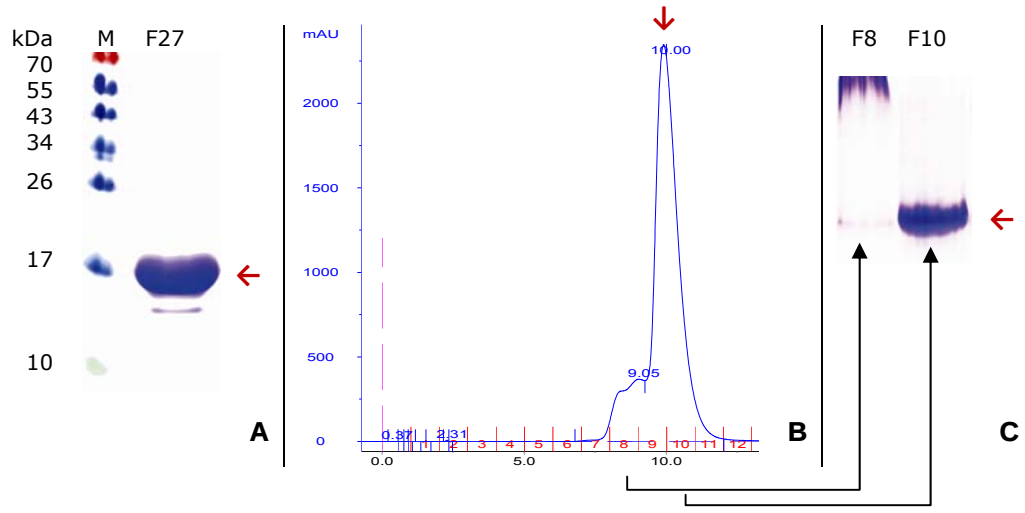

Figure 20 - Purification of Strep-tagged RsbW after expression from pPRIBA1:RsbW
RsbW in pPRIBA1:RsbW was recombinantly expressed in *E. coli* BL 21 (DE3) plys S for 2.5 h at 37°C after induction with 1 mM IPTG. Protein was extracted, affinity purified and protein aggregates were removed by gelfiltration. The RsbW containing non aggregated fractions/bands are indicated by red arrows. M: molecular weight marker in kDa. (A) Coomassie stained 15% SDS-PAGE analysis of RsbW containing fraction 27 after affinity purification by the Strep-tag. 10 µl of the eluted fraction were loaded. (B, C) Removal of protein aggregates by SEC with a superdex 75 column. (B) SEC chromatogram with aggregates in fractions 8 and 9 (F8, F9) and the RsbW homodimer in fractions 10 and 11 (F9, F10). Protein retention intensity was measured in milli Absorbance Units (mAU) at 280 nm (blue line). Fractions are indicated in red and the retention volume (in ml) in black at the x-axis. (C) Coomassie stained 15% native PAGE analysis of a RsbW aggregate containing fraction (F8) and the fraction with homodimeric RsbW (F10) after the SEC. 10 µl of fractions were loaded per lane.

Using the same protocol the natural RsbW substrate, RsbV and the transcription factor SigB were also recombinantly produced in *E. coli* by plasmids pPRIBA1:RsbV and pPRIBA1:SigB, respectively. The purified Strep-tagged proteins were stored in aliquots at -80°C until further experiments or directly used. They were used for testing the inhibition and binding ability of SP1-1 and the structural analysis of the peptide – kinase interaction by NMR.

3.4.6 Characterization of the SP1-1 – RsbW interaction

The identified strong interaction between SP1-1 and RsbW was analyzed regarding their structural interaction to elucidate the structural characteristics of the two partners that are important for binding. To analyze the relevance of this binding for the mode of action of SP1-1, the impact of the binding of SP1-1 on the kinase function was furthermore elucidated *in vitro* and *in vivo*.

3.4.6.1 Structural analysis of the interaction between SP1-1 and RsbW

The structural analysis of a binding event between an enzyme such as the RsbW kinase and its interaction partner such as SP1-1, can provide helpful knowledge about the interaction between both partners and the mechanism of interaction can be elucidated. With this knowledge targeted engineering of the peptide can be conducted in regard to binding efficiency. As there was a strong interaction between peptide SP1-1 and RsbW of *S. aureus* identified within the Y2H screen, the interaction of those two partners should be investigated by NMR analysis and structurally important domains of both binding partners should be identified.

To analyze binding domains of SP1-1 at the kinase by NMR, RsbW was recombinantly produced in *E. coli* and purified as explained in chapter 3.4.5 with ^{15}N as the single nitrogen source in the cell culture medium (^{15}N-M9 medium). The ^{15}N labeled protein was analyzed by NMR, with titration of SP1-1 to the sample during the measurement. Thereby conformational changes induced by the binding of the peptide should be observed. Unfortunately, the NMR did not provide an analyzable signal. Presumably RsbW is not stable in solution, as it not only forms dimers as the active form but also aggregates of much bigger size. The aggregating behavior of RsbW was already observed during purification and aggregates had to be removed by gelfiltration (Figure 20). Thus, several attempts were made to prevent aggregate formation and stabilize RsbW in solution, before further NMR measurements together with SP1-1 could be conducted.

Firstly, to get more information about the stability of RsbW in solution and about changes in stability by the use of stabilizing additives, melting curve measurements were performed. To record the melting curves, a fluorescent dye was used, adhering non-specifically to hydrophobic protein regions. This leads to an enhanced fluorescence when the protein unfolds and hydrophobic parts are exposed. Fluorescence intensity of the dye was recorded while the protein sample was stepwise heated from 25 to 95°C. With this approach, the melting temperature of the protein can be determined at the inflection point of the resulting melting curve and the stability can be deducted.

For other analyses regarding influence of SP1-1 on RsbW, recombinantly produced protein was used that was stored in aliquots at -80°C prior to the subsequent

experiments. It was tested whether the freezing and thawing of the protein caused the instability. Hence, RsbW stored at -80 °C prior to the experiment, or a fresh preparation of RsbW was used for the melting curve measurements and the behavior of both was compared. Furthermore, the stabilizing influence of nucleotide analogues on the ATP/ADP binding pocket and thereby on the whole protein was studied. Additives, such as ADP or alternatively 5'-Adenylylimidodiphosphate (AMPPNP), an ATP derivate with assumed higher affinity than ADP but without cleavability like ATP, were incubated at 4°C with freshly purified RsbW protein before the melting curves. With the obtained information about stabilizing conditions, RsbW should be stabilized in solution for a next NMR analysis. As control the natural substrate of RsbW, the protein RsbV, was used. This protein did not show aggregation during purification. It was used after freezing to -80°C and thawing prior to the measurement. RsbV showed typical melting curves with an increase in the fluorescence signal starting at ~45°C, reaching maximum intensities at 65°C. The signals slowly decreased, due to disintegration of the dye, and the baseline was reached again at around 85 – 95°C (Figure 21B). In contrast, atypical melting curves were observed for RsbW. The melting curves of freshly purified RsbW (50 – 200 µg protein, dye concentration: 0.5 – 5 fold) are shown in Figure 21A as a representative and typical example for all obtained RsbW melting curves. The curves started with high fluorescence intensities at initial low temperatures (beginning from 25 °C). Then they decreased until 65°C. The signal then increased again with a maximum at around 78°C and slightly decreased when the temperature approximated 95°C (Figure 21A). The shape of the melting curve was not changed by any of the used conditions or additives. So, neither the use of freshly purified protein instead of frozen and thawed preparations nor the use of nucleotide additives like ADP and AMPPNP could stabilize RsbW.

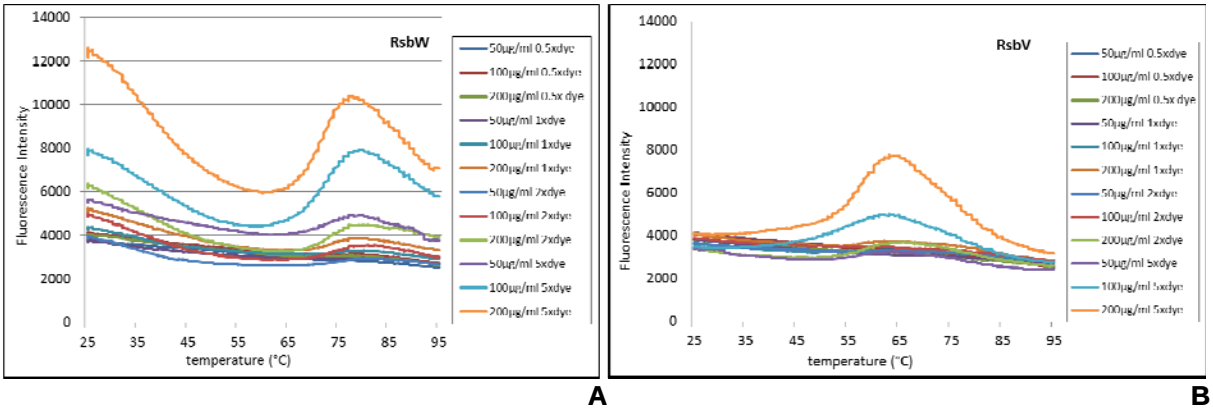

Figure 21 - Melting curves of RsbW and RsbV
Protein preparations of RsbW (A) or RsbV (B) in different concentrations (50, 100, 200 µg/ml) were used for melting curve measurements with different concentrations of hydrophobic protein dye SYBR@ Orange (0.5, 1, 2, 5 fold concentrated). Fluorescence intensities of the dye were monitored during stepwise slow heating of the proteins from 25 to 95°C.

The primary amino acid sequence of RsbW does not include any lengthy hydrophobic parts or clusters that could be faced outside the protein and cause such behavior of the

fluorescent dye (Supplementary Figure 11). Thus, those atypical melting curves were assumed to be caused by the aggregating behavior of RsbW.

Due to this unexpected melting behavior we decided to have a closer look at the aggregating behavior of RsbW samples using different conditions and different additives. RsbW was separated by gelfiltration after the incubation with additives or under different pH conditions. Subsequently corresponding masses of retending protein peaks were detected by a light scattering detector. ADP, AMPPNP, SP1-1 or SP1-13 were used as additives. Also a co-purification approach with RsbV was tested, for which purified RsbV protein was added to RsbW in a molar ratio of 1:1 after affinity chromatography and incubated 2 h on ice before the next step of purification. Alternatively, buffer exchange was performed. Conditions were changed from the usually used buffer with pH 8 (25 mM Tris, 150 mM NaCl) to a buffer with pH 5 (50 mM Na_2HPO_4, 150 mM NaCl), as for sigma factor regulating proteins from other organisms stability at lower pH values had been reported (Etezady-Esfarjani and Wuthrich, 2004). The use of SP1-1 or SP1-13 or low buffer pH did not increase stability of RsbW. In contrast, under those conditions a rapid precipitation of the samples occurred (Figure 22, samples 4, 5, 7).

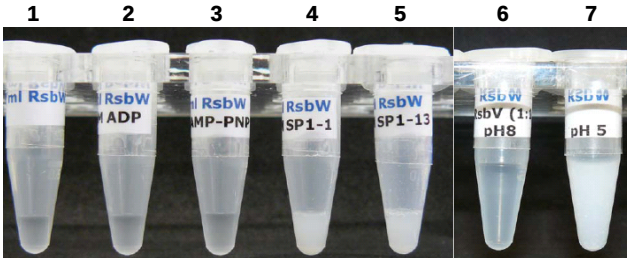

Figure 22 - RsbW incubated with additives for gelfiltration and light-scattering detection
RsbW was recombinantly produced from pPRIBA1:RsbW, purified and used in a concentration of 2 mg/ml with additives. The sample should be conducted to SEC separation and light scattering detection. (1) RsbW, pH 8; (2) RsbW + 2 mM ADP, pH 8; (3) RsbW + 2 mM AMPPNP, pH 8; (4) RsbW + 0.5 mM SP1-1, pH 8; (5) RsbW + 0.5 mM SP1-1, pH 8; (6) 2 mg/ml RsbW, co-purified with 1.3 mg/ml RsbV, pH 8; (7) RsbW, pH 5. Samples 4, 5 and 7 show precipitation of the proteins.

From the subsequent SEC separation and light scattering detection of the non precipitated samples, retending peaks with masses of 40 kDa of homodimeric RsbW complexed with nucleotide analogues, or of 50 kDa for dimeric RsbW complexed with RsbV should be obtained. Earlier retending peaks with bigger masses, containing RsbW aggregates, should be prevented by the additives or the co-expression approach. The samples with either no additive, ADP, AMPPNP or with co-purified RsbV, showed all similar SEC and mass chromatograms. As a representative and typical example, the results from co-purification of RsbW with RsbV are given in Figure 23. The main peak (M), with a retention volume of 15 - 19 ml, reflected partly dimeric RsbW, complexed with the 12 kDa protein RsbV (50 kDa). But the formation of the upstream retending shoulder peak (S), with 12.8 - 15 ml retention volume, could not be avoided by the co-purification. The earlier retending shoulder peak (S) was in fact smaller than the main peak, but masses of not only tri- or tetramers were calculated but even aggregates

bigger than 124 kDa (Figure 23B). Even the majority of the main peak (M), consisted partly of aggregates with bigger masses compared to the target mass (Figure 23B). The later retending peak (22 - 24.5 ml) is due to salt components from the buffer (Figure 23A).

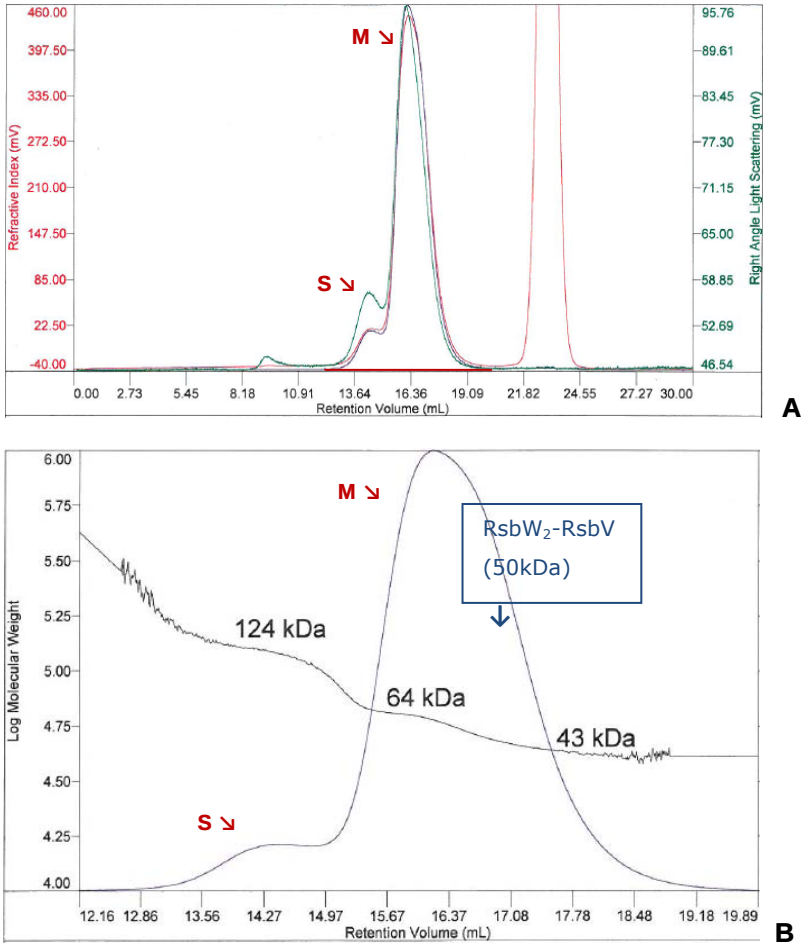

Figure 23 - SEC chromatogram and correlating light scattering of RsbW with co-purified RsbV
After recombinant production of RsbW and co-purification with RsbV in a molar ratio of 1:1 the sample was incubated at 4°C oN and separated again on a superdex 200 gelfiltration column including a downstream light scattering detector (LSD). (A) The chromatogram of the SEC and the LSD shows a main peak (M) with retention volume of 15 – 19 ml with a preceding shoulder peak (S) retending between 12.8 – 15 ml. The later retending peak (22 – 24.5 ml) is due to salt components of the buffer. Retention volume in ml (black) is indicated on the x-axis. Refractive Index (red) and right angle light scattering (green) are indicated in mV on the y-axis (B). By light scattering measured masses show that the main peak (M) consisted of RsbW homodimers, complexed with one molecule of RsbV ($RsbW_2$-RsbV), with a size of 50 kDa and bigger aggregates. The shoulder (S) at earlier retention volumes consisted of protein aggregates (average size 124 kDa). Retention volume in ml is indicated on the x-axis and molecular weight on a log-scale on the y-axis.

Successful stabilization of related proteins from *Staphylococcus sp.* or related *Bacillales* bacteria was reported by recombinant co-expression with the transcription factor as an *in vivo* pre-assembled complex (Campbell and Darst, 2000; Campbell et al., 2002). Therefore, a co-expression approach of RsbW with SigB in *E. coli* was attempted to prevent RsbW from aggregation.

For co-expression with RsbW the transcription factor SigB had to be sub-cloned from pPRIBA1:SigB (f1 origin) into a plasmid with a different kind of origin of replication. pCDF11 with N-terminal 6x His-tag and untagged pCDF13 (kindly provided by Dr. A.

Geerlof, Protein Expression and Purification Facility, Helmholtz Zentrum München, Munich, Germany) were used. After amplification of *sigB* from pPRIBA1:SigB and restriction with NcoI and HindIII, the gene was ligated into pCDF11 and pCDF13. The resulting plasmids pCDF11:SigB and pCDF13:SigB were expressed in *E. coli*. Unfortunately, after induction of SigB expression in the mid-logarithmic phase, bacterial growth decreased within 5 h and no recombinant protein could be detected by SDS-PAGE analysis. Due to similar findings of other researchers (Campbell and Darst, 2000), it was assumed that SigB from *S. aureus* had toxic effects on *E. coli* during expression. When SigB and RsbW were expressed from double transformed *E. coli* (pPRIBA1:RsbW and pCDF11/pCDF13:SigB) the toxic effect of SigB was partly prevented by binding to RsbW. However, the expression levels of SigB were still very low (Figure 24A). The attempt to isolate at least a small amount of the SigB - RsbW complex by affinity purification of the 6x His-tag from pCDF11:SigB yielded only negligible amounts of protein in the correct mass range. Additionally, within the isolated proteins a lot of false positive protein bands occurred that were co-purified unspecifically during the 6x His-tag purification (Figure 24B and C). The presence of SigB protein was additionally verified by western blotting and immunodetection of the 6x His-tag (Figure 24C).

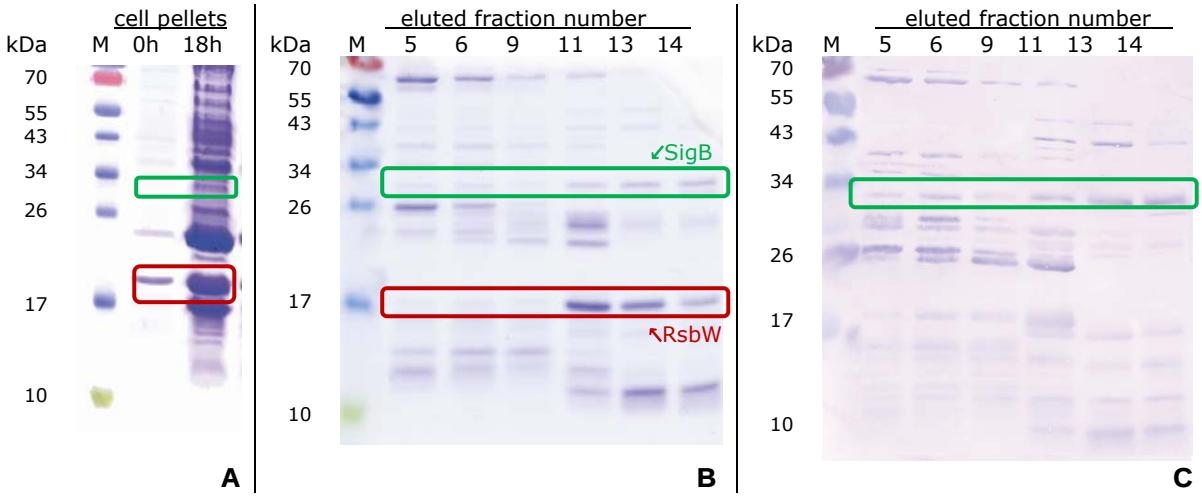

Figure 24 – Analysis of expression levels and affinity purified eluted fractions of co-expressed SigB and RsbW
N-terminal 6x His-tagged SigB (expressed from pCDF11:SigB) and RsbW (expressed from pPRIBA1:RsbW) were co-expressed in *E. coli* BL 21 (DE3) plys S. Protein was extracted and SigB-RsbW complexes were affinity purified by the 6x His-tag by FPLC. SigB (29.6 kDa), indicated by green boxes and RsbW (19 kDa), indicated by red boxes were analyzed by reducing SDS-PAGE analysis and Coomassie staining or western blotting and immunodetection of *E. coli* cell pellets during expression, or of eluted fractions after affinity chromatography. M: molecular weight marker in kDa. (A) Cell pellets of 1 ml samples of cell culture, directly (0 h) and 18 h after induction of recombinant protein expression by 1 mM IPTG. Cell pellets were resuspended in 50 µl and 10 µl were loaded per lane of 15% reducing SDS-PAGE. (B + C) Analysis of eluted fractions of affinity chromatography. 1 ml fractions were concentrated to 100 µl and 10 µl were used for separation by reducing 15% SDS-PAGE. (B) Gels were Coomassie stained or (C) subsequently western blotted and the 6x His-tag was immunodetected by Anti-Histidine-tagged protein mouse mAb OB05 (Calbiochem, Darmstadt, Germany).

After affinity purification, fractions containing at least a small amount of SigB (29.6 kDa) and additional RsbW (19 kDa) were selected (Figure 24B and C, fractions 11, 13 and 14). The collected samples were subjected to SEC separation and light scattering detection,

like for the above described samples. But peak separation and mass detection failed, as the signal was not analyzable due to the low amount of protein and a diffuse signal from many small peaks. They displayed mainly false-positive purified proteins and no mass could be defined due to the big number of diffuse peaks.
Hence, it was not possible to stabilize RsbW in solution by copurification with additives or its substrate or by co-expression with SigB. Therefore, the structural interaction between SP1-1 and RsbW could not be elucidated within this study.

3.4.6.2 SP1-1 and related peptides inhibit the function of RsbW in vitro

To test the relevance of the strong interaction between SP1-1 on RsbW function *in vitro*, inhibition assays regarding the kinase phosphorylation activity of its natural substrate RsbV and the binding potential to transcription factor SigB were tested. For the inhibition assays, recombinant kinase RsbW, substrate RsbV and transcription factor SigB were used.
The phosphate residue, attached to RsbV by RsbW, changes isoelectric point and size of the phosphorylated protein (RsbV-P). Hence, RsbV-P shows elongated running distances during separation by native PAGE as compared to the non-phosphorylated form RsbV. The influence on this protein pattern of SP1-1 was tested. SP1-13 was also used for the experiment. This AMP belongs to the same structural group as the RsbW interacting SP1-1. It differs mainly by several phenylalanine residues in its sequence (Table 1) and shows higher activity against *S. aureus* (Table 2). Again SP8 was used as control with no activity against *S. aureus*. Different amounts of peptides (0.5, 1, 2, 4, 6, 8 µg) or only buffer were incubated with the recombinant RsbW. The inhibition of the following phosphorylation reaction of added RsbV by RsbW was detected by native PAGE analysis. Dose dependent inhibition of the enzymatic reaction could be detected for SP1-1 and SP1-13. The band of RsbV-P on the native polyacrylamide gel faded with increasing SP1-1 concentrations, starting at 4 µg SP1-1. Additionally, the band of the non-phosphorylated RsbV re-appeared when 4 – 8 µg SP1-1 were used (Figure 25). Furthermore, the RsbW – RsbV indicating double band on the gel disappeared starting with an applied amount of 1 µg SP1-1. SP1-13 with 10 fold lower MIC (1 µg/ml) for *S. aureus* compared to SP1-1 (10 µg/ml) also showed a bigger impact on the kinase function of RsbW. For SP1-13 the complex indicating double band and the RsbV band faded already when 0.5 µg were used and the band of RsbV re-appeared (Figure 25). When high amounts of SP1-13 (4 – 8 µg) were used, a precipitation of the reaction mixture occurred. This partly prevented the protein samples from migration into the gel during electrophoresis. The inhibition of RsbW phosphorylation activity could not be detected for peptide SP8.

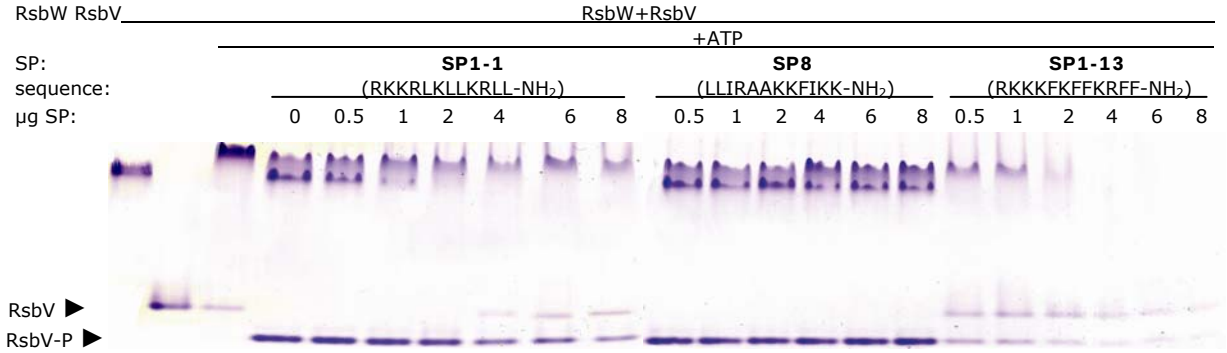

Figure 25 - Inhibition of the phosphorylation reaction of RsbW by SP1-1 and SP1-13
Recombinant RsbW (0.1 µM) was pre-incubated with 0.5 – 8 µg of SP1-1, SP8 or SP1-13 for 15 min. After the addition of recombinant substrate RsbV and 2 mM ATP, phosphorylation was carried out for 5 min. The reaction was stopped by the addition of 50 mM EDTA and incubation on ice and the samples were separated by 15% native PAGE and Coomassie stained. The inhibition of the phosphorylation reaction can be shown by the disappearance of the phosphorylated substrate (RsbV-P) and the re-appearance of the unphosphorylated substrate (RsbV) on the Coomassie stained gel.

The inhibitory potential was also compared to the SP1 derivates SP1-3, SP1-7, SP1-12 (Supplementary Figure 10A) with different MIC ranges (SP1-3: 100 µg/ml, SP1-7: >100 µg/ml, SP1-12: 5 µg/ml). Comparing these data to that of SP1-1, SP1-13 and SP8 the inhibitory potential could be associated with activity against *S. aureus* (Supplementary Figure 10B).

The ability of SP1-1 to influence the binding of RsbW to the transcription factor SigB was also analyzed. SP8 was again used as peptide with no activity against *S. aureus*. In addition to SP1-1, the related SP1 derivates SP1-3 and SP1-13 with their different MICs against *S. aureus* (SP1-1: 10, SP1-3: 100, SP1-13: 1 µg/ml, Table 2) were included. Again, the peptides or only the same volume of buffer were pre-incubated with the kinase, followed by an incubation step with SigB and analysis by native PAGE. The used low amounts of transcription factor were not visible on the Coomassie stained gel. However, the complex formation of SigB and RsbW resulted in a mobility shift and a double band when both proteins were incubated together (Figure 26, lane 3).

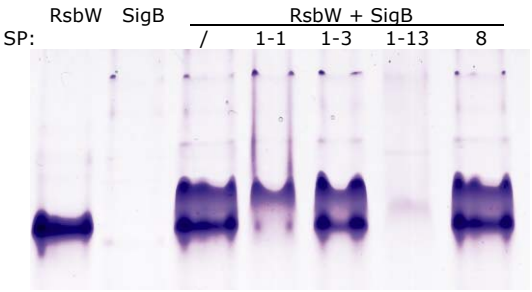

Figure 26 - Inhibition of complex formation between RsbW and SigB by different peptides
Recombinant RsbW (0.1 µM) was pre-incubated with 6 µg SP1-1, SP1-3, SP1-13 or SP8 for 15 min. After the addition of recombinant transcription factor SigB (0.05 µM), the complex formation of RsbW and SigB was proceeded further 5 min. The reaction was stopped by the addition of 50 mM EDTA and incubation on ice. The samples were separated by 15% native PAGE and Coomassie stained. The used amount of SigB cannot be detected by Coomassie stain but the complex formation can be observed by appearance of a shifted RsbW double band. SP1-1 and SP1-13 disturbed the RsbW – SigB complex. SP1-3 and SP8 had no influence on the complex formation.

After pre-incubation with peptide SP1-1, the RsbW-SigB-complex indicating double band was disturbed. The upper, complex associated band showed decreased intensity. The lower band, mainly associated to free RsbW, disappeared (Figure 26, lane 4). Thereby, the inhibition of the complex formation by SP1-1 could be shown.
SP1-13 abolished both bands (Figure 26, lane 6). In contrast, the peptides SP1-3 and SP8 did not interfere with the kinase and the RsbW-SigB complex was formed and could be detected on the gel (Figure 26, lanes 5 and 7). So, inhibition ability of the RsbW – SigB complex formation was again correlated with activity against *S. aureus*.

3.4.6.3 RsbW is an in vivo *target of SP1-1*

To proof the relevance of the inhibitory influence of SP1-1 on RsbW *in vivo*, antibacterial activity tests were carried out with *S. aureus* RN1HG and its mutant strains of the *sigB* operon. The strains were kindly provided by Dr. S. Engelmann from the Institute of Microbiology, Ernst-Moritz-Arndt-University Greifswald (Greifswald, Germany). In the RN1HG mutant strain *ΔsigB*, the operon *sigB*, containing the genes *rsbW*, *rsbV* and *sigB* was deleted. The upstream located gene of phosphatase *rsbU* was also impaired by an 11 bp deletion within the coding region (Bruckner, 1992; Kullik et al., 1998; Pane-Farre et al., 2006). For comparison, the original RN1HG strain (wt) and a complemented mutant (Δ*sigB* complemented) with episomal generated complementation of the *ΔsigB* mutation were used. The mutant strain Δ*sigB* complemented was generated by the use of a pPB473 plasmid derivate (Bruckner, 1992). Microbroth dilution assays were carried out as described in chapter 2.2.10.6 with 0 (buffer), 0.5, 5, 10, 40 or 100 µg/ml SP1-1 and the three strains (RN1HG wt, *ΔsigB* and *ΔsigB* complemented*)*. SP10-2 served as control for higher activity (MIC: 1 µg/ml for strain 90857) than SP1-1 (MIC: 10 µg/ml for strain 90857) and a putative different mode of action and SP8 served again as control with no detectable anti-*Staphylococcus* activity. The control peptides SP10-2 and SP8 showed no differences in MIC values between the 3 strains, as expected (Supplementary Table 3). The obtained OD_{600nm} values after 18 hours of SP1-1 treatment were compared among the strains (Figure 27). In RN1HG wild type strain (wt) and in the complemented mutant (Δ*sigB* complemented) 100 µg/ml SP1-1 could inhibit bacterial growth and the OD_{600nm} values decreased to 9.4 and 7.9%. In the deletion mutant *ΔsigB* only very marginal growth inhibition of less than 30% was detectable with the same SP1-1 concentration (Figure 27A, B: highlighted in yellow). This indicates influence of SP1-1 on RsbW *in vivo*.

However, the growth inhibition of the *S. aureus* RN1HG strains was generally much lower than expected from the previous tests with strain 90857 (Table 2). SP1-1, that showed MIC / MBC of 10 / 20 µg/ml for *S. aureus* 90857, was active at 100 µg/ml with strain RN1HG, which was the highest tested concentration (Figure 27B). SP10-2 with a previous activity of 1 µg/ml showed 5-fold higher MIC values of 5 µg/ml (compare Table 2 and Supplementary Table 1).

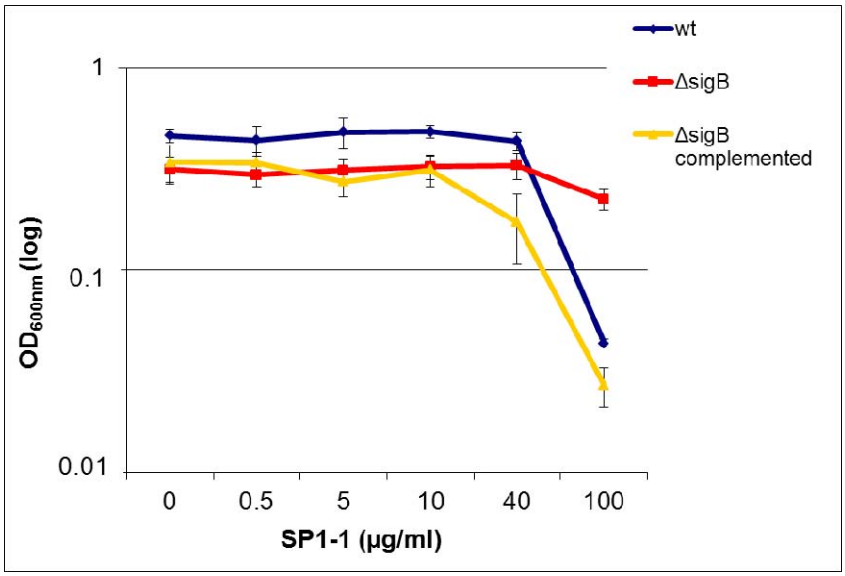

A

SP1-1 (µg/ml) → *S. aureus* strain ↓		0µg/ml	0.5µg/ml	5µg/ml	10µg/ml	40µg/ml	100µg/ml
RN1HG wt	OD_{600nm}	0.462	0.439	0.480	0.483	0.434	0.044
	%growth	100	95	103.8	104.5	93.8	9.4
RN1HG *ΔsigB*	OD_{600nm}	0.314	0.296	0.311	0.324	0.329	0.225
	%growth	100	94.4	99.2	103.2	104.7	71.6
RN1HG *ΔsigB* complemented	OD_{600nm}	0.343	0.340	0.273	0.313	0.173	0.027
	%growth	100	99.4	79.9	91.7	50.5	7.9

B

Figure 27 - Antibacterial activity of SP1-1 against *S. aureus* RN1HG *sigB*-regulon mutant strains
S. aureus RN1HG (wt), the deletion mutant of this strain of operon *sigB* and upstream *rsbU* (*ΔsigB*) and the complemented mutant (*ΔsigB complemented*) were used for antibacterial activity tests with SP1-1 by incubation of 10^5 bacteria cells with 0, 0.5, 5, 10, 40 or 100µg/ml SP1-1. The cultures were incubated at 37°C for 18 h and growth was determined by OD_{600nm} measurement. (A) Bacterial growth on an OD_{600nm} log-scale after treatment with different SP1-1 concentrations. (B) Corresponding OD_{600nm} measurements and calculated percentage growth normalized to 100% growth of buffer treated bacteria. The shown values represent mean values of 4 replicates. Error bars represent standard deviation of the 4 replicates.

4 Discussion

The rise of multi-resistant pathogenic microorganisms urgently necessitates new antimicrobial agents to cope with the problem of severe infections and massive costs for the health care systems world-wide (Livermore, 2004; Wilke, 2010). Similar problems occur in plant protection, where pathogenic microorganisms are the major cause of crop losses. As a consequence, the ongoing use of pesticides unavoidably leads to environmental pollution, carry overs into food-production and processing (Flury, 1996; Dabrowski et al., 2002; Gonzalez-Rodriguez et al., 2011) and to the emergence of increasingly resistant pathogen strains (Marcos et al., 2008). Antimicrobial peptides are deemed alternatives to the established antibiotics because of their often differing mode and site of action thus making it more difficult for the bacteria to acquire resistance. AMPs have been considered as mostly membrane active agents for a long time (Sahl et al., 1987; Kordel et al., 1988; Dalmau et al., 2002; Shai, 2002). However, recent studies have demonstrated that there are a number of possible different targets addressed, occasionally at the membrane, but also at intracellular sites (Otvos et al., 2000; 2005; Hancock and Sahl, 2006; Andres, 2011). The numerous AMPs, sharing the features of short length, an overall positive net charge and high portions of hydrophobic and cationic amino acid residues can thereby act in many different ways. As the *de novo* designed antimicrobial peptides showed high activities against plant pathogens and multi-resistant *S. aureus*, their possible target sites were analyzed and their mode of action was elucidated within this study.

4.1 Activity against multi-resistant *Staphylococcus aureus*

The human pathogen *Staphylococcus aureus* represents a particular problematic bacterium with an increasing number of resistances to common antibiotics. Most of the strains acquired multiple resistances against numerous different antibiotics over the years. They are responsible for outbreaks world-wide and cause a number of severe illnesses. Due to this fact, there is an urgent necessity for new antibiotic agents (Chambers and Deleo, 2009).

Previous to this study the *de novo* designed antimicrobial peptides have been shown to display a broad range activity against a number of plant pathogenic bacteria, including several *Pseudomonas* strains, *Clavibacter michiganensis*, *Xanthomonas vesicatoria* and *Pectobacterium carotovorum*. Especially SP10 and its derivates were highly active (Supplementary Table 1). To test the activity of our AMPs also against the important human pathogenic bacterium *S. aureus,* a clinical isolate was used, which displayed a

high level of multiple antibiotic resistances against methicillin, penicillin, oxacillin, erythromycin, clindamycin, gentamycin, amikacin, ciprofloxacin and moxifloxacin. Interestingly, during this study several peptides were identified, especially derivates of SP1 and SP10, with high activity against this multi-resistant strain (Table 2). SP1-13, SP10-2, SP10-4 and SP10-8 have to be highlighted as they showed activities at only 1 µg/ml. But also the antibacterial activities of SP1-11, SP1-14, SP10-4 (MIC: 2.5 µg/ml) as well as of SP1-12, SP10, and SP10-5 (MIC: 5 µg/ml) remain within low micromolar range, as 1 µg/ml equals roughly 1.5 µM of the 12 amino acid peptides. Additionally, peptides that show moderate activity, like SP1 (40 µg/ml) and SP13 (20 µg/ml) are not negligible in comparison to examples of other peptides applied against *S. aureus* and other highly resistant bacteria. Recently the newly characterized antimicrobial peptide BmKbpp, for example, was published as a potential agent for therapeutic applications. It showed strong antibacterial activity in the range of 2.3 – 68.3 µM against several gram-positive and gram-negative bacteria including some antibiotic-resistant strains (Zeng et al., 2011). Several other AMPs and their derivates, mainly derived from human defensins, with similar ranges of activity, are also currently under investigation as anti-*Staphylococcus* candidates. For example, GF-17, derived from the major antimicrobial region of human LL-37. It has a MIC value for *S. aureus* of 7.5 µM (Wang et al., 2011), comparable to SP1-12, SP10, and SP10-5 from this study. Furthermore, the recombinantly produced peptide hPAB-ß, designed from the natural model human ß-defensin 2, yielded MIC values of 8 - 64 µM against 22 tested different MRSA isolates and is therefore a potential antimicrobial agent against MRSA infections (Chen et al., 2011b). Human α-defensin 5 (HD5) as well as its oxidized form HD5ox exhibit high anti-*Staphylococcus* activity in the low micromolar range, with bactericidal activity for $HBD5_{ox}$ at 3 – 4 µM (Wanniarachchi et al., 2011). In contrast, the antibacterial activity against *Staphylococcus sp.* of all HD5 disulfide array mutants, deleted in one or all of the intramolecular three disulphide bridges through an exchange of cysteine for serine residues, was attenuated within the tested range (Wanniarachchi et al., 2011). This demonstrates that small differences in peptide structures can have important influence on activity, what was also identified in this study. For example, derivates of SP1 exhibit very similar sequences (Table 1) but MIC values ranged from 1 µg/ml for SP1-3 to no detectable activity for SP1-10 (Table 2). Regarding the differences between *S. aureus* strains and their susceptibility to antimicrobial peptides Midorikawa and coworkers (2003) tested a total of 44 *S. aureus* clinical isolates, including 22 MRSA strains for their sensitivity against human ß-defensins and the AMP CAP18, expressed in keratinocytes. The resistant strains tendentially showed less sensitivity to the antimicrobial peptides, but a synergistic effect of the peptides applied could be observed (Midorikawa et al., 2003).

From these data it can be concluded that the activity range against MRSA of our newly designed peptides is at a promising high level and further investigation and development of the most potent AMPs is very reasonable. With regard to previously analyzed toxicity (Supplementary Table 1) there are few representatives (SP10, SP10-8, SP13, SP13-2, SP13-5, SP13-12, SP13-14) that should be regarded with care as they showed hemolytic activity at 100 and 50 µg/ml. However, all other AMPs with high anti-*Staphylococcus* activity (Table 2) had a very low or no detectable toxicity to erythrocytes. Having several AMP candidates with moderate to high antibacterial activity against a highly resistant *S. aureus* strain and low toxicity on hand is a very promising starting point for developing new generations of peptides with improved activity of single peptides or also of synergistic combinations, when mode and site of action have been elucidated.

Hence, for the representatives of the new AMPs with broad range and high activity, mode and site of action regarding the major putative target sites, such as membranes, nucleic acids and bacterial proteins were analyzed and their impact was evaluated.

4.2 Membrane interactions of the antimicrobial peptides

Due to their negative net charge prokaryotic membranes are preferred targets for cationic antimicrobial peptides (Yeaman and Yount, 2003) and have been reported to be affected by many known AMPs, including α-helical peptides (Bechinger, 2010) such as cathelicidins (Lee et al., 2011) and magainins (Tamba et al., 2010). The design of the peptides of this study suggested besides hydrophobic and cationic amino acid clusters α-helical secondary structures, which is generally associated with membrane interaction (Matsuzaki, 1999; Zelezetsky and Tossi, 2006). For members of all structural groups (SP1-1, SP8, SP10-10 and SP13) CD-spectra and NMR analyses revealed a randomly coiled structure in aqueous solutions and the formation of an α-helix in phosphatidylglycerol-micelle suspensions (Zeitler, 2011; Zeitler et al., 2012). This behavior has also been reported for membrane disturbing antimicrobial peptides in aqueous solutions and membrane mimicking environments previously (Bhattacharjya and Ramamoorthy, 2009; Haney et al., 2009). For longicin, a defensin-like peptide from the hard tick *Haemaphysalis longicornis* even the transition from a ß-sheet structure to an α-helix was shown under membrane mimicking conditions (Rahman et al., 2010).

Following different possibilities of types of interaction with bacterial membranes are discussed for our designed AMPs.

Pore formation

Despite the structural features mentioned above, no pore forming activity could be detected in experiments with artificial membranes (Figure 6). The relatively short length of peptides from group I, II and III with their 12 amino acids could be a reason for the inability to span the membrane and form pores. Surprisingly, even SP13 from group IV did not show stronger effects. Its elongated chain length of 20 amino acids and its assembly of a hydrophobic part in the center of the molecule, bordered by smaller cationic parts (Figure 4), did also not lead to a membrane spanning and an enhanced pore forming ability. Additionally, the used peptides did not show selectivity for negatively charged lipids (Figure 6 and 7), characteristic for prokaryotic membranes. In contrast, for dermaseptin, a membrane active AMP from the skin secretion of frogs of the genus *Phyllomedusa* (Galanth et al., 2009), stronger interactions with negatively charged compared to zwitterionic lipids were reported (Salay et al., 2011). Pore formation by AMPs is characterized by a stepwise increase of membrane conductance curves with conductance plateaus (Figure 5, Stipani et al., 2001; Manich et al., 2008; Polzien et al., 2009). For this behavior at lipid bilayers, the matrix protein porin, derived from *E. coli*, with its function of forming large ion permeable channels stands as a standard (Benz et al., 1978). Also a number of other AMPs showed pore formation in experiments using measurement of lipid bilayer conductance like in this study. For example lactacin F, inducing channels in a voltage dependent manner (Dalmau et al., 2002) or nisin, produced by *Lactococcus lactis*. The latter is active against several gram-positive bacteria and is often used as food-preservative. It was shown to build pores at artificial membranes when a negative trans-membrane potential of 110 mV was applied. When the cell wall precursor lipid II, the actual target molecule of nisin was incorporated into the membrane, the pore forming ability of nisin could be enhanced further and was already observed at applied voltages of 5 – 10 mV (Wiedemann et al., 2004). Despite this, for the peptides used in this study, relatively high voltages of around ± 150 mV had to be applied to initiate interaction with the membrane. But the interaction was only observed as spikes of the conductance curve plots and no clear pore formation occurred when peptide concentrations between 0.1 and 10 µg/ml were used (Figure 6).

Integration into membranes and lysis

The fluctuation in conductance, caused by our peptides, rather indicates other membrane associated effects than pore formation. With a colorimetric approach established by Kolusheva and colleagues (2000a; 2000b) phospholipid membrane perturbations by the antimicrobial peptides melittin, magainin and alamethicin could be demonstrated at concentrations of 10 µM. In a similar concentration range of 10 – 20 µg/ml, the AMPs used in this study only showed interaction and to a certain extent insertion into the membranes, as expected from the conductance measurements with artificial lipid

bilayers, but no lysis (Figure 7). Preference for negatively charged membranes was only shown by the pore forming peptide protegrin 1. Using the same method, pronounced bilayer surface interactions could be identified for the α-defensin cryptdin-4 (Crp4) and to a certain extent also for its disordered, disulfide-null variant of mouse cryptdin-4 in negatively charged liposomes (Hadjicharalambous et al., 2008).

Membrane homeostasis

Membrane activity of AMPs can also have less obvious effects than those discussed above which can be analyzed by the influence on membrane permeability or potential. Magainin 2 from the African clawed frog *Xenopus laevis*, causes calcein leakage by membrane permeabilization of *Bacillus megaterium* (Imura et al., 2008). The same was shown for its equipotent analog F5W-magainin 2, by microscopically visible influx of calcein into the cells (Imura et al., 2008). Cathelicidin-BF (BF-30) causes β-galactosidase leakage and EtBr accumulation, by what its antimicrobial activity is attributed on cytoplasmic membrane permeability (Zhou et al., 2011). However, for such leaking substances and dyes also drawbacks are reported. Fluorescein, used for leakage experiments, for example, can even be actively transported by the bacteria and accumulates in the environment without membrane damage (Chitarra et al., 2006). As the AMPs of this study did neither show channel formation (Figure 6) nor lytic effects on micelles (Figure 7), an also frequently applied method using a membrane potential sensitive dye ($DiSC_3(5)$) was carried out with selected peptides. This detects not only permeabilization endpoints, but more subtle changes in the membrane potential and the degree of membrane depolarization (Wu et al., 1999; Zhang et al., 2000; Nan et al., 2009; Kim et al., 2010). The peptides SP10-4, SP10-8 (structural group III) and SP13-2 (structural group IV) revealed strong membrane depolarization levels in the range of membrane-active indolicidin (Falla et al., 1996; Friedrich et al., 2001). In gram-positive bacteria SP10-8 showed depolarizing effects similar to tensidic SDS. In contrast, SP1-1 and SP8 exhibited only moderate or no depolarization activity (Figure 8). Indolicidin has been shown before to cause almost complete membrane depolarization in *S. aureus*, measured by $DiSC_3(5)$ treatment like in this study, in a concentration of 10 µg/ml. Probably, this peptide acts via dissipation of the membrane potential by application of one of the three major models of membrane perturbation, introduced in chapter 1.1.3.1 (Nan et al., 2009). For our peptides these membrane disturbing mechanisms could be excluded. So, the membrane depolarization of SP10-4, SP10-8 and SP13-2 has to be associated with more tenuous changes in the membrane environment and its ion fluxes. Also for piscidin 1, a cationic α-helical peptide isolated from the mast cells of hybrid striped bass, membrane depolarization was observed using the same technique with *S. aureus*. 90% membrane depolarization was observed, when the MIC of the peptide was applied. After application of the double MIC of the AMP the membrane depolarized even to 100%.

When glycine at position 8 was substituted by proline the observed depolarization decreased to 40%. When this amino acid was replaced by a lysine peptoid-residue, the depolarization was nearly abolished with values of less than 10%. The authors assumed the bacterial membranes to be the major target of the parental peptide piscidin 1, whereas the antibacterial activity of the derivates might not be caused by permeabilizing actions (Kim et al., 2010). A similar situation could be identified for the peptides used in this study. Although they all are quite similar regarding their sequences (Table 1), the structures seem to be different enough to exhibit membrane depolarizing action for specific members of structural group III and group IV, but not for SP1-1 from group I.

Sequence features important for depolarization

The impact of single amino acids on the antibacterial activity was elucidated for SP10-4, which was identified as a highly antibacterially active (Table 2) and membrane depolarizing (Figure 8) AMP candidate. Alanine scans are an often used tool for sequence-activity studies for AMPs (Munoz et al., 2007; Dings et al., 2008; Wei et al., 2010). With the alanine scan of SP10-4 it could be shown that the hydrophobic amino acids were particularly important for activity against the tested *S. aureus* strain (Table 3). Especially when hydrophobic leucine residues were replaced by alanine, the antibacterial activity decreased dramatically or was even attenuated in the tested concentration range. Thereby, leucines at positions 8 and 11 seemed to be most crucial. The importance of hydrophobic amino acid residues for AMP activity was also observed by other groups. The alanine scan of human α-defensin 1 (HNP-1) showed that especially the bulky hydrophobic residue of tryptophan at position 26 of the peptide was essential for the functional versatility in *S. aureus*. When in this peptide alanine again was replaced by non-coded, straight chain aliphatic amino acids with increasing chain length, the activity could progressively be restored by stepwise enhancing hydrophobicity (Wei et al., 2010). For fallaxin, an antimicrobial peptide isolated from West Indian mountain chicken frog, the replacement of especially hydrophobic leucine with alanine decreased the antibacterial activity, as it was the case for SP10-4. In reverse, the exchange of alanines of the original peptide with leucines resulted in an improved antibacterial activity against MRSA and other gram-positive bacteria (Nielsen et al., 2007). According to those findings and keeping the importance of the hydrophobic amino acids for the anti-*Staphylococcus* activity of SP10-4 in mind, those hydrophobic leucine residues should be considered of special interest for future structure-activity studies. Possibly by the addition of leucine residues at special positions the antibacterial activity of SP10-4 can be further enhanced. However, toxicity, although to a lower extent, followed the same trend as activity. The low toxicity of SP10-4 slightly increased following the exchange of cationic arginine at position 5 or 10 to alanine but was not detected anymore when hydrophobic amino acids were replaced. Toxicity and the therapeutic window, regarded as the range

between effective doses and concentrations with adverse effects, have to be regarded as critical points. Especially as it is known that toxicity for human cells often increases with increasing hydrophobicity of AMPs (Brogden, 2005; Jiang et al., 2008). However, for our AMPs no strong increase in toxicity could be observed by increasing hydrophobicity in general (Table 2, Supplementary Table 1). But the molecular mechanism of insertion of amphipathic peptides into membranes remains unknown for most known AMPs (Boland and Separovic, 2006; Leontiadou et al., 2006). Furthermore, the membrane active mechanisms seem to be very specific for peptides with distinct structures. The histidine rich peptide LAH4, for example, undergoes structural changes during interaction with lipid micelles. The α-helix formation and incorporation into the membranes reacts with pH dependency due to the high density of histidine residues (Georgescu et al., 2010). Hydrophobic amino acids like leucine may lead to other structural changes and further elucidation of their impact might be helpful for developing highly active peptides.

Membrane passage

There is only a thin borderline between membrane destruction and membrane penetration, since single changes in the amino acid composition of a peptide can have severe effects on how they act. For example, the exchange of only one amino acid, glutamic acid (E) to lysine (K) at position 2, led to a change from a cell penetrating and cargo carrier peptide Pep-1, to a membrane destructive peptide Pep-1-K (Bobone et al., 2011). Although our peptides all exhibit similar sequence characteristics, small differences can result in different modes of action. Translocation through the bacterial membrane can as well affect the membrane features, e.g. the membrane potential to a minor extent. The ^{15}N labeled peptide SP1-1 was shown to enter the intracellular space of *S. aureus* cells (Figure 11, Figure 12). SP1-1 only caused small changes in membrane potential behavior, unlike for example SP10-4 that affected membrane potential strongly (Figure 8). So it is conceivable that this particular peptide only translocates through the bacterial membrane. In conclusion, the different peptide groups seem to interact differentially with bacterial membranes (Figure 28).

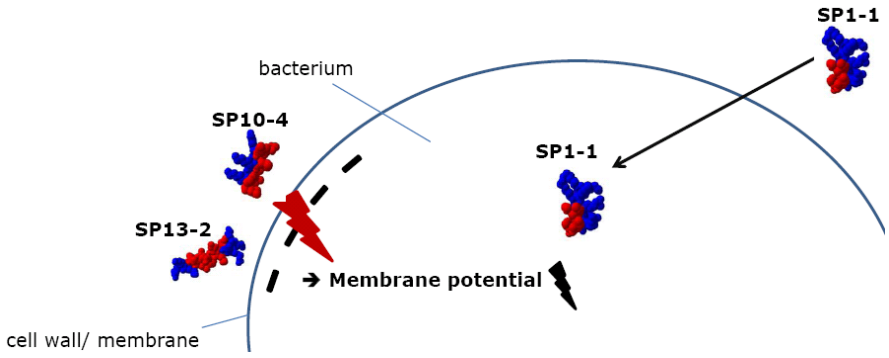

Figure 28 - Model of the membrane interactions of SP1-1, SP10-4 and SP13-2
SP10-4 and SP13-2 influenced the bacterial membrane potential strongly. SP1-1 showed only minor effects on the membrane potential and accumulated in the intracellular space of *S. aureus*. Hence, it was supposed to translocate through the bacterial membrane.

Additionally, the fact that the antibacterial action of SP1-1 proceeded slower than that of SP10 and SP13 derivates (chapter 3.2.3, Supplementary Figure 2) indicated that possibly intracellular targets apart from the membrane were affected, which the peptide needed to reach first. Regarding the question as to how the AMP translocated through the membrane a more detailed view on the sequence of SP1-1 opened an interesting parallel to cell penetrating peptides (CPPs). For CPPs, an arginine rich structure is an important feature for interaction with the membrane during their translocation through it. Well studied examples for this feature are the TAT peptide from the HIV transactivator protein TAT, penetratin, a 16 amino acid domain from the antennapedia protein of *Drosophila*, and oligoarginines (Schmidt et al., 2010). This arginine rich structure is also part of the design of SP1-1 and other representatives of our AMPs. With regard to the mentioned TAT peptide, SP1-1 exhibits sequence homology of the first four amino acids (RKKR-) starting from the C-terminus (Sawant and Torchilin, 2009). However, the CPPs are used for delivery of cargo into mammalian and not prokaryotic cells. But uptake mechanisms for CPPs are under discussion and there is still need for a detailed investigation (Jones, 2007; Nakase et al., 2008). So, some steps of the internalization mechanism, due to the given structures, may be conserved between CPPs and AMPs, and the uptake of SP1-1 and some arginine rich CPPs may hypothetically - at least in some details - rely on the same structural basics.

4.3 Interaction of AMPs with intracellular bacterial targets

Not all of the highly active *de novo* designed antimicrobial peptides affected membrane stability (discussed in chapter 4.2). Especially as SP1-1 seemed to translocate through the membranes and, furthermore, was shown to be able to enter bacterial cells and accumulate inside, also intracellular targets attracted attention. The results showed interaction with nucleic acids and transcriptional changes (chapters 3.4.1 and 3.4.2). In addition, RsbW kinase from *S. aureus* was identified and evaluated as an intracellular interaction partner of SP1-1 (chapters 3.4.3 to 3.4.6).

4.3.1 Localization of the AMPs at treated bacteria

Several attempts were necessary to identify the subcellular localization of the peptides. Finally SP1-1 could be detected inside of *S. aureus*. Light microscopy did not turn out to be the method of choice, due to the narrow potential regarding magnification and resolution. The peptides clearly colocalized with the treated bacterial cells. But it could not be distinguished with certainty in which part of the cell the peptides accumulated. Neither was it possible to ascertain whether the fluorescence emitting peptides were attached to the membranes or accumulated in the intracellular space as the signal

covered the whole cell (Figure 9). Since a bacterial cell roughly measures one micrometer in size, the maximum magnifications of the used microscope of 630 fold was not enough to allow a defined subcellular localization with a sufficient differentiation of fluorescent signal emitting and non-emitting regions within the subcellular space. However, in other studies localization of peptide compounds at bacterial cells was possible by similar techniques when the signal could be clearly attributed to membrane regions by ring-like signal structures. For example, the horseshoe crab peptide polyphemusin exhibited ring like structures on treated bacteria and the signal could be clearly defined to be related to the bacterial membrane when fluorescent labeled peptide was incubated with *E. coli* (Powers et al., 2006). With the fluorescence labeled AMPs, I could only detect ring like signal structures when fungal spores were incubated with sub-lethal peptide concentrations, which could prove the performance of the assay (Figure 10). To overcome the magnification and resolution problem of fluorescence signal localization with light microscopy, antibodies against SP1-1, SP10-2 and SP13 were generated. Those should be used for an imaging of immunogold stained peptides with bacteria by a transmission electron microscopy approach. But all 25 different antibody containing, primary supernatants of hybridoma cells were neither specific nor sensitive enough to detect and distinguish pure peptides or peptides out of mixtures with BSA or crude bacterial extracts (Supplementary Figure 3). By the short length such peptides exhibit only one to two epitopes. Additionally, the hydrophobicity can adversely affect immunization efficiency (Feng et al., 2011). So, generation of antibodies against such molecules is often difficult, protracted and unsuccessful (Bhargava et al., 2007; Feng et al., 2011). However, for some antimicrobial peptides specific antibody generation has been reported, for example against indolicidin (Lomash et al., 2010), human ß-defensin (Ortega et al., 2000) or dermcidin, derived from human sweat glands (Minami et al., 2004). But the researchers also faced problems during antibody-development. For example, three sub-cloning steps from previously positively tested hybridoma cell lines had to be performed to obtain working anti-tachyplesin antibodies (Feng et al., 2011). Finally, in 2011 the localization of immunogold stained peptides in bacteria cells via an transmission electron microscopy approach was reported for the first time (Huttunen-Hennelly et al., 2011). But as the generation of antibodies against the AMPs from this study did not yield specific and sensitive material, alternatively nanometer-scaled Secondary Ion Mass Spectrometry (NanoSIMS) imaging of SP1-1 with an exchange of ^{14}N by ^{15}N at three leucine residues was applied. This technique was used the first time to localize AMPs in bacterial cells. The approach of using this technique for the incorporation of heavy isotope labeled ions at a single cell level has often been used for identification of nitrogen assimilation in marine microorganisms (Pernice et al., 2012; Woebken et al., 2012), or, in conjunction with other techniques, like in-situ hybridization for the phylogenetic identification and quantification of metabolic activities (Musat et al., 2008).

Using this technique we were able to show accumulation of ^{15}N-SP1-1 inside the bacterial cells (Figure 11, Figure 12). By slicing the cells in a number of Z-layers it was made sure that signals obtained originated from the intracellular part of the cells and were not due to scattering by the membrane or cell surface. Thus, the localization via NanoSIMS imaging proved that SP1-1 can reach possible intracellular targets, like nucleic acids and proteins. It was also shown that translocation into the cells is fast and takes places in a time frame of less than 10 minutes. In conclusion, the conditions for the AMP to reach intracellular targets and affect metabolism within one generation cycle are favourable.

4.3.2 Interactions of the antimicrobial peptides with nucleic acids

Nucleic acids exhibit a net negative charge and are therefore another possible major target for the cationic antimicrobial peptides. Numerous AMPs are known that unfold their antimicrobial action by binding to bacterial nucleic acids. Buforin II is probably the most prominent example of an antimicrobial peptide, that has been shown to penetrate the cell-membrane of bacteria without lysis, but binding to DNA and RNA and thereby leading to a rapid cell death (Park et al., 1998). Nucleic acid binding of buforin II has been analyzed by similar gel retardation experiments used for the *de novo* designed peptides in this study. Already in the 1990s, tachyplesin has been shown to bind to the minor groove of the DNA double strand leading to inhibited macromolecular synthesis (Yonezawa et al., 1992). Also PR-39, an antibacterial peptide derived from pig intestine, has been shown by isotope incorporation experiments to act via inhibition of DNA and protein synthesis in *E. coli,* probably by binding to nucleic acids after a lag-period of 8 min that is needed to penetrate the outer membrane (Boman et al., 1993). Human pre-elafin/trappin-2 and elafin also possess the ability to translocate through the membrane of *Pseudomonas aeruginosa* and to bind to DNA in *in vitro* gel retardation experiments. Thereby, they decrease the expression of virulence factors necessary for biofilm formation and the secretion of pyoverdine (Bellemare et al., 2010). Additionally, it has been shown for several of those classical antibiotics - which are inhibitors of macromolecular synthesis - that their binding to the ribosomal sub-unit overwhelmingly targets the rRNA part rather than ribosomal proteins. In fact, they show different ways of interaction with the rRNA. Examples are tetracycline, interacting with magnesium ions, streptomycin reacting with the RNA´s phosphate groups, or spectinomycin interacting with the bases themselves (Wirmer and Westhof, 2006).

The antimicrobial peptides SP1-1, SP10-2, and SP13 tested in this study were active against pathogenic bacteria and showed DNA and RNA binding as well, both in a dose dependent manner. Peptide SP8, without any antibacterial activity against the tested microorganisms, did not show clear binding to DNA. Only at very high concentrations it bound to RNA, which can probably be explained by charge compensation. In general,

however, the different activities with regard to DNA and RNA binding cannot solely be explained by charge compensation effects. Peptides with the same net charge did not influence nucleic acid migration to similar extents. For example, SP8 and SP10-2 both have a net charge of +5 (Table 1), whereas only SP10-2 binds strongly to DNA starting at a ratio of 1.0 (Figure 13). Also, a higher net charge does not necessarily lead to a higher effect on nucleic acid migration. SP13 with a net charge of +9 did not show higher effects than SP1-1 (net charge of +7) for DNA and RNA (Figure 13, Figure 14) and similar effects for RNA migration compared to SP10-2 with a net charge of only +5 (Figure 14). The differences in nucleic acid binding are rather corresponding to the structural design and antibacterial activity ranges of the tested peptides. It was not surprising that SP1-1 from structural group I, with its big cationic part, showed the strongest interaction with negatively charged nucleic acids, compared to peptides from other groups (Figure 4). Those consist of extended hydrophobic parts (groups II and IV) or hydrophobic and cationic parts of identical size (group III). Groups I, III and IV (including derivates of SP1, SP10 and SP13) also exhibited higher activities against bacteria than group II (SP8) and also stronger DNA binding activity. Due to the interaction of the negative control SP8 with RNA at high concentrations, but not with DNA, binding events with DNA could be more clearly associated with highly active peptides and influences in transcription may play a bigger role than in translation.

Due to these reasons, alteration of gene expression after treatment of *S. aureus* with sub-lethal doses of strongly DNA binding SP1-1 was investigated by microarray analysis. SP1-1 induced 18 genes belonging to a variety of metabolic pathways (Table 4). They have, for example, functions in cell wall metabolism (atl, *lytM*, SACOL1062, *sceD*), oxidative phosphorylation (cytochrome d ubiquinol oxidase), biofilm formation (*ica* group), pigmentation and virulence (staphyloxanthin biosynthesis, *ssaA*). SP1-1 also repressed a large number of 97 genes with very diverse functions (Table 5). *Vra* genes (*vraD, E, F*) were affected, which encode for transport proteins with influence on resistance to antibiotics (Pietiainen et al., 2009), as well as several ABC transporters for maltose, peptides and amino acids. Amino acid metabolism and synthesis pathways were also cut back, like histidine, lysine and glutamate biosynthesis. Pietiäinen and coworkers followed a similar approach investigating the gene expression changes in *S. aureus* caused by the membrane active antimicrobial peptides temporin L, ovospirin-1 and dermaseptin K4 (Pietiainen et al., 2009). Interestingly, SP1-1 showed a different pattern of up- and down-regulation regarding the overlapping genes. It repressed most of the genes that were induced by the membrane active peptides. This was the case for genes *vraD* and *vraE*, encoding for an ABC transporter, similar to putative bacitracin efflux pump (Pietiainen et al., 2009), the histidine biosynthesis (*his*) operon, aspartate kinase (*lysC*), diaminopimelate decarboxylase (*lysA*), genes *citC* and *citZ* and several peptide ABC transporters (SACOL1915, SACOL1916, SACOL2472 – SACOL2476). The same was

true for genes *drp35* and *sgtB*. The gene products with lactonase and glycosyltransferase activity belong to the cell wall stimulon. They are contributing to bacterial resistance and are induced by membrane active antibiotics such as ß-lactams, vancomycin, bacitracin, fosomycin (Murakami et al., 1999; Steidl et al., 2008) and also by detergents (Morikawa et al., 2005) but repressed by SP1-1. In contrast, genes *ssaA* and *cspB* were up-regulated by SP1-1. However, the other cell wall active peptides showed down-regulation. Only a few genes (*arcB, arcD*) were redundantly repressed by SP1-1 and cell wall active peptides, analyzed by Pietiäinen and colleagues (2009). So, SP1-1 showed a strongly opposed expression pattern, compared to cell-wall active compounds like pore-forming temporin L (Rinaldi et al., 2002), ovospirin and dermaseptin that disrupt membranes by the carpet mechanism (Brogden, 2005) and other membrane active antibiotics and detergents. It can therefore be concluded that the mode of action of SP1-1 must be different from the other substances mentioned and that it has no impact on membrane integrity. However, the down-regulated genes involved in amino acid biosynthesis (*dapA, B, D, gltA, B, D, hisA, B, C, D, F, G, H, I, Z*) could either to a certain extent reflect changes of availability of amino acids by the sub-lethal doses of the AMP SP1-1 or a general stress response. The effects caused by the other peptides could also be secondary resulting from membrane perturbation, whereas SP1-1 directly binds to DNA due to its cationic structure. Thereby, transcription seems to be affected. Repression of the large number of genes can be caused by direct DNA binding. Inhibition of transcription can take place by blocking of binding sites for transcription factors, enhancers or the RNA polymerase. Inhibition of the synthesis of metabolic important compounds can severely influence fitness of the bacteria and be part of the mode of action. However, within this context the microarray data can only elucidate a section of possible influences at a low concentration (4 µg/ 10^6 cfu) of less than half MIC (10 µg/ 10^6 cfu) and for one timepoint after application. The full inhibiting impact of SP1-1 on gene expression at its MIC and over a longer period of time may be even stronger.

4.3.3 Interaction with bacterial proteins in *S. aureus*

In addition to bacterial nucleic acids, proteins are the major group of possible intracellular peptide targets. Inhibition of enzyme functions is the mode of action for classic antibiotic substances and was also elucidated for several antimicrobial peptides. For example, the antibiotics of the sulphonamide group and Trimethoprim that are often applied together, are acting via the competitive inhibition of the enzymes dihydropteroate synthase and dihydrofolate reductase of folic acid synthesis (Zander et al., 2009). Proline rich AMPs, derived from various insect species, interfere with enzyme functions inside the bacterial cells (Andreu and Rivas, 1998; Markossian et al., 2004). Salivary histatins have been discovered to be able to inhibit a trypsin-like proteinase

from *Bacteroides gingivalis,* occurring in the human oral cavity (Nishikata et al., 1991). The antimicrobial peptide eNAP-2, isolated from equine neutrophils selectively inactivates microbial serine proteases subtilisin A and proteinase K (Couto et al., 1993).
As SP1-1 can enter bacteria and binds to DNA (discussed in chapters 4.3.1 and 4.3.2), interaction with intracellular proteins would also be conceivable. In most cases it is difficult to identify and characterize single protein-protein interactions in complex mixtures like crude protein extracts of bacteria. In most cases successful protein-protein interaction studies have been performed with purified proteins (Neely et al., 2002; Ishmael et al., 2003). But for this hints for possible interactions have to be available previous to the analysis. To be able to elucidate protein - peptide interactions in bacteria without the problem of complex cell extract mixtures but with ability to cover the majority of the cellular proteins, the decision fell to apply an ORFeome based yeast-two-hybrid screen. This technique covered not only possible binding partners within cytoplasmic proteins but more than 95% of the ORFs of the corresponding strain (Brandner et al., 2008; Maier et al., 2008). With this approach, RsbW was identified as an intracellular interaction partner of SP1-1 in *S. aureus* (Figure 15), in addition to nucleic acids. This kinase performs a partner switching between the transcription factor Sigma B (SigB) and a substrate for phosphorylation, RsbV (Figure 18). It can thereby directly prevent SigB dependent transcription by binding to it or initiate transcription by release of SigB and binding and phosphorylation of RsbV (Miyazaki et al., 1999).

SP1-1 inhibits kinase and anti-sigma-factor functions of RsbW

The interaction between RsbW and SP1-1 seemed to be very strong. This could be shown by ß-galactosidase quantification (Figure 16). The inhibiting influence of SP1-1 on the phosphorylation of RsbV and the complex formation with SigB, by binding to RsbW was also demonstrated in a dose dependent manner in an *in-gel* analysis (Figure 25 and 26). Peptide SP1-13, structurally strongly related to SP1-1, differing mainly by several phenylalanine residues in the primary peptide sequence (Table 1) had stronger antibacterial activity against *S. aureus.* Interestingly, this peptide exhibited an even stronger inhibition of the phosphorylation reaction. The same was true for the binding of RsbW to the transcription factor SigB *in vitro (*Figure 25*,* Figure 26*)*. Interestingly, when including further SP1 derivates in the test for phosphorylation inhibition, a correlation between activity against *S. aureus* and kinase inhibition became obvious. This provides a connection between AMP interaction with RsbW and the mode of action, which can result in a permanent unbound and uncontrolled transcription factor SigB and thereby uncontrolled transcription (Figure 29). Furthermore, antibacterial activity via the inhibiting influence on RsbW seems to increase with the occurrence of phenylalanine residues in the peptide, when SP1-1 (no F), SP1-12 (4 F) and SP1-13 (5 F) were compared (Supplementary Figure 10).

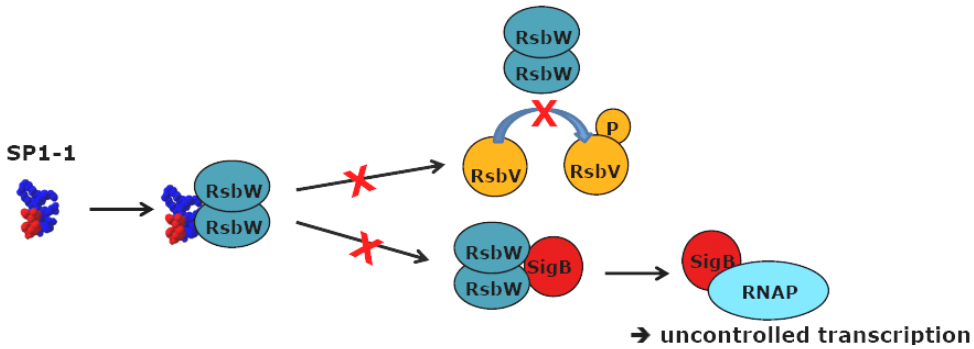

Figure 29 - Model of the inhibiting influence of SP1-1 on RsbW
RsbW was identified as interaction partner of SP1-1 in *S. aureus*. The binding of SP1-1 to RsbW was shown to inhibit the phosphorylation reaction of RsbV and the binding to transcription factor Sigma B (SigB). Thereby, SigB is free and can bind to the RNA polymerase (RNAP) core enzyme and SigB dependent genes can be transcribed without negative control of RsbW.

The *in vivo* tests with *S. aureus* deletion mutants of operon *sigB*, brought further evidence for a RsbW based killing mechanism, deduced from the ability of SP1-1 to kill wild type and complemented mutant strains of *S. aureus* RN1HG but not the *ΔsigB* deletion mutant (Figure 27). However, this deletion mutant is viable with the apparent phenotypical change of reduced pigmentation. In *sigB* deletion mutants of different genetic backgrounds the phenotypical changes covered reduced pigmentation, accelerated sedimentation and increased sensitivity to hydrogen peroxide during stationary growth phase (Kullik et al., 1998). Since there are no severe phenotypic disadvantages in the deletion mutant, RsbW and its influence in SigB dependent transcription can only be one mechanism of action among others that are required for killing, such as the detected DNA binding and the resulting changes of transcription.
Furthermore, Y2H approaches, using predefined ORFs and a common assay for the detection of any pair-wise interaction with the proteome, are prone to a high level of false negative results, due to their strict selective pressure for avoiding false positives (Legrain and Selig, 2000). Although the result could be confirmed under less stringent conditions, the possibility of further non identified intracellular targets of SP1-1 still remains. Further evidence for this hypothesis was brought by the microarray analysis of SP1-1 treated *S. aureus*, as SP1-1 clearly affected SigB dependent genes but also others.

Influences on SigB dependent transcription

Influencing the function of RsbW can have a big impact on SigB dependent transcription in *S. aureus*. This alternative transcription factor has influence on resistance of *S. aureus* to multiple stresses, such as heat, alkaline and acidic shock, hydrogen peroxide, pulsed electric fields and high hydrostatic pressure. This has been shown by analyzing the survival rates of *S. aureus* Newman *sigB* deletion strains (*ΔsigB)* after the application of different stress factors (Cebrian et al., 2009). In a microarray comparative analysis of wild type and *sigB* deleted mutant strains a total number of 251 ORFs have been discovered as SigB dependent genes, of which 198 were positively and 53 negatively

regulated by SigB (Bischoff et al., 2004). Within another study the comparison of wild type and *sigB* deleted strains delivered the expression of 122 distinct genes as positively *sigB* dependent. 72 of these genes were found to be inducible by alkaline shock (Pane-Farre et al., 2006). SigB thereby influences the transcription of regulatory elements as well as genes for antibiotic resistance, internalization into endothelial cells and general stress response (Senn et al., 2005). Furthermore, the regulated genes have functions related to the cell envelope, like in capsular polysaccharide synthesis or autolysins. Additionally, the expression of several transporters is up-regulated by SigB (Pane-Farre et al., 2006). Also virulence associated genes are SigB dependent, such as adhesins, exoproteins and different toxins (Bischoff et al., 2004; Entenza et al., 2005). SigB can influence genes directly or indirectly, as genes with as well as without known promoter consensus sequences are affected (Pane-Farre et al., 2006). The genes of global *S. aureus* regulators Sar and Agr, important for cell wall associated proteins and virulence factors are also SigB dependent, respectively. Firefly luciferase reporter gene assay in combination with SigB overexpression showed that *sar* correlated positively and *agr* expression negatively with SigB activity, which in general peaked in the late exponential phase and diminished towards the stationary phase under non stress conditions (Bischoff et al., 2001).

The genes of ornithine carbamoyltransferase (*arcB)* and arginine/ornithine antiporter *(arcD)* are under positive control of the global regulator Agr (Pietiainen et al., 2009). Due to the influence of SigB on *agr*, the down-regulation of *arcB* and *arcD* by SP1-1 reflects the impact on RsbW and SigB. Additionally, a number of other genes altered by SP1-1, especially significantly up-regulated ones could also be correlated with SigB dependency. The virulence determinant *SsaA* and the putative transglycosylase SceD, up-regulated by SP1-1, are positively SigB dependent (Bischoff et al., 2004; Stapleton et al., 2007). Microarray analysis of *S. aureus* under different stress conditions correlated many genes with functions of cell wall envelope with SigB (Pane-Farre et al., 2006), as for example autolysin (SACOL1062). SP1-1 also induced several genes involved in cell wall metabolism, like as well autolysins (*atl,* SACOL1062), peptidoglycan hydrolase (*lytM*), and LysM domain-containing protein SACOL0507, which displays a cell wall binding domain (Visweswaran et al., 2012). Furthermore, the up-regulated autolysin *atl* is regulated by the SigB dependent global regulator Sar (Pietiainen et al., 2009). Cytochrome d ubiquinol oxidase subunits I and II (*cydA* and *cydB*) were the most up-regulated genes by SP1-1 with fold changes of 4.64 and 5.34. Until now no influence of SigB on these genes had been identified in *S. aureus,* but in the related system of *B. cereus* subunit II was induced by SigB (van Schaik et al., 2004). Additionally, *icaA, B* and *D* from the ica operon were up-regulated by SP1-1. This operon is known to function in biofilm production, it has been established as a virulence factor and allows *Staphylococcus* to adhere to and persist in medical devices (Diemond-Hernandez et al.,

2010). At least *icaA* is positively regulated by SigB in *S. epidermis* (Knobloch et al., 2004). Regulation of the ica group by SigB and Agr of *S. aureus* is also under discussion (Rachid et al., 2000; Lauderdale et al., 2009). It is moreover known that SigB affects pigmentation (Kullik et al., 1998) and that *S. aureus* mutant strains, lacking SigB and its positive regulator RsbU, are unable to accumulate the pigment staphyloxanthin (Giachino et al., 2001). Three genes encoding for proteins with function in staphyloxanthin biosynthesis (SACOL2291, SACOL2295, SACOL2581) were up-regulated by SP1-1. These three genes were classified to be positively SigB dependent by Pané-Farré and coworkers (2006). They also characterized the group SACOL2441, SACOL2471 – 2476 as negatively SigB dependent, which is again in agreement with the down-regulation by SP1-1. The same is true for iron compound ABC transporter gene *sirA* (SACOL0099). In sum, 61% of the SP1-1 up-regulated and 10% of the down-regulated genes are overlapping with direct or indirect SigB dependency in *S. aureus* or at least assumed dependency, because SigB dependency has been proven in related bacteria (Figure 30, in comparison to Table 4 and Table 5).

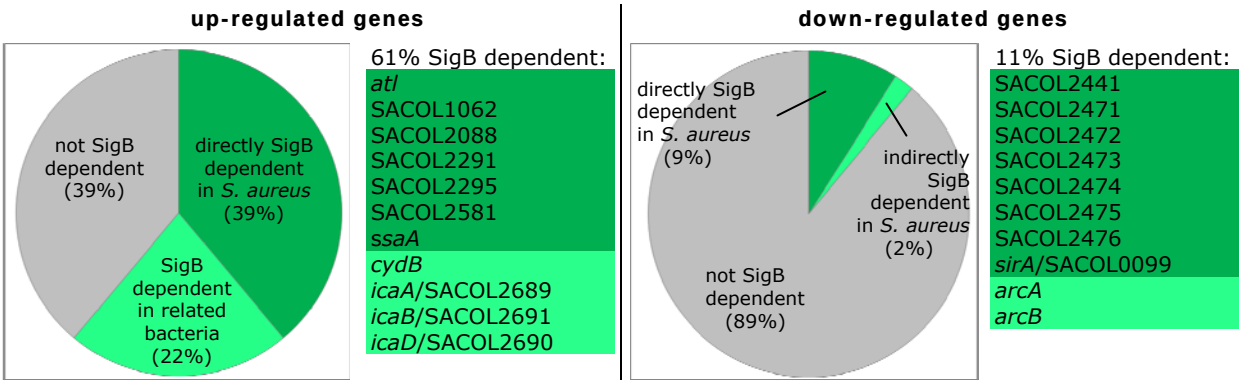

Figure 30 - SigB dependent genes with altered expression by SP1-1 in *S. aureus*
Data extracted from Table 4 and Table 5. Exponential growing *S. aureus* cells were treated 10 min with 4 µg/10^6 cfu SP1-1. Cells were harvested, RNA was extracted and transcriptional changes were analyzed with a *S. aureus* whole genome oligoarray (Charbonnier et al., 2005). Data from triplicates were analyzed by variance analysis and fold changes of more than 3 were considered as significant. Genes with a proven SigB dependency in *S. aureus* are indicated in dark green and genes with an assumed SigB dependency, due to indirect effects of SigB or SigB dependency in related organisms are indicated in light green.

Thus, especially the SP1-1 up-regulated genes correlate with SigB dependent genes. This is a further piece of evidence for the causality between SP1-1 antibacterial activity and the influence on RsbW and SigB. It can therefore be concluded that the influence on this regulatory system by SP1-1 plays a role in the mode of action of SP1-1. However, none of the genes for which SigB dependency was most clearly identified and which are used as SigB marker genes like *asp23*, *csb7* and *clpL* (Gertz et al., 2000; Pane-Farre et al., 2006) was significantly changed by SP1-1 treatment. So, it could be concluded that, in addition to the inhibiting influence of SP1-1 on transcription by more unspecific DNA binding, influencing SigB via RsbW is part of the mode of action of SP1-1. Precisely, the binding of SP1-1 to RsbW may to a certain extent prevent the binding of SigB to RsbW

and the unbound SigB can initiate transcription of several genes uncontrolled (Figure 29). The influence of SP1-1 on the regulatory system of SigB, although not being the exclusive mechanism of action can trigger changes in the resistance or stress response. On the one hand cell wall thickening and resistance to ß-lactams and even to the antimicrobial peptide ASABF-alpha were shown for *sigB* overexpressing lines (Morikawa et al., 2001; Zhang et al., 2005). But on the other hand the fitness of the *S. aureus* cells suffers heavily when solely *sigB* is expressed in a *rsbV/rsbW/sigB* deleted mutant (Pané-Farré, 2011, personal communication). This situation with a permanent unbound SigB lacks the influence from the regulatory anti-sigma factor RsbW. This scenario comes most probably closest to the situation when peptide SP1-1 is inhibiting kinase RsbW and prevents the binding to SigB.

RsbW – SP1-1 binding – a structural biology approach

The investigation of the interaction between enzymes, like RsbW and corresponding inhibitors, like SP1-1, by NMR or crystallography is often adducted to understand structural features that are important for binding (Martorell et al., 1994; Morgan et al., 1999; Gong et al., 2010; Rhodes et al., 2011). With the knowledge about binding events at a structural level the structure of the inhibitory drug can subsequently be altered to yield better and selective binding (Morgan et al., 1999; Gong et al., 2010; Orcajo-Rincon et al., 2011).

With NMR studies of $^{13}C/^{15}N$ labeled SP1-1 and ^{15}N labeled RsbW, insight into the binding reaction and the conformational changes during the binding event should be gained. This could support the future design of improved SP1-1 derivates with regard to binding efficiency. But no analyzable signal could be extracted from the NMR even when RsbW without SP1-1 addition was analyzed. After addition of peptide the sample precipitated and the signal became even more inarticulate. The aggregating behavior, known for RsbW and homologues (Campbell and Darst, 2000; Etezady-Esfarjani et al., 2006b) could be an explanation for the problems during the NMR measurement. It had been reported before that protein aggregation in general could be prevented by the use of only freshly purified protein (Etezady-Esfarjani and Wuthrich, 2004). But neither the use of freshly purified RsbW nor all other attempts to stabilize the protein in solution by different additives, such as nucleotide analogues, or SP1-1 or SP1-13 with their strong binding ability, could stabilize the protein in solution (Figure 21 - Figure 23). Also co-purification with the natural substrate RsbV or purification at low pH, although this was reported to stabilize the anti-sigma antagonist in *Thermogata maritima* (Etezady-Esfarjani and Wuthrich, 2004) could not prevent aggregation of RsbW. Samples precipitated or consisted of large amounts of protein aggregates, detected by mass separation and following light scattering detection (Figure 23). In the related system of RsbW homologue SpoIIAB and transcription factor Sigma F (SigF) in *B. stearothermophilus* as well as of

kinase UsfX and SigF in *Mycobacterium tuberculosis,* co-expression of the two-proteins delivered a stable pre-assembled complex (Campbell and Darst, 2000; Malik et al., 2009). But when RsbW was co-expressed with SigB not only stability problems but additional problems regarding SigB expression occurred. Campbell and Darst (2000) faced similar problems when they tried to study the sigma factor - kinase interaction in *B. subtilis*. They switched over to the homologues from *B. stearothermophilus* when they observed that *B. subtilis* SigF was toxic to *E. coli* cells and SpoIIAB insoluble when recombinantly expressed. In the present study the toxic effect of SigB from *S. aureus* to *E. coli* could be decreased when co-expressed as an *in vivo* pre-assembled complex with RsbW, but not completely neutralized. Furthermore, the low expression levels of SigB resulted in purification of only minimal amounts of 6x His-tagged complex together with numerous false positive proteins (Figure 24). Due to all these reasons the structural interaction between SP1-1 and RsbW could not be analyzed in full detail during this study. However, recombinant $^{13}C/^{15}N$ labeled peptide SP1-1 was already successfully expressed and purified in this study (Supplementary chapter 6.8).

The following considerations might be helpful to stabilize RsbW in solution for an analysis of the SP1-1 binding event in future studies: The RsbW homologue TM0733 of the gram-positive bacterium *Thermogata maritima* was found to aggregate and precipitate in solution with low expression levels in *E. coli*. Thus, the interaction of TM1442 and TM0733 (homologue to the RsbV-RsbW interaction) was successfully studied with an approach in cell extracts without purification of TM0733 (Etezady-Esfarjani et al., 2006a; 2006b). As SigF from *B. stearothermophilus* was observed to have lower but still detectable toxicity to *E. coli* than the homologue from *B. subtilis*, an included mutation known from the gene of *B. subtilis* helped to slightly decrease toxicity (Yudkin, 1987). When SigB from *S. aureus* was recombinantly expressed as a thioredoxin fusion protein, high protein levels could be produced in *E. coli* without toxic effects (Miyazaki et al., 1999). Similar approaches could putatively be considered for further RsbW stabilization and co-expression experiments. Also the co-expression of SigF and anti-sigma factor SpoIIAB together in one co-expression vector which placed *spoIIAB* and *sigF* in a transcriptional operon, similar to that found in the *spoA* operon of *B. stearothermophilus in vivo*, led to stable recombinant proteins (Campbell and Darst, 2000). Such arrangements could also be helpful to overcome the problems of low expression and aggregation. Alternatively, for further studies also different expression systems, for example in yeast, should be kept in mind.

4.4 Conclusion and Outlook

The threat of an already large and still increasing number of bacterial strains resistant to common antibiotics necessitates the search for new antibiotic agents. Especially multi-resistant strains of *Staphylococcus aureus* cause severe health problems. Antimicrobial peptide candidates analyzed in this study with high level and broad range activity against phytopathogens and multi-resistant *S. aureus* and at the same time low toxicity against eukaryotic cells might be a possible alternative.

In this study *de novo* designed AMPs were investigated regarding their antibacterial mode of action. The former assumption, that AMPs are mostly membrane active agents, was found to be only true for representatives of structural groups III and IV (SP10-4, SP10-8 and SP13-2). Derivates of SP1, especially SP1-1 of structural group I with the characteristic large cationic and smaller hydrophobic amino acid cluster, however, had no observable influence on membrane homeostasis. Localization studies revealed that this AMP translocates through the cell wall and accumulates inside the bacteria. Regarding possible intracellular target sites, we identified strong binding of SP1-1 and several other AMPs to bacterial nucleic acids, thus influencing gene expression (Figure 31).

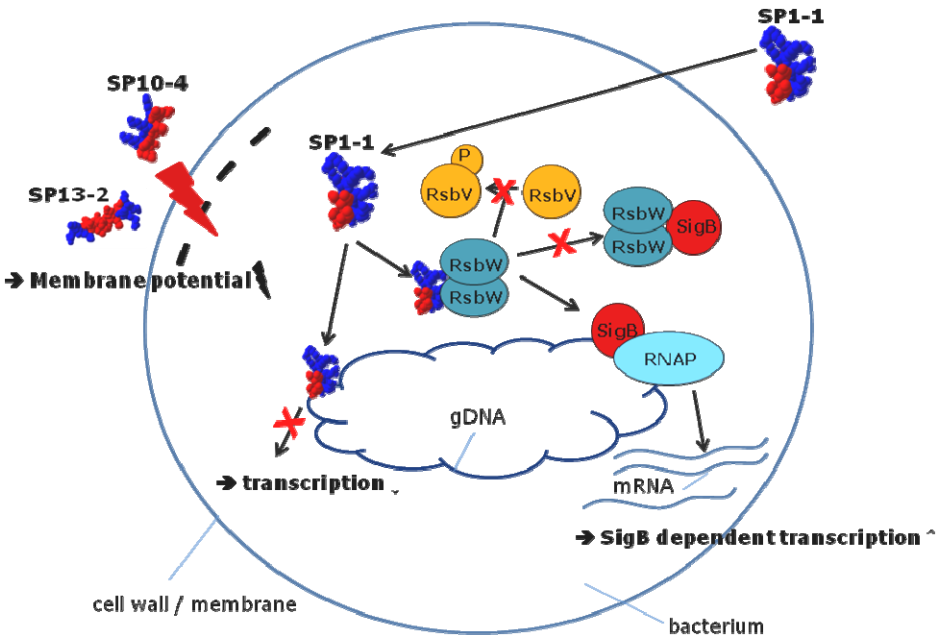

Figure 31 - Model of the multiple modes of action of SP1-1, SP10-4 and SP13-2
The shown peptides have diverse targets and multiple modes of action. Representative peptides from structural groups III (SP10-4) and IV (SP13-2) influence the bacterial membrane potential strongly. Furthermore, the peptides show dose dependent nucleic acid binding. SP1-1 can enter bacterial cells and interact with DNA and regulatory kinase RsbW, leading to transcriptional changes. gDNA: genomic DNA; mRNA: messenger RNA, RNAP: RNA polymerase

Additionally, for SP1-1 a strong inhibiting effect on the RsbW kinase in *S. aureus* was identified as part of the mode of action. Due to the regulatory impact of RsbW on transcription factor SigB, expression of SigB dependent genes was found to be altered. But also a huge number of further genes with functions in cell wall metabolism, amino

acid and carbohydrate transport and metabolism showed expression changes. However, the distinct affected genes and pathways still need further investigation.

Hence, it can be concluded that *de novo* designed AMPs with their different clusters of hydrophobic and charged residues have diverse target sites and multiple modes of action, not constricted to a certain target site. They have partly very specific target molecules, like RsbW kinase for SP1-1 in *S. aureus,* but show also unspecific or generalized targeting by binding to nucleic acids or by influencing membrane homeostasis (Figure 31).

The mechanisms of the different AMPs are thereby also depending on the pathogenic bacterial strain, which is exposed to the peptides. However, by antibacterial activity tests a number of further candidates were identified with high activity against phytopathogens and multi-resistant *S. aureus*. Alternative derivates of SP1, the highly active derivates of SP10 or even synergistic combinations can serve as a toolbox in the fight against diseases.
Kinase inhibitors fulfill important functions in modern medicine regarding cancer or inflammation processes (Janne et al., 2009; Roychowdhury et al., 2010; Dufies et al., 2011). Having with SP1-1 an agent on hand with strong kinase inhibitory activity might serve as a very promising starting point for future studies. For SP1-1 a screen for interactions with other *S. aureus* kinases has already started. Together with further analysis of the structural peptide kinase interaction, which has already been initiated within this study, this may lead to further elucidation of possible use and application of this and additional related peptides in future studies.

Additionally, immune-modulatory effects of well characterized antimicrobial peptides as well as for newly described ones attract increasing attention of researchers (Barlow et al., 2011; Bridle et al., 2011; Kim et al., 2011; Pasikowski et al., 2011). This still has to be elucidated with suitable *in vivo* models for the AMPs on hand and might open a further, additional opportunity for putative application. Furthermore, improved production techniques for antimicrobial peptides have allowed synthesis in a more cost-effective way by classical solid phase or enzymatic synthesis in recent years (Bruckdorfer et al., 2004; Guzman et al., 2007). Also alternative technologies like production in plants (Donini et al., 2005; Zeitler, 2011) or recombinant production in cell cultures (Bommarius et al., 2010; Li, 2011) are progressing. Additionally, several antimicrobial peptides, for example derived from magainin or histatins already entered the developing phase of clinical trials (Melo et al., 2006; Andres, 2011).

Taken together, the multiple modes of action of several new AMPs, highly active against *S. aureus,* could be characterized within this study, with membrane potential influencing ability (SP10 and SP13 derivates) on the one hand and a strong kinase inhibitor (SP1-1) and transcription-influencing agent on the other hand. In the future the use of these AMPs, after further developmental steps in human or animal medicine or plant protection is conceivable, with particular importance in the fight against resistant pathogens.

5 References

Agerberth, B., Charo, J., Werr, J., Olsson, B., Idali, F., Lindbom, L., Kiessling, R., Jornvall, H., Wigzell, H., and Gudmundsson, G.H. (2000). The human antimicrobial and chemotactic peptides LL-37 and alpha-defensins are expressed by specific lymphocyte and monocyte populations. Blood **96,** 3086-3093.

Agrios G. N. (2005). Plant Pathology. Academic Press Inc., London **Fifth Edition**.

Amiche, M., and Galanth, C. (2011). Dermaseptins as models for the elucidation of membrane-acting helical amphipathic antimicrobial peptides. Curr Pharm Biotechnol **12,** 1184-1193.

Andres, E. (2011). Cationic antimicrobial peptides in clinical development, with special focus on thanatin and heliomicin. Eur J Clin Microbiol Infect Dis.

Andreu, D., and Rivas, L. (1998). Animal antimicrobial peptides: an overview. Biopolymers **47,** 415-433.

Baba, T., Bae, T., Schneewind, O., Takeuchi, F., and Hiramatsu, K. (2008). Genome sequence of Staphylococcus aureus strain Newman and comparative analysis of staphylococcal genomes: polymorphism and evolution of two major pathogenicity islands. J Bacteriol **190,** 300-310.

Baba, T., Takeuchi, F., Kuroda, M., Yuzawa, H., Aoki, K., Oguchi, A., Nagai, Y., Iwama, N., Asano, K., Naimi, T., Kuroda, H., Cui, L., Yamamoto, K., and Hiramatsu, K. (2002). Genome and virulence determinants of high virulence community-acquired MRSA. Lancet **359,** 1819-1827.

Barlow, P.G., Svoboda, P., Mackellar, A., Nash, A.A., York, I.A., Pohl, J., Davidson, D.J., and Donis, R.O. (2011). Antiviral Activity and Increased Host Defense against Influenza Infection Elicited by the Human Cathelicidin LL-37. PLoS ONE **6,** e25333.

Baron, S. (1996). Medical Microbiology **4th edition**.

Barry, A.L., Craig, W.A., Nadler, H., Reller, L.B., Sanders, C.C., and Swenson, J.M. (1999). Methods for Determining Bactericidal Activity of Antimicrobial Agents; Approved Guideline M26-A. In Clinical and Laboratory Standards Institute (NCCLS).

Bechinger, B. (2010). Membrane association and pore formation by alpha-helical peptides. Adv Exp Med Biol **677,** 24-30.

Bellemare, A., Vernoux, N., Morin, S., Gagne, S.M., and Bourbonnais, Y. (2010). Structural and antimicrobial properties of human pre-elafin/trappin-2 and derived peptides against Pseudomonas aeruginosa. BMC Microbiol **10,** 253.

Benz, R., Janko, K., Boos, W., and Lauger, P. (1978). Formation of large, ion-permeable membrane channels by the matrix protein (porin) of Escherichia coli. Biochim Biophys Acta **511,** 305-319.

Bhargava, A., Osusky, M., Hancock, R.E., Forward, B., Kay, W., and Misra, S. (2007). Antiviral indolicidin variant peptides: Evaluation for broad-spectrum disease resistance in transgenic Nicotiana tabacum Plant Sci. **172** 515-523

Bhattacharjya, S., and Ramamoorthy, A. (2009). Multifunctional host defense peptides: functional and mechanistic insights from NMR structures of potent antimicrobial peptides. FEBS J **276,** 6465-6473.

Bischoff, M., Entenza, J.M., and Giachino, P. (2001). Influence of a functional sigB operon on the global regulators sar and agr in Staphylococcus aureus. J Bacteriol **183,** 5171-5179.

Bischoff, M., Dunman, P., Kormanec, J., Macapagal, D., Murphy, E., Mounts, W., Berger-Bachi, B., and Projan, S. (2004). Microarray-based analysis of the Staphylococcus aureus sigmaB regulon. J Bacteriol **186,** 4085-4099.

Bobone, S., Piazzon, A., Orioni, B., Pedersen, J.Z., Nan, Y.H., Hahm, K.S., Shin, S.Y., and Stella, L. (2011). The thin line between cell-penetrating and antimicrobial peptides: the case of Pep-1 and Pep-1-K. J Pept Sci **17,** 335-341.

Bocchinfuso, G., Palleschi, A., Orioni, B., Grande, G., Formaggio, F., Toniolo, C., Park, Y., Hahm, K.S., and Stella, L. (2009). Different mechanisms of action of

antimicrobial peptides: insights from fluorescence spectroscopy experiments and molecular dynamics simulations. J Pept Sci **15,** 550-558.

Boland, M.P., and Separovic, F. (2006). Membrane interactions of antimicrobial peptides from Australian tree frogs. Biochim Biophys Acta **1758,** 1178-1183.

Boman, H.G., Agerberth, B., and Boman, A. (1993). Mechanisms of action on Escherichia coli of cecropin P1 and PR-39, two antibacterial peptides from pig intestine. Infect Immun **61,** 2978-2984.

Boman, H.G., Faye, I., Gudmundsson, G.H., Lee, J.Y., and Lidholm, D.A. (1991). Cell-free immunity in Cecropia. A model system for antibacterial proteins. Eur J Biochem **201,** 23-31.

Bommarius, B., Jenssen, H., Elliott, M., Kindrachuk, J., Pasupuleti, M., Gieren, H., Jaeger, K.E., Hancock, R.E., and Kalman, D. (2010). Cost-effective expression and purification of antimicrobial and host defense peptides in Escherichia coli. Peptides **31,** 1957-1965.

Bouarab, K., Adas, F., Gaquerel, E., Kloareg, B., Salaun, J.P., and Potin, P. (2004). The innate immunity of a marine red alga involves oxylipins from both the eicosanoid and octadecanoid pathways. Plant Physiol **135,** 1838-1848.

Brandner, C.J., Maier, R.H., Henderson, D.S., Hintner, H., Bauer, J.W., and Onder, K. (2008). The ORFeome of Staphylococcus aureus v 1.1. BMC Genomics **9,** 321.

Bridle, A., Nosworthy, E., Polinski, M., and Nowak, B. (2011). Evidence of an antimicrobial-immunomodulatory role of Atlantic salmon cathelicidins during infection with Yersinia ruckeri. PLoS ONE **6,** e23417.

Brogden, K.A. (2005). Antimicrobial peptides: pore formers or metabolic inhibitors in bacteria? Nat Rev Microbiol **3,** 238-250.

Bruckdorfer, T., Marder, O., and Albericio, F. (2004). From production of peptides in milligram amounts for research to multi-tons quantities for drugs of the future. Curr Pharm Biotechnol **5,** 29-43.

Bruckner, R. (1992). A series of shuttle vectors for Bacillus subtilis and Escherichia coli. Gene **122,** 187-192.

Bucki, R., Leszczynska, K., Namiot, A., and Sokolowski, W. (2010). Cathelicidin LL-37: a multitask antimicrobial peptide. Arch Immunol Ther Exp (Warsz) **58,** 15-25.

Burda, W.N., Fields, K.B., Gill, J.B., Burt, R., Shepherd, M., Zhang, X.P., and Shaw, L.N. (2011). Neutral metallated and meso-substituted porphyrins as antimicrobial agents against Gram-positive pathogens. Eur J Clin Microbiol Infect Dis.

CAMECA. (2009). NanoSIMS 50: Cell biolology application booket "Multiple Isotope Mass Spectrometry for simultaneous stable isotope tracer imaging and measurements at subcellular level. A revolution in cellular biology".

Campbell, E.A., and Darst, S.A. (2000). The anti-sigma factor SpoIIAB forms a 2:1 complex with sigma(F), contacting multiple conserved regions of the sigma factor. J Mol Biol **300,** 17-28.

Campbell, E.A., Masuda, S., Sun, J.L., Muzzin, O., Olson, C.A., Wang, S., and Darst, S.A. (2002). Crystal structure of the Bacillus stearothermophilus anti-sigma factor SpoIIAB with the sporulation sigma factor sigmaF. Cell **108,** 795-807.

Cebrian, G., Sagarzazu, N., Aertsen, A., Pagan, R., Condon, S., and Manas, P. (2009). Role of the alternative sigma factor sigma on Staphylococcus aureus resistance to stresses of relevance to food preservation. J Appl Microbiol **107,** 187-196.

Chambers, H.F., and Deleo, F.R. (2009). Waves of resistance: Staphylococcus aureus in the antibiotic era. Nat Rev Microbiol **7,** 629-641.

Charbonnier, Y., Gettler, B., Francois, P., Bento, M., Renzoni, A., Vaudaux, P., Schlegel, W., and Schrenzel, J. (2005). A generic approach for the design of whole-genome oligoarrays, validated for genomotyping, deletion mapping and gene expression analysis on Staphylococcus aureus. BMC Genomics **6,** 95.

Chen, H.Y., Chen, C.C., Fang, C.S., Hsieh, Y.T., Lin, M.H., and Shu, J.C. (2011a). Vancomycin Activates sigma in Vancomycin-Resistant Staphylococcus aureus Resulting in the Enhancement of Cytotoxicity. PLoS ONE **6,** e24472.

Chen, Z., Wang, D., Cong, Y., Wang, J., Zhu, J., Yang, J., Hu, Z., Hu, X., Tan, Y., Hu, F., and Rao, X. (2011b). Recombinant antimicrobial peptide hPAB-beta expressed in Pichia pastoris, a potential agent active against methicillin-resistant Staphylococcus aureus. Appl Microbiol Biotechnol **89,** 281-291.

Chitarra, G.S., Breeuwer, A.J., Abee, T., and Bulk, R.W. (2006). The Use of Fluorescent Probes to Assess Viability of the Plant Pathogenic Bacterium *Clavibacter michiganensis* subsp. *michiganensis* by Flow Cytometry. Fitopatol. Bras. **31**.

Chroma, M., and Kolar, M. (2010). Genetic methods for detection of antibiotic resistance: focus on extended-spectrum beta-lactamases. Biomed Pap Med Fac Univ Palacky Olomouc Czech Repub **154,** 289-296.

Couto, M.A., Harwig, S.S., and Lehrer, R.I. (1993). Selective inhibition of microbial serine proteases by eNAP-2, an antimicrobial peptide from equine neutrophils. Infect Immun **61,** 2991-2994.

Craik, D.J., Gruber, C.W., Cemazar, M., and Anderson, M.A. (2007). Insecticidal plant cyclotides and related cystine knot toxins. Toxicon **49,** 561-575.

Dabrowski, J.M., Peall, S.K., Van Niekerk, A., Reinecke, A.J., Day, J.A., and Schulz, R. (2002). Predicting runoff-induced pesticide input in agricultural sub-catchment surface waters: linking catchment variables and contamination. Water Res **36,** 4975-4984.

Dale, B.A., and Fredericks, L.P. (2005). Antimicrobial peptides in the oral environment: expression and function in health and disease. Curr Issues Mol Biol **7,** 119-133.

Dalmau, M., Maier, E., Mulet, N., Vinas, M., and Benz, R. (2002). Bacterial membrane injuries induced by lactacin F and nisin. Int Microbiol **5,** 73-80.

Defres, S., Marwick, C., and Nathwani, D. (2009). MRSA as a cause of lung infection including airway infection, community-acquired pneumonia and hospital-acquired pneumonia. Eur Respir J **34,** 1470-1476.

Delumeau, O., Lewis, R.J., and Yudkin, M.D. (2002). Protein-protein interactions that regulate the energy stress activation of sigma(B) in Bacillus subtilis. J Bacteriol **184,** 5583-5589.

Derossi, D., Calvet, S., Trembleau, A., Brunissen, A., Chassaing, G., and Prochiantz, A. (1996). Cell internalization of the third helix of the Antennapedia homeodomain is receptor-independent. J Biol Chem **271,** 18188-18193.

Diemond-Hernandez, B., Solorzano-Santos, F., Leanos-Miranda, B., Peregrino-Bejarano, L., and Miranda-Novales, G. (2010). Production of icaADBC-encoded polysaccharide intercellular adhesin and therapeutic failure in pediatric patients with Staphylococcal device-related infections. BMC Infect Dis **10,** 68.

Diep, B.A., Gill, S.R., Chang, R.F., Phan, T.H., Chen, J.H., Davidson, M.G., Lin, F., Lin, J., Carleton, H.A., Mongodin, E.F., Sensabaugh, G.F., and Perdreau-Remington, F. (2006). Complete genome sequence of USA300, an epidemic clone of community-acquired meticillin-resistant Staphylococcus aureus. Lancet **367,** 731-739.

Dings, R.P., Haseman, J.R., and Mayo, K.H. (2008). Probing structure-activity relationships in bactericidal peptide betapep-25. Biochem J **414,** 143-150.

Dommett, R., Zilbauer, M., George, J.T., and Bajaj-Elliott, M. (2005). Innate immune defence in the human gastrointestinal tract. Mol Immunol **42,** 903-912.

Donini, M., Lico, C., Baschieri, S., Conti, S., Magliani, W., Polonelli, L., and Benvenuto, E. (2005). Production of an engineered killer peptide in Nicotiana benthamiana by using a potato virus X expression system. Appl Environ Microbiol **71,** 6360-6367.

Duchesne, L., and Fernig, D.G. (2007). Silver and gold nanoparticle-coated membranes for femtomole detection of small proteins and peptides by Dot and Western blot. Anal Biochem **362,** 287-289.

Dufies, M., Jacquel, A., Robert, G., Cluzeau, T., Puissant, A., Fenouille, N., Legros, L., Raynaud, S., Cassuto, J.P., Luciano, F., and Auberger, P. (2011). Mechanism of action of the multikinase inhibitor Foretinib. Cell Cycle **10**.

Duthie, E.S. (1952). Variation in the antigenic composition of staphylococcal coagulase. J Gen Microbiol **7,** 320-326.

Entenza, J.M., Moreillon, P., Senn, M.M., Kormanec, J., Dunman, P.M., Berger-Bachi, B., Projan, S., and Bischoff, M. (2005). Role of sigmaB in the expression of Staphylococcus aureus cell wall adhesins ClfA and FnbA and contribution to infectivity in a rat model of experimental endocarditis. Infect Immun **73,** 990-998.

Epand, R.M., and Vogel, H.J. (1999). Diversity of antimicrobial peptides and their mechanisms of action. Biochim Biophys Acta **1462,** 11-28.

Etezady-Esfarjani, T., and Wuthrich, K. (2004). NMR assignment of TM1442, a putative anti-sigma factor antagonist from Thermotoga maritima. J Biomol NMR **29,** 99-100.

Etezady-Esfarjani, T., Herrmann, T., Horst, R., and Wuthrich, K. (2006a). Automated protein NMR structure determination in crude cell-extract. J Biomol NMR **34,** 3-11.

Etezady-Esfarjani, T., Placzek, W.J., Herrmann, T., and Wuthrich, K. (2006b). Solution structures of the putative anti-sigma-factor antagonist TM1442 from Thermotoga maritima in the free and phosphorylated states. Magn Reson Chem **44 Spec No,** S61-70.

Ezekowitz, R.A.B., and Hoffmann, J.A. (2003). Innate Immunity. Humana Press.

Falla, T.J., Karunaratne, D.N., and Hancock, R.E. (1996). Mode of action of the antimicrobial peptide indolicidin. J Biol Chem **271,** 19298-19303.

Feng, X., Han, W., Song, Z., Zhao, H., Gao, Y., Diao, Y., Liu, S., and Lei, L. (2011). Development and characterization of a mouse monoclonal antibody against antimicrobial peptide tachyplesin I. Hybridoma (Larchmt) **30,** 355-359.

Flury, M. (1996). Experimental Evidence of Transport of Pesticides through Field Soils—A Review. Journal of Environmental Quality **Vol. 25** p. 25-45.

Friedrich, C.L., Moyles, D., Beveridge, T.J., and Hancock, R.E. (2000). Antibacterial action of structurally diverse cationic peptides on gram-positive bacteria. Antimicrob Agents Chemother **44,** 2086-2092.

Friedrich, C.L., Rozek, A., Patrzykat, A., and Hancock, R.E. (2001). Structure and mechanism of action of an indolicidin peptide derivative with improved activity against gram-positive bacteria. J Biol Chem **276,** 24015-24022.

Galanth, C., Abbassi, F., Lequin, O., Ayala-Sanmartin, J., Ladram, A., Nicolas, P., and Amiche, M. (2009). Mechanism of antibacterial action of dermaseptin B2: interplay between helix-hinge-helix structure and membrane curvature strain. Biochemistry **48,** 313-327.

Ganz, T., Selsted, M.E., and Lehrer, R.I. (1990). Defensins. Eur J Haematol **44,** 1-8.

Georgescu, J., Munhoz, V.H., and Bechinger, B. (2010). NMR structures of the histidine-rich peptide LAH4 in micellar environments: membrane insertion, pH-dependent mode of antimicrobial action, and DNA transfection. Biophys J **99,** 2507-2515.

Gertz, S., Engelmann, S., Schmid, R., Ziebandt, A.K., Tischer, K., Scharf, C., Hacker, J., and Hecker, M. (2000). Characterization of the sigma(B) regulon in Staphylococcus aureus. J Bacteriol **182,** 6983-6991.

Giachino, P., Engelmann, S., and Bischoff, M. (2001). Sigma(B) activity depends on RsbU in Staphylococcus aureus. J Bacteriol **183,** 1843-1852.

Gill, S.R., Fouts, D.E., Archer, G.L., Mongodin, E.F., Deboy, R.T., Ravel, J., Paulsen, I.T., Kolonay, J.F., Brinkac, L., Beanan, M., Dodson, R.J., Daugherty, S.C., Madupu, R., Angiuoli, S.V., Durkin, A.S., Haft, D.H., Vamathevan, J., Khouri, H., Utterback, T., Lee, C., Dimitrov, G., Jiang, L., Qin, H., Weidman, J., Tran, K., Kang, K., Hance, I.R., Nelson, K.E., and Fraser, C.M. (2005). Insights on evolution of virulence and resistance from the complete genome analysis of an early methicillin-resistant Staphylococcus aureus strain and a biofilm-producing methicillin-resistant Staphylococcus epidermidis strain. J Bacteriol **187,** 2426-2438.

Gillaspy, A.F., Worell, V., Orvis, J., Roe, B.A., and Dyer, D.W. (2007). *Staphylococcus aureus* subsp. aureus NCTC 8325, complete genome. Ref Type: Internet Communication.

Girish, T.S., Navratna, V., and Gopal, B. (2011). Structure and nucleotide specificity of Staphylococcus aureus dihydrodipicolinate reductase (DapB). FEBS Lett **585,** 2561-2567.

Giuliani, A., Pirri, G., and Nicoletto, S.F. (2007). Antimicrobial peptides: an overview of a promising class of therapeutics. Central European Journal of Biology **2,** 1-33.

Glaser, R. (2011). Research in practice: Antimicrobial peptides of the skin. J Dtsch Dermatol Ges **9,** 678-680.

Gong, Q., Menon, L., Ilina, T., Miller, L.G., Ahn, J., Parniak, M.A., and Ishima, R. (2010). Interaction of HIV-1 reverse transcriptase ribonuclease H with an acylhydrazone inhibitor. Chem Biol Drug Des **77,** 39-47.

Gonzalez-Rodriguez, R.M., Rial-Otero, R., Cancho-Grande, B., Gonzalez-Barreiro, C., and Simal-Gandara, J. (2011). A review on the fate of pesticides during the processes within the food-production Chain. Crit Rev Food Sci Nutr **51,** 99-114.

Gorwitz, R.J., Kruszon-Moran, D., McAllister, S.K., McQuillan, G., McDougal, L.K., Fosheim, G.E., Jensen, B.J., Killgore, G., Tenover, F.C., and Kuehnert, M.J. (2008). Changes in the prevalence of nasal colonization with Staphylococcus aureus in the United States, 2001-2004. J Infect Dis **197,** 1226-1234.

Grieco, P., Luca, V., Auriemma, L., Carotenuto, A., Saviello, M.R., Campiglia, P., Barra, D., Novellino, E., and Mangoni, M.L. (2011). Alanine scanning analysis and structure-function relationships of the frog-skin antimicrobial peptide temporin-1Ta. J Pept Sci **17,** 358-365.

Gruber, T.M., and Gross, C.A. (2003). Multiple sigma subunits and the partitioning of bacterial transcription space. Annu Rev Microbiol **57,** 441-466.

Guerquin-Kern, J.L., Wu, T.D., Quintana, C., and Croisy, A. (2005). Progress in analytical imaging of the cell by dynamic secondary ion mass spectrometry (SIMS microscopy). Biochim Biophys Acta **1724,** 228-238.

Guzman, F., Barberis, S., and Illanes, A. (2007). Peptide sythesis: chemical or enzymatic. Electronic Journal of Biotechnology **Vol.10 No.2**.

Hadjicharalambous, C., Sheynis, T., Jelinek, R., Shanahan, M.T., Ouellette, A.J., and Gizeli, E. (2008). Mechanisms of alpha-defensin bactericidal action: comparative membrane disruption by Cryptdin-4 and its disulfide-null analogue. Biochemistry **47,** 12626-12634.

Haigh, B., Hood, K., Broadhurst, M., Medele, S., Callaghan, M., Smolenski, G., Dines, M., and Wheeler, T. (2008). The bovine salivary proteins BSP30a and BSP30b are independently expressed BPI-like proteins with anti-Pseudomonas activity. Mol Immunol **45,** 1944-1951.

Haines, L.R., Thomas, J.M., Jackson, A.M., Eyford, B.A., Razavi, M., Watson, C.N., Gowen, B., Hancock, R.E., and Pearson, T.W. (2009). Killing of Trypanosomatid Parasites by a Modified Bovine Host Defense Peptide, BMAP-18. PLoS Negl Trop Dis **3,** e373.

Hancock, R.E., and Lehrer, R. (1998). Cationic peptides: a new source of antibiotics. Trends Biotechnol **16,** 82-88.

Hancock, R.E., and Diamond, G. (2000). The role of cationic antimicrobial peptides in innate host defences. Trends Microbiol **8,** 402-410.

Hancock, R.E., and Sahl, H.G. (2006). Antimicrobial and host-defense peptides as new anti-infective therapeutic strategies. Nat Biotechnol **24,** 1551-1557.

Haney, E.F., Hunter, H.N., Matsuzaki, K., and Vogel, H.J. (2009). Solution NMR studies of amphibian antimicrobial peptides: linking structure to function? Biochim Biophys Acta **1788,** 1639-1655.

Harris, F., Dennison, S.R., and Phoenix, D.A. (2009). Anionic antimicrobial peptides from eukaryotic organisms. Curr Protein Pept Sci **10,** 585-606.

Hartley, J.L., Temple, G.F., and Brasch, M.A. (2000). DNA cloning using in vitro site-specific recombination. Genome Res **10,** 1788-1795.

Hecker, M., Pane-Farre, J., and Volker, U. (2007). SigB-dependent general stress response in Bacillus subtilis and related gram-positive bacteria. Annu Rev Microbiol **61,** 215-236.

Hecker, M., Reder, A., Fuchs, S., Pagels, M., and Engelmann, S. (2009). Physiological proteomics and stress/starvation responses in Bacillus subtilis and Staphylococcus aureus. Res Microbiol **160,** 245-258.

Herbert, S., Ziebandt, A.K., Ohlsen, K., Schafer, T., Hecker, M., Albrecht, D., Novick, R., and Gotz, F. (2010). Repair of global regulators in Staphylococcus aureus 8325 and comparative analysis with other clinical isolates. Infect Immun **78,** 2877-2889.

Hernandez-Aponte, C.A., Silva-Sanchez, J., Quintero-Hernandez, V., Rodriguez-Romero, A., Balderas, C., Possani, L.D., and Gurrola, G.B. Vejovine, a new antibiotic from the scorpion venom of Vaejovis mexicanus. Toxicon **57,** 84-92.

Herzner, A.M., Dischinger, J., Szekat, C., Josten, M., Schmitz, S., Yakeleba, A., Reinartz, R., Jansen, A., Sahl, H.G., Piel, J., and Bierbaum, G. (2011). Expression of the Lantibiotic Mersacidin in Bacillus amyloliquefaciens FZB42. PLoS ONE **6,** e22389.

Holden, M.T., Feil, E.J., Lindsay, J.A., Peacock, S.J., Day, N.P., Enright, M.C., Foster, T.J., Moore, C.E., Hurst, L., Atkin, R., Barron, A., Bason, N., Bentley, S.D., Chillingworth, C., Chillingworth, T., Churcher, C., Clark, L., Corton, C., Cronin, A., Doggett, J., Dowd, L., Feltwell, T., Hance, Z., Harris, B., Hauser, H., Holroyd, S., Jagels, K., James, K.D., Lennard, N., Line, A., Mayes, R., Moule, S., Mungall, K., Ormond, D., Quail, M.A., Rabbinowitsch, E., Rutherford, K., Sanders, M., Sharp, S., Simmonds, M., Stevens, K., Whitehead, S., Barrell, B.G., Spratt, B.G., and Parkhill, J. (2004). Complete genomes of two clinical Staphylococcus aureus strains: evidence for the rapid evolution of virulence and drug resistance. Proc Natl Acad Sci U S A **101,** 9786-9791.

Huang, Y., Huang, J., and Chen, Y. (2010). Alpha-helical cationic antimicrobial peptides: relationships of structure and function. Protein Cell **1,** 143-152.

Huttunen-Hennelly, H.E.K., Azad, M.A., and Friedman, C.R. (2011). Bioactivity and the First Transmission Electron Microscopy Immunogold Studies of Short De Novo-Designed Antimicrobial Peptides. Antimicrobial Agents and Chemotherapy **55,** 2137-2145.

Imura, Y., Choda, N., and Matsuzaki, K. (2008). Magainin 2 in action: distinct modes of membrane permeabilization in living bacterial and mammalian cells. Biophys J **95,** 5757-5765.

Ishmael, F.T., Trakselis, M.A., and Benkovic, S.J. (2003). Protein-protein interactions in the bacteriophage T4 replisome. The leading strand holoenzyme is physically linked to the lagging strand holoenzyme and the primosome. J Biol Chem **278,** 3145-3152.

Jagadish, K., and Camarero, J.A. (2010). Cyclotides, a promising molecular scaffold for peptide-based therapeutics. Biopolymers **94,** 611-616.

Janne, P.A., Gray, N., and Settleman, J. (2009). Factors underlying sensitivity of cancers to small-molecule kinase inhibitors. Nat Rev Drug Discov **8,** 709-723.

Jiang, Z., Kullberg, B.J., van der Lee, H., Vasil, A.I., Hale, J.D., Mant, C.T., Hancock, R.E., Vasil, M.L., Netea, M.G., and Hodges, R.S. (2008). Effects of hydrophobicity on the antifungal activity of alpha-helical antimicrobial peptides. Chem Biol Drug Des **72,** 483-495.

Jones, A.T. (2007). Macropinocytosis: searching for an endocytic identity and role in the uptake of cell penetrating peptides. J Cell Mol Med **11,** 670-684.

Kenny, J.G., Ward, D., Josefsson, E., Jonsson, I.M., Hinds, J., Rees, H.H., Lindsay, J.A., Tarkowski, A., and Horsburgh, M.J. (2009). The Staphylococcus aureus response to unsaturated long chain free fatty acids: survival mechanisms and virulence implications. PLoS ONE **4,** e4344.

Kim, J.K., Lee, S.A., Shin, S., Lee, J.Y., Jeong, K.W., Nan, Y.H., Park, Y.S., Shin, S.Y., and Kim, Y. (2010). Structural flexibility and the positive charges are the

key factors in bacterial cell selectivity and membrane penetration of peptoid-substituted analog of Piscidin 1. Biochim Biophys Acta.

Kim, J.K., Lee, E., Shin, S., Jeong, K.W., Lee, J.Y., Bae, S.Y., Kim, S.H., Lee, J., Kim, S.R., Lee, D.G., Hwang, J.S., and Kim, Y. (2011). Structure and Function of Papiliocin with Antimicrobial and Anti-inflammatory Activities Isolated from the Swallowtail Butterfly, Papilio xuthus. J Biol Chem **286,** 41296-41311.

King, J.D., Mechkarska, M., Coquet, L., Leprince, J., Jouenne, T., Vaudry, H., Takada, K., and Conlon, J.M. (2011). Host-defense peptides from skin secretions of the tetraploid frogs Xenopus petersii and Xenopus pygmaeus, and the octoploid frog Xenopus lenduensis (Pipidae). Peptides.

Kluytmans, J., van Belkum, A., and Verbrugh, H. (1997). Nasal carriage of Staphylococcus aureus: epidemiology, underlying mechanisms, and associated risks. Clin Microbiol Rev **10,** 505-520.

Knobloch, J.K., Jager, S., Horstkotte, M.A., Rohde, H., and Mack, D. (2004). RsbU-dependent regulation of Staphylococcus epidermidis biofilm formation is mediated via the alternative sigma factor sigmaB by repression of the negative regulator gene icaR. Infect Immun **72,** 3838-3848.

Koessler, T., Francois, P., Charbonnier, Y., Huyghe, A., Bento, M., Dharan, S., Renzi, G., Lew, D., Harbarth, S., Pittet, D., and Schrenzel, J. (2006). Use of oligoarrays for characterization of community-onset methicillin-resistant Staphylococcus aureus. J Clin Microbiol **44,** 1040-1048.

Kolusheva, S., Boyer, L., and Jelinek, R. (2000a). A colorimetric assay for rapid screening of antimicrobial peptides. Nat Biotechnol **18,** 225-227.

Kolusheva, S., Shahal, T., and Jelinek, R. (2000b). Peptide-membrane interactions studied by a new phospholipid/polydiacetylene colorimetric vesicle assay. Biochemistry **39,** 15851-15859.

Kordel, M., Benz, R., and Sahl, H.G. (1988). Mode of action of the staphylococcinlike peptide Pep 5: voltage-dependent depolarization of bacterial and artificial membranes. J Bacteriol **170,** 84-88.

Kordel, M., Schuller, F., and Sahl, H.G. (1989). Interaction of the pore forming-peptide antibiotics Pep 5, nisin and subtilin with non-energized liposomes. FEBS Lett **244,** 99-102.

Kragol, G., Lovas, S., Varadi, G., Condie, B.A., Hoffmann, R., and Otvos, L., Jr. (2001). The antibacterial peptide pyrrhocoricin inhibits the ATPase actions of DnaK and prevents chaperone-assisted protein folding. Biochemistry **40,** 3016-3026.

Kullik, I., Giachino, P., and Fuchs, T. (1998). Deletion of the alternative sigma factor sigmaB in Staphylococcus aureus reveals its function as a global regulator of virulence genes. J Bacteriol **180,** 4814-4820.

Kuroda, M., Ohta, T., Uchiyama, I., Baba, T., Yuzawa, H., Kobayashi, I., Cui, L., Oguchi, A., Aoki, K., Nagai, Y., Lian, J., Ito, T., Kanamori, M., Matsumaru, H., Maruyama, A., Murakami, H., Hosoyama, A., Mizutani-Ui, Y., Takahashi, N.K., Sawano, T., Inoue, R., Kaito, C., Sekimizu, K., Hirakawa, H., Kuhara, S., Goto, S., Yabuzaki, J., Kanehisa, M., Yamashita, A., Oshima, K., Furuya, K., Yoshino, C., Shiba, T., Hattori, M., Ogasawara, N., Hayashi, H., and Hiramatsu, K. (2001). Whole genome sequencing of meticillin-resistant Staphylococcus aureus. Lancet **357,** 1225-1240.

Laemmli, U.K. (1970). Cleavage of structural proteins during the assembly of the head of bacteriophage T4. Nature **227,** 680-685.

Landon, C., Barbault, F., Legrain, M., Guenneugues, M., and Vovelle, F. (2008). Rational design of peptides active against the gram positive bacteria Staphylococcus aureus. Proteins **72,** 229-239.

Larkin, E.A., Carman, R.J., Krakauer, T., and Stiles, B.G. (2009). Staphylococcus aureus: the toxic presence of a pathogen extraordinaire. Curr Med Chem **16,** 4003-4019.

Lauderdale, K.J., Boles, B.R., Cheung, A.L., and Horswill, A.R. (2009). Interconnections between Sigma B, agr, and proteolytic activity in Staphylococcus aureus biofilm maturation. Infect Immun **77,** 1623-1635.

Lee, C.C., Sun, Y., Qian, S., and Huang, H.W. (2011). Transmembrane pores formed by human antimicrobial peptide LL-37. Biophys J **100,** 1688-1696.

Legrain, P., and Selig, L. (2000). Genome-wide protein interaction maps using two-hybrid systems. FEBS Lett **480,** 32-36.

Leontiadou, H., Mark, A.E., and Marrink, S.J. (2006). Antimicrobial peptides in action. J Am Chem Soc **128,** 12156-12161.

Li, Y. (2011). Recombinant production of antimicrobial peptides in Escherichia coli: a review. Protein Expr Purif **80,** 260-267.

Liu, G.Y., and Nizet, V. (2009). Color me bad: microbial pigments as virulence factors. Trends Microbiol **17,** 406-413.

Livermore, D.M. (2004). The need for new antibiotics. Clin Microbiol Infect **10 Suppl 4,** 1-9.

Lomash, S., Nagpal, S., and Salunke, D.M. (2010). An antibody as surrogate receptor reveals determinants of activity of an innate immune peptide antibiotic. J Biol Chem **285,** 35750-35758.

Lu, Y., Ma, Y., Wang, X., Liang, J., Zhang, C., Zhang, K., Lin, G., and Lai, R. (2008). The first antimicrobial peptide from sea amphibian. Mol Immunol **45,** 678-681.

Madani, F., Lindberg, S., Langel, U., Futaki, S., and Graslund, A. (2011). Mechanisms of cellular uptake of cell-penetrating peptides. J Biophys **2011,** 414729.

Maier, R., Brandner, C., Hintner, H., Bauer, J., and Onder, K. (2008). Construction of a reading frame-independent yeast two-hybrid vector system for site-specific recombinational cloning and protein interaction screening. Biotechniques **45,** 235-244.

Mainous, A.G., 3rd, Diaz, V.A., Matheson, E.M., Gregorie, S.H., and Hueston, W.J. (2011). Trends in hospitalizations with antibiotic-resistant infections: U.S., 1997-2006. Public Health Rep **126,** 354-360.

Malik, S.S., Luthra, A., and Ramachandran, R. (2009). Interactions of the M. tuberculosis UsfX with the cognate sigma factor SigF and the anti-anti sigma factor RsfA. Biochim Biophys Acta **1794,** 541-553.

Maloy, W.L., and Kari, U.P. (1995). Structure-activity studies on magainins and other host defense peptides. Biopolymers **37,** 105-122.

Mangoni, M.L. (2011). Host-defense peptides: from biology to therapeutic strategies. Cell Mol Life Sci **68,** 2157-2159.

Manich, M., Knapp, O., Gibert, M., Maier, E., Jolivet-Reynaud, C., Geny, B., Benz, R., and Popoff, M.R. (2008). Clostridium perfringens delta toxin is sequence related to beta toxin, NetB, and Staphylococcus pore-forming toxins, but shows functional differences. PLoS ONE **3,** e3764.

Marcos, J.F., Munoz, A., Perez-Paya, E., Misra, S., and Lopez-Garcia, B. (2008). Identification and rational design of novel antimicrobial peptides for plant protection. Annu Rev Phytopathol **46,** 273-301.

Markossian, K.A., Zamyatnin, A.A., and Kurganov, B.I. (2004). Antibacterial proline-rich oligopeptides and their target proteins. Biochemistry (Mosc) **69,** 1082-1091.

Marti, M., Trotonda, M.P., Tormo-Mas, M.A., Vergara-Irigaray, M., Cheung, A.L., Lasa, I., and Penades, J.R. (2009). Extracellular proteases inhibit protein-dependent biofilm formation in Staphylococcus aureus. Microbes Infect **12,** 55-64.

Martorell, G., Gradwell, M.J., Birdsall, B., Bauer, C.J., Frenkiel, T.A., Cheung, H.T., Polshakov, V.I., Kuyper, L., and Feeney, J. (1994). Solution structure of bound trimethoprim in its complex with Lactobacillus casei dihydrofolate reductase. Biochemistry **33,** 12416-12426.

Matsuzaki, K. (1999). Why and how are peptide-lipid interactions utilized for self-defense? Magainins and tachyplesins as archetypes. Biochim Biophys Acta **1462,** 1-10.

Melo, M.N., Dugourd, D., and Castanho, M.A. (2006). Omiganan pentahydrochloride in the front line of clinical applications of antimicrobial peptides. Recent Pat Antiinfect Drug Discov **1,** 201-207.

Midorikawa, K., Ouhara, K., Komatsuzawa, H., Kawai, T., Yamada, S., Fujiwara, T., Yamazaki, K., Sayama, K., Taubman, M.A., Kurihara, H., Hashimoto, K., and Sugai, M. (2003). Staphylococcus aureus susceptibility to innate antimicrobial peptides, beta-defensins and CAP18, expressed by human keratinocytes. Infect Immun **71,** 3730-3739.

Minami, Y., Uede, K., Sagawa, K., Kimura, A., Tsuji, T., and Furukawa, F. (2004). Immunohistochemical staining of cutaneous tumours with G-81, a monoclonal antibody to dermcidin. Br J Dermatol **151,** 165-169.

Miyazaki, E., Chen, J.M., Ko, C., and Bishai, W.R. (1999). The Staphylococcus aureus rsbW (orf159) gene encodes an anti-sigma factor of SigB. J Bacteriol **181,** 2846-2851.

Montesinos, E. (2007). Antimicrobial peptides and plant disease control. FEMS Microbiol Lett **270,** 1-11.

Morgan, W.D., Birdsall, B., Nieto, P.M., Gargaro, A.R., and Feeney, J. (1999). 1H/15N HSQC NMR studies of ligand carboxylate group interactions with arginine residues in complexes of brodimoprim analogues and Lactobacillus casei dihydrofolate reductase. Biochemistry **38,** 2127-2134.

Morikawa, K., Hidaka, T., Murakami, H., Hayashi, H., and Ohta, T. (2005). Staphylococcal Drp35 is the functional counterpart of the eukaryotic PONs. FEMS Microbiol Lett **249,** 185-190.

Morikawa, K., Maruyama, A., Inose, Y., Higashide, M., Hayashi, H., and Ohta, T. (2001). Overexpression of sigma factor, sigma(B), urges Staphylococcus aureus to thicken the cell wall and to resist beta-lactams. Biochem Biophys Res Commun **288,** 385-389.

Munoz, A., Lopez-Garcia, B., Perez-Paya, E., and Marcos, J.F. (2007). Antimicrobial properties of derivatives of the cationic tryptophan-rich hexapeptide PAF26. Biochem Biophys Res Commun **354,** 172-177.

Murakami, H., Matsumaru, H., Kanamori, M., Hayashi, H., and Ohta, T. (1999). Cell wall-affecting antibiotics induce expression of a novel gene, drp35, in Staphylococcus aureus. Biochem Biophys Res Commun **264,** 348-351.

Musat, N., Foster, R., Vagner, T., Adam, B., and Kuypers, M.M. (2011). Detecting metabolic activities in single cells, with emphasis on nanoSIMS. FEMS Microbiol Rev.

Musat, N., Halm, H., Winterholler, B., Hoppe, P., Peduzzi, S., Hillion, F., Horreard, F., Amann, R., Jorgensen, B.B., and Kuypers, M.M. (2008). A single-cell view on the ecophysiology of anaerobic phototrophic bacteria. Proc Natl Acad Sci U S A **105,** 17861-17866.

Nakase, I., Takeuchi, T., Tanaka, G., and Futaki, S. (2008). Methodological and cellular aspects that govern the internalization mechanisms of arginine-rich cell-penetrating peptides. Adv Drug Deliv Rev **60,** 598-607.

Nan, Y.H., Park, K.H., Park, Y., Jeon, Y.J., Kim, Y., Park, I.S., Hahm, K.S., and Shin, S.Y. (2009). Investigating the effects of positive charge and hydrophobicity on the cell selectivity, mechanism of action and anti-inflammatory activity of a Trp-rich antimicrobial peptide indolicidin. FEMS Microbiol Lett **292,** 134-140.

Neely, K.E., Hassan, A.H., Brown, C.E., Howe, L., and Workman, J.L. (2002). Transcription activator interactions with multiple SWI/SNF subunits. Mol Cell Biol **22,** 1615-1625.

Nguyen, L.T., Haney, E.F., and Vogel, H.J. (2011). The expanding scope of antimicrobial peptide structures and their modes of action. Trends Biotechnol.

Nielsen, S.L., Frimodt-Moller, N., Kragelund, B.B., and Hansen, P.R. (2007). Structure--activity study of the antibacterial peptide fallaxin. Protein Sci **16,** 1969-1976.

Nishikata, M., Kanehira, T., Oh, H., Tani, H., Tazaki, M., and Kuboki, Y. (1991). Salivary histatin as an inhibitor of a protease produced by the oral bacterium Bacteroides gingivalis. Biochem Biophys Res Commun **174,** 625-630.

O'Gara, J.P. (2007). ica and beyond: biofilm mechanisms and regulation in Staphylococcus epidermidis and Staphylococcus aureus. FEMS Microbiol Lett **270,** 179-188.

Orcajo-Rincon, A.L., Ortega-Gutierrez, S., Serrano, P., Torrecillas, I.R., Wuthrich, K., Campillo, M., Pardo, L., Viso, A., Benhamu, B., and Lopez-Rodriguez, M.L. (2011). Development of non-peptide ligands of growth factor receptor-bound protein 2-SRC homology 2 domain using molecular modeling and NMR spectroscopy. J Med Chem **54,** 1096-1100.

Oren, Z., and Shai, Y. (1998). Mode of action of linear amphipathic alpha-helical antimicrobial peptides. Biopolymers **47,** 451-463.

Ortega, M.R., Ganz, T., and Milner, S.M. (2000). Human beta defensin is absent in burn blister fluid. Burns **26,** 724-726.

Otvos, L., Jr. (2000). Antibacterial peptides isolated from insects. J Pept Sci **6,** 497-511.

Otvos, L., Jr. (2005). Antibacterial peptides and proteins with multiple cellular targets. J Pept Sci **11,** 697-706.

Otvos, L., Jr., O, I., Rogers, M.E., Consolvo, P.J., Condie, B.A., Lovas, S., Bulet, P., and Blaszczyk-Thurin, M. (2000). Interaction between heat shock proteins and antimicrobial peptides. Biochemistry **39,** 14150-14159.

Palffy, R., Gardlik, R., Behuliak, M., Kadasi, L., Turna, J., and Celec, P. (2009). On the physiology and pathophysiology of antimicrobial peptides. Mol Med **15,** 51-59.

Pane-Farre, J., Jonas, B., Forstner, K., Engelmann, S., and Hecker, M. (2006). The sigmaB regulon in Staphylococcus aureus and its regulation. Int J Med Microbiol **296,** 237-258.

Pane-Farre, J., Jonas, B., Hardwick, S.W., Gronau, K., Lewis, R.J., Hecker, M., and Engelmann, S. (2009). Role of RsbU in controlling SigB activity in Staphylococcus aureus following alkaline stress. J Bacteriol **191,** 2561-2573.

Park, C.B., Kim, M.S., and Kim, S.C. (1996). A novel antimicrobial peptide from Bufo bufo gargarizans. Biochem Biophys Res Commun **218,** 408-413.

Park, C.B., Kim, H.S., and Kim, S.C. (1998). Mechanism of action of the antimicrobial peptide buforin II: buforin II kills microorganisms by penetrating the cell membrane and inhibiting cellular functions. Biochem Biophys Res Commun **244,** 253-257.

Park, Y., and Hahm, K.S. (2005). Antimicrobial peptides (AMPs): peptide structure and mode of action. J Biochem Mol Biol **38,** 507-516.

Pasikowski, P., Gozdziewicz, T., Stefanowicz, P., Artym, J., Zimecki, M., and Szewczuk, Z. (2011). A novel immunosuppressory peptide originating from the ubiquitin sequence. Peptides.

Patrzykat, A., Friedrich, C.L., Zhang, L., Mendoza, V., and Hancock, R.E. (2002). Sublethal concentrations of pleurocidin-derived antimicrobial peptides inhibit macromolecular synthesis in Escherichia coli. Antimicrob Agents Chemother **46,** 605-614.

Pernice, M., Meibom, A., Van Den Heuvel, A., Kopp, C., Domart-Coulon, I., Hoegh-Guldberg, O., and Dove, S. (2012). A single-cell view of ammonium assimilation in coral-dinoflagellate symbiosis. ISME J.

Perron, G.G., Zasloff, M., and Bell, G. (2006). Experimental evolution of resistance to an antimicrobial peptide. Proc Biol Sci **273,** 251-256.

Peschel, A., and Sahl, H.G. (2006). The co-evolution of host cationic antimicrobial peptides and microbial resistance. Nat Rev Microbiol **4,** 529-536.

Pietiainen, M., Francois, P., Hyyrylainen, H.L., Tangomo, M., Sass, V., Sahl, H.G., Schrenzel, J., and Kontinen, V.P. (2009). Transcriptome analysis of the responses of Staphylococcus aureus to antimicrobial peptides and characterization of the roles of vraDE and vraSR in antimicrobial resistance. BMC Genomics **10,** 429.

Podorieszach, A.P., and Huttunen-Hennelly, H.E. (2010). The effects of tryptophan and hydrophobicity on the structure and bioactivity of novel indolicidin derivatives with promising pharmaceutical potential. Org Biomol Chem **8,** 1679-1687.

Polzien, L., Baljuls, A., Roth, H.M., Kuper, J., Benz, R., Schweimer, K., Hekman, M., and Rapp, U.R. (2010). Pore-forming activity of BAD is regulated by specific phosphorylation and structural transitions of the C-terminal part. Biochim Biophys Acta **1810,** 162-169.

Polzien, L., Baljuls, A., Rennefahrt, U.E., Fischer, A., Schmitz, W., Zahedi, R.P., Sickmann, A., Metz, R., Albert, S., Benz, R., Hekman, M., and Rapp, U.R. (2009). Identification of novel in vivo phosphorylation sites of the human proapoptotic protein BAD: pore-forming activity of BAD is regulated by phosphorylation. J Biol Chem **284,** 28004-28020.

Poole, R.K., and Cook, G.M. (2000). Redundancy of aerobic respiratory chains in bacteria? Routes, reasons and regulation. Adv Microb Physiol **43,** 165-224.

Powers, J.P., and Hancock, R.E. (2003). The relationship between peptide structure and antibacterial activity. Peptides **24,** 1681-1691.

Powers, J.P., Martin, M.M., Goosney, D.L., and Hancock, R.E. (2006). The antimicrobial peptide polyphemusin localizes to the cytoplasm of Escherichia coli following treatment. Antimicrob Agents Chemother **50,** 1522-1524.

Rachid, S., Ohlsen, K., Wallner, U., Hacker, J., Hecker, M., and Ziebuhr, W. (2000). Alternative transcription factor sigma(B) is involved in regulation of biofilm expression in a Staphylococcus aureus mucosal isolate. J Bacteriol **182,** 6824-6826.

Rahman, M., Tsuji, N., Boldbaatar, D., Battur, B., Liao, M., Umemiya-Shirafuji, R., You, M., Tanaka, T., and Fujisaki, K. (2010). Structural characterization and cytolytic activity of a potent antimicrobial motif in longicin, a defensin-like peptide in the tick Haemaphysalis longicornis. J Vet Med Sci **72,** 149-156.

Renzoni, A., Barras, C., Francois, P., Charbonnier, Y., Huggler, E., Garzoni, C., Kelley, W.L., Majcherczyk, P., Schrenzel, J., Lew, D.P., and Vaudaux, P. (2006). Transcriptomic and functional analysis of an autolysis-deficient, teicoplanin-resistant derivative of methicillin-resistant Staphylococcus aureus. Antimicrob Agents Chemother **50,** 3048-3061.

Rhodes, D.I., Peat, T.S., Vandegraaff, N., Jeevarajah, D., Le, G., Jones, E.D., Smith, J.A., Coates, J.A., Winfield, L.J., Thienthong, N., Newman, J., Lucent, D., Ryan, J.H., Savage, G.P., Francis, C.L., and Deadman, J.J. (2011). Structural basis for a new mechanism of inhibition of HIV-1 integrase identified by fragment screening and structure-based design. Antivir Chem Chemother **21,** 155-168.

Rinaldi, A.C., Mangoni, M.L., Rufo, A., Luzi, C., Barra, D., Zhao, H., Kinnunen, P.K., Bozzi, A., Di Giulio, A., and Simmaco, M. (2002). Temporin L: antimicrobial, haemolytic and cytotoxic activities, and effects on membrane permeabilization in lipid vesicles. Biochem J **368,** 91-100.

Roychowdhury, A., Sharma, R., and Kumar, S. (2010). Recent advances in the discovery of small molecule mTOR inhibitors. Future Med Chem **2,** 1577-1589.

Rzepiela, A.J., Sengupta, D., Goga, N., and Marrink, S.J. (2010). Membrane poration by antimicrobial peptides combining atomistic and coarse-grained descriptions. Faraday Discuss **144,** 431-443; discussion 445-481.

Sahl, H.G., Kordel, M., and Benz, R. (1987). Voltage-dependent depolarization of bacterial membranes and artificial lipid bilayers by the peptide antibiotic nisin. Arch Microbiol **149,** 120-124.

Salay, L.C., Nobre, T.M., Colhone, M.C., Zaniquelli, M.E., Ciancaglini, P., Stabeli, R.G., Leite, J.R., and Zucolotto, V. (2011). Dermaseptin 01 as antimicrobial peptide with rich biotechnological potential: study of peptide interaction with membranes containing Leishmania amazonensis lipid-rich extract and membrane models. J Pept Sci **17,** 700-707.

Sambrook, J., and Russell, D.W. (2001). Molecular Cloning: A Laboratory Manual Cold Spring Harbor Laboratory Press, Cold Spring Harbor, New York **3rd Edition**.

Sass, P., Jansen, A., Szekat, C., Sass, V., Sahl, H.G., and Bierbaum, G. (2008). The lantibiotic mersacidin is a strong inducer of the cell wall stress response of Staphylococcus aureus. BMC Microbiol **8,** 186.

Sawant, R., and Torchilin, V. (2009). Intracellular transduction using cell-penetrating peptides. Mol Biosyst **6,** 628-640.

Schagger, H. (2006). Tricine-SDS-PAGE. Nat Protoc **1,** 16-22.

Scherl, A., Francois, P., Charbonnier, Y., Deshusses, J.M., Koessler, T., Huyghe, A., Bento, M., Stahl-Zeng, J., Fischer, A., Masselot, A., Vaezzadeh, A.,

Galle, F., Renzoni, A., Vaudaux, P., Lew, D., Zimmermann-Ivol, C.G., Binz, P.A., Sanchez, J.C., Hochstrasser, D.F., and Schrenzel, J. (2006). Exploring glycopeptide-resistance in Staphylococcus aureus: a combined proteomics and transcriptomics approach for the identification of resistance-related markers. BMC Genomics **7,** 296.

Schmidt, N., Mishra, A., Lai, G.H., and Wong, G.C. (2010). Arginine-rich cell-penetrating peptides. FEBS Lett **584,** 1806-1813.

Scocchi, M., Tossi, A., and Gennaro, R. (2011). Proline-rich antimicrobial peptides: converging to a non-lytic mechanism of action. Cell Mol Life Sci **68,** 2317-2330.

Semrau, S., Monster, M.W., van der Knaap, M., Florea, B.I., Schmidt, T., and Overhand, M. (2010). Membrane lysis by gramicidin S visualized in red blood cells and giant vesicles. Biochim Biophys Acta **1798,** 2033-2039.

Senn, M.M., Giachino, P., Homerova, D., Steinhuber, A., Strassner, J., Kormanec, J., Fluckiger, U., Berger-Bachi, B., and Bischoff, M. (2005). Molecular analysis and organization of the sigmaB operon in Staphylococcus aureus. J Bacteriol **187,** 8006-8019.

Shafer, W.M., and Iandolo, J.J. (1979). Genetics of staphylococcal enterotoxin B in methicillin-resistant isolates of Staphylococcus aureus. Infect Immun **25,** 902-911.

Shai, Y. (1999). Mechanism of the binding, insertion and destabilization of phospholipid bilayer membranes by alpha-helical antimicrobial and cell non-selective membrane-lytic peptides. Biochim Biophys Acta **1462,** 55-70.

Shai, Y. (2002). Mode of action of membrane active antimicrobial peptides. Biopolymers **66,** 236-248.

Sinha, B., and Fraunholz, M. (2010). Staphylococcus aureus host cell invasion and post-invasion events. Int J Med Microbiol **300,** 170-175.

Sokolov, Y., Mirzabekov, T., Martin, D.W., Lehrer, R.I., and Kagan, B.L. (1999). Membrane channel formation by antimicrobial protegrins. Biochim Biophys Acta **1420,** 23-29.

Sperstad, S.V., Haug, T., Blencke, H.M., Styrvold, O.B., Li, C., and Stensvag, K. (2011). Antimicrobial peptides from marine invertebrates: Challenges and perspectives in marine antimicrobial peptide discovery. Biotechnol Adv.

Stapleton, M.R., Horsburgh, M.J., Hayhurst, E.J., Wright, L., Jonsson, I.M., Tarkowski, A., Kokai-Kun, J.F., Mond, J.J., and Foster, S.J. (2007). Characterization of IsaA and SceD, two putative lytic transglycosylases of Staphylococcus aureus. J Bacteriol **189,** 7316-7325.

Steidl, R., Pearson, S., Stephenson, R.E., Ledala, N., Sitthisak, S., Wilkinson, B.J., and Jayaswal, R.K. (2008). Staphylococcus aureus cell wall stress stimulon gene-lacZ fusion strains: potential for use in screening for cell wall-active antimicrobials. Antimicrob Agents Chemother **52,** 2923-2925.

Steiner, H., Hultmark, D., Engstrom, A., Bennich, H., and Boman, H.G. (1981). Sequence and specificity of two antibacterial proteins involved in insect immunity. Nature **292,** 246-248.

Stipani, V., Gallucci, E., Micelli, S., Picciarelli, V., and Benz, R. (2001). Channel formation by salmon and human calcitonin in black lipid membranes. Biophys J **81,** 3332-3338.

Talaat, A.M., Howard, S.T., Hale, W.t., Lyons, R., Garner, H., and Johnston, S.A. (2002). Genomic DNA standards for gene expression profiling in Mycobacterium tuberculosis. Nucleic Acids Res **30,** e104.

Tamba, Y., Ariyama, H., Levadny, V., and Yamazaki, M. (2010). Kinetic pathway of antimicrobial peptide magainin 2-induced pore formation in lipid membranes. J Phys Chem B **114,** 12018-12026.

Tang, M., and Hong, M. (2009). Structure and mechanism of beta-hairpin antimicrobial peptides in lipid bilayers from solid-state NMR spectroscopy. Mol Biosyst **5,** 317-322.

Taylor, K., Barran, P.E., and Dorin, J.R. (2008). Structure-activity relationships in beta-defensin peptides. Biopolymers **90,** 1-7.

Terras, F.R., Eggermont, K., Kovaleva, V., Raikhel, N.V., Osborn, R.W., Kester, A., Rees, S.B., Torrekens, S., Van Leuven, F., Vanderleyden, J., and et al. (1995). Small cysteine-rich antifungal proteins from radish: their role in host defense. Plant Cell **7,** 573-588.

Thennarasu, S., Tan, A., Penumatchu, R., Shelburne, C.E., Heyl, D.L., and Ramamoorthy, A. (2010). Antimicrobial and membrane disrupting activities of a peptide derived from the human cathelicidin antimicrobial peptide LL37. Biophys J **98,** 248-257.

van Schaik, W., Zwietering, M.H., de Vos, W.M., and Abee, T. (2004). Identification of sigmaB-dependent genes in Bacillus cereus by proteome and in vitro transcription analysis. J Bacteriol **186,** 4100-4109.

van Schaik, W., Tempelaars, M.H., Zwietering, M.H., de Vos, W.M., and Abee, T. (2005). Analysis of the role of RsbV, RsbW, and RsbY in regulating {sigma}B activity in Bacillus cereus. J Bacteriol **187,** 5846-5851.

Visweswaran, G.R., Dijkstra, B.W., and Kok, J. (2011). Murein and pseudomurein cell wall binding domains of bacteria and archaea--a comparative view. Appl Microbiol Biotechnol **92,** 921-928.

Visweswaran, G.R., Dijkstra, B.W., and Kok, J. (2012). A genetically engineered protein domain binding to bacterial murein, archaeal pseudomurein, and fungal chitin cell wall material. Appl Microbiol Biotechnol.

Walhout, A.J., Temple, G.F., Brasch, M.A., Hartley, J.L., Lorson, M.A., van den Heuvel, S., and Vidal, M. (2000). GATEWAY recombinational cloning: application to the cloning of large numbers of open reading frames or ORFeomes. Methods Enzymol **328,** 575-592.

Wang, G., Epand, R.F., Mishra, B., Lushnikova, T., Thomas, V.C., Bayles, K.W., and Epand, R.M. (2011). Decoding the Functional Roles of Cationic Side Chains of the Major Antimicrobial Region of Human Cathelicidin LL-37. Antimicrob Agents Chemother.

Wanniarachchi, Y.A., Kaczmarek, P., Wan, A., and Nolan, E.M. (2011). Human defensin 5 disulfide array mutants: disulfide bond deletion attenuates antibacterial activity against Staphylococcus aureus. Biochemistry **50,** 8005-8017.

Wei, G., Pazgier, M., de Leeuw, E., Rajabi, M., Li, J., Zou, G., Jung, G., Yuan, W., Lu, W.Y., Lehrer, R.I., and Lu, W. (2010). Trp-26 imparts functional versatility to human alpha-defensin HNP1. J Biol Chem **285,** 16275-16285.

Werner, G., Strommenger, B., and Witte, W. (2008). Acquired vancomycin resistance in clinically relevant pathogens. Future Microbiol **3,** 547-562.

Wiedemann, I., Benz, R., and Sahl, H.G. (2004). Lipid II-mediated pore formation by the peptide antibiotic nisin: a black lipid membrane study. J Bacteriol **186,** 3259-3261.

Wiegand, I., Hilpert, K., and Hancock, R.E. (2008). Agar and broth dilution methods to determine the minimal inhibitory concentration (MIC) of antimicrobial substances. Nat Protoc **3,** 163-175.

Wilke, M.H. (2010). Multiresistant bacteria and current therapy - the economical side of the story. Eur J Med Res **15,** 571-576.

Wimley, W.C., and Hristova, K. (2011). Antimicrobial peptides: successes, challenges and unanswered questions. J Membr Biol **239,** 27-34.

Wirmer, J., and Westhof, E. (2006). Molecular contacts between antibiotics and the 30S ribosomal particle. Methods Enzymol **415,** 180-202.

Woebken, D., Burow, L.C., Prufert-Bebout, L., Bebout, B.M., Hoehler, T.M., Pett-Ridge, J., Spormann, A.M., Weber, P.K., and Singer, S.W. (2012). Identification of a novel cyanobacterial group as active diazotrophs in a coastal microbial mat using NanoSIMS analysis. ISME J.

Woodford, N., and Ellington, M.J. (2007). The emergence of antibiotic resistance by mutation. Clin Microbiol Infect **13,** 5-18.

Wu, M., Maier, E., Benz, R., and Hancock, R.E. (1999). Mechanism of interaction of different classes of cationic antimicrobial peptides with planar bilayers and with the cytoplasmic membrane of Escherichia coli. Biochemistry **38,** 7235-7242.

Yeaman, M.R., and Yount, N.Y. (2003). Mechanisms of antimicrobial peptide action and resistance. Pharmacol Rev **55,** 27-55.

Yonezawa, A., Kuwahara, J., Fujii, N., and Sugiura, Y. (1992). Binding of tachyplesin I to DNA revealed by footprinting analysis: significant contribution of secondary structure to DNA binding and implication for biological action. Biochemistry **31,** 2998-3004.

Yudkin, M.D. (1987). Structure and function in a Bacillus subtilis sporulation-specific sigma factor: molecular nature of mutations in spoIIAC. J Gen Microbiol **133,** 475-481.

Zander, J., Besier, S., Ackermann, H., and Wichelhaus, T.A. (2009). Synergistic antimicrobial activities of folic acid antagonists and nucleoside analogs. Antimicrob Agents Chemother **54,** 1226-1231.

Zanetti-Polzi, L., Anselmi, M., D'Alessandro, M., Amadei, A., and Di Nola, A. (2009). Structural, thermodynamic, and kinetic properties of Gramicidin analogue GS6 studied by molecular dynamics simulations and statistical mechanics. Biopolymers **91,** 1154-1160.

Zasloff, M. (1987). Magainins, a class of antimicrobial peptides from Xenopus skin: isolation, characterization of two active forms, and partial cDNA sequence of a precursor. Proc Natl Acad Sci U S A **84,** 5449-5453.

Zasloff, M. (2002). Antimicrobial peptides of multicellular organisms. Nature **415,** 389-395.

Zeitler, B. (2011). Production of Antimicrobial Peptides in different *Nicotiana* species. Technische Universität München, dissertation.

Zeitler, B., Dangel, A., Thellmann, M., Meyer, H., Sattler, M., and Lindermayr, C. (2012). *De-novo* Design of Antimicrobial Peptides for Plant Protection. submitted to Molecular Plant-Microbe Interactions (MPMI), in resubmission process.

Zelezetsky, I., and Tossi, A. (2006). Alpha-helical antimicrobial peptides--using a sequence template to guide structure-activity relationship studies. Biochim Biophys Acta **1758,** 1436-1449.

Zeng, X.C., Wang, S., Nie, Y., Zhang, L., and Luo, X. (2011). Characterization of BmKbpp, a multifunctional peptide from the Chinese scorpion Mesobuthus martensii Karsch: Gaining insight into a new mechanism for the functional diversification of scorpion venom peptides. Peptides.

Zhang, H., Morikawa, K., Ohta, T., and Kato, Y. (2005). In vitro resistance to the CSalphabeta-type antimicrobial peptide ASABF-alpha is conferred by overexpression of sigma factor sigB in Staphylococcus aureus. J Antimicrob Chemother **55,** 686-691.

Zhang, L., Scott, M.G., Yan, H., Mayer, L.D., and Hancock, R.E. (2000). Interaction of polyphemusin I and structural analogs with bacterial membranes, lipopolysaccharide, and lipid monolayers. Biochemistry **39,** 14504-14514.

Zhang, R., Eggleston, K., Rotimi, V., and Zeckhauser, R.J. (2006). Antibiotic resistance as a global threat: evidence from China, Kuwait and the United States. Global Health **2,** 6.

Zhou, H., Dou, J., Wang, J., Chen, L., Wang, H., Zhou, W., Li, Y., and Zhou, C. (2011). The antibacterial activity of BF-30 in vitro and in infected burned rats is through interference with cytoplasmic membrane integrity. Peptides **32,** 1131-1138.

6 Supplement

6.1 Antibacterial activity of the designed AMPs against phytopathogenic bacteria

Supplementary Table 1 - MIC values against phytopathogenic bacteria and hemolytic activity of the first and second design-generation of the AMPs

A

	SP1	SP2	SP3	SP4	SP5	SP6	SP7	SP8
MIC (µg/ml)								
Pseudomonas corrugata (2d)	2	5	> 40	> 40	> 40	20	10	> 40
Pseudomonas syringae pv. tomato (1d)	10	2	5	10	> 40	10	5	> 40
Clavibacter michiganensis (2d)	1	2	20	40	20	> 40	5	> 40
Pectobacterium carotovorum (1d)	>40	> 40	> 40	> 40	> 40	> 40	> 40	> 40
Pseudomonas syringae pv. syringae (1d)	2	2	> 40	> 40	40	5	10	> 40
Xanthomonas vesicatoria (2d)	2	2	> 40	> 40	40	40	5	> 40
Hemolytic activity (µg/ml)	-	> 200	> 200	> 200	> 200	> 200	> 200	> 200

	SP9	SP10	SP11	SP12	SP13	SP14	SP15	SP16
MIC (µg/ml)								
Pseudomonas corrugata (2d)	>40	20	> 40	> 40	2.5	> 40	> 40	2.5
Pseudomonas syringae pv. tomato (1d)	10	10	> 40	2.5	20	40	40	5
Clavibacter michiganensis (2d)	10	10	> 40	>40	2.5	20	2.5	5
Pectobacterium carotovorum (1d)	>40	20	5	>40	>40	> 40	> 40	> 40
Pseudomonas syringae pv. syringae (1d)	10	10	> 40	10	10	> 40	> 40	5
Xanthomonas vesicatoria (2d)	5	5	10	20	2.5	> 40	20	5
Hemolytic activity (µg/ml)	50	100	> 200	> 200	100	> 200	< 20	> 200

B

	SP1-1	SP1-2	SP1-3	SP1-4	SP1-5	SP1-6	SP1-7	SP1-8
MIC (µg/ml)								
Pseudomonas corrugata (2d)	< 0.1	0.5	2.5	> 10	5.0	> 10	0.5	2.5
Pseudomonas syringae pv. tomato (1d)	>10	5.0	5.0	2.5	1.0	1.0	10	10
Clavibacter michiganensis (2d)	2.5	10	> 10	> 10	> 10	10	2.5	5.0
Pectobacterium carotovorum (1d)	> 10	> 10	> 10	> 10	> 10	> 10	> 10	>10
Pseudomonas syringae pv. syringae (1d)	0.1	2.5	0.25	5.0	> 10	5.0	0.1	0.25
Xanthomonas vesicatoria (2d)	0.1	5.0	> 10	> 10	> 10	> 10	1.0	2.5
Hemolytic activity (µg/ml)	-	-	-	-	-	-	-	-

	SP1-9	SP1-10	SP1-11	SP1-12	SP1-13	SP1-14	SP1-15	SP1-16
MIC (µg/ml)								
Pseudomonas corrugata (2d)	5.0	10	0.25	0.25	< 0.1	0.5	< 0.1	0.5
Pseudomonas syringae pv. tomato (1d)	5.0	>10	>10	>10	2.5	1.0	1.0	1.0
Clavibacter michiganensis (2d)	2.5	> 10	2.5	0.5	0.25	1.0	5.0	>10
Pectobacterium carotovorum (1d)	> 10	> 10	> 10	> 10	> 10	> 10	> 10	> 10
Pseudomonas syringae pv. syringae (1d)	0.5	1.0	1.0	0.1	0.1	< 0.1	0.1	0.1
Xanthomonas vesicatoria (2d)	2.5	>10	2.5	0.5	0.5	1.0	5.0	10
Hemolytic activity (µg/ml)	-	-	-	-	-	-	-	-

Supplementary Table 1 – continued

	SP1-17	SP1-18	SP1-19	SP1-20	SP1-21	SP1-22	SP10-1	SP10-2
MIC (µg/ml)								
Pseudomonas corrugata (2d)	5.0	0.25	0.5	0.5	2.5	> 10	2.5	0.5
Pseudomonas syringae pv. tomato (1d)	1.0	1.0	>10	10	2.5	1.0	1.0	0.5
Clavibacter michiganensis (2d)	>10	5.0	5.0	5.0	>10	>10	1.0	0.25
Pectobacterium carotovorum (1d)	> 10	> 10	> 10	> 10	> 10	> 10	2.5	1.0
Pseudomonas syringae pv. syringae (1d)	< 0.1	0.1	< 0.1	0.25	0.5	2.5	2.5	0.1
Xanthomonas vesicatoria (2d)	> 10	5.0	5.0	10	> 10	>10	2.5	0.25
Hemolytic activity (µg/ml)	-	-	-	-	-	-	>200	>200

	SP10-3	SP10-4	SP10-5	SP10-6	SP10-7	SP10-8	SP10-9	SP10-10
MIC (µg/ml)								
Pseudomonas corrugata (2d)	1.0	2.5	0.5	2.5	2.5	0.5	0.5	0.25
Pseudomonas syringae pv. tomato (1d)	0.25	1.0	0.25	1.0	1.0	1.0	0.25	0.5
Clavibacter michiganensis (2d)	2.5	0.25	0.5	2.5	5.0	0.5	1.0	0.25
Pectobacterium carotovorum (1d)	> 10	2.5	2.5	2.5	> 10	2.5	2.5	2.5
Pseudomonas syringae pv. syringae (1d)	0.25	0.25	0.5	2.5	> 10	0.5	0.25	0.25
Xanthomonas vesicatoria (2d)	2.5	0.1	0.25	1.0	5.0	0.5	1.0	0.1
Hemolytic activity (µg/ml)	-	>200	-	>200	-	50	-	-

	SP10-11	SP13-1	SP13-2	SP13-3	SP13-4	SP13-5	SP13-6	SP13-7
MIC (µg/ml)								
Pseudomonas corrugata (2d)	0.5	2.5	5.0	> 10	5.0	10	2.5	0.5
Pseudomonas syringae pv. tomato (1d)	0.5	1.0	10	10	>10	2.5	2.5	10
Clavibacter michiganensis (2d)	5.0	0.5	0.25	2.5	1.0	2.5	0.1	0.25
Pectobacterium carotovorum (1d)	> 10	> 10	> 10	> 10	> 10	> 10	> 10	> 10
Pseudomonas syringae pv. syringae (1d)	0.1	1.0	5.0	> 10	10	> 10	1.0	> 10
Xanthomonas vesicatoria (2d)	0.5	0.5	0.25	2.5	2.5	1.0	0.1	0.1
Hemolytic activity (µg/ml)	-	> 200	50	> 200	50	100	20	200

	SP13-8	SP13-9	SP13-10	SP13-11	SP13-12	SP13-13	SP13-14
MIC (µg/ml)							
Pseudomonas corrugata (2d)	0.25	0.25	0.25	> 10	10	0.25	2.5
Pseudomonas syringae pv. tomato (1d)	10	>10	1.0	2.5	5.0	2.5	2.5
Clavibacter michiganensis (2d)	0.1	0.25	0.1	2.5	2.5	0.5	0.5
Pectobacterium carotovorum (1d)	> 10	> 10	> 10	> 10	> 10	> 10	> 10
Pseudomonas syringae pv. syringae (1d)	> 10	> 10	> 10	> 10	> 10	0.5	5.0
Xanthomonas vesicatoria (2d)	0.1	0.1	0.1	2.5	2.5	0.25	0.25
Hemolytic activity (µg/ml)	>200	-	200	200	50	>200	50

Antibacterial activity was determined by incubation of dilution series of synthetic AMPs with 10^5 cfu of bacterial suspension cultures in LB medium in a total volume of 100 µl for 1 (1d) or 2 (2d) days (24 or 48 h). OD_{600nm} was measured and minimal inhibitory concentration (MIC) values were determined. (A) MIC values for the first development generation of synthetic AMPs. 0.1 – 40 µg/ml were incubated with the bacteria. (B) MIC values for the second development generation of synthetic AMPs. 0.1 – 10 µg/ml were incubated with the bacteria. Hemolytic activity was determined by incubation of 0.1 – 200 µg/ml peptides with human erythrocytes and measurement of the released hemoglobin. Shown are the peptide concentrations leading to 25 % hemoglobin release from human blood cells. > 200 describes a slight hemolytic activity at 200 µg/ml but below the above mentioned threshold. No value indicates no detectable hemolytic activity up to the highest concentration tested. (Zeitler et al., 2012).

6.2 Bacterial membrane potential measurements

The measurements of bacterial membrane potential with different concentrations of peptides (Supplementary Figure 1) showed by trend the same differences as presented in chapter 3.2.3, Figure 8. Additionally, plating of aliquots at every measurement timepoint revealed active concentrations and killing speed with the used amount of 5 x 10^7 cfu cells (Supplementary Figure 2), in comparison to the 10^5 cfu bacteria cells that were used for standard antibacterial activity assays.

A

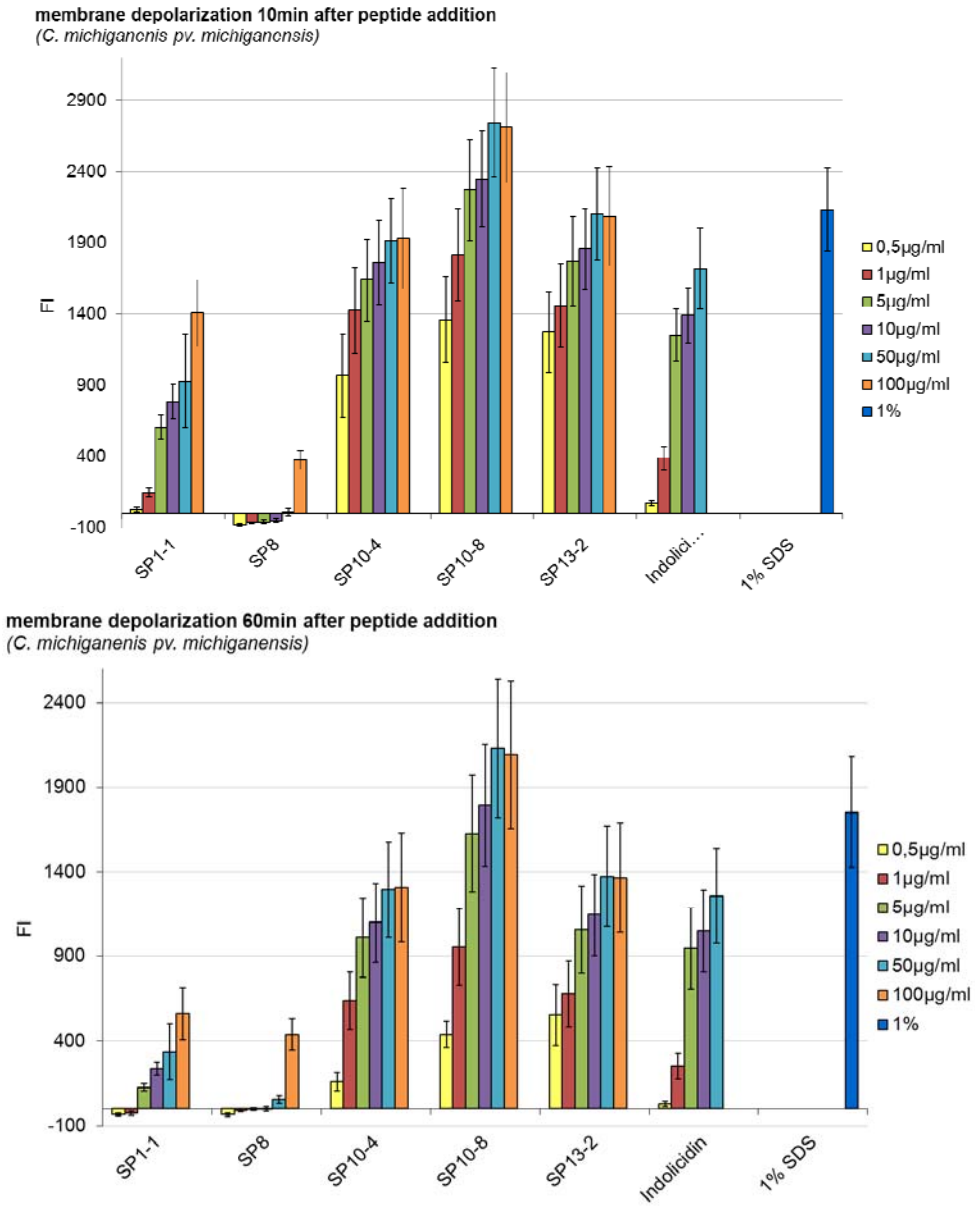

B

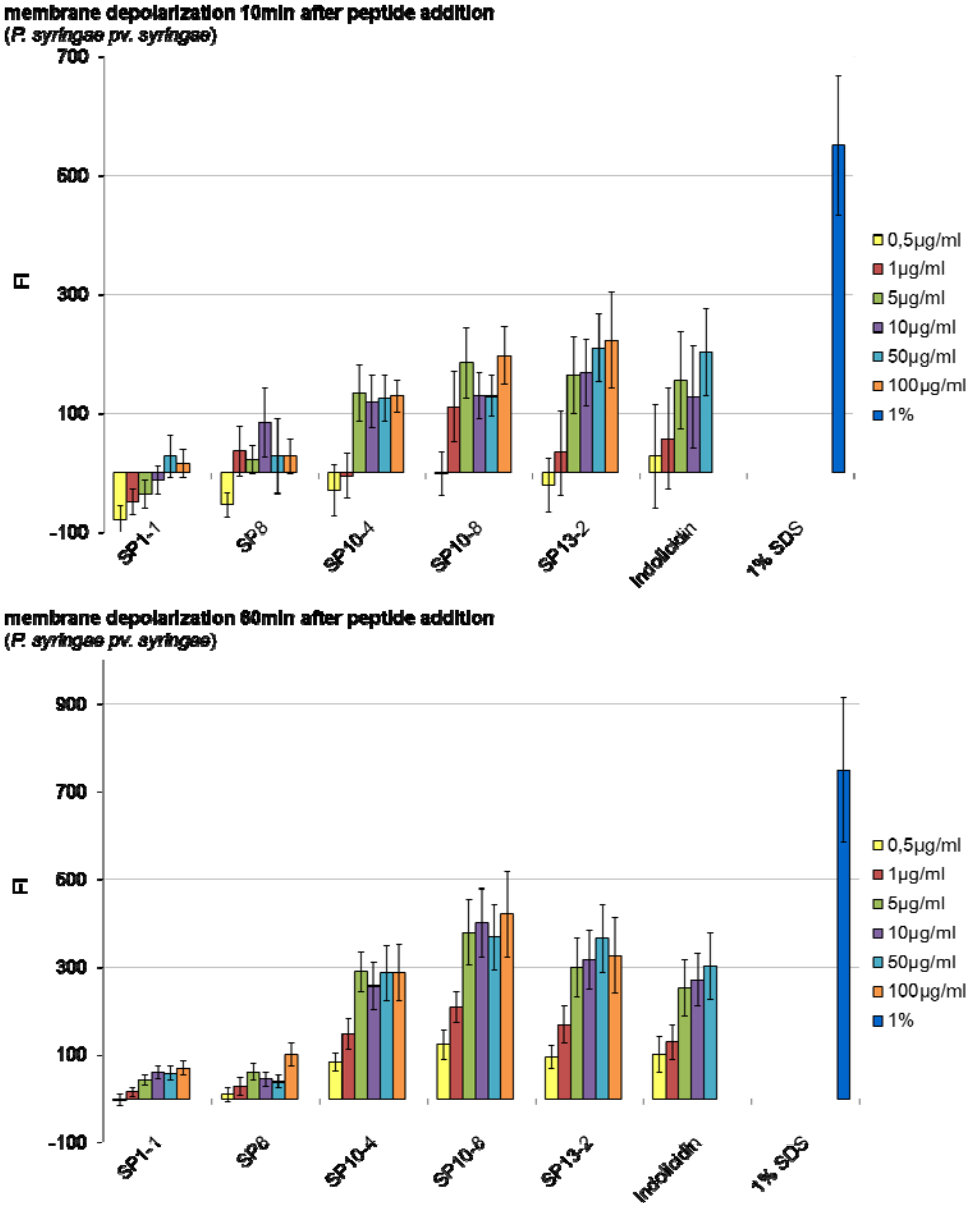

Supplementary Figure 1 - Measurement of bacterial membrane depolarization
Depolarization of bacterial membranes was determined by loading 5 x 10^7 cfu/ml (A) gram-positive *C. michiganensis ssp. michiganensis* or (B) gram-negative *P. syringae pv. syringae* with $DiSC_3(5)$ and measuring fluorescence intensity (FI) after addition of 0.5, 1, 5, 10, 50 or 100 µg/ml peptides (λ_{ex}: 622nm λ_{em}: 670nm). Shown are FI values 10 and 60 min after peptide addition. Peptides SP1-1, SP10-4, 10-8 and 13-2 were used. Indolicidin and 1% SDS were used as positive controls and SP8 as control with no antibacterial activity, respectively. Data were normalized against FI after buffer treatment. Error bars represent standard deviation of three independent experiments.

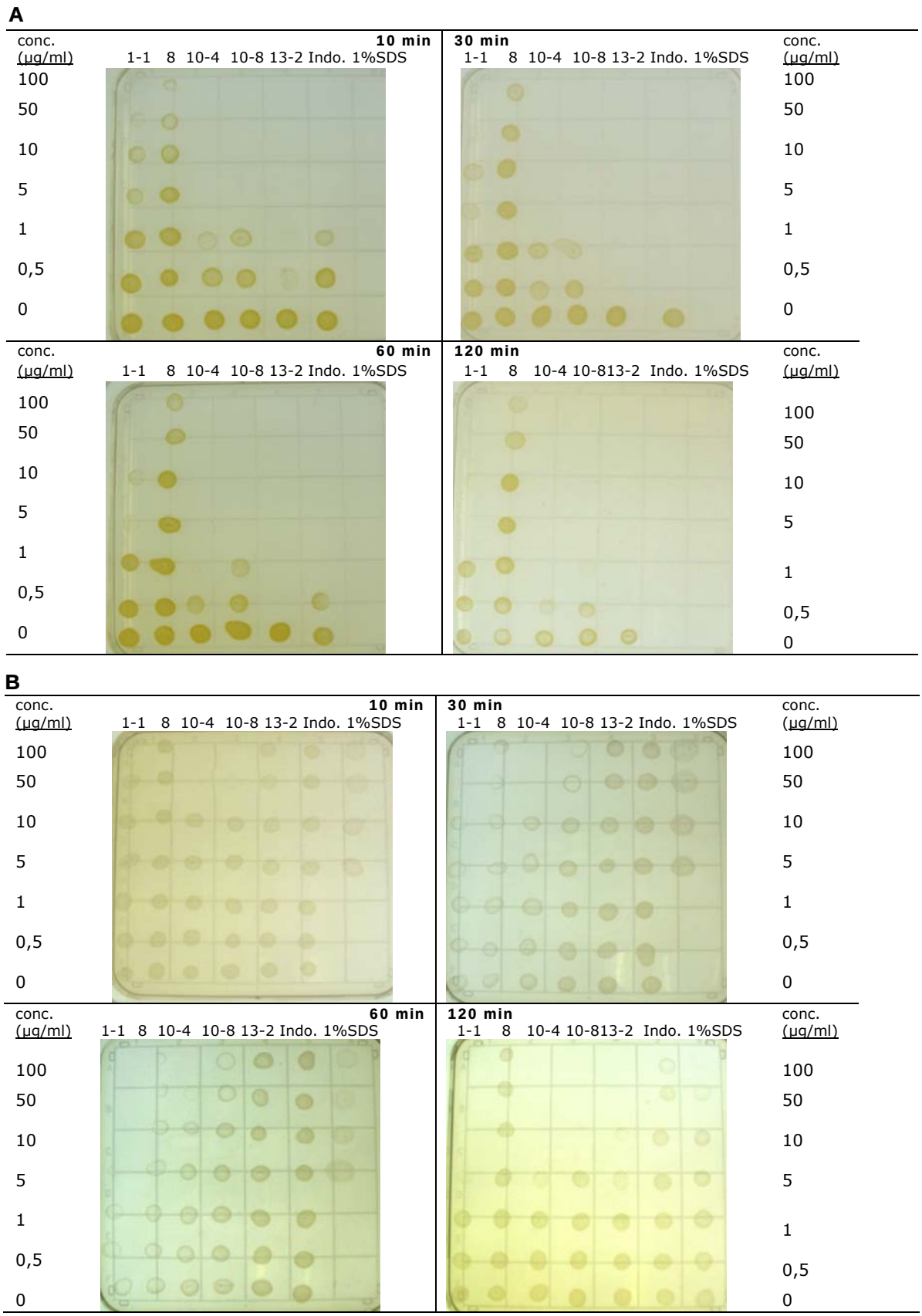

Supplementary Figure 2 - Plating of bacterial suspensions during membrane potential measurements

10 µl aliquots of the reaction mixtures of $DiSC_3(5)$ loaded and peptide treated (A) *C. michiganensis ssp. michiganensis* or (B) *P. syringae pv. syringae* were plated on LB agar plates at 10, 30, 60 and 120 minutes after treatment with 0, 0.5, 1, 5, 10, 50, 100 µg/ml SP1-1, SP8, SP10-4, SP10-8, SP13-2 or indolicidin (Indo.). 1% SDS (4 -5 replicates) served as control for growth under membrane depolarization. The plates were incubated for 24 h at 30°C and checked for bacteria growth.

6.3 Anti-peptide antibody testing for immunogold stain

Monoclonal antibodies were generated at the Core Facility for Generation of Monoclonal Antibodies and Cell Sorting of the Institute of Molecular Immunology (Helmholtz Zentrum München, Munich, Germany). Therefor SP1-1 and 10-2 were synthesized coupled to Keyhole Limpet Hemocyanin (KLH) carrier protein by Peptide Speciality Laboratories GmbH (Heidelberg, Germany) and used for immunization. The primary supernatants of the monoclonal antibody producing hybridoma cell lines were initially tested for cross reactivity at the Core Facility for Generation of Monoclonal Antibodies and Cell Sorting (Supplementary Table 2). The delivered primary hybridoma supernatants were tested for sensitivity and selectivity by immunodetection of peptides, BSA (as negative control) and bacterial protein extracts on dot blots or western blots from Tricine–SDS-PAGE (example in Supplementary Figure 3).

Supplementary Table 2 - List of tested monoclonal antibodies and reactivity

mAb species	sub class	developed against	Theoretical activity and cross reactivity		
mAb from rat-hybridoma cells			**SP1**	**SP10-2**	**SP13**
2D12	2a	SP1-1, SP102, SP13	positive	positive	((positive))
5A10	2a	SP1-1, SP102, SP13	positive	positive	((positive))
5C10	M	SP1-1, SP102, SP13	positive	positive	((positive))
5C10	2a	SP1-1, SP102, SP13	positive	positive	((positive))
7C5	2b	SP1-1, SP102, SP13	positive	positive	((positive))
8F4	2b	SP1-1, SP102, SP13	positive	positive	((positive))
7B8	M	SP1-1	((positive))	positive	Negative
7B8	2a	SP10-2	((positive))	positive	Negative
7F12	2b	SP1-1	((positive))	positive	Negative
4H8	2b	SP10-2	positive	positive	Positive
6A4	2b	SP1-1	(positive)	negative	((positive))
6B4	2b	SP1-1	(positive)	negative	((positive))
8G11	2a	SP1-1	positive	positive	Positive
4F2	M/G1	SP10-2	positive	(positive)	(positive)
7D6	2c	SP10-2	negative	positive	Positive
8A8	2c	SP10-2	negative	positive	Positive
4C9	2c	SP10-2	negative	positive	Positive
3C12	2c	SP10-2	negative	positive	(positive)
4F2	M/G1	SP1, SP10-2, SP13	positive	(positive)	Positive
4F3	2a	SP10-2	negative	positive	Negative
3F7	2b	SP1-1, SP102, SP13	positive	negative	Positive
2H9	2b	SP1-1, SP102, SP13	positive	negative	Positive
8A1	2b	SP1-1, SP102, SP13	positive	negative	Positive
mAb from mouse-hybridoma cells					
7F7	2a	SP1-1	n.d	n.d.	n.d.

The shown antibodies were generated against SP1-1, SP10-2 and/or SP13 at the Core Facility for Generation of Monoclonal Antibodies and Cell Sorting of the Institute of Molecular Immunology (Helmholtz Zentrum München). Origin, species and subclass of the antibodies are shown in the left column. Peptides used for immunization and antibody generation are shown in the middle column and initial tested reactivity and cross-reactivity, tested by the Core Facility for Generation of Monoclonal Antibodies and Cell Sorting are shown in the right column. Reactivity against the used peptides was classified from no reactivity to high reactivity as follows: negative< ((positive)) < (positive) < positive. mAB 2D12 (highlighthed in yellow) serves as an example for sensitivity and specificity test, shown in Supplementary Figure 3. mAB: monoclonal antibody; n.d.: not determined.

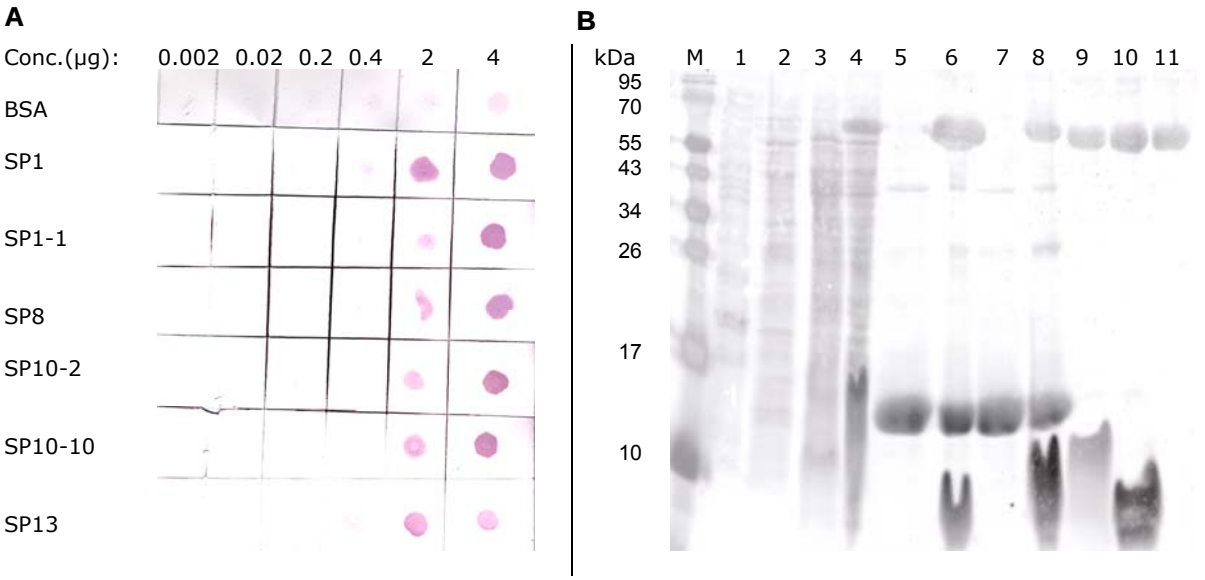

Supplementary Figure 3 - Example of the anti-SP antibody testing (mAb 2D12/2a)
Antibodies were tested for sensitivity and specificity for immunogold stain. The testing was done by (A) dot blotting and immunodetection by secondary Anti-Rat IgG-AP or by (B) 16% Tricine-SDS-PAGE followed by western blotting and immunodetection by secondary Alexa-Fluor-546 goat ant-Rat IgG (B). Shown is the example for mAB 2D12 (highlighted in yellow in Supplementary Table 2).
(A) For dot blots dilutions 0.002 µg – 4 µg of SP1-1, SP8, SP10-2, SP10-10 and SP13 and BSA were used. (B) For western blots 25 µg crude protein extract with or without 10 µg peptide addition, or 10 µg pure peptides (in 0.02% BSA, 0.01% acetic acid) or 10 µg BSA were used: (1) BSA (2) SP1-1, (3) SP13, (4) protein extract of *Clavibacter michiganensis ssp. michiganensis* + SP1-1, (5) protein extract of *Clavibacter michiganensis ssp. michiganensis*, (6) protein extract of *Pectobacterium carotovorum* ssp. *carotovorum* + SP10, (7) protein extract of *Pectobacterium carotovorum ssp. carotovorum*, (8) protein extract of *Pseudomonas syringae pv. syringae* + SP13, (9) protein extract of *Pseudomonas syringae pv. syringae*, (10) protein extract of *Pseudomonas corrugata*, (11) protein extract of *Xanthomonas vesicatoria*. M: molecular weight marker (in kDa)

6.4 NanoSIMS measurements

Usage of sub-lethal ^{15}N-SP1-1 concentrations was made sure by plating of 10 µl aliquots of the peptide treated reaction mixtures and checking for growth.

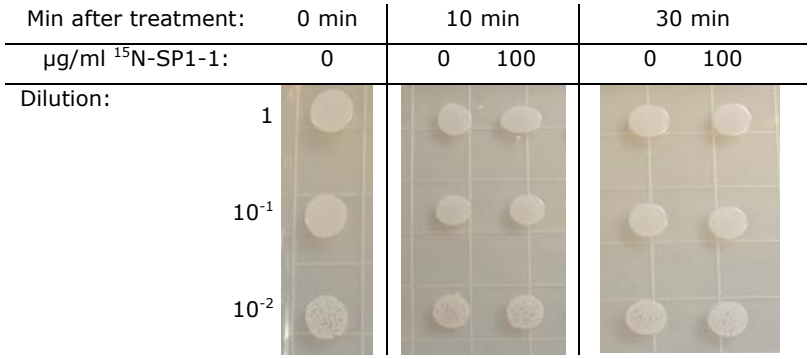

Supplementary Figure 4 - Plating of ^{15}N-SP1-1 treated samples
4x 10^6 cfu *S. aureus* 90857 were treated with either 0 (mock) or 100 µg/ml ^{15}N-SP1-1. To make sure that sub-lethal concentrations of ^{15}N-SP1-1 were used for the NanoSIMS analysis 10 µl aliquots of the reaction mixtures, 1/10 and 1/100 dilutions of it were plated on LB agar plates. The samples were plated directly before peptide treatment, 10 and 30 min after treatment before the cells were harvested for the analysis. The agar plates were incubated oN at 37°C and checked for growth.

For calculation of the accumulation of ^{15}N over the natural ^{14}N background of the ^{15}N-SP1-1 treated *S. aureus* cells, regions of interests (ROIs) were built on selected Nano SIMS image spots covering *S. aureus* cells or filter area for measurement of nitrogen background levels. Ratios of $^{12}C^{15}N/^{12}C^{14}N$ of the recorded SIMS counts were calculated. By comparing the $^{12}C^{15}N/^{12}C^{14}N$ signal count ratios of ROIs of 30 min ^{15}N-SP1-1 treated *S. aureus* cells (Supplementary Figure 5, red ROIs), to ROIs either from the background filter area (Supplementary Figure 5, green ROIs) or from *S. aureus* cells from 30 min buffer treatment (Supplementary Figure 7), elevated ^{15}N levels of a factor of 2.75 - 5.5 were identified (comparison of Supplementary Figure 5C (red to green table) to 7C). By comparing the $^{12}C^{15}N/^{12}C^{14}N$ signal count ratios of ROIs of 10 min ^{15}N-SP1-1 treated *S. aureus* cells (Supplementary Figure 6), with either ROIs from the background filter area (Supplementary Figure 5, green ROIs) or from *S. aureus* cells from the 30 min buffer treatment (Supplementary Figure 7), elevated ^{15}N levels of a factor of 5 - 10 were identified (comparison of Supplementary Figure 6C, to 5C (green table) and 7C). By recording of ^{12}C, ^{13}C, ^{16}O ^{32}S and the sum of all secondary electrons, the analysis of *S. aureus* cells and not artefacts was ensured (Supplementary Figure 8).

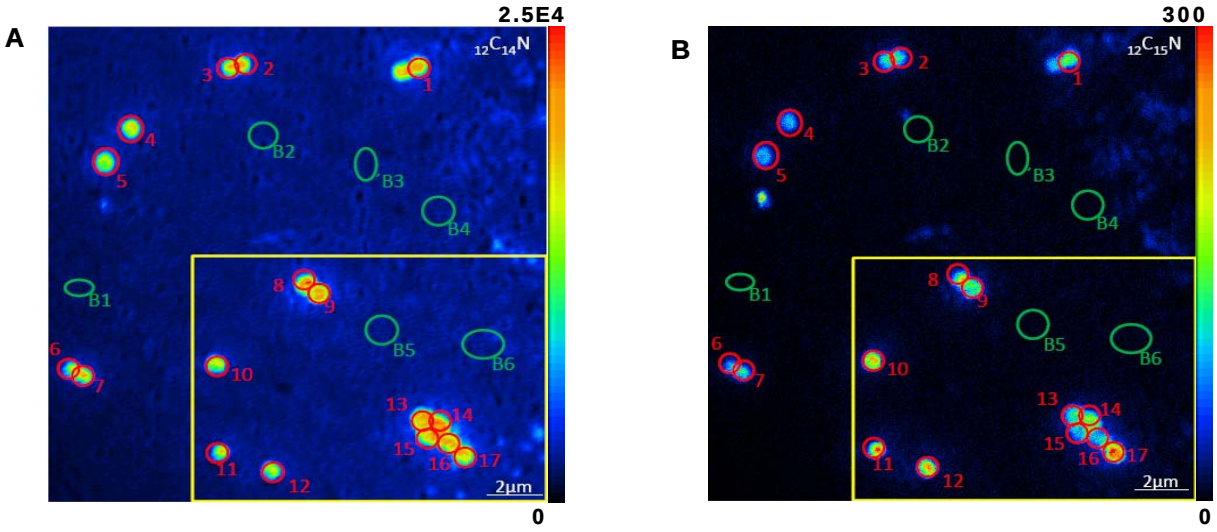

C

region of interest	1	2	3	4	5	6	7	8	9
$^{12}C^{15}N/^{12}C^{14}N$	0.0094	0.0085	0.0089	0.0071	0.0085	0.0080	0.0087	0.0096	0.0089
region of interest	10	11	12	13	14	15	16	17	mean
$^{12}C^{15}N/^{12}C^{14}N$	0.0173	0.0198	0.0189	0.0082	0.0085	0.0077	0.0082	0.0183	0.011

region of interest (background area)	B1	B2	B3	B4	B5	B6	mean
$^{12}C^{15}N/^{12}C^{14}N$	0.00383	0.00421	0.00391	0.00395	0.00387	0.00399	0.004

Supplementary Figure 5 - $^{12}C^{15}N/^{12}C^{14}N$ ratios of 30 minutes SP1-1 treated *S. aureus* samples
NanoSIMS analysis of 30 min SP1-1 treated *S. aureus* was carried out and data were processed as described in chapter 2.2.9.2. Regions of interest (ROIs) were built over representative image spots covering *S. aureus* cells (red) or only filter area for nitrogen background levels (green). (A) $^{12}C^{14}N$ signal images were compared to (B) $^{12}C^{15}N$ signal images and (C) ratios of $^{12}C^{15}N/^{12}C^{14}N$ signal counts of the ROIs were calculated. Mean values (mean) of the signal count ratios from ROIs covering *S. aureus* cells (red) or background (green) are indicated. Data analysis was done with WinImage Software (Cameca, Genneviliers Cedex, France). The yellow box markes the image section, shown in Figure 11. Shown are drift-corrected, accumulated signals from cycles 10 to 50 of 60. The color scale illustrates signal counts from low (0) in black to high of (A) 2.5x 10^4 or (B) 300 in red.

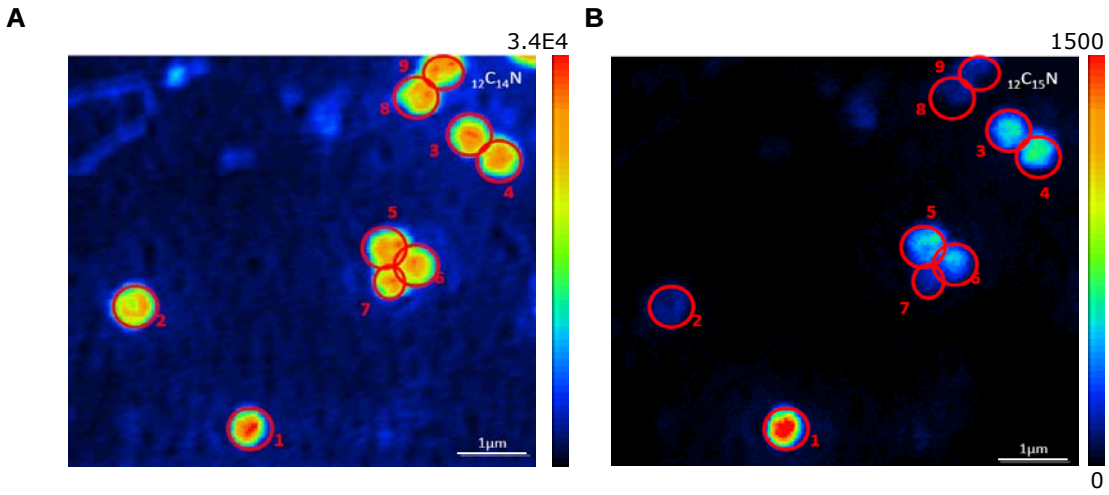

C

region of interest	1	2	3	4	5	6
$^{12}C^{15}N/^{12}C^{14}N$	0.053	0.0066	0.0191	0.023	0.0185	0.0173

region of interest	7	8	9	mean value
$^{12}C^{15}N/^{12}C^{14}N$	0.00844	0.0065	0.0080	**0.02**

Supplementary Figure 6 - $^{12}C^{15}N/^{12}C^{14}N$ ratios of 10 minutes SP1-1 treated *S. aureus* samples
NanoSIMS analysis of 10 minutes SP1-1 treated *S. aureus* samples was carried out and data were processed as described in chapter 2.2.9.2. Regions of interest (ROIs) were built over representative image spots covering *S. aureus* cells (red). (A) $^{12}C^{14}N$ signal images were compared to (B) $^{12}C^{15}N$ signal images by (C) calculation of ratios of $^{12}C^{15}N/^{12}C^{14}N$ signal counts of the ROIs. Data analysis was performed with WinImage Software (Cameca, Genneviliers Cedex, France). Shown is the same MS image area as in Figure 12 from drift-corrected and accumulated signals of cycles 5 to 50 of 63. The color scale illustrates signal counts from low (0) in black to high of (A) 3.4x 10^4 or (B) 1500 in red.

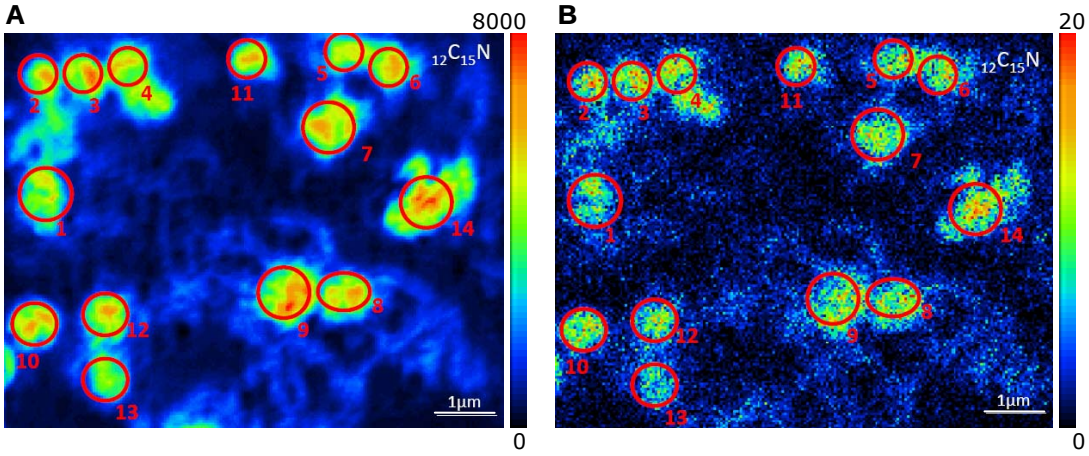

C

region of interest	1	2	3	4	5	6	7	8
$^{12}C^{15}N/^{12}C^{14}N$	0.00216	0.00218	0.00213	0.00221	0.00217	0.00181	0.00175	0.00195

region of interest	9	10	11	12	13	14	mean value
$^{12}C^{15}N/^{12}C^{14}N$	0.00175	0.00193	0.00186	0.00181	0.00170	0.00185	**0.002**

Supplementary Figure 7 - $^{12}C^{15}N/^{12}C^{14}N$ ratios of untreated *S. aureus* samples
NanoSIMS analysis of 30 minutes buffer treated *S. aureus* samples was carried out and data were processed as described in chapter 2.2.9.2. Regions of interest (ROIs) were built over representative image spots covering *S. aureus* cells (red) for measurement of nitrogen background levels. (A) $^{12}C^{14}N$ signal images were compared to (B) $^{12}C^{15}N$ signal images by (C) calculation of ratios of $^{12}C^{15}N/^{12}C^{14}N$ signal counts of the ROIs. Data analysis was performed with WinImage Software (Cameca, Genneviliers Cedex, France). Shown are accumulated signals from cycles 10 to 50 of 65. The color scale illustrates signal counts from low (0) in black to high of (A) 8000 or (B) 20 in red.

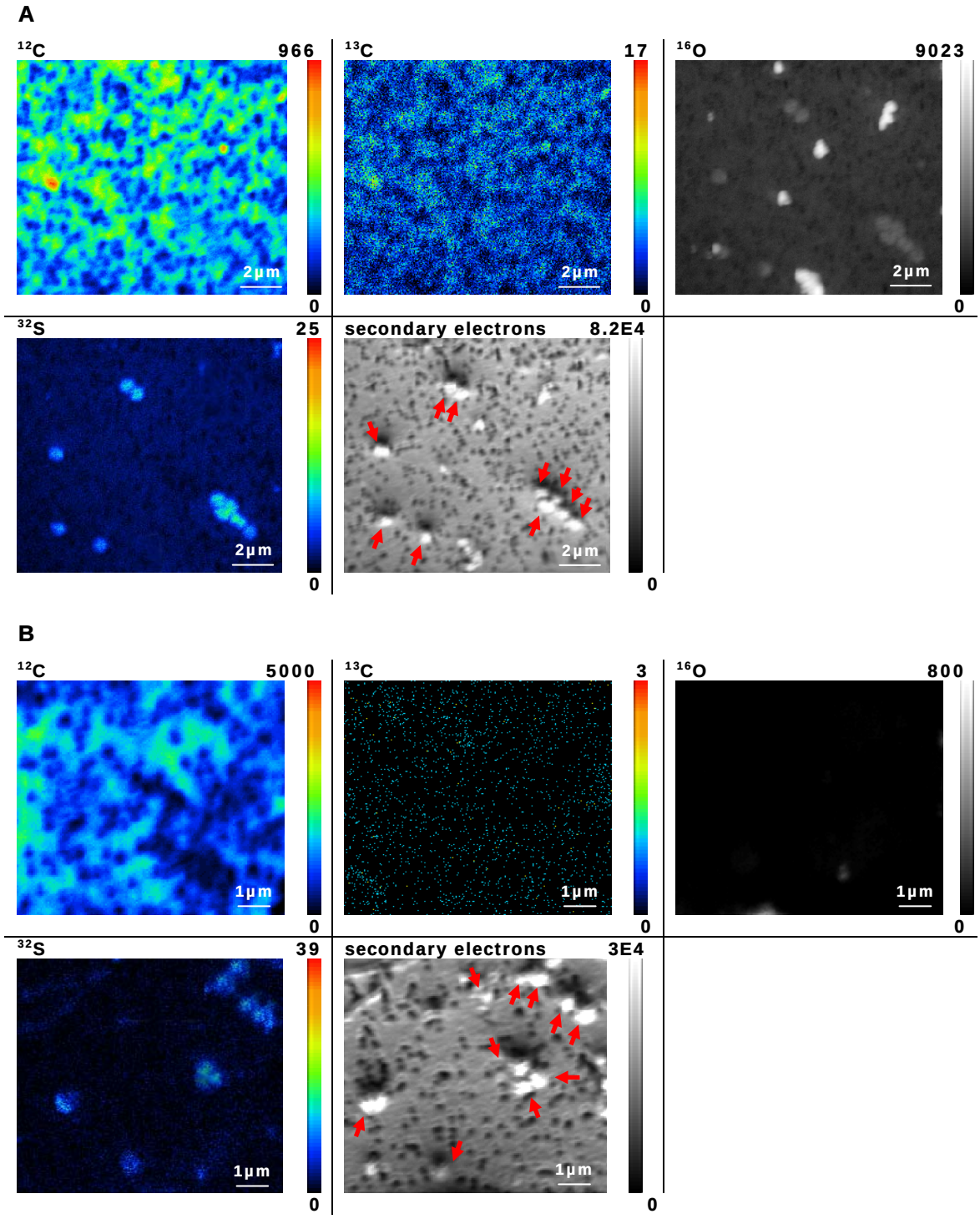

Supplementary Figure 8 - Secondary NanoSIMS images of ^{12}C, ^{13}C, ^{16}O, ^{32}S, and recorded secondary electrons

S. aureus cells (4 x 10^6 cfu) were incubated with 100 µg/ml ^{15}N-SP1-1 for 10 min or 30 min at 37°C, harvested by centrifugation and fixed with 1% paraformaldehyde oN at 4°C. The cells were washed with PBS and filtered on gold/palladium sputtered filters. They were analyzed by NanoSIMS 50L with 60 – 63 cycles of ion beam sections and generation of according secondary ion mass spectrums. Image processing and analysis was performed with WinImage (Cameca, Gennevilliers Cedex, France). Shown are MS images of ^{12}C, ^{13}N, ^{16}O, ^{31}P, ^{32}S and the image of all measured secondary electrons to exclude artefacts being analyzed. The analyzed cells are indicated by arrows on the secondary electron image. (A) Shown are secondary MS signals of *S. aureus* cells from cycles 10 to 50 of 60 after 30 min of SP1-1 treatment. (B) Shown are secondary MS signals of *S. aureus* cells from cycles 5 to 50 of 63 after 10 min of SP1-1 treatment. The color scale illustrates signal counts from low (0) in black to high in red. The gray scale illustrates signal counts from low (0) in black to high in white.

6.5 Determination of SP1-1 concentration for the microarray analysis

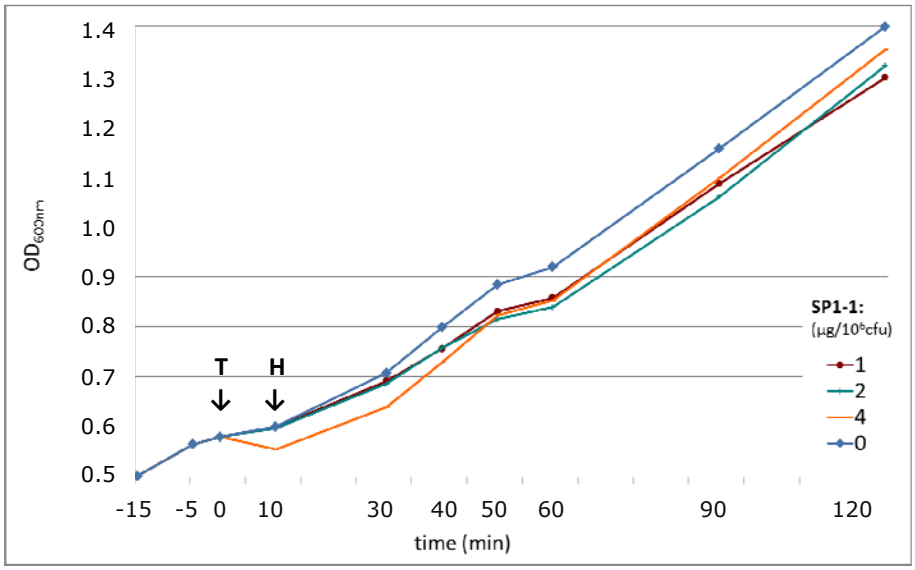

Supplementary Figure 9 - Growth of *S. aureus* COL after SP1-1 treatment
S. aureus COL from an oN culture in BHI broth was diluted to OD_{600nm} and grown to mid–logarithmic phase. The cells were treated with 0 (mock), 1, 2, or 4 µg SP1-1/10^6 cfu and growth was monitored for 120 min by measurement of OD_{600nm}. The concentration of SP1-1 (4 µg / 10^6 cfu, indicated in orange) leading to a slight growth reduction, was used for microarray experiments. The timepoints for SP1-1 treatment (T) and harvest (H) of the following microarray experiments are indicated. The timepoint of peptide treatment is characterized as timepoint 0.

6.6 Inhibiting effect on the phosphorylation reaction of RsbW by SP1 derivates

A

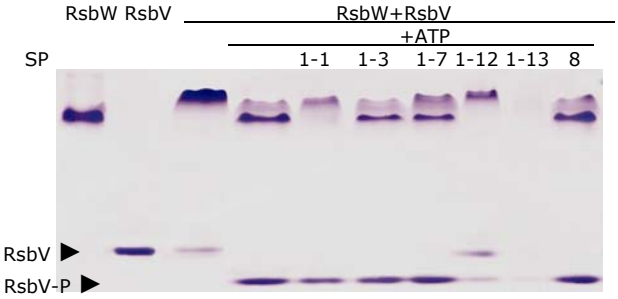

B

Activity in *S. aureus*

peptide	Sequence	MIC (µg/ml)
SP1-1	RKKRLKLLKRLV	**10**
SP1-3	RKKKVKLLKRLV	**100**
SP1-7	RKKKLKIIKRLI	**>100**
SP1-12	RKKKFKFFKRLF	**5**
SP1-13	RKKKFKFFKRFF	**1**
SP8	LLIRAAKKFIKK	**>100**

Supplementary Figure 10 - Inhibition of the kinase function of RsbW by SP1 derivates
(A) RsbW (0.1 µM) was pre-incubated with 6 µg SP1-1, SP1-3, SP1-7, SP1-12, SP1-13, and SP8 (used as control) for 15 min. After the addition of the substrate RsbV and 2 mM ATP, phosphorylation was carried out for 5 min. The reaction was stopped by the addition of 50 mM EDTA and incubation on ice. The samples were separated by 15% native PAGE. The inhibition of the phosphorylation reaction can be shown by the disappearance of the phosphorylated substrate (RsbV-P) and the re-appearance of the unphosphorylated substrate (RsbV) on the Coomassie stained gel. (B) By comparison of MIC values against *S. aureus* 90857 (from Table 2) of the peptides, tested for RsbW inhibition, inhibition ability can be correlated with activity.

6.7 MIC values for antibacterial activity tests with *S. aureus* mutant strains

Supplementary Table 3 - MIC values of SP1-1 and control peptides tested against *S. aureus* mutant strains

***S. aureus* strain**	**SP1-1**	**SP8**	**SP10-2**
	MIC (µg/ml)		
RN1HG	100	>100	5
RN1HG *ΔsigB*	>100	>100	5
RN1HG *ΔsigB* comp.	100	>100	5

Antibacterial activity was determined by incubation of 0.1 – 100 µg/ml of SP1-1, SP10-4 or SP8 with 10^5 cfu of bacterial suspension cultures in LB medium in a total volume of 100 µl for 18 h. OD_{600nm} was measured and minimal inhibitory concentration (MIC) values were determined.
S. aureus strains RN1HG, RN1HG *ΔsigB (*deletion mutant of *sigB* operon *(rsbV, rsbW and sigB*) and *rsbU*) and RN1HG *ΔsigB* complemented (comp.; complemented strain of the deletion mutant *ΔsigB*) were used.

6.8 Amino acid sequence of RsbW

1 MQSKEDFIEM RVPASAEYVS LIRLTLSGVF SRAGATYDDI EDAKIAVSEA

50 VTNAVKHAYK EN*NNVGIINI YFEILEDKIK IVISDKGDSF DYETTKSKIG

100 PYDKDENIDF LREGGLGLFL IESLMDEVTV YKESGVTISM TKYIKKEQVR

150 NNGERVEISs awshpqfek STOP

Supplementary Figure 11 - Amino acid sequence of strep-tagged recombinant RsbW
The RsbW amino acid sequence displays no big highly hydrophobic clusters (strongly hydrophobic amino acids are indicated in red). Shown is the amino acid sequence of RsbW from *S. aureus* Mu50 / COL (accession-numbers from http://www.ncbi.nlm.nih.gov: YP_186871 (COL), NP_372589.1 (Mu50)) with a length of 159 amino acids (black, capital letters) with N-terminal strep tag (blue, small letters), including the 2 aa linker in between (green, small letters) from plasmid pPRIBA1:RsbW. The given sequence in plasmid pPRIBA1:RsbW, derived from *S. aureus* COL, was used for recombinant production, interaction and structural analyses. The ORF library for the Y2H screen was generated from *S. aureus* Mu50. The RsbW sequences from *S. aureus* Mu50 and COL display 100% sequence similarity. The RsbW sequence translated from the Y2H prey plasmid had due to a mutation an exchange in N at position 62 (marked by an asterisk) to K and showed thereby 100% homology to RsbW from strain MRSA 252 (Gene-ID: 2861460).

6.9 Recombinant SP1-1 expression

For structural interaction studies with RsbW by NMR analysis, SP1-1 was recombinantly produced in *E. coli* and labeled with ^{15}N during production. The coding sequence of SP1-1 from plasmid pAGRO:T2SB:SP1-1cc for tobacco transformation with N-terminal charge compensation and TMV coat protein as fusion partner (Zeitler, 2011) was used. The peptide sequence was recombined into bacterial expression plasmids pDest15 (GST-tagged) and pDest17 (6x His-tagged) as described in chapter 2.2.4.1. The peptide was expressed in *E. coli* BL 21 Star (DE3) RARE 2, a special expression host capable of the production of rare codons. Overnight expression of pDest15:T2SB:SP1-1 at 30°C incubation temperature after induction with 1 mM IPTG delivered a high amount of expressed protein (Supplementary Figure 12).

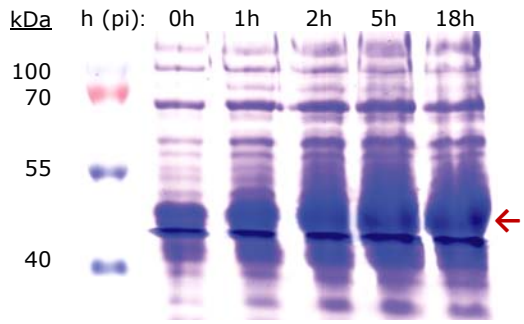

Supplementary Figure 12 - Expression levels of the SP1-1-TMVcoat fusion protein in *E. coli* BL 21 Star (DE3) RARE2
The plasmid pDest15:T2SB:SP1-1 was generated by gateway cloning and transformed into *E. coli* BL 21 Star (DE3) RARE 2. From an oN culture LB medium (Carb) was inoculated to OD_{600nm}: 0.1 and grown to OD_{600nm} of 0.5. Protein expression was induced by addition of 1mM IPTG and carried out for 18 h at 30°C. 1 ml samples were taken after 0 – 4 h post induction (pi), the samples were pelleted and concentrated 1/20. 1/5 Vol was analyzed by 12% SDS-PAGE. The produced fusion protein (indicated by a red arrow) was detected at a size of 48 kDa.

The fusion protein was affinity purified with a GSTrap column, by the plasmid derived GST-tag. Protein concentration was determined and pure fusion protein was detected in eluted fractions by 12% SDS-PAGE analysis (Supplementary Figure 13). However, the amount of the purified fusion protein was only 0.5 mg per 1l culture volume. As the 1.5 kDa peptide represents only 3% of the 48 kDa fusion protein, the purified protein amount was not sufficient for structural analysis as 1 mg of pure peptide was needed.

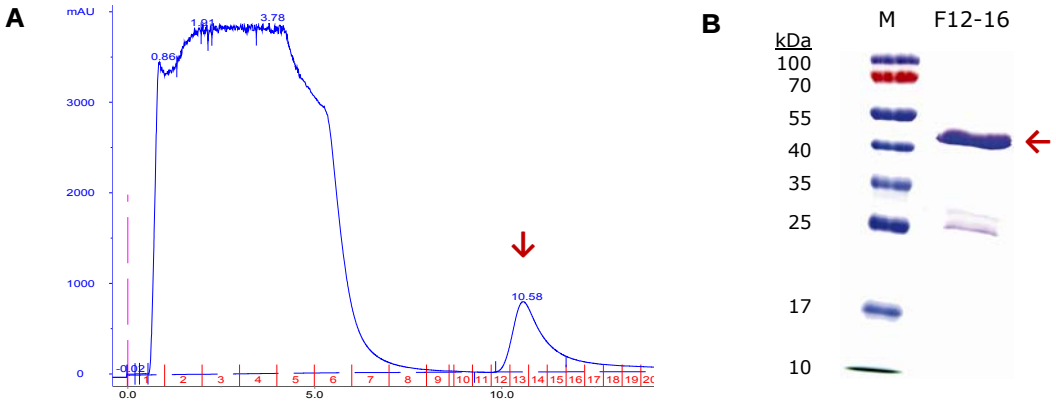

Supplementary Figure 13 - Purification of the recombinant GST-TMVcoat-SP1-1 fusion protein
Crude protein extract from an *E. coli* culture was purified with a GSTrap column by FPLC and analyzed by 12% SDS-PAGE. The fusion protein is indicated by red arrows. M: molecular weight marker (in kDa). (A) Chromatogram of the affinity purification and detection of protein retention in milli Absorbance Units (mAU) at 280 nm (blue line). Fractions are indicated in red and retention volume (in ml) in black on the x-axis. (B) 10 µl of pooled fractions 12-15 after affinity chromatography were separated by 12% SDS-PAGE and Coomassie stained. The fusion protein with a size of 48 kDa could be detected

Due to the low amount of purified protein from pDest15:T2SB:SP1-1, SP1-1 was sub-cloned with codons optimized for *E. coli* usage and plasmids pETGB1a, pETTrx1a, or pETZ1a with different fusion proteins (1 - B1 Ig binding domain gene fragment derived from *Streptococcus (GB1)*, 2- Thioredoxin A gene (Trx), or 3 - Z-Tag 2: gene fragment of staphylococcal protein A (Z1)). The used fusion partners are known to compensate the cationic charge and hydrophobicity to a higher extent and therefore lead to higher expression levels and to better solubility of the fusion protein. The SP1-1 coding DNA sequence including stop codon was built of primer pairs with *E. coli* transcription optimized codons and flanking sites, coding for enzyme restriction cleavage sites for recombination into the expression vector. Cloning, recombinant production and purification was done as described in chapter 2.2.4.2, with the help of Franziska Carmienke during an internship and a Bachelor´s thesis. The single stranded primers were annealed to double stranded constructs, ligated into the expression vectors (pETGB1a, pETTrx1a, pETZ1a) and transformed in *E. coli* DH5α. Only with pETGB1a:SP1-1 positive *sp1-1* containing plasmids could be obtained and the plasmid was transformed into *E. coli* BL 21 (DE3) plys S and used for expression. High expression yields were obtained by oN incubation at 30°C (Supplementary Figure 14A, lane PE). The extracted protein was affinity purified by Ni-NTA agarose (Qiagen, Hillden, Germany) and yielded roughly 15 – 20 mg fusion protein per 1l culture volume (Supplementary Figure 14A, lanes E1 – E4). As the portion of the pure peptide SP1-1 is 14% of the 10.8 kDa fusion protein the amount, obtained from 2 l culture volume, was estimated high enough for the NMR analysis including losses in purification steps. Further purification was done according to the protocol of Zeitler (2011). Oxidized methionine residues were reduced, the peptide was cleaved by CNBr treatment and SEC purified with a superdex Peptide 10/300 GL column. The retended recombinant peptide fraction could be compared with synthetic peptide retention (Supplementary Figure 14A – B). The expected chromatographic behavior according to Zeitler (2011) could be shown with a slightly earlier retention time (Supplementary Figure 14B, red line) compared to the synthetic standard peptide (green line), due to the missing C-terminal amidation. The collected SEC fractions were further separated by reversed phase chromatography and checked for size and purity on Tricine-SDS-PAGE, where the recombinant purified SP1-1 as well as the synthetic peptide used as a standard, showed the according to Zeitler (2011) expected shifted running behavior, due to hydrophobicity and positive charge, with bands at 3 kDa (Supplementary Figure 14C).

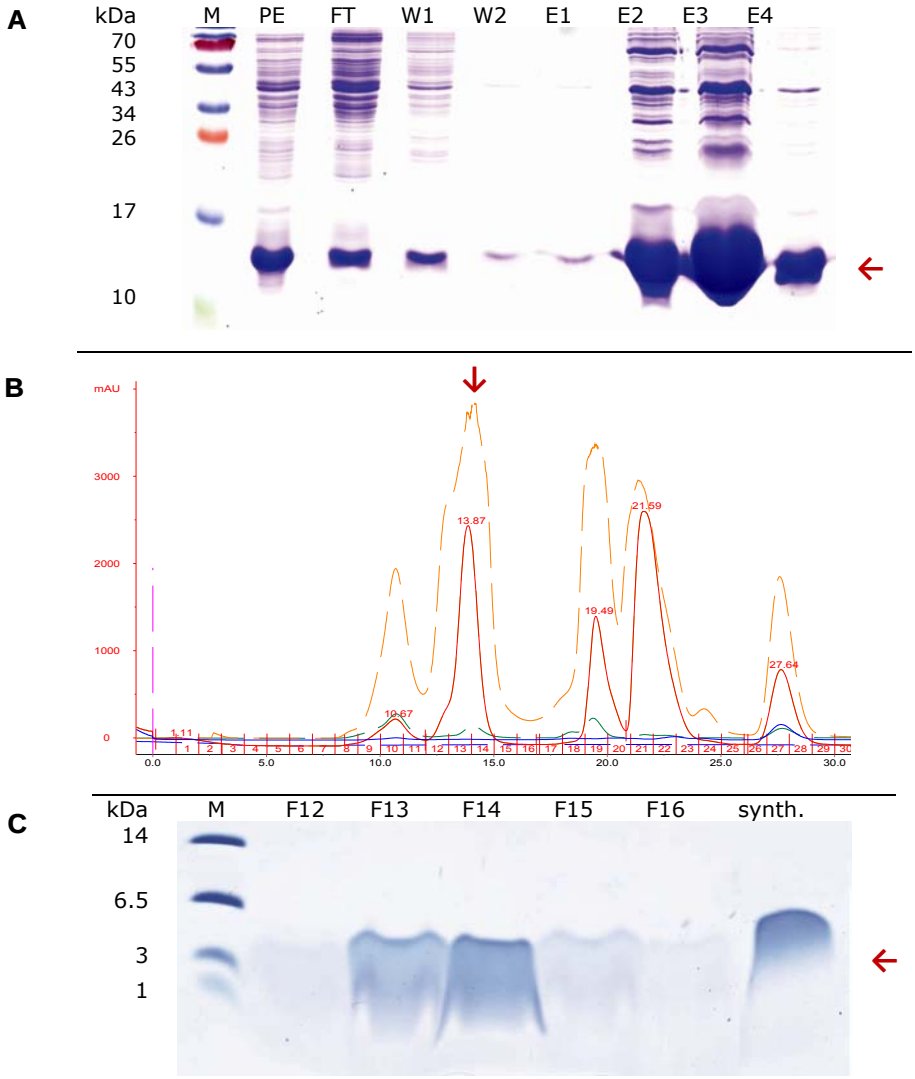

Supplementary Figure 14 - Recombinant expression and purification of recombinant SP1-1 from plasmid pET-GB1a
SP1-1 (pETGB1a:SP1-1) was recombinantly expressed in in *E. coli* oN at 30°C. Protein was extracted and affinity purified. SP1-1 was cleaved by CNBr and purified by size exclusion (SEC) and reverse phase chromatography (RPC). M: molecular weight marker (in kDa). (A) 18% SDS-PAGE analysis of protein extract (PE), flow through (FT), different washing (W1-2) and elution steps (E1-4) from affinity purification with Ni-NTA agarose (Qiagen, Hillden, Germany). The fusion protein (10.8 kDa) is indicated by a red arrow. (B) SEC chromatogram after cleavage with CNBr. Peptide retention is measured in milli Absorbance Units (mAU) at 215 nm, indicated on the y-axis. Fractions are indicated in red and retention volume in black on the x-axis. SP1-1 retends with a maximum at 13.87 ml (red arrow). The peaks of 50 µg synthetic SP1-1 standard (green line), the CNBr cleaved sample of 900 ml culture of recombinantly expressed (red line) and the the CNBr cleaved sample of 1.2 l culture of ^{15}N-labeled recombinantly expressed SP1-1 (orange line) overlap. (C) 16% Tricine-SDS-PAGE analysis of 10 µl of eluted fractions 12-16 (F12-16) from RPC. 2 µg synthetic SP1-1 served as standard. SP1-1 samples show shifted running behavior, due to hydrophobicity and positive charge, with bands at 3 kDa (indicated by a red arrow).

A sufficient amount of pure SP1-1 could be obtained with this expression and purification technique. SP1-1 was expressed with ^{13}C and ^{15}N as single carbon and nitrogen sources by growing the cells in ^{13}C^{15}N-M9 minimal medium. It was purified according to the same protocol, resulting in around 2 mg pure SP1-1 from 1.2 l culture volume, to be used for NMR analysis with the RsbW kinase.

Acknowledgements

First of all I would like to thank my Ph.D. supervisor Prof. Jörg Durner, for the opportunity to perform my Ph.D. thesis at the Institute of Biochemical Plant Pathology. Thank you as well for the open minded discussions and experienced advices throughout the whole time.

I also would like to thank my second examiner, Prof. Siegfried Scherer and the head of the examination, Prof. Wolfgang Liebl, for reviewing this work and organizing the examination process.

I want to thank my group leader, Dr. Christian Lindermayr, for supervision throughout the entire project, his experienced advice regarding the peptide topic, all the discussions and new ideas and the proof reading of this work.

A big thank you also to Dr. Nikolaus Ackermann from the Max-von-Pettenkofer Institute of Hygiene and Microbiology of the Ludwig-Maximilian-University in Munich, who gave me the opportunity to perform most of the work with the *Staphylococcus aureus* strains in their S2 lab facilities, and together with his technician Theresa Anding for their constant helpfulness and excellent cooperation.

A special thank also to Dr. Kamil Önder, Dr. Omar Abdel-Hadi and Dr. Richard Maier from the Department of Dermatology, at the Paracelsus Medical University Salzburg for performing the yeast-two hybrid screen, which led to the important finding of the kinase target. Also, thank you for the continuous and still ongoing excellent cooperation, the good ideas and the support.

Thank you very much also to Prof. Michael Hecker, Dr. Susanne Engelmann and Dr. Jan Panné-Farré for the cooperation regarding the work of the kinase – peptide interactions and for the opportunity to perform the activity tests with the *S. aureus* deletion mutants in their S2 lab facilities at the Institute of Microbiology, of the Ernst-Moritz-Arndt University of Greifswald.

Furthermore I want to thank Prof. Roland Benz from the Rudolf-Virchow-Center, DFG-Research Center for Experimental Biomedicine University of Würzburg. He enabled me to perform the measurements with artificial membranes in his laboratories in Wurzburg. In this context also thank you to his technician, Elke Meyer, who introduced me in the experimental setup.

Thank you also to Prof. Michael Sattler, Dr. Arie Geerlof and Dr. Ana Messias of the Institute of Structural Biology for the support regarding the structural analysis of the kinase – peptide interaction. Ana, who carried out the NMR measurements and Arie (Protein Expression and Purification Facility of the Helmholtz Zentrum München), who

carried out the stability studies of the kinase together with me and also supported me with plasmids and bacteria strains, both spent much effort on my project. So, thank you a lot.

I also want to thank Prof. Jaques Schrenzel and Dr. Patrice Francois, from the Genomic Research Laboratory, University Hospital of Geneva for their good cooperation and performance of the *Staphylococcus* Microarray.

Many thanks to the NanoSIMS Facility at the Chair of Soil Science under the direction of Prof. Ingrid Kögel-Knabner, at the Department Ecology and Ecosystem Management of the Center of Life and Food Sciences Weihenstephan (TU München). In particular I would like to say thank you to Dr. Carsten Müller, Dr. Carmen Höschen and Johann Lugmeier, for the NanoSIMS analyses of my samples.

I would like to acknowledge Dr. Elisabeth Kremmer from the Core Facility for Generation of Monoclonal Antibodies and Cell Sorting of the Institute of Molecular Immunology (Helmholtz Zentrum München) for the generation of antibodies against our peptides.

Thanks are also due, of course, to all my "BIOP" colleagues and former colleagues for the nice working atmosphere, for help whenever needed and for fruitful discussions. I am particularly grateful to one of my former colleagues, Dr. Cristina Palmieri, who introduced me to many techniques and helped me to orient myself in the lab during my first months at the Institute. Thanks also to my former trainee students, who contributed to this work: Stefanie Tischer working on RNA binding ability of the peptides and Franziska Carmienke who helped with cloning, recombinant production and purification of $^{15}N^{13}C$ labeled SP1-1 in *E. coli* in the course of an internship and her Bachelor´s thesis work.

Among the (former) BIOP members I particularly want to thank Dr. Günther Bahnweg for the English-proofreading of this work. Thank you very much for the very quick readiness to help.

Lastly I wish to thank Dr. Benjamin Zeitler, for introducing me into FPLC technique and many other practical advices regarding my lab-work. Especially thank you, Benny, for helping with the proofreading of this work, standing and improving my mood during writing and the continuous support.